Cerebello-Thalamic Connection:
A study of development, physiology and anatomy

Simona Veronica Gornati

The research described in this thesis was performed at the Department of Neuroscience, Erasmus Medical Center Rotterdam.

The research in this thesis was financially supported by the Netherlands Organisation for Scientific Research (NWO-VIDI) and by ERC-Adv, ERC-PoC, NWO-ALW and Zon-MW grants.

Cover design by Monia Giannotta
Printing and layout by Ridderprint BV, www.ridderprint.nl

© Simona Veronica Gornati, 2018.

All rights reserved. No parts of this publication may be reproduced, stored in retrieval system or transmitted in any form by any means, electronical, mechanical, photocopying, recording or otherwise without permission of the author or, when appropriate, the scientific journal in which parts of this thesis have been published.

.

Cerebello-Thalamic Connection:
A study of development, physiology and anatomy

De ontwikkeling, fysiologie en anatomie
van de cerebello-thalamische verbinding

Proefschrift

ter verkrijging van de graad van doctor aan de
Erasmus Universiteit Rotterdam
op gezag van de rector magnificus

Prof.dr. R.C.M.E. Engels

en volgens besluit van het College voor Promoties.

De openbare verdediging zal plaatsvinden op

woensdag 12 september 2018 om 13.30

door
Simona Veronica Gornati
geboren te Novara, Italy

Erasmus University Rotterdam

Promotiecommissie:

Promotoren: Prof.dr. C.I. De Zeeuw
Prof.dr. F.E. Hoebeek

Overige leden: Dr. T.J.H Ruigrok
Prof.dr. S.A. Kushner
Prof.dr. H.W.H.G Kessels

“Patty, Teto, ce l’abbiamo fatta!”

Part Lies

Part Heart

Part Truth

Part Garbage

Contents

"Lector intende: laetaberis"

Metamorphoseon – Apuleio

Chapter 1

General introduction

1

General introduction

The aim of neuroscience has always been the understanding of the mechanisms behind neuronal activity and brain function. The nervous system, in its totality, is highly complex and fascinating: mouse nervous system is made of 71.000.000 neurons [1], whereas humans have 16.000.000.000 [2] and all of these neurons are highly heterogeneous both for their chemistry, role and activity.

How neurons communicate to each other has always been of mayor importance to understand the basis of brain function and the mechanism by which we accomplish daily life tasks. Neurons never function alone or in couple, they organize in circuits that process specific kinds of information. The fundament of these interaction between neurons are the synapses. They connect two (or more) neurons aiding the passage of information through the system, converting an electrical signal to a chemical one, and then back again. The basic features of the synaptic connection are well conserved, however the arrangement of neuronal circuits varies greatly according to the intended function.

Among all, the cerebello-thalamic connection, which has always been appreciated for its role in movement, is the focus of this work. The main goal of this thesis is to characterize in detail this synapse from development to pathological conditions and investigate the potential role of this in non-motor function.

Starting from the basics: anatomy and physiology

The brain is clearly subdivided in two parts, which are distinguishable by the naked eye. They are called the big brain (cerebrum) which contains cerebral cortex and other subcortical structures, such as the thalamus, and the small brain (cerebellum).

Cerebellum anatomy and function

In the caudal part of the brain, dorsal to the brain stem, there is a separate structure tucked underneath the cerebral hemispheres: the cerebellum. It is separated from the overlying cerebrum by a layer of dura mater called "tentorium cerebelli" and it receives the main connections coming from other parts of the brain through the pons. The cerebellar structure has a very peculiarly organized and conserved cellular organization that caught the attention of anatomists and neuroscientists since the beginning of modern neuroscience (y Cajal 1888-1889). We can recognize two main structures in the cerebellum: the cerebellar cortex and the cerebellar nuclei.

Cerebellar cortex

The cerebellar cortex gives the cerebellum an unusual appearance as the bulk of the structure is made of a very tightly folded layer of gray matter (called folia). Underneath the gray matter lies the white matter, which consists of myelinated nerve fibers running to and from cortex [3]. Within the cerebellar cortex the cytoarchitecture is highly uniform, in that there are three layers to the cerebellar cortex from outer to inner layer: the molecular, Purkinje cells and granular layer (Figure 1).

The molecular layer contains the dendritic trees of Purkinje cells (PCs), which receives inputs from two types of inhibitory neurons: the stellate and basket cells. Moreover, on the proximal branches, PCs are contacted by a single climbing fiber coming from inferior olive and by granule cell axons that form ~10 to 20 synapses with PCs dendritic trees before they bifurcate into parallel fibers (PFs), running perpendicular to the Purkinje tree.

The middle layer is exclusively formed by a monolayer of Purkinje cell somata. These neurons are the only cells in cerebellar cortex that are sending inhibitory projections to the nuclei and therefore they play a central role in modulating the information flow from the cerebellar cortex to the cerebellar nuclei.

The innermost layer contains the cell bodies and dendrites of granule cells, which give rise to the parallel fibers, the unipolar brush cells, the Golgi cells and the mossy fibers.

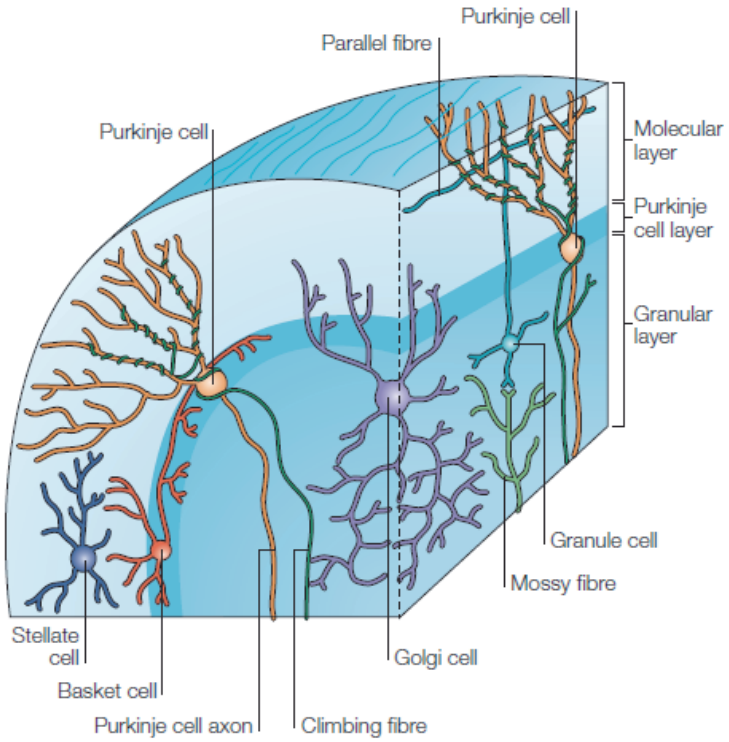

Figure 1. Organization of cerebellar cortex. There are different types of cells and fibers found within the three cell layers of the cortex. The climbing fiber, originating from inferior olivary neurons, and the parallel fiber form a connection with the Purkinje cells' dendrites in the moleculr layer. PCs soma and axons are in PCs and granular layer and descend further to reach their output in the cerebellar nuclei. From [4]

Cerebellar nuclei

The mouse cerebellar nuclei are divided in Lateral, Interpositus and Medial [5]. The cerebellar nuclei are the major output of the cerebellum with projections to pre-motor centres of the brainstem, like the red nucleus, and to thalamus [6, 7]. Classically CN neurons have been classified in two main categories, glutamatergic and GABAergic cells, but a more detailed categorization has been reported [8], including local neurons and glycinergic neurons. All of these cells are distributed heterogeneously among the three nuclei. Nevertheless, the circuits that these neurons are forming are different: glutamatergic cells are the one that are projecting outside the CN, although they also send projections to the cerebellar cortex [9], GABAergic cells provides feedback to inferior olive (IO) and glycinergic cell not only project outside of the cerebellum to the vestibular nuclei [10] but are also sending projections back to cerebellar cortex [11, 12].

Among the neurons of the cerebellar nuclei, the glutamatergic cells are the easiest to identify. They are characterized by a soma with a large diameter of 20-30 µm, with 2 to 5 primary dendrites expanding from the soma [12, 13]. These cells fire with a spontaneous high rate, which is independent of synaptic input [12, 14]. Glutamatergic projection cell dendrites contain voltage sensitive calcium channels, which produce transient events [15] and it has been shown in isolated neurons that a tonic cation current is promoting spontaneous firing as it drives the membrane potential above threshold [16]. Sodium ions carry the main flux, and are partially gated by voltage independent, tetrodoxin-insensitive channels that can depolarize neurons near action potential threshold. However these cells receive four different inputs that can affect their firing: excitatory inputs from collaterals of the climbing fibers and mossy fibers (Figure 2) [17, 18], local inhibitory interneurons and inhibitory input arising from the axonal terminals of ~30 to 40 of PCs, i.e., the majority of synapses on CN cells [19].

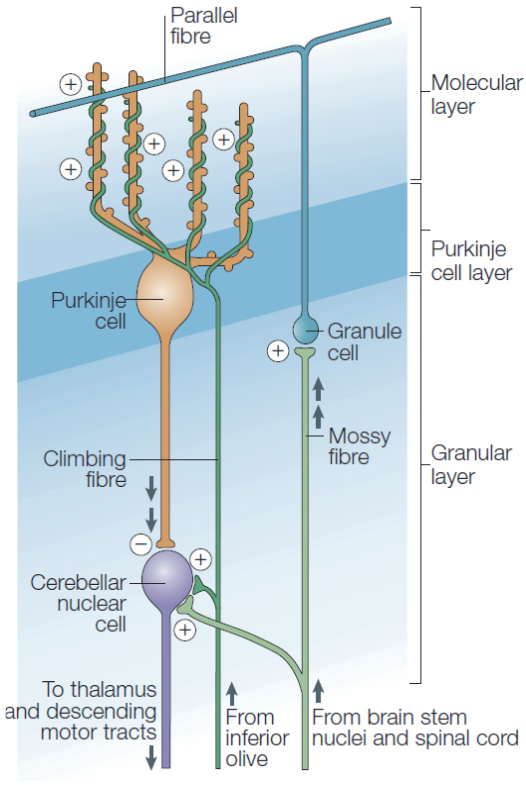

Figure 2. Cerebellar nuclei cell. CN neurons receive inputs from different sources: inhibitory inputs from PCs and excitatory inputs from collaterals of the climbing fibers and mossy fibers

The effect of the excitatory input is still unclear as the CN spontaneous firing overlap with any basal mossy fiber input [20], therefore in order to detect the effect of the excitatory input, a reduction of spontaneous firing is required. Purkinje-mediated inhibition is responsible for the decrease of nuclear cells firing and given the big convergence of Purkinje cells onto a single CN neuron and considering their high firing rate, it is assumed that the CN neuron is under a constant tonic inhibition [21].

Beside the difference in cellular organization, there is evidence of the existence of several molecular markers that divided the cerebellum into distinct bands [22]. One is Zebrin that is expressed in specific subgroups of PCs that are organized in symmetric stripes [23]. This organization, conserved in both birds and mammals, is reflected also in the inputs these cells receive as PCs located in the same band receive CF inputs from the same part of the inferior olive and project their axon to the same part of cerebellar nuclei [24]. Rostral nuclei as anterior interposed receives Zebrin negative inputs whereas the caudal part, posterior interposed and lateral, mostly Zebrin-positive inputs [25]. The Zebrin positive and Zebrin negative PCs cells fire at different frequencies in vivo (i.e. approximately 60 Hz vs 90 Hz) and this has been suggested to be due to a difference in intrinsic properties of PCs [26]. This reflects in a diverse influence on cerebellar nuclei firing, as previous works suggested that the synchronized inhibition of the PCs is phase locking the spiking activity of the glutamatergic cells [19, 27] but a differentiation by Zebrin identity of the cerebellar nuclei [25] has not been characterized yet.

As most of the axonal terminals of the glutamatergic CN cells are found in various parts of the brain [6], it is of interest characterizing how this cell type communicates to downstream target, like the thalamus.

Thalamus anatomy and function

The mouse thalamus forms the largest part of dienchepalon. It is located just above the brain stem between the cerebral cortex and the midbrain and has extensive nerve connections to both. The word “thalamus” in greek means inner room as in the greek archaic house the “thalamus” was the chamber connecting directly or via passageway the rest of the house to the yard; so the thalamus is positioned in a way that connects midbrain and cortex. This football-shaped structure is located in the origin of the two neocortical hemispheres, like the atom of a large molecule. The purpose of this geometrical arrangement could be that being equidistant from all cortical areas demands the least length of reciprocal wiring and provides the fastest axonal communication. The main function of the thalamus is to relay motor and sensory signals to the cerebral cortex and it also regulates sleep, alertness and wakefulness. It has been described as

the "gateway" to the cortex as everything we know about the outside world or about ourselves, is based on messages that have to pass through the thalamus.

It is a paired structured made by two main components: the dorsal thalamus that comprised of nuclei that projects to cerebral cortex and the ventral thalamus composed mostly of the reticular nucleus, a group of inhibitory cells that organize like a shell around the lateral part of dorsal thalamus (figure 3). Beside GABA neurons from the reticular nucleus and the relay neurons of the dorsal thalamus in rat and primates there are interneurons which however are not present in mice except for the Lateral Geniculate Nucleus (LGN).

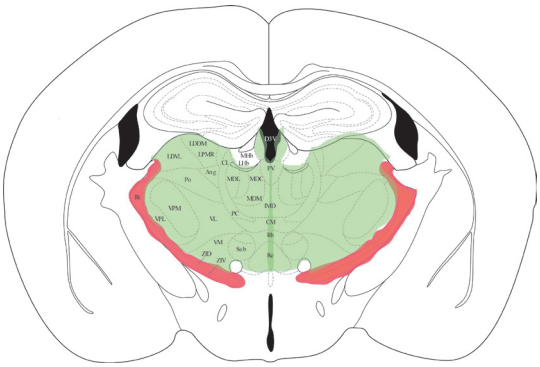

Figure 3. Mouse Thalamus. Thalamus is divided in dorsal (green) and ventral (red). Each of these structures is further divided in nuclei that receive projections from specific subcortical areas. Adapted from Paxinos 2001

Another difference between rodents and higher species is that in mice and rats it is critical to discern between the nuclei as the cytoarchitecture of relay cells is not well defined. The classical categorization of thalamic nuclei is primarily based on the kind of information that is transferred through a particular nucleus or group of nuclei to the cerebral cortex. The main category is formed by the principal "relay" nuclei, which receives specific sensory, motor or associative information through ascending or descending fiber pathways and transmit this information to particular areas of cortex. How the incoming stimuli are integrated by thalamic neurons is quite a mystery, even neighboring neurons cannot chat with each other directly, since they do not possess local axon collaterals, or only very sparse ones in some nuclei. Their axons rush up to the neocortex, terminating predominantly in layer 4 but also in layers 5 and 6 [28].

Thalamic afferents are divided into two main categories: drivers and modulators. This definition comes from the scientist Sherman and Guillery that in 1998 made a distinction between drivers that carries the message, defining the essential patterns

of activity, and the modulators that can alter the effectiveness of the driver without contributing significantly to the general pattern of the message. The distinction between these fibers is based on peculiar characteristics: driver inputs are thick axons that form very large terminals (several µm in diameter) and these synapses evoke large-amplitude post-synaptic responses, activate only ionotropic receptors, and show paired-pulse depression [29] whereas modulators are usually smaller in size, activate metabotropic receptors and show paired pulse facilitation. A typical example of driver input comes from lateral geniculate studies in which retinal afferents are listed as drivers, whereas the layer 6 cortical inputs are modulators. (All the main characteristics are listed in the table 1and figure 4)

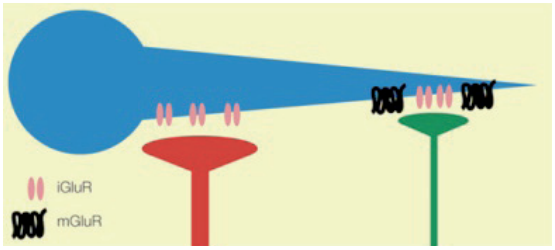

Figure 4. Summary of the anatomical and synaptic features of driver (Class 1) and modulators (Class 2). Adapted from Sherman Neuroscientist 2013

Table 1.

Driver (Class1)	Modulators (class2)
Large and small terminals	Small terminals
Contact on proximal dendrites	Contact on distal dendrites
Thick axons	Thin axons
Less convergence on target	More convergence on target
Large EPSPs	Small EPSPs
Paired-pulse depression	Paired-pulse facilitation
Activate ionotropic glutamate receptors	Activate ionotropic and metabotropic glutamate receptors

Thalamus and cortex are highly interconnected and the thalamocortical relationship is organized so that each cortical area receiving an input from a specific thalamic nucleus, faithfully connects back to this input through a topographically organized cortical projection to the same thalamic area.

The afferents that provide driver input to the thalamus are of two distinct types: one comes from ascending pathways, carrying information from sensory periphery (visual, auditory, tactile etc.) and from other parts of the brain such as the cerebellum; on the

other hand we have input coming from the cerebral cortex itself. These connections defines two different types of thalamic nuclei, respectively the first order and higher order [30, 31]. Both these nuclei receive corticothalamic afferents from pyramidal cells in cortical layer, which also send branches to the thalamic reticular nucleus and have a modulatory function [30, 32, 33] (figure 5).

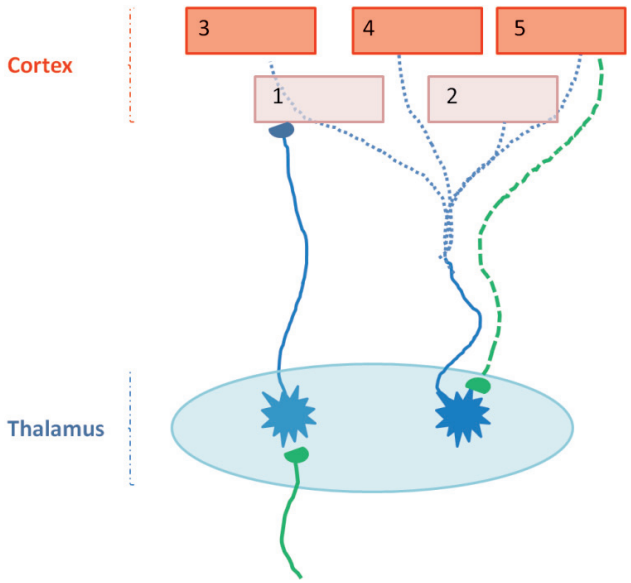

Figure 5. Schematic of first and higher order thalamic nuclei. On the left an example of first order thalamic nucleus receiving its afferents from subcortical areas. On the right higher order thalamic nuclei that receives afferents from layer 5 and send widespread thalamocortical axons (dotted lines) to higher cortical areas. Adapted from Guillery Sherman 2002

All these inputs together can control the state of thalamic relay cell that is known to generate two distinct patterns of action potential: burst and tonic. The firing mode is partially determined by the (in)activation state of voltage gated T-type Ca^{2+} channels in somatic and dendritic membrane [34, 35] (Figure 6).

The firing modes strongly affect the way thalamic relay cells respond to inputs and how this is relayed to the cortex [36]. In general bursting activity is related to sleep, periods of inattention or drowsiness whereas tonic activity is present during waking and rapid-eye-movement sleep. Apart from sleep a lot of essential brain functions, such as memory consolidation and spatial navigation are based on synchronized, rhythmic firing among smaller or larger neuronal cell populations [37, 38], therefore

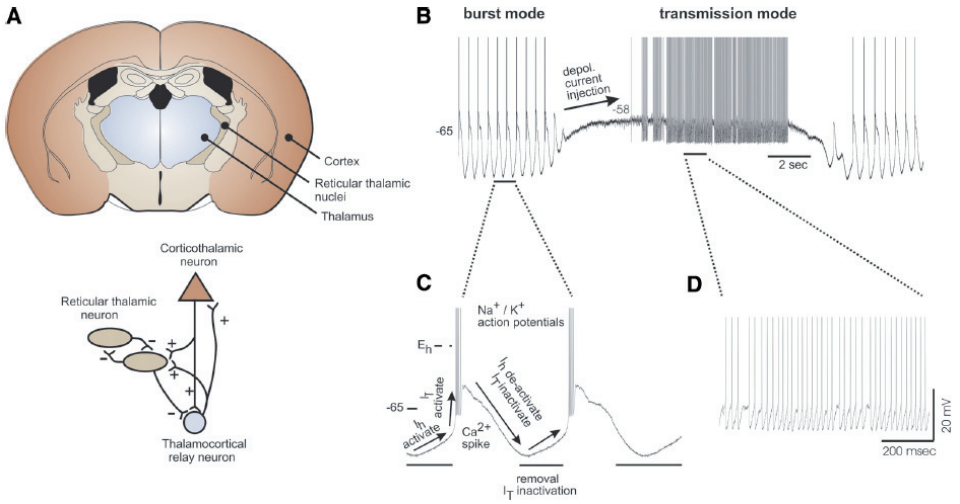

Figure 6. Thalamocortical circuit. Schematic of the thalamocortical system. **A** The thalamus is reciprocally connected with the cerebral cortex and with the thalamic reticular nucleus (TRN). Thalamocortical and corticothalamic neurons are glutamatergic and innervate the TRN where they branch axon collaterals. **B** firing modes of thalamocortical neurons and insets enlarged in C and D. Adapted from McCormick and Bal 1995

thalamocortical activity has to be protected from any perturbation that might lead to pathological conditions of hypersynchronicity, such as during epileptic seizures.

Scope of the thesis

Despite major advances in research, complete understanding of how brain networks work is still an unsolved mystery. In order to decipher the rules governing interactions among neurons and neuronal systems that give rise to behaviors, we need to reveal the basic connectivity and connections starting from synapses.

The cerebello-thalamic connection is historically known for its role in motor behavior, however there is a raising consensus over its involvement in higher functions and even in controlling pathological conditions such as epilepsy. Studying this connection from development to optogenetic control of its activity helped us to characterize better this synapse.

In chapter 2 we focused on the time period during embryonic development when this connection is established to reveal from what point in time cerebellar axons innervate thalamic neurons. In chapter 3 we then explored the difference in the activity of the big glutamatergic CN cells originating from different Zebrin domains in vivo and in vitro in

order to elucidate if there are differences in the transmission mode of information based on the input CN glutamatergic neurons receive. In chapter 4 we questioned whether the cerebellar input from glutamatergic cells of Interposed and Lateral nucleus shows a different impact on thalamic relay cells in Ventrolateral (VL) Ventromedial (VM) and Centrolateral (CL). These findings address the idea that cerebellum do not only influence motor areas (as VL and VM), but also non-motor domains (CL). In chapter 5 we aimed to test the efficacy of CN-TC stimulation in controlling seizures in epileptic mouse models. Finally, in chapter 6 we provide an overview of how cerebellar stimulation in animal models are utilized to investigate therapeutic options for neurological disorders, like epilepsy.

References

1. Herculano-Houzel, S., B. Mota, and R. Lent, *Cellular scaling rules for rodent brains.* Proc Natl Acad Sci U S A, 2006. 103(32): p. 12138-43.
2. Azevedo, F.A., et al., *Equal numbers of neuronal and nonneuronal cells make the human brain an isometrically scaled-up primate brain.* J Comp Neurol, 2009. 513(5): p. 532-41.
3. ER, K. and S. JH, *The cerebellum*, in *Principles of Neural Science, 2nd edition*, Elsevier, Editor.: New York
4. Apps, R. and M. Garwicz, *Anatomical and physiological foundations of cerebellar information processing.* Nat Rev Neurosci, 2005. 6(4): p. 297-311.
5. Voogd, J. and M. Glickstein, *The anatomy of the cerebellum.* Trends Cogn Sci, 1998. 2(9): p. 307-13.
6. Teune, T.M., et al., *Topography of cerebellar nuclear projections to the brain stem in the rat.* Prog Brain Res, 2000. 124: p. 141-72.
7. Sawyer, S.F., et al., *Cerebellar-responsive neurons in the thalamic ventroanterior-ventrolateral complex of rats: in vivo electrophysiology.* Neuroscience, 1994. 63(3): p. 711-24.
8. Uusisaari, M.Y. and T. Knopfel, *Diversity of neuronal elements and circuitry in the cerebellar nuclei.* Cerebellum, 2012. 11(2): p. 420-1.
9. Gao, Z., et al., *Excitatory Cerebellar Nucleocortical Circuit Provides Internal Amplification during Associative Conditioning.* Neuron, 2016. 89(3): p. 645-57.
10. Bagnall, M.W., et al., *Glycinergic projection neurons of the cerebellum.* J Neurosci, 2009. 29(32): p. 10104-10.
11. Ankri, L., et al., *A novel inhibitory nucleo-cortical circuit controls cerebellar Golgi cell activity.* Elife, 2015. 4.
12. Uusisaari, M., K. Obata, and T. Knopfel, *Morphological and electrophysiological properties of GABAergic and non-GABAergic cells in the deep cerebellar nuclei.* J Neurophysiol, 2007. 97(1): p. 901-11.
13. V, C.-P., *Fine Structure of the Large Neurons and Their Processes: Dendritic Thorns and Their Synapses.*, in *Cerebellar Dentate Nucleus: Organization, Cytology and Transmitters.* 1977, Springer Berlin Heidelberg: Berlin, Heidelberg. p. 86-124.
14. Najac, M. and I.M. Raman, *Integration of Purkinje cell inhibition by cerebellar nucleo-olivary neurons.* J Neurosci, 2015. 35(2): p. 544-9.
15. Schneider, E.R., E.F. Civillico, and S.S. Wang, *Calcium-based dendritic excitability and its regulation in the deep cerebellar nuclei.* J Neurophysiol, 2013. 109(9): p. 2282-92.
16. Raman, I.M., A.E. Gustafson, and D. Padgett, *Ionic currents and spontaneous firing in neurons isolated from the cerebellar nuclei.* J Neurosci, 2000. 20(24): p. 9004-16.
17. Shinoda, Y., et al., *The entire trajectory of single climbing and mossy fibers in the cerebellar nuclei and cortex.* Prog Brain Res, 2000. 124: p. 173-86.
18. Anchisi, D., B. Scelfo, and F. Tempia, *Postsynaptic currents in deep cerebellar nuclei.* J Neurophysiol, 2001. 85(1): p. 323-31.
19. Person, A.L. and I.M. Raman, *Purkinje neuron synchrony elicits time-locked spiking in the cerebellar nuclei.* Nature, 2011. 481(7382): p. 502-5.
20. Pugh, J.R. and I.M. Raman, *Potentiation of mossy fiber EPSCs in the cerebellar nuclei by NMDA receptor activation followed by postinhibitory rebound current.* Neuron, 2006. 51(1): p. 113-23.

21. Bengtsson, F., C.F. Ekerot, and H. Jorntell, *In vivo analysis of inhibitory synaptic inputs and rebounds in deep cerebellar nuclear neurons.* PLoS One, 2011. 6(4): p. e18822.
22. Apps, R. and R. Hawkes, *Cerebellar cortical organization: a one-map hypothesis.* Nat Rev Neurosci, 2009. 10(9): p. 670-81.
23. Brochu, G., L. Maler, and R. Hawkes, *Zebrin II: a polypeptide antigen expressed selectively by Purkinje cells reveals compartments in rat and fish cerebellum.* J Comp Neurol, 1990. 291(4): p. 538-52.
24. Voogd, J. and T.J. Ruigrok, *The organization of the corticonuclear and olivocerebellar climbing fiber projections to the rat cerebellar vermis: the congruence of projection zones and the zebrin pattern.* J Neurocytol, 2004. 33(1): p. 5-21.
25. Sugihara, I., *Compartmentalization of the deep cerebellar nuclei based on afferent projections and aldolase C expression.* Cerebellum, 2011. 10(3): p. 449-63.
26. Zhou, H., et al., *Cerebellar modules operate at different frequencies.* Elife, 2014. 3: p. e02536.
27. Steuber, V. and D. Jaeger, *Modeling the generation of output by the cerebellar nuclei.* Neural Netw, 2013. 47: p. 112-9.
28. Jones, E.G., *A new view of specific and nonspecific thalamocortical connections.* Adv Neurol, 1998. 77: p. 49-71; discussion 72-3.
29. Sherman, S.M. and R.W. Guillery, *On the actions that one nerve cell can have on another: distinguishing "drivers" from "modulators".* Proc Natl Acad Sci U S A, 1998. 95(12): p. 7121-6.
30. Guillery, R.W., *Anatomical evidence concerning the role of the thalamus in corticocortical communication: a brief review.* J Anat, 1995. 187 (Pt 3): p. 583-92.
31. Sherman, S.M. and R.W. Guillery, *The role of the thalamus in the flow of information to the cortex.* Philos Trans R Soc Lond B Biol Sci, 2002. 357(1428): p. 1695-708.
32. Reichova, I. and S.M. Sherman, *Somatosensory corticothalamic projections: distinguishing drivers from modulators.* J Neurophysiol, 2004. 92(4): p. 2185-97.
33. Sherman, S.M., *Thalamus plays a central role in ongoing cortical functioning.* Nat Neurosci, 2016. 19(4): p. 533-41.
34. Jahnsen, H. and R. Llinas, *Electrophysiological properties of guinea-pig thalamic neurones: an in vitro study.* J Physiol, 1984. 349: p. 205-26.
35. Llinas, R. and H. Jahnsen, *Electrophysiology of mammalian thalamic neurones in vitro.* Nature, 1982. 297(5865): p. 406-8.
36. Sherman, S.M., *Tonic and burst firing: dual modes of thalamocortical relay.* Trends Neurosci, 2001. 24(2): p. 122-6.
37. Kim, S.Y., E. Pardilla-Delgado, and S.E. Alger, *Enhancing Memory Consolidation through Slow Oscillation and Spindle Synchronization.* J Neurosci, 2017. 37(48): p. 11517-11519.
38. Jacobs, J., *Hippocampal theta oscillations are slower in humans than in rodents: implications for models of spatial navigation and memory.* Philos Trans R Soc Lond B Biol Sci, 2014. 369(1635): p. 20130304.

1

"Facts do not cease to exist because they are ignored"

Aldous Huxley

Chapter 2

Anatomical development of the Cerebellothalamic tract in embryonic mice

Daniël B. Dumas
Simona V. Gornati
Youri Adolfs
Jeroen R. Pasterkamp
Freek E. Hoebeek

In preparation for Journal of Neuroscience

Abstract

The cerebellum, connects to neocortex through thalamus and it has a fundamental role in development and maturation of neocortical circuits. Disruption in the cerebello thalamo cortical loop is associated with neurodevelopmental disorders such as autism. In spite of the implications of both the dorsal thalamus (dTh) and the cerebellum in developmental diseases, only few studies have attempted a description of this connection in prenatal animals. Using the transgenic mouse Ntsr1-Cre/Ai14 we were able to tag with the red fluorescent protein (RFP) a restricted population of cerebellar nuclei cells (CNs) and follow their growth in mouse embryos between E14.5 and E18.5. With confocal and light microscopy, we found that the cerebello-thalamic (CbT) fibers arrive in the ventral thalamus between E14.5 and E15.5 and travels further rostrally invading the dorsal thalamic complex at E17.5. We could observe cerebellar fibers spread with a gradient in many dorsal thalamic nuclei, such as the ventromedial, ventrolateral, parafascicular, mediodordsal and the posterior complex, at E18.5. Axonal varicosities were visible at E18.5, some of which colocalize with vGluT2, a marker for subcortical synaptic contacts, suggesting the existence of active CbT synapses in the prenatal mouse brain. Our results contribute to the generation of a frame of reference on the anatomical development of the CbT, which can help to guide future experiments into the investigation of how this synapse develops and if perturbations of the correct development could lead to the onset of neurodevelopmental disorders.

Introduction

Cerebello-cerebral connectivity is known to be involved in motor activity, but also several non-motor functions are controlled by the long range cerebellar and cerebral projection neurons [1-5]. The most direct route from the cerebellum to the cerebral cortex runs through the thalamic complex and it is this cerebello-thalamic (CbT) tract that has been implicated in a wide range of neurological conditions, like rapid onset dystonia, epilepsy and autism spectrum disorder (ASD) [6-8]. Several of these pathologies have a developmental aspect, and thus put a focus on the ontogeny and maturation of the CbT tract. Imaging data from children with cerebellar lesions, which are at high-risk of developing ASD [9], revealed concomitant cerebral impairments that have been suggested to be mediated by impairments of the CbT. Yet, the time of onset of the CbT abnormalities in ASD and other neurodevelopmental disorders remains unknown. Despite recent feasibility studies that allow clinicians to investigate the developing cerebello-cerebral connectivity in very pre-term born children [10], it even remains to be elucidated from which embryonic or fetal stage cerebellar axons reach the thalamic primordium.

In animal models the development of the cerebello-thalamic connectivity is equally understudied. Although it is well understood that the cerebellar nuclei (CN) neurons are the sole source of CbT tract, there are few studies available on the development of their axonal connections to the thalamic complex. Some sparse reports on a developing CbT tract in the post-natal opossum [11] and a single report in mouse embryo [12] indicate that CN axons reach the thalamic primordium at the late embryonic stages, but any data on the progress of CbT growth and synaptogenesis is currently lacking. Given that early synaptic afferents have recently been shown to modulate thalamic activity patterns, gene expression profiles and the thalamo-cortical connectivity [13-15]; it is of upmost importance to elucidate at what embryonic stage cerebellar axons start to innervate the developing thalamus. Moreover, given that in the adult rodent the cerebello-thalamic tract diverges to many first-order and higher-order nuclei (including ventrolateral (VL), ventromedial (VM), centrolateral (CL), posteriomedial (POm), parafascicular (Pf) and mediodorsal (MD) [16-19] each of which has critical periods for growth and maturation of its afferents and efferents. For instance, the somatosensory ventrobasal nuclei receive brainstem afferents from E17.5 [20] and during the following 2 weeks its efferents start to innervate various neuronal populations in the developing cerebral cortex [21]; during this critical period disruptions will result in permanent disturbance of long-range connections and functional aberrations [22]. In order to study critical periods and the impact of disruptions of the developing cerebello-thalamic connection in early life, a thorough understanding is required of how this connection comes about.

Here we investigated the embryonic development of the CbT tract using transgenic mice in which CbT fibers are tagged with red fluorescent protein (RFP). Using this approach we found that from E15.5 CN axons innervate ventral diencephalon. Our results reveal how from this time point on the CN axons appear to reside in the ventral thalamus and from E16.5 continue to grow into the dorsal thalamus. By E18.5 even the rostrally located VL nucleus is innervated by CN axons and CN axon varicosities are co-labeled markers of active glutamatergic synapses.

Materials & Methods

All experiments were performed in accordance with the European Communities Council Directive. Protocols were reviewed and approved by the Dutch national experimental animal committees (DEC) and every precaution was taken to minimize stress and the number of animals used in each series of experiments.

Mice

To visualize the fibers from the cerebellar nuclei (CN), mice carrying an *Ntsr1-Cre* allele [23] Mutant Mouse Regional Resource Center; Stock Tg(Ntsr1-cre)GN220Gsat/Mmucd) were crossed with an Ai14 reporter line [24] (Jackson laboratories strain 007908) to generate mice expressing RFP in Ntsr1$^+$ cells. The line was genotyped by PCR and only positive mice were used for further studies. To investigate the prenatal development of the CbT fibers, we used Ntsr1-Cre/Ai14 embryos aged from embryonic day (E) 14.5 to E18.5. The morning of the day of vaginal plug detection was counted as E0.5. Before sacrificing the mother, she was deeply anesthetized with isofluorane. In total, we used four E14.5, two E15.5, five E16.5, seven E17.5 and six E18.5 embryos. There were no gross morphological abnormalities present in any of these embryos. We also used three adult mice (P48-75) for characterization of the Ntsr1$^+$ CN neurons.

Tissue preparation for immunohistochemistry

Embryos were collected at E14.5, E15.5, E16.5, E17.5 and E18.5. Those of E14.5 and E15.5 were immediately immersion fixed in 4% PFA; E16.5 and E17.5 were first decapitated before immersion fixation in 4% PFA; and E18.5 brains were immediately dissected in phosphate buffer saline (PBS) over ice before immersion fixation in 4% PFA. All embryo tissue was fixed for 36 hours at 4°C. After fixation, the embryos were cryoprotected in 20% sucrose for at least 3 days at 4°C. After cryoprotection, the embryo tissue was embedded in 22% bovine serum albumin in 7% gelatin solution. The embedded brains were stored at -80°C until sectioning. Sagittal and coronal sections (20 µm) were

produced and glass-mounted on chrome alum-gelatin coated slides using a Microm HM560 cryostat (Walldorf, Germany) and then stored at -20°C until processing for immunohistochemistry.

After anesthetizing the adult mice with 0.15 mL pentobarbital (i.p. injection), they were perfused with 4% paraformaldehyde (PFA).The brains of the adult mice were removed after perfusion and post-fixed on a shaker for 2 hours in 4% PFA at room temperature. After perfusion, the pia mater was removed. Thereafter, the brains were embedded in 12% gelatin/10% sucrose. The gelatin blocks containing the brains were then incubated in 30% sucrose/0.1M PB overnight at 4°C. Thereafter, the brains were cut into 40 µm thick sections using a Leica SM 2000 R sliding microtome (Nussloch, Germany).

Immunohistochemistry

For 3, 3 -diaminobenzidine (DAB) staining, slides with embryonic sections were immersed in 0.3% H_2O_2 in methanol to block endogenous peroxidase activity. After three times of 10 min rinsing with PBS, the cell membranes were permeabilized by immersion in 0.3% Triton in PBS for 60 min. After another three times of 10 min rinsing with PBS, the slides were immersed in a 5% normal horse serum (NHS) in PBS blocking solution for 60 min. Afterwards, the slides were rinsed three times 10 min with PBS and subsequently incubated in primary antibodies in 2% NHS/PBS overnight at 4°C. After three times of 10 min rinsing with PBS, the slides were incubated in secondary antibodies in 2% NHS/PBS for 2 hours at room temperature. After another three times of 10 min rinsing with PBS, the slides were incubated in avidin biotin complex (ABC) solution for 2 hours. The ABC solution was prepared 40 minutes before incubation. The ABC solution consists of 0.7% avidin, 0.7% biotin and 0.5% Triton in PBS. After incubation in ABC solution, the slides were rinsed three times 10 min with PBS and two times 10 min with 0.05M phosphate buffer (PB). After rinsing, slides were incubated for 15 min in DAB solution, which consisted of 0.5% DAB 0.665% DAB in 0.1M PB. The DAB reaction was catalyzed by adding H_2O_2 to the solution (final concentration 0.01%) right before immersion. Afterwards, the slides were rinsed three times 10 min in 0.05M PB. After an additional short rinse in MilliQ, the slides were incubated in thionin for 5 min. Thereafter, the slides were incubated two times 10 min in 96% ethanol, followed by three incubation steps of 2 min in 100% ethanol. Afterwards, the slides were incubated three times 2 min in xylene and subsequently covered with Permount (Fisher Chemical™ SP15-500) and coverslipped.

To stain embryonic sections with immunofluorescence the slides were first rinsed three times 10 min with PBS and subsequently permeabilized by immersion in 0.3% Triton in PBS for1 hour. The slides were then incubated in 1% sodium dodecyl sulfate

in PBS for 5 min to facilitate antigen retrieval. This was followed by times 5 min rinsing with PBS. Thereafter, the slides were immersed in a 5% NHS/PBS blocking solution for 1 hour. Afterwards, the slides were rinsed three times 10 min with PBS and subsequently incubated in primary antibodies in 2% NHS/PBS overnight at 4°C. After three times of 10 min rinsing with PBS, the slides were incubated in secondary antibodies in 2% NHS/PBS for 2 hours at room temperature. After incubation, the slides were rinsed two times 10 min with PBS and 10 min with 0.05M PB. The slides were then incubated in 1:10000 4',6-diamidino-2-fenylindool (DAPI) solution for the visualization of cell nuclei. Afterwards, the slides were rinsed two times 10 min with 0.05M PB and subsequently covered with Mowiol (Sigma Aldrich 4-88) and coverslipped.

For immunofluorescence on adult tissue, the adult brain sections were first rinsed four times 10 min with PBS and subsequently preincubated in 10% NHS/ 0.5% Triton/ PBS for 1 hour. This was followed incubation in primary antibodies in 2% NHS/ 0.4% Triton/ PBS for 48 hours at 4°C. Afterwards, the sections were rinsed four times 10 min with PBS and subsequently incubated in secondary antibodies in 2% NHS/ 0.4% Triton/ PBS. The sections were then rinsed two times 10 min with PBS and 5 min with 0.1M PB. After rinsing, the sections were incubated in 1:10000 DAPI solution for 10 min. The sections were then rinsed two times 5 min with 0.1M PB, after which they were immersed in 5% gelatin/ 1% chrome alum/ MilliQ. Afterwards, the sections were glass-mounted and coverslipped using Mowiol. Except for the incubation in primary antibody solution, all the steps were performed at room temperature.

3DISCO

For this procedure, embryos were collected at E15.5, E16.5, E17.5 and E18.5. The brains of E16.5-18.5 embryos were immediately dissected in phosphate buffer saline (PBS) over ice before immersion fixation in 4% PFA. Younger animals were decapitated and their heads were immediately immersion fixated in 4% PFA. The brains were fixed for 24 hours at 4°C. The brains were then incubated in 0.2% gelatin/ 0.5% Triton/ PBS (PBSGT) for 24 hours on a shaker (~70 rounds per min (rpm)) at room temperature. The PBSGT was filtered with a 0.2 µm filter before use. After incubation in PBSGT, the brains were incubated in a 0.2 µm filtered primary antibody solution in 0.1% saponin (Sigma Aldrich S-7900)/PBSGT at 37°C on a shaker (~100 rpm) for 1 week. Afterwards, the brains were rinsed six times for 60 min with PBSGT and subsequently incubated overnight in a 0.2 µm filtered secondary antibody solution in 0.1% saponin/PBSGT at 37°C on a shaker (~100 rpm). Afterwards, the brains were rinsed six times for 1 hour with PBSGT. Then the brains were incubated in 50% tetrahydrofuran (THF) (Sigma Aldrich 186562-1L) in H_2O overnight to start dehydration. Thereafter, the brains were incubated for 60 min in 80% THF/H_2O, then for two times for 1 hour in 100% THF. The brains were then incubated

in dichloromethane (Sigma Aldrich 270997-1L) for 20 min for clearing the brains, after which they were incubated and stored in dibenzylether (Sigma Aldrich 108014-1KG) at room temperature. From the first THF incubation step onwards, care was taken to have the least amount of air possible in the vials containing the brains.

Antibodies

An overview of the antibodies used is presented in Tables 1 and 2. For DAB staining, we used a primary rabbit anti-RFP antibody (1:000, *Rockland*) and a secondary donkey anti-rabbit antibody (1:200, *Jackson*). For immunofluorescence, we used chicken anti-Calbindin (1:500, *Synaptic Systems*), goat anti-FoxP2 (1:500, *Santa Cruz*), guinea pig anti-vGluT2 (1:500, *MilliPore*), rabbit anti-RFP (1:000, *Rockland*), and mouse anti-NeuN (1:1000, *MilliPore*) as primary antibodies. Cy5 anti-chicken (1:200, *Jackson*), Alexa488 anti-goat (1:200, *Jackson*), Cy5 anti-guinea pig (1:200, *Jackson*), Cy3 anti-rabbit (1:400, *Jackson*), and Alexa488 anti-Mouse (1:200, *Jackson*) antibodies were used as secondary antibodies.

For 3DISCO, we used chicken anti-Calbindin (1:500, *Synaptic Systems*), goat anti-FoxP2 (1:500, *Santa Cruz*) and rabbit anti-RFP (1:000, *Rockland*) as primary antibodies. Cy5 anti-chicken (1:200, *Jackson*), Alexa488 anti-goat (1:200, *Jackson*) and Cy3 anti-rabbit (1:400, *Jackson*) antibodies were used as secondary antibodies.

Imaging

An overview of the microscopes used is presented in Table 3. Light microscopy pictures of DAB stained slides were made using a Nanozoomer 2.0-HT (Hamamatsu, Japan) with 40X magnification. The pixel size was 230 nm x 460 nm. Confocal microscopy pictures were taken with a Zeiss LSM700 Meta (Carl Zeiss Microscopy, LLC, USA) and an Opera Phenix™ HCS system (Perkin Elmer, Hamburg, Germany). Confocal pictures on the Zeiss LSM700 Meta were taken with a 63X oil Plan-Apochromat lens with an NA of 1.4. Z-stacks were taken with a voxel size of 50 nm x 50 nm x 150 nm, a pinhole of 1 Airy unit and bit depth of 8-bits. Signal-to-noise ratio was improved by 4X line averaging. For the different fluorophores, the following lasers were used: 405 nm for DAPI, 488 nm for Alexa488, 543 nm for Cy3 and 633 nm for Cy5. The confocal pictures on the Opera Phenix™ HCS system were taken with a 20X lens with an NA of 0.4. The pixel size was 598 nm x 598 nm. The bit depth was 16-bits. For the different fluorophores, the following lasers were used: 488 nm for Alexa488, 561 nm for Cy3 and 640 nm for Cy5. Z-stacks consisting of two 10 µm spaced slices were taken to correct for shifts in the z-axis. Before further analysis, a maximum intensity projection of the images was produced, which was subsequently converted to 8-bits.

The 3DISCO cleared brains were imaged with the LaVision biotec light sheet microscope Ultramicroscope II (LaVision biotec, Bielefeld, Germany). Overview pictures

were taken with a 1.6X zoom, detailed pictures were taken with a 6.3X zoom. The lens had an NA of 0.5 and the bit depth was 16-bits. Overview pictures had a voxel size of 2030 nm x 2030 nm x 2500 nm and detailed pictures had a voxel size of 515.9 nm x 515.9 nm x 2500 nm. We solely used a 561 nm laser to image Cy3.

Delineation and intensity measurements

Any images containing structural artefacts were discarded. The delineation of anatomical regions and measurements were performed with FIJI software (version 1.51). To delineate the thalamic nuclei across the different ages studied, we used the chemoarchitectonic atlas of the developing mouse brain (Jacobowitz and Abbott, 1998), the atlas of the prenatal mouse brain (Schambra et al., 1992), the atlas of the developing mouse brain (Paxinos, 2007), the Allen brain atlas (Thompson et al., 2014) and descriptive studies of FoxP2 expression in developing mice [25-28]. With FoxP2, we could delineate the parafascicular nucleus (Pf), the mediodorsal nucleus (MD), the ventrobasal complex (VB), the posterior complex (Po), the ventromedial nucleus (VM) and parts of the midline nuclei (ML). Our definition of ML includes the centromedial, paraventricular, intermediodorsal, reunions, retroreuniens, intermediodorsal, rhomboid, xyphoid, retroxyphoid, interanteromedial, anteromedial and posteromedian nuclei of the thalamus. When combining FoxP2 with calbindin staining, we could delineate the VM and the ML more specifically than with FoxP2 alone [29]. In addition to these markers, we also used the atlases described in the materials and methods section. The border between the ventrolateral nucleus of the thalamus (VL) and the intralaminar nuclei could not consistently be accurately delineated in all slices. Therefore, the size of the nucleus might be slightly underestimated in some instances. Moreover, at E16.5, the border between the VL and the LP could not be delineated. We therefore did not measure the VL at this age. The delineation of thalamic nuclei was performed in the fluorescent channels representing the FoxP2 and calbindin expression, so that the researcher was blinded for the location of RFP signal, which represents the location of Ntsr1Cre-Ai14-positive axons. For further measurements, nuclei were delineated with the ROI manager in FIJI. If a nucleus could not be delineated in two or more sequential sections, this particular nucleus was not quantified.

To measure the amount of Cy3 signal in each nucleus, the mean plus two times the standard deviation of the histogram was used as threshold to binarize the image into background and foreground. To measure the area of detected objects within each nucleus ($A_{detected}$) we used the "analyze particle function".

Colocalization

Colocalization of vGluT2 and RFP signals were determined using FIJI in the 63X images

of the different thalamic nuclei. Confocal z-stacks were taken and after applying user defined thresholds in the separate channels of the raw image, sites of putative localization were subjectively identified by the appearance of structures showing the presence of both colors and then deconvolved using Huygens (Scientific Volume Imaging). After deconvolution, a user defined threshold was applied to confirm the colocalization, which was defined as a complete overlap of vGluT2 and RFP structures. vGluT2 positive terminals' volume in VL and VM was measured using a custom-written Fiji macro (see also[16]).

Statistical Analysis

The fluorescence of a whole thalamic nucleus was calculated for each mouse by summing the $A_{detected}$ and the $A_{delineated}$ of all the sections containing the nucleus in question, yielding the $\sum A_{detected}$ and $\sum A_{delineated}$, respectively, per nucleus per hemipshere. Dividing $\sum A_{detected}$ by $\sum A_{delineated}$ gives the sum of the relative area occupied by RFP^+ fibers, expressed by the percentage of Summed Area Occupied (pSAO). For each mouse, data from both hemispheres were averaged. Thereafter, the average pSAO per nucleus was calculated for E16.5, E17.5 and E18.5. For each nucleus, significant differences between the ages were first tested with a Kruskal-Wallis (K-W) test (degrees of freedom = 2). When a significant difference was found, Dunn's post-hoc test was used to compare pairwise between the age groups. For the latter test, a Šidák corrected *p*-value of 0.017 was used as threshold for significance. To compare the data of nuclei gathered from two ages we used a Mann Whitney U test. In this case, a Šidák corrected *p*-value of 0.0253 was used as threshold for significance.

The relative amount of RFP^+ fibers per section was calculated by dividing the $A_{detected}$ by the $A_{delineated}$. These values were then plotted against the relative caudal-to-rostral distance. This distance was calculated as a linear scale from 0 to 100, with 0 indicating the most caudal section in which a particular nucleus was delineated and 100 indicating the most rostral section in which that nucleus was delineated. To determine whether there was caudal-to-rostral gradient of the relative amount of RFP^+ fibers, a Spearman's rank correlation coefficient 'rho' was calculated per nucleus per age. To measure differences in correlation between groups, the Fisher's Z-transformation was used, after which a Z-test was conducted for pairwise comparison. Since the same dataset was used for whole nucleus analysis, a Šidák corrected p-value of 0.0253 was used as threshold for significance. Šidák corrected p-values are calculated using $\alpha per\ comparison = 1 - (1-\alpha)1/k$, where α is the overall significance level, which was chosen to be 0.05, and k was chosen as the amount of times a same dataset was analyzed, or the amount of comparisons in the case of the Dunn's post-hoc test. Data are represented as mean ± SD.

Results

Characterization of the Ntsr1-Cre/Ai14 mouse line:

To study the embryonic development of the CbT, we crossed the Ntsr1-Cre and Ai14 mouse lines. The offspring is characterized by RFP$^+$ expression in previously characterized large diameter CN neurons (Fig. 1A-D) (see also [30]). To assess the distribution of Cre expression in the cerebellum we measured the proportion of RFP$^+$ CN cells and the number of NeuN$^+$ cells in the CN, (Table 4, Fig. 1E). Since there are non-CN neurons migrating through the cerebellum during embryonic stages [31] we quantified the RFP$^+$ CN population in adult mice. The quantification revealed that ~1/3 of CN neurons are RFP$^+$ (Fig. 1E).

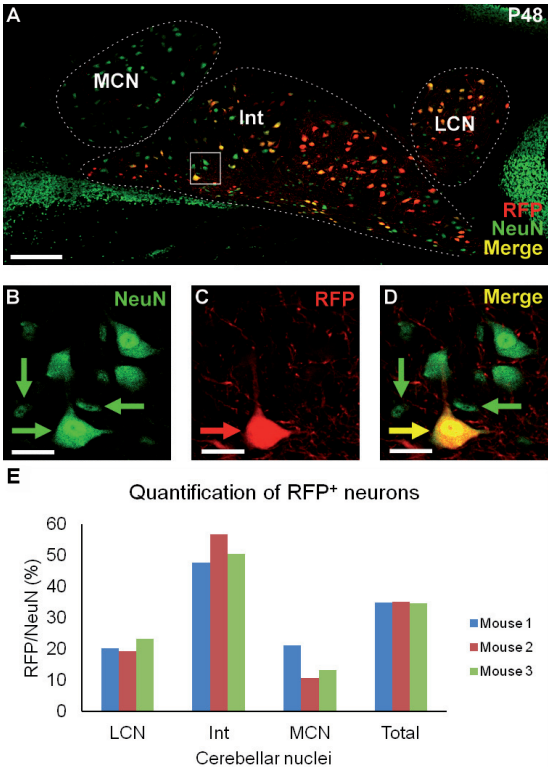

Figure 1. Example of NeuN and RFP staining in adult CN. A) 20x tilescan of a coronal P48 cerebellar slice, zoomed in on the left CN. Stainings: red fluorescent protein (RFP) in red, NeuN in green, yellow indicating colocalization of these two stainings. **B-D)** Zoom in of boxed region in A. **B)** NeuN stained cells. **C)** RFP stained cells and fibers. **D)** Merge of B and C. Note that the RFP$^+$ somata are relatively big compared to the RFP$^-$ somata. **E)** A barplot representation of the quantification of RFP$^+$ cells as a proportion of NeuN$^+$ cells (see also Table 4). Scale bars: A = 150 µm, C-D = 5 µm.

Most of these RFP$^+$ neurons reside in the interposed nucleus (Fig. 1E). We found that RFP$^+$ somata appeared larger than RFP$^-$ somata. In contrast to the CN, no RFP$^+$-neurons were found in the nearby vestibular nuclei or in the cerebellar cortex.

During embryonic development, RFP$^+$ neurons are also found outside of the CN (Fig. 2A,B). Following an immunohistochemical amplification of the RFP signal, we found that at E18.5 also layer VI pyramidal neurons are RFP$^+$ (Fig. 2A,C), which has previously been acknowledged in adult *Ntsr1-Cre* mice [23, 32]. Some sparse RFP$^+$ neurons were also found throughout the posterior and lateral hypothalamus, hippocampus, lateral

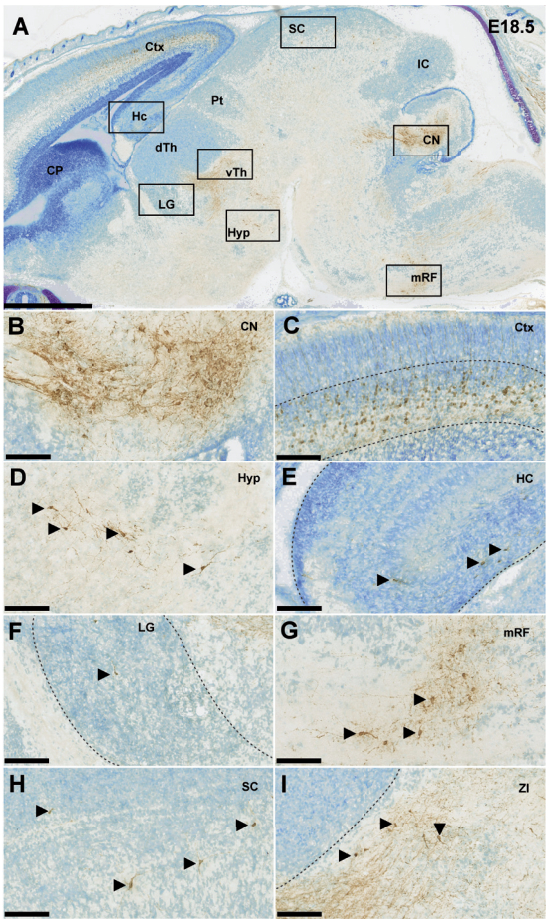

Figure 2. Distribution of Ntsr1$^+$ cells in an E18.5 embryonic mouse brain. A) Sagittal section showing all the regions in which Ntsr1$^+$ is expressed. **(B-I)** 20x zoom in pictures of CN, Ctx, Hyp, Hc, LG, mRF, SC, and ZI, respectively. Note the abundance of Ntsr1+ cells in CN and Ctx. Scale bars: A = 1000 µm, others = 100 µm.

geniculate nucleus, medial reticular formation, superior colliculus and zona incerta (ZI) (Fig. 2D-I). Apart from the cortical layer VI neurons, which project throughout the dorsal thalamic complex from E17.5 onwards [33], these other nuclei do not provide dense input to the thalamic nuclei that receive dense CN input in the adult brain (see discussion).

We found that at E18.5 RFP$^+$ axons from cortical layer VI had descended through the internal capsule and reached the VB nucleus, but remained lateral of VM (Fig. 3). The RFP$^+$ CN axons populate the more medially located bundle that progresses from the mesencephalic and subthalamic regions into VM. Thus although the Ntsr1Cre-Ai14 mutants do not provide exclusive RFP-expression in CN neurons, we were able to study the embryonic development of CN axons in the mouse brain.

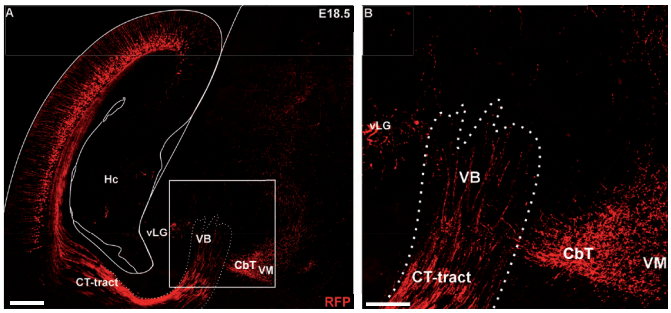

Figure 3. RFP$^+$ cortical fibers entering the dorsal thalamus, specifically the ventrobasal thalamic nucleus, at E18.5. A) Zoomed out confocal tile scan showing the RFP$^+$ corticothalamic fibers and another, separate, RFP$^+$ fiber bundle, presumably originating from the CN. **B)** Zoom in of inset in A. Scale bars: A = 250 µm, B = 100 µm.

RFP$^+$ axons of the CbT reside in ventral thalamus until E16.5

After characterizing the origin of RFP$^+$ axons in the embryonic thalamus, we next sought to determine at what age the RFP$^+$ axons that putatively originate from CN neurons arrive at the thalamic primordium. Using a combination of light-sheet imaging of 3DISCO-treated brains, confocal and light-microscopy we visualized the CbT tract at 15.5 and E16.5 (Fig. 4). We found that rostral of the decussation the CbT is located medially and follows the mesencephalic curvature dorsally (Fig. 4C,D,G,H). At these ages the CbT RFP$^+$ axons progress beyond the red nucleus (see also Hara et al., 2016) and reside in the ventral thalamus at E15.5 and E16.5; the adjacent dorsal thalamus remains devoid of CbT axons.

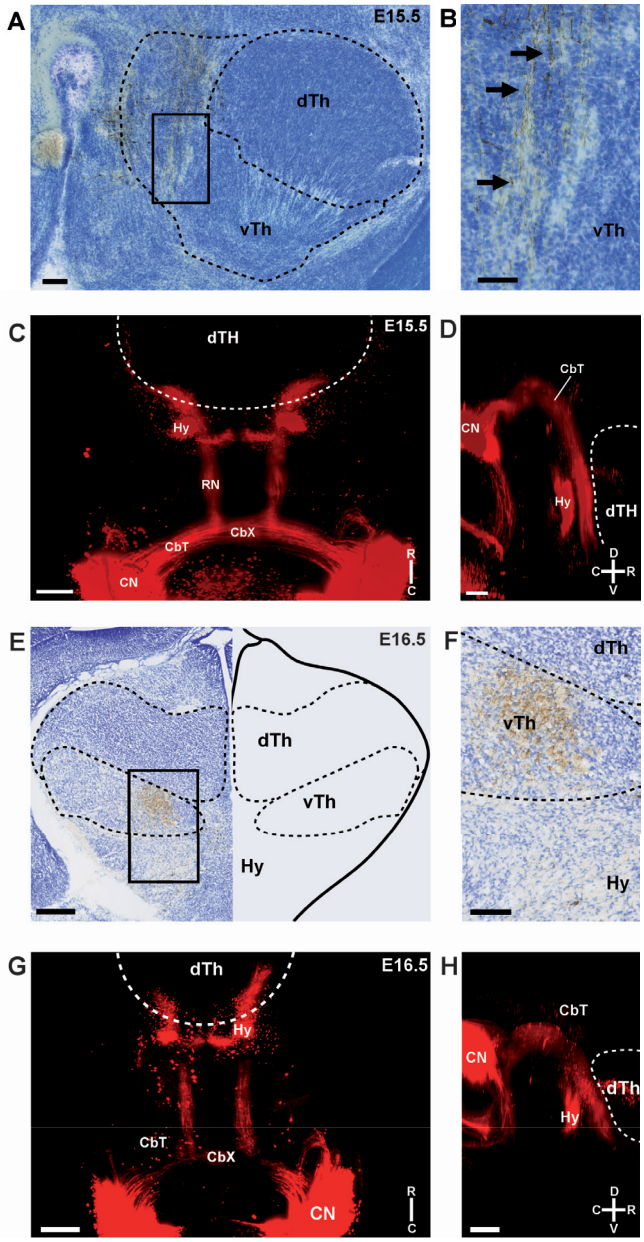

Figure 4. RFP⁺ fibers in the thalamic complex at E15.5 and E16.5. A-D) E15.5 RFP⁺ fibers innervate the ventral thalamus (vTh), but not the dorsal thalamus (dTh). A,B Nissl stained sagittal section; C,D Horizontal view of a maximum intensity projection of a 3DISCO cleared mouse brain. B and D are enlarged from boxed areas in A and C, respectively. **E-H)** similar to A-D for E16.5. Scale bars: A = 250 µm, B = 50 µm, C = 100 µm, D = 50 µm.

CbT RFP$^+$ axons progressively innervate specific nuclei in dorsal thalamus from E17.5

From E17.5 the CbT commences to innervate the dorsal thalamic nuclei (Fig. 5A-E). To establish which nuclei are invaded by RFP$^+$ axons we combined immunofluorescence staining for FoxP2 and calbindin-d28K with RFP-stainings to identify the neuronal populations that form the separate nuclei (Fig. 5F). We found from E17.5 that the bundle of RFP$^+$ axons extended from the ventral thalamus into the nearby VM nucleus and diverged into other nuclei.

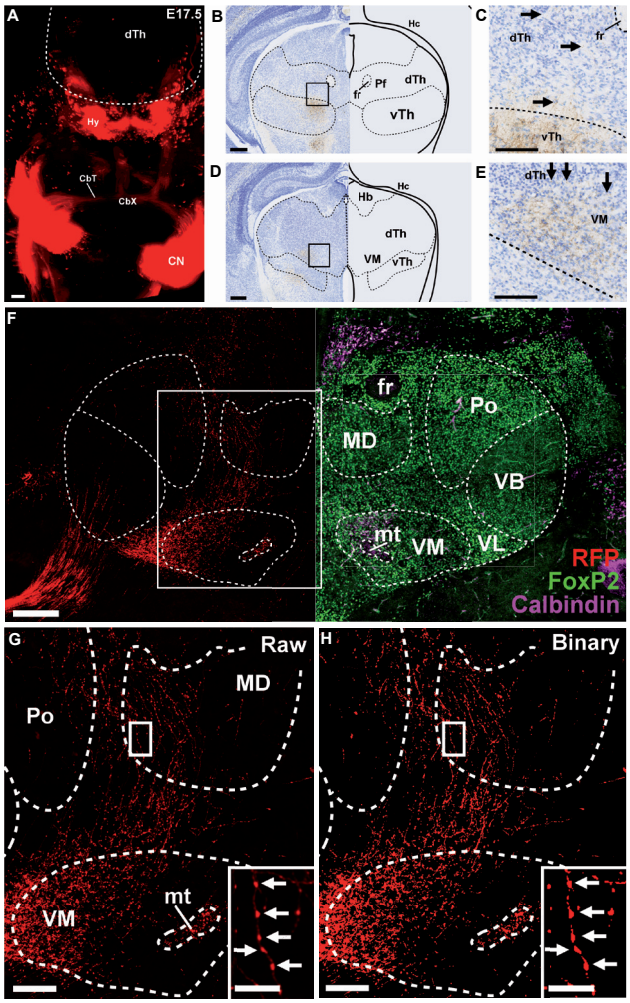

Figure 5. Innervation of the dorsal thalamic complex from E17.5. A) Horizontal view of a maximum intensity projection of a 3DISCO cleared E17.5 mouse brain. **B-E)** Coronal section of an

E17.5 mouse brain at two rostro-caudal planes in which DAB-stained RFP+ fibers diverge in dTh. (B,D) and their magnified insets (C,E). Note that RFP+ fibers in dorsal thalamus (dTh) appear less dense than in the medial vTh. **F)** Expression of FoxP2 (green) and Calbindin (purple) in E18.5 mouse brain with delineated nuclei adapted from Schambra (1992). **G, H)** Magnification of boxed region in F, showing raw (G) and binarized (H) versions of RFP-signal in different nuclei. Arrows in insets indicate putative boutons. Scale bar: A = 250 µm B,D = 500 µm, C,E = 100 µm, F = 200 µm, G,H = 100 µm and insets G,H = 25 µm.

To assess the innervation of the individual nuclei by RFP$^+$ axons, we selected all sections available for all the identified nuclei and summed for each nucleus the percentage of the area that was RFP$^+$ (Fig. 6A) (see methods section). This analysis of fluorescence revealed that at E17.5 VM, VL and Pf, i.e., nuclei which receive dense CN innervation in the adult brain, at least 1% of the section's surface was RFP$^+$ (Fig. 6A,C,E; see Table 5 for all nuclei). In E18.5 tissue the surface of RFP-signal further increased: in VM we found 14.7 ± 2,05% of the section's surface to be RFP$^+$; in VL and Pf 9.6 ± 2,95% and 3.3 ± 1,55%, respectively (Fig. 6B,D,F). Also beyond the VM, VL and Pf nuclei we found that in the last days of embryonic development the RFP$^+$ signal increased. In the MD, POm, VB and ML nuclei the RFP+ section's surface tended to increase, but remained fairly limited in that at E18.5, MD (1.45 ± 0,48%), POm (0.89 ± 0,54%), VB (0,92 ± 0,52%) and ML (0,34 ± 0,14%) all remained well below the RFP fluorescence levels found in VM, VL and Pf nuclei (see also Table 5).

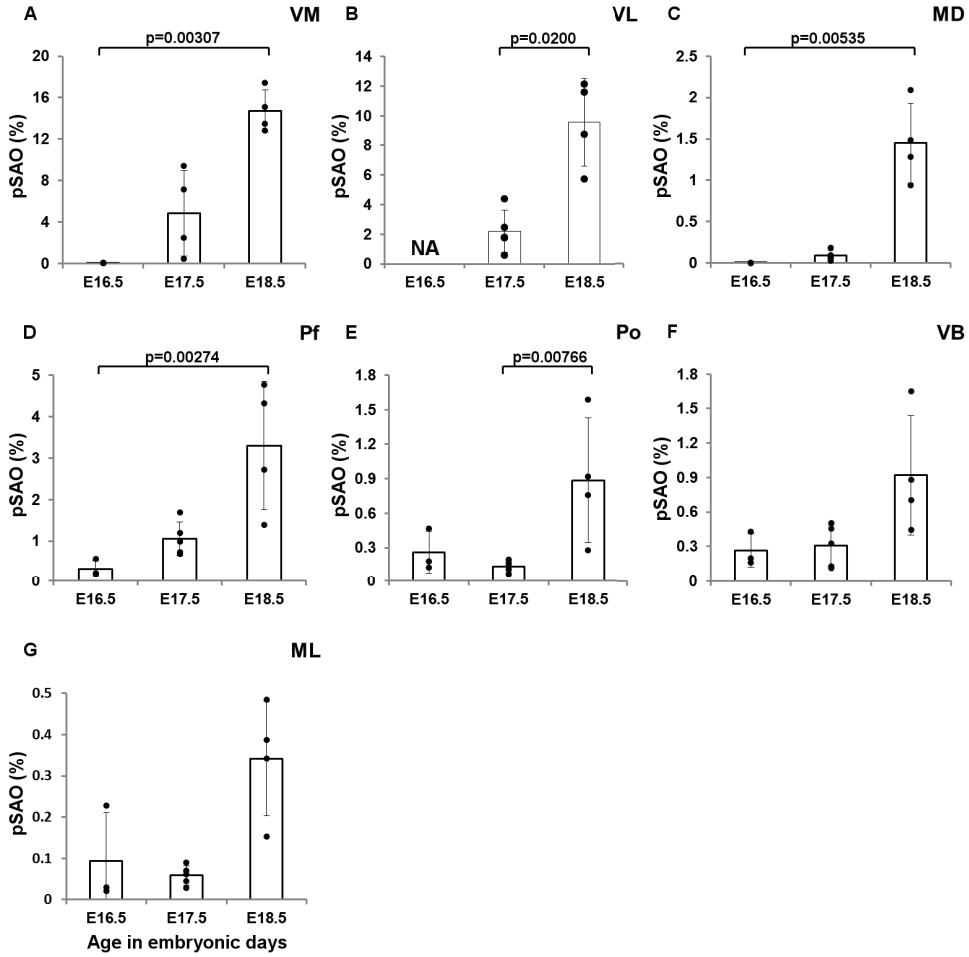

Figure 6. RFP signal quantification in the thalamic nuclei. Percentage of summed area occupied by above-threshold RFP-signal (pSAO) in **A)** VM (E16.5, n=3, E17.5, n=4, E18.5, n=4), **B)** VL (E16.5, n=0, E17.5, n=4, E18.5, n=4) **C)** MD (E16.5, n=2, E17.5, n=5, E18.5, n=4), **D)** Pf (E16.5, n=3, E17.5, n=5, E18.5, n=4), **E)** Po (E16.5, n=3, E17.5, n=5, E18.5, n=4) **F)** VB (E16.5, n=3, E17.5, n=5, E18.5, n=4), **G)** ML (E16.5, n=3, E17.5, n=5, E18.5, n=4).

To describe the development of the CbT in more detail, we focused on the VM, VL and Pf nuclei and analysed the caudal-to-rostral gradient of the relative amount of RFP^+ fibers (Fig. 7). We calculated the Spearman's correlation value rho (r) for E17.5 and E18.5 tissue pooled from various embryos (see methods) and found that in all these nuclei the fluorescence was relatively higher in the most caudal sections. In the VM at E17.5 there was a negative correlation between the level of rostrallity and the relative amount of RFP^+ fibers ($r=-0.550$, $df=48$, $p=3.57*10^{-5}$) (Fig. 7A). At E18.5, all embryos

showed a negative correlation value (pooled r=-0.790, df=57, p=1.06*10^{-13}) (Fig. 7B). The correlation was significantly stronger at E18.5 as compared to E17.5 (-0.790 vs. -0.550, Z=-2.29, p=0.0226; for E18.5 vs. E17.5, respectively). In the VL at E17.5, there was a negative correlation between the level of rostrallity and the relative amount of RFP^+ fibers (r=-0.711, df=44, p=3.11*10^{-8}) (Fig. 7C). At E18.5 this correlation (r=-0.591, df=50, p=4.06^{-6}) (Fig. 7D) did not differ significantly from that of the E17.5 animals (Z=1.01, p=0.844). In the Pf at E17.5, there was a negative correlation between the level of rostrallity and the relative amount of RFP^+ fibers (r=-0.658, df=39, p=2.99*10^{-6}) (Fig. 7E). At E18.5 we did not observe a significant correlation between the level of rostrallity and the relative amount of RFP^+ fibers (pooled r=-0.265, df=39, p=0.0946) (Fig. 7F). At E17.5, the correlation was significantly stronger than at E18.5 (Z=-2.26, p=0.0244).

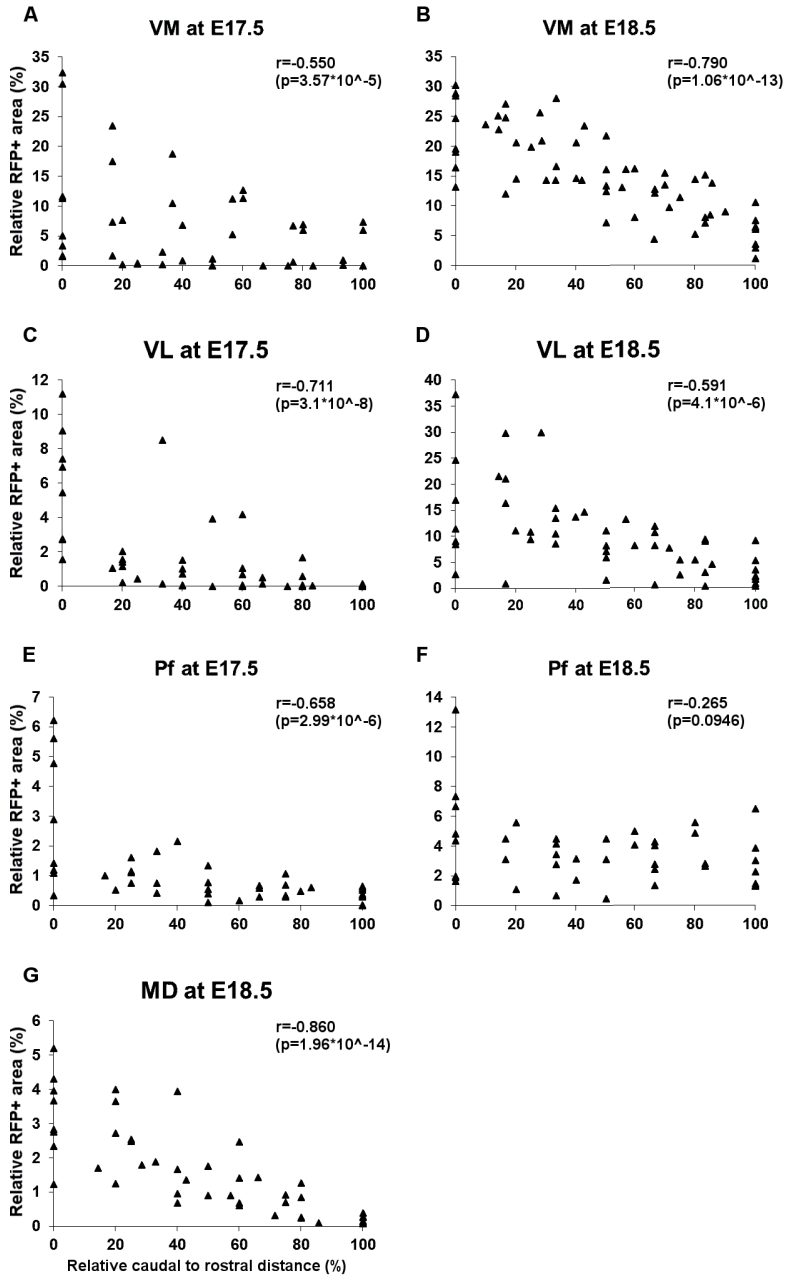

Figure 7. RFP signal quantification from caudal to rostral in the thalamic nuclei. The surface of the section that is RFP$^+$ positive (in %) against the relative rostral to caudal distance (in %) in VL, VM, and Pf. **A)** VL at E17.5 (n=46); **B)** VL at E18.5 (n=52); **C)** VM at E17.5 (n=48) **D)** VM at E18.5 (n=57) **E)** Pf at E17.5 (n=39) **F)** Pf at E18.5 (n=39). r = Spearman's rho.

Boutons and synapses

So far we identified the location of RFP$^+$ axons and the growth of the CbT in the dorsal thalamic complex. We next evaluated whether RFP$^+$ axons formed synaptic contacts using confocal microscopy and FoxP2-stained tissue (Fig. 8A,B). Whereas at our DAB and immunofluorescent staining of E17.5 tissue did not provide any hint for RFP$^+$ bouton-like varicosities in thalamus (data not shown), at E18.5 found that throughout the thalamic complex RFP$^+$ axons to show morphological characteristics of pre-synaptic terminal formation (Fig. 8C-N). In adult brain the cerebellothalamic projection has been shown to be glutamatergic [34] and positive to vGluT2 staining [35, 36]. Note that cortical layer VI projections, i.e., the other main source of RFP$^+$ axons (see Figure 2) are vGluT1-positive [35, 37]. We acquired stacks of high-magnification confocal images of VM, VL and Pf, which allowed us to confirm the colocalization of vGluT2 and RFP putative axon terminals in VM (Fig. 8C-F), the VL (Fig. 8G-J) and the Pf (Fig. 8K-N). We then assessed the morphological characteristics of the identified vGluT2-positive varicosities in VL and VM nuclei; the number of terminals did not vary significantly between the two nuclei (in VL: 5, VM 4), however in VL the boutons volume showed a tendency towards bigger size (VL: 5.79±2.18 μm^3, VM: 1.07±0.31 μm^3) although the difference was not significantly relevant ($p=0.11$, Mann Whitney test).

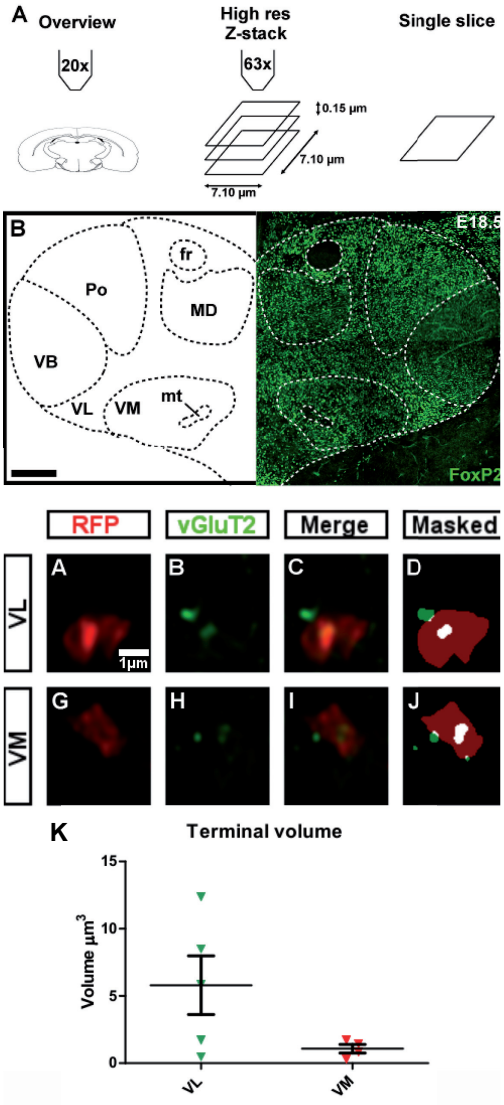

Figure 8. Putative boutons and colocalization with vGluT2. A) Schematic overview of the workflow. After acquiring an overview image at 20x, we zoomed in on the region of interest and acquired a z-stack with voxel dimensions of 50 nm * 50 nm * 150 nm. After deconvolution, a threshold was applied to the different channels and areas of overlap were determined. An RFP^+ bouton or terminal was considered to be colocalizing with vGluT2 only if this vGluT2 region was overlapping a 100% in x, y and z dimensions. For the examples shown in C-R, a single slice was taken from the z-stack. **B)** Overview image taken with a 20x objective before switching to higher magnification. **C-F)** Example of a deconvolved image showing a putative CbT bouton in VL, with RFP in red (C), vGluT2 in green (D), and the result after thresholding (F). **G-J)** same for VM, K-N) same for Pf. Scale bars: B = 200 µm, C-R = 1 µm).

Discussion

We describe the final stages of the outgrowth of CN axons into the thalamic complex. Our data reveal that at E15.5 and E16.5 the CbT is found in the part of the ventral thalamus that in postnatal life will form the ZI. From E17.5 onwards we found CN axons throughout the developing dorsal thalamus. Notably, several of the thalamic nuclei that in the adult life receive the most dense CN axon projections, like VM, VL and Pf, were already invaded by RFP^+ axons. In these nuclei we found that RFP^+ axon varicosities colocalized with vGluT2, a marker for glutamatergic inputs from subcortical sources [16].

Technical considerations

Using the Ntsr1Cre-AI14 brains for our current study allowed us to investigate the development of CbT axonal projections, but also resulted in the endogenous staining of other cell populations, some of which are known to innervate the thalamic complex. Apart from the obvious CN labelling (see also[30]), RFP^+ neurons and axons were also readily identified in the deeper layers of the cerebral cortex, where $Ntsr1^+$ are known to label a subpopulation of L6 pyramidal cells [23, 32]. As we have shown in our analysis the corticothalamic tract, which contains the L6 fibers, and the CbT tract are positioned differently in the embryonic mouse brain (Fig. 3). Also the time of thalamic invasion by the corticothalamic and CbT fibers is different: our data reveals that already from E17.5 RFP^+ fibers start invading the thalamic complex, which precedes the innervation of thalamic nuclei by corticothalamic fibers, which has been shown by detailed analyses to occur from E18.5 (as reviewed by [38]). Finally, also the nuclei that are innervated appear to differ between the corticothalamic and CbT tracts, in that the corticothalamic fibers initially innervate the ventrobasal nuclei and appear to diverge from their onwards [33], whereas the CbT shows arrives in the ventromedial and ventrolateral nuclei. These lines of evidence indicate that we can reliably isolate the RFP-labelling in cortical L6 neurons.

We also found sparse labelling in several other brain regions, which clearly has implications for the interpretability of our data on thalamic innervation in the embryonic stages. Of these regions (see Figure 2) we found that mRF cells that project to the thalamus are located more dorsally than where we observed $Ntsr1^+$ cells [39]. Moreover, we found that the few $Nstr1^+$ cells in ZI at E18.5 were undetectable in adult mouse tissue (data not shown). For the hypothalamic $Ntsr1^+$ cells it may be that these have already connected to the thalamic nuclei, of which the Pf is one of the prime targets in the adult mouse brain [40, 41]. Finally, to our knowledge CN neurons are the predominant source of vGluT2-positive terminals in the $Ntsr1^+$ population of cells, in that ZI regions that primarily target the dorsal thalamic complex, i.e., dorsal and ventral ZI, are practically void of vGluT2-expressing cells ([42]; [43]), although a subpopulation of hypothalamic

and superior colliculus neurons also express vGluT2 [35] in the adult stages. Our data set lacks dedicated retro- and anterograde tracing experiments that allow a detailed quantification of the CN fibers to the embryonic thalamic complex, but based upon previous work in adult rodent brain we advocate that the bulk of RFP^+ fibers in the VL and VM in our current dataset are most likely originating from $Ntsr1^+$ CN neurons [16].

Development of the CbT in mouse embryos

In the present study, we investigated the anatomical development of the CbT in mouse embryos aged E15.5 to E18.5 and found that prior to the entry of the dorsal thalamus, the CbT tract appears to stall its growth and reside in the ventral thalamus between E15.5 and E16.5. This apparent waiting period of ~48 hours might be compared to the second waiting period of the corticothalamic (CT) pathway in the reticular nucleus [33]. In our knowledge, a similar waiting period has not been described for other subcortical thalamic afferents in the rodent brain [20]. We speculate that the CbT waiting period could possibly be related to axonal energy supplies for branching within the ventral thalamus, or in mesencephalic targets of the CbT, such as the red nucleus, which are innervated prior to the thalamic complex[12]. Another likely option is that CbT axonal growth is stalled due to chemical signaling. These nuclei could possibly send out chemical signals that prevent CbT fibers to enter the dorsal thalamus, like the Sema3E/PlexinD1 signaling responsible for one of the CT waiting period in the reticular nucleus [44]. A function of this waiting period might be that CN fibers, which originate from CN neurons that are sequentially born [31], arrest their growth and reorganize in the ventral thalamus before entering the dorsal complex – a mechanism again described for the corticothalamic tract as well [38].

Upon entry in the dorsal thalamus, CbT fibers appeared to swiftly locate the VM and VL nuclei, which are also in the adult mouse brain their prime target nuclei [16, 17]. We found that the most caudal portions of VM and VL nuclei were more RFP^+ labelled than the rostral portions, indicating that the afferents arise from caudal, which matches with the position of the CbT tract. The fact that the caudal-rostral gradient disappeared in Pf could suggest that also fibers that arrive in a different orientation start to innervate this nucleus, like the corticothalamic or hypothalamic-thalamic fibers [33, 41]. Further investigations of the various thalamic afferents shall reveal more insights in how their growth is organized.

In this study, the development of the CbT tract was described as a whole, as if the axons arise from a single cerebellar nucleus. The current approach did not allow a detailed analysis of the individual axons and thereby we were not able to dissociate between axons from the lateral, interposed or medial nuclei. Since in the adult rodent brain the innervation of CbT fibers originating from the separate CN differs extensively

(e.g.[17]), and the fact that CN neurons are born sequentially under control of various transcription factors ([45]; [31]), it is likely that the CbT ontogeny can be differentiated. Future experiments, which potentially utilize co-cultures of CN and thalamic neurons, analogous to studies performed on cocultures of thalamus and cerebral cortex [46-48], may provide more insights in how the various the connectivity of the individual CN with their thalamic targets comes about.

Timing of thalamic innervation by CbT and functional relevance

The invasion of CbT fibers into the dTh starts from E17.5 and most likely continues well into the postnatal period. This is relatively late when compared to other subcortical thalamic afferents. Both primary sensory afferents and serotonergic afferents start invading the dTh at earlier time points. The retinogeniculate pathway is present in the LG as early as E15.5 in mouse [14] and the trigeminothalamic pathway starts to invade the dTh between E14 and E17 in mouse [20]. Serotonergic afferents enter the thalamus at approximately E16 in rat [49]. As has been proposed before the ascending fibers of the brainstem may provide a passage for the CbT fibers through the mesencephalon [11], but whether there is active interaction between these thalamic afferents remains to be elucidated.

Although for several of the afferent systems it is quite evident what the role is of forming a connection during late embryonic stages, this remains speculative for the CbT tract, not in the least because the cerebellar cortex is developing relatively late and its impact on the CN neurons is rudimentary at best in the antenatal period. One option is that the CbT fibers are present in the thalamic complex to interact with thalamic neurons and guide their axonal growth. The invasion of thalamocortical (TC) fibers into the cortical plate starts from E18.5-P0.5, but already before that the activity levels of thalamic neurons are thought to direct the axonal growth speed [14, 47, 48]. Thus, since the CbT tract seems to have established connections with the thalamus starting at E18.5, there is ample time for the cerebellar output to affect thalamo-cortical development.

Both the thalamocortical system and the cerebellum have been implicated to undergo critical periods [9, 20], disruptions of which are suggested to contribute to a whole range of neurodevelopmental disorders and psychiatric diseases, like autism spectrum disorder and schizophrenia [9, 50]. These neurological conditions are thought to be related to malformations in the neuronal wiring caused by early life events [51, 52] and our current study indicates that in the murine brain cerebellar aberrations can derail thalamocortical wiring from E17.5 onwards, which translates to early fetal stages in human development.

List of abbreviations

3V = third ventricle
4V = fourth ventricle
APT = anterior pretectal nucleus
Aq = Aquaduct
CbT = cerebellothalamic tract
CbX = decussation of the cerebellothalamic tract
CN = cerebellar nuclei
CP = Caudate Putamen
CT = corticothalamic
Ctx = cerebral cortex
dTh = dorsal thalamus
EGL = external granular layer of the cerebellum
fr = fasciculus retroflexus
Hb = Habenula
Hc = hippocampus
Hyp = Hypothalamus
IC = inferior colliculus
Int = interposed nucleus of the cerebellum
LC = lateral nucleus of the cerebellum
LG = lateral geniculate nucleus of the thalamus
LHb = Lateral habenula
LP = lateral posterior nucleus of the thalamus
MCN = medial nucleus of the cerebellum
MD = mediodorsal nucleus of the thalamus
MG = medial geniculate nucleus of the thalamus
MHb = Medial habenula
ML = midline nuclei
mRF = medullary reticular formation
mt = mamillothalamic tract
NHS = normal horse serum
PBS = phosphate buffer saline
PBSGT = phosphate buffer saline with gelatin and triton
Pf = parafascicular nucleus of the thalamus
Po = Posterior complex of the thalamus
pSAO = percentage of summed area occupied by above threshold RFP signal
Pt = pretectum
PV = paraventricular nucleus of the thalamus
RFP = red fluorescent protein
Rh = rhomboid nucleus
RN = red nucleus
rpm = rounds per minute
RRE = retroreuniens nucleus
Rt = reticular nucleus of the thalamus
SC = superior colliculus
TC = thalamocortical
THF = tetrahydrofuran
VB = ventrobasal complex of the thalamus
VL = ventrolateral nucleus of the thalamus
VM = ventromedial nucleus of the thalamus
vTh = ventral thalamus
ZI = zona incerta
ZLI = zona limitans intrathalamica

Table 1. Primary antibodies

Host species	Antigen	Concentration	Manufacturer
Rabbit	Red fluorescent protein	1:1000	Rockland 600-401-379
Guinea Pig	Vesicular glutamate transporter 2	1:500	MilliP AB2251
Goat	FoxP2	1:500	SC-21069
Chicken	Calbindin	1:500	Syn Sys 214006
Mouse	NeuN	1:1000	MilliP MAB377

Table 2. Secondary antibodies

Host species	Target species	Conjugate	Concentration	Manufacturer
Donkey	Rabbit	Cy3	1:400	Jackson 711-165-152
Goat	Rabbit	Biotin	1:1000	Jackson 111-065-144
Donkey	Guinea Pig	Cy5	1:200	Jackson 706-175-148
Donkey	Goat	Alexa488	1:200	Jackson 705-545-147
Donkey	Chicken	Cy5	1:200	Jackson 703-175-155
Donkey	Mouse	Alexa488	1:200	Jackson 715-545-150

Table 3. Laser and filters per microscope per dye

	Lightsheet Ultramicroscope II		Opera Phenix™ HCS		Zeiss LSM700 Meta		
Dyes	Laser	Filters	Lasers	Filters	Lasers	Filters	Beamsplitter
DAPI	-	-	-	-	-	-	-
Alexa 488	488nm	525/50	488nm	500/50	488nm	0/590	520
Cy3	561nm	615/40	561nm	570/30	555nm	/640	600
Cy5	647nm	676/29	640nm	650/60	633nm	640/	630

Table 4. Relative amount of RFP^+ neurons (RFP/NeuN in %) per cerebellar nucleus and the relative amount of RFP^+ neurons in each nucleus compared to the total amount of RFP+ CN neurons (RFP/totalRFP in %).

	Mouse 1		Mouse 2	
	RFP/NeuN in %	RFP/totalRFP	RFP/NeuN in %	RFP/totalRFP
LCN	33.3	22.1	22.5	13.3
Int	56.6	64.8	64.6	77.5
MCN	19.0	13.1	12.7	9.25
Total	40.0	100	39.7	100

Table 5. pSAO values (in %) of the investigated thalamic nuclei and the Z- and p-values of the differences between the age groups of each of these nuclei.

	E16.5	E17.5	E18.5	E16.5 vs. E17.5		E16.5 vs. E18.5		E17.5 vs. E18.5	
	pSAO	pSAO	pSAO	Z	p	Z	p	Z	p
VM	0.0480%	4.85%	14.7%	-1.38	0.167	-2.96	0.00307	-1.71	0.0881
MD	0.00147%	0.0590%	1.45%	-1.26	0.207	-2.79	0.00535	-2.02	0.0431
Pf	0.330%	1.06%	3.30%	-1.60	0.111	-3.00	0.00274	-1.67	0.0940
ML	0.0930%	0.0586%	0.342%	-1.77	0.859	-2.15	0.0317	-2.25	0.0242
Po	0.0261%	0.137%	0.885%	0.836	0.403	-1.54	0.123	-2.67	0.00766

References

1. Brooks, J.X., J. Carriot, and K.E. Cullen, *Learning to expect the unexpected: rapid updating in primate cerebellum during voluntary self-motion.* Nat Neurosci, 2015. 18(9): p. 1310-7.
2. De Zeeuw, C.I. and M.M. Ten Brinke, *Motor Learning and the Cerebellum.* Cold Spring Harb Perspect Biol, 2015. 7(9): p. a021683.
3. Manto, M., et al., *Consensus paper: roles of the cerebellum in motor control--the diversity of ideas on cerebellar involvement in movement.* Cerebellum, 2012. 11(2): p. 457-87.
4. Schmahmann, J.D., J. Macmore, and M. Vangel, *Cerebellar stroke without motor deficit: clinical evidence for motor and non-motor domains within the human cerebellum.* Neuroscience, 2009. 162(3): p. 852-61.
5. Stoodley, C.J., E.M. Valera, and J.D. Schmahmann, *Functional topography of the cerebellum for motor and cognitive tasks: an fMRI study.* Neuroimage, 2012. 59(2): p. 1560-70.
6. Chen, C.H., et al., *Short latency cerebellar modulation of the basal ganglia.* Nat Neurosci, 2014. 17(12): p. 1767-75.
7. Kros, L., et al., *Controlling Cerebellar Output to Treat Refractory Epilepsy.* Trends Neurosci, 2015. 38(12): p. 787-99.
8. Stoodley, C.J., et al., *Altered cerebellar connectivity in autism and cerebellar-mediated rescue of autism-related behaviors in mice.* Nat Neurosci, 2017. 20(12): p. 1744-1751.
9. Wang, S.S., A.D. Kloth, and A. Badura, *The cerebellum, sensitive periods, and autism.* Neuron, 2014. 83(3): p. 518-32.
10. Pieterman, K., et al., *Cerebello-cerebral connectivity in the developing brain.* Brain Struct Funct, 2017. 222(4): p. 1625-1634.
11. Martin, G.F., et al., *Development of brainstem and cerebellar projections to the diencephalon with notes on thalamocortical projections: studies in the North American opossum.* J Comp Neurol, 1987. 260(2): p. 186-200.
12. Hara, S., et al., *Interstitial branch formation within the red nucleus by deep cerebellar nuclei-derived commissural axons during target recognition.* J Comp Neurol, 2016. 524(5): p. 999-1014.
13. Mire, E., et al., *Spontaneous activity regulates Robo1 transcription to mediate a switch in thalamocortical axon growth.* Nat Neurosci, 2012. 15(8): p. 1134-43.
14. Moreno-Juan, V., et al., *Prenatal thalamic waves regulate cortical area size prior to sensory processing.* Nat Commun, 2017. 8: p. 14172.
15. Chou, S.J., et al., *Geniculocortical input drives genetic distinctions between primary and higher-order visual areas.* Science, 2013. 340(6137): p. 1239-42.
16. Gornati, S.V., et al., *Differentiating Cerebellar Impact on Thalamic Nuclei.* Cell Rep, 2018. 23(9): p. 2690-2704.
17. Teune, T.M., et al., *Topography of cerebellar nuclear projections to the brain stem in the rat.* Prog Brain Res, 2000. 124: p. 141-72.
18. Shinoda, Y., T. Futami, and M. Kano, *Synaptic organization of the cerebello-thalamo-cerebral pathway in the cat. II. Input-output organization of single thalamocortical neurons in the ventrolateral thalamus.* Neurosci Res, 1985. 2(3): p. 157-80.
19. Sawyer, S.F., J.M. Tepper, and P.M. Groves, *Cerebellar-responsive neurons in the thalamic ventroanterior-ventrolateral complex of rats: light and electron microscopy.* Neuroscience, 1994. 63(3): p. 725-45.

20. Kivrak, B.G. and R.S. Erzurumlu, *Development of the principal nucleus trigeminal lemniscal projections in the mouse.* J Comp Neurol, 2013. 521(2): p. 299-311.
21. Marques-Smith, A., et al., *A Transient Translaminar GABAergic Interneuron Circuit Connects Thalamocortical Recipient Layers in Neonatal Somatosensory Cortex.* Neuron, 2016. 89(3): p. 536-49.
22. Tolner, E.A., et al., *Subplate neurons promote spindle bursts and thalamocortical patterning in the neonatal rat somatosensory cortex.* J Neurosci, 2012. 32(2): p. 692-702.
23. Gong, S., et al., *Targeting Cre recombinase to specific neuron populations with bacterial artificial chromosome constructs.* J Neurosci, 2007. 27(37): p. 9817-23.
24. Madisen, L., et al., *A robust and high-throughput Cre reporting and characterization system for the whole mouse brain.* Nat Neurosci, 2010. 13(1): p. 133-40.
25. Ferland, R.J., et al., *Characterization of Foxp2 and Foxp1 mRNA and protein in the developing and mature brain.* J Comp Neurol, 2003. 460(2): p. 266-79.
26. Vargha-Khadem, F., et al., *FOXP2 and the neuroanatomy of speech and language.* Nat Rev Neurosci, 2005. 6(2): p. 131-8.
27. Thompson, C.L., et al., *A high-resolution spatiotemporal atlas of gene expression of the developing mouse brain.* Neuron, 2014. 83(2): p. 309-323.
28. Nagalski, A., et al., *Molecular anatomy of the thalamic complex and the underlying transcription factors.* Brain Struct Funct, 2016. 221(5): p. 2493-510.
29. Bodor, A.L., et al., *Structural correlates of efficient GABAergic transmission in the basal ganglia-thalamus pathway.* J Neurosci, 2008. 28(12): p. 3090-102.
30. Houck, B.D. and A.L. Person, *Cerebellar Premotor Output Neurons Collateralize to Innervate the Cerebellar Cortex.* J Comp Neurol, 2015. 523(15): p. 2254-71.
31. Leto, K., et al., *Consensus Paper: Cerebellar Development.* Cerebellum, 2016. 15(6): p. 789-828.
32. Olsen, S.R., et al., *Gain control by layer six in cortical circuits of vision.* Nature, 2012. 483(7387): p. 47-52.
33. Jacobs, E.C., et al., *Visualization of corticofugal projections during early cortical development in a tau-GFP-transgenic mouse.* Eur J Neurosci, 2007. 25(1): p. 17-30.
34. Schwarz, C. and Y. Schmitz, *Projection from the cerebellar lateral nucleus to precerebellar nuclei in the mossy fiber pathway is glutamatergic: a study combining anterograde tracing with immunogold labeling in the rat.* J Comp Neurol, 1997. 381(3): p. 320-34.
35. Fremeau, R.T., Jr., et al., *The expression of vesicular glutamate transporters defines two classes of excitatory synapse.* Neuron, 2001. 31(2): p. 247-60.
36. Hisano, S., et al., *Expression of inorganic phosphate/vesicular glutamate transporters (BNPI/VGLUT1 and DNPI/VGLUT2) in the cerebellum and precerebellar nuclei of the rat.* Brain Res Mol Brain Res, 2002. 107(1): p. 23-31.
37. Kaneko, T. and F. Fujiyama, *Complementary distribution of vesicular glutamate transporters in the central nervous system.* Neurosci Res, 2002. 42(4): p. 243-50.
38. Grant, E., A. Hoerder-Suabedissen, and Z. Molnar, *Development of the corticothalamic projections.* Front Neurosci, 2012. 6: p. 53.
39. Newman, D.B. and C.Y. Ginsberg, *Brainstem reticular nuclei that project to the thalamus in rats: a retrograde tracer study.* Brain Behav Evol, 1994. 44(1): p. 1-39.
40. Vertes, R.P., et al., *Ascending projections of the posterior nucleus of the hypothalamus: PHA-L analysis in the rat.* J Comp Neurol, 1995. 359(1): p. 90-116.

41. Shimogawa, Y., Y. Sakuma, and K. Yamanouchi, *Efferent and afferent connections of the ventromedial hypothalamic nucleus determined by neural tracer analysis: implications for lordosis regulation in female rats.* Neurosci Res, 2015. 91: p. 19-33.
42. Mitrofanis, J., *Some certainty for the "zone of uncertainty"? Exploring the function of the zona incerta.* Neuroscience, 2005. 130(1): p. 1-15.
43. Ziegler, L., et al., *Synaptic consolidation: from synapses to behavioral modeling.* J Neurosci, 2015. 35(3): p. 1319-34.
44. Deck, M., et al., *Pathfinding of corticothalamic axons relies on a rendezvous with thalamic projections.* Neuron, 2013. 77(3): p. 472-84.
45. Fink, A.J., et al., *Development of the deep cerebellar nuclei: transcription factors and cell migration from the rhombic lip.* J Neurosci, 2006. 26(11): p. 3066-76.
46. Metin, C. and P. Godement, *The ganglionic eminence may be an intermediate target for corticofugal and thalamocortical axons.* J Neurosci, 1996. 16(10): p. 3219-35.
47. Uesaka, N., et al., *Interplay between laminar specificity and activity-dependent mechanisms of thalamocortical axon branching.* J Neurosci, 2007. 27(19): p. 5215-23.
48. Matsumoto, N., et al., *Synapse-dependent and independent mechanisms of thalamocortical axon branching are regulated by neuronal activity.* Dev Neurobiol, 2016. 76(3): p. 323-36.
49. Lauder, J.M., et al., *In vivo and in vitro development of serotonergic neurons.* Brain Res Bull, 1982. 9(1-6): p. 605-25.
50. Mizuno, A., et al., *Partially enhanced thalamocortical functional connectivity in autism.* Brain Res, 2006. 1104(1): p. 160-74.
51. Di Martino, A., et al., *The autism brain imaging data exchange: towards a large-scale evaluation of the intrinsic brain architecture in autism.* Mol Psychiatry, 2014. 19(6): p. 659-67.
52. Nair, A., et al., *Regional specificity of aberrant thalamocortical connectivity in autism.* Hum Brain Mapp, 2015. 36(11): p. 4497-511.

2

"Nothing in life is to be feared, it is only to be understood"

Marie Curie

Chapter 3

Zebrin identity of murine cerebellar afferents corroborate neuronal firing frequency

Gerco Beekhof*
Simona V. Gornati*
Cathrin Canto
Avi Libster
M. Schonewille
C.I. De Zeeuw
Freek E. Hoebeek

*These authors contributed equally

In preparation for Journal of Neuroscience

Abstract

The heterogeneity of the murine cerebellar cortex has been highlighted in the past decade by results of anatomical and physiological experiments that supplement its behavioral specification. Although an increasing amount of data indicates that the output of the cerebellar cortex is linked to regionally variable molecular identity, i.e., inhibitory Purkinje cells (PCs), which are either positive or negative for the expression of aldolase-C, or Zebrin, can be recognized by their intrinsic firing frequencies. However, little is known about the impact of this dichotomous firing frequency on the downstream neurons in the cerebellar nuclei (CN). Here we investigated whether the firing frequency of neurons in the CN innervated by Zebrin-positive (Z^+) PC axons, which are the interpositus posterior, lateral and part of the medial nuclei, is different from that in Zebrin-negative (Z^-) nuclei, i.e., the interpositus anterior and a part of the medial nuclei. We recorded action potential firing in awake adult mice and found that the Z^- CN firing frequency was consistently higher than in Z^+ CN. Subsequent *in vitro* recordings of the intrinsic pacemaking activity did not reveal a significant difference in firing frequency between the CN neurons in Z^+ and Z^- nuclei, nor did we find morphological difference in the large-somata CN neurons. Further *in vivo* recordings in juvenile mice indicated that already during the postnatal days P17-19 the firing frequency of CN neurons correlates to the zebrin identitiy of the PC afferents. Our findings indicate that in the absence of overt differences in the neuronal morphology or intrinsic activity, the neurons in Z+ CN fire at a lower frequency than those in Z^- CN. Thereby these CN neurons tend to adhere to the increased firing frequency of Z^- PCs.

Introduction

Traditionally the cerebellum is seen as an integrator of sensory and motor information to control and adjust the motor system. However, studies in humans and primates showed that the cerebellum is also granted a modulatory function in higher-order cognitive and emotional disorders, which have their onset during development [1, 2]. Information from many brain structures enters via the mossy fiber and climbing fiber systems and the output is transferred through the cerebellar nuclei (CN) neurons to diverse brain areas, such as mesencephalic pre-motor nuclei and the diencephalic thalamus[3]. The cerebellar cortex receives vast amounts of input [4] and its principle output neurons, the Purkinje cells (PCs), converge onto the CN neurons with a ratio of ~40:1 ratio [5]. Moreover, CN neurons, most of which are intrinsically active [6], receive input from an unknown number of mossy fiber and climbing fiber collaterals [7].The precise impact of these afferents has been discussed in various detailed *in silico*, *in vitro* and *in vivo* studies[5, 8, 9] but so far it remains to be elucidated how the modular organization of the olivo-cerebellar system correlates to the actual output of the cerebellum, i.e., the CN firing pattern.

The CN population is very heterogeneous in its cell composition and in its extracerebellar afferents. Yet, the PC input to the CN is organized according to the modular organization of the so-called 'Zebrin-bands' [10]. There are several molecular markers that subdivide cerebellar cortex in different bands; staining of aldolase-C, which is the same protein as zebrin II, clearly reveal that CN can be divided into zebrin-positive (Z^+) and zebrin-negative (Z^-), based upon the density of Z^+ and Z^- PC axons. The lateral, interpositus posterior and caudal portion of the medial CN are mostly innervated by Z^+ PCs whereas the interpositus anterior and rostral portion of the medial CN are mostly innervated by Z^- PCs [10]. Recent studies in adult mice have shown that the Z^+ PCs fire action potentials on average at lower frequencies than Z- Purkinje cells [11]. Under the assumption that the convergence of the PC input to Z^+ and Z^- CN neurons is equal, the Z^- CN neurons receive increased inhibition compared to Z^+. Although the synchrony of the inhibitory inputs to CN neurons is decisive over its effect on CN action potential firing [5, 8], there has been no quantitative comparison of the synchrony of PC firing in Z^+ and Z^- bands. Here, we aimed to answer whether the firing frequency of Z^+ and Z^- neurons differs. Using *in vivo* electrophysiology we found that Z^- CN neurons fire at a higher rate than the Z^+ neurons, whereas *in vitro* we could not observe a significant difference. Moreover morphological reconstruction of patched neurons showed no difference in the structure of the dendritic tree.

Materials and Methods

Subjects

A total of 60 mice, aged P12 to P133, where used for extracellular recordings in the CN. We used both males and females and selected the pups randomly from a litter. We used either EAAT4-eGFP mutant mice, in which eGFP is expressed in EAAT4-expressing Purkinje cells, i.e., in Zebrin-positive Purkinje cells[12] or C57BL/6J mice. The EAAT4-eGFP mice were bred in-house; the C57Bl/6J mice were obtained from a time-pregnant mother imported from the vendor (Charles River or Janvier Labs). All experiments were performed in accordance with the European Communities Council Directive. Protocols were reviewed and approved by the Dutch national experimental animal committees (DEC) and every precaution was taken to minimize stress, discomfort and the number of animals used.

Surgery

Mice were subcutaneously injected with Buprenorphine (0.015 mg/kg) (RB Pharmaceuticals Ltd., Slough, UK) and Rimadyl cattle (5mg/kg) (Zoetis, Parsippany, NJ, USA) sixty minutes before surgery. The mice were anesthetized with isoflurane (3% in 0.4 L/min O_2 for induction and for maintenance 0.5-1.3% in 0.2-0.4 L/min O_2) (TEVA Pharmachemie, Haarlem, The Netherlands). During the surgery the temperature was maintained at 37°C using a heating pad and anal probe in an automated feedback system. Before and after shaving of the skin 2% lidocaine (AstraZeneca, Cambridge, UK) was applied, and to expose the skull the skin was opened over the rostro-caudal midline. The skull was covered with a layer of Optibond (Kerr, Salerno, Italy) for stability and five holes were drilled using a high speed, diamond-tipped drill (Foredome, Bethel, CT, USA). To obtain ECoG signals, five pure silver ball-tipped electrodes (custom-made from 0.125 mm diameter silver wire; Advanced research materials LTD, Eynsham, Oxford, UK) were placed on the meningeal layer of the dura mater. Two silver electrodes were positioned bilateral above the primary cortex (M1, 1 mm rostral; 1 mm lateral; relative to Bregma), two were placed above the primary sensory cortex (S1, 1 mm caudal; 3. mm lateral; relative to Bregma), and one in the interparietal bone (1 mm caudal; 1 mm lateral; relative to Lambda). UV-sensitive composites, a layer of Optibond (Kerr, Salerno, Italy) and Charisma or Charisma Flow (Heraeas Kulzer, Hesse, Germany), were used to fixate the silver electrodes and the pedestal and included M1.4 nuts to fixate the mouse head. To obtain extracellular recordings a craniotomy was made in the occipital bone and temporarily closed with Kwik-Cast sealant (World Precision Instruments Inc, Sarasota, Fl, USA) to prevent cooling of the brain. At the end of the surgery the mice received 0.1-0.2 mL saline for hydration and 0.2 L/min O_2.

In vivo awake extracellular recordings

Within two hours of the start of the surgical procedure the mice were relocated to the setup where the body temperature was supported via a feedback controlled heating pad. We evaluated the state of the mice using the behaviour (spontaneous whisking, response to auditory stimuli) and ECoG (presence of slow-wave, high-amplitude activity indicating drowsiness, or fast, low-amplitude activity indicating alert state). ECoG and extracellular recordings were sampled at 20 kHz (setup 1: Digidata 1322A, Molecular Devices LLC., Axon instruments, Sunnyvale, CA, USA) or at 50 kHz (setup 2: ECoG: adapted MEA60, Multichannel system, Reutlingen, Germany; extracellular: Multiclamp 700B amplifier with a DigiData 1440; Molecular Devices). Single-unit recordings were made using borosilicate glass capillaries (Harvard apparatus, Holliston, MA, USA) with 0.5-1.0 µm tips and a resistance of 6-12 MΩ. We recorded with a K^+-based internal solution containing 2% biocytin or 0.5% Evans Blue (both from Sigma-Aldrich, Merck KGaA, Darmstadt, Germany). At the recording location biocytin was released with iontophoresis with 1 s pulses of 4 µA for 3 min (custom-built device, Erasmus MC, Rotterdam, The Netherlands), or Evans Blue injections were made with air pressure.

Slice preparation

19 adult mice (P>90) isoflurane-anesthetized were decapitated, their brain quickly removed and placed in warm (~34ºC) aCSF containing the following (in mM): 123 NaCl, 2.5 KCl, 1 $MgCl_2$, 1.3 NaH_2PO_4, 26 $NaHCO_3$, 10 glucose, 2 $CaCl_2$, bubbled with 95%O_2/5%CO_2, pH 7.4 [13]. Coronal slices (250 µm) of cerebellar tissue including the CN were cut using a Leica vibratome VT1000S (Leica Biosystems, Wetzlar, Germany). For the recovery, cerebellar slices were incubated in oxygenated aCSF and maintained at 34ºC. After 30 min, the slices were transferred to a recording chamber and maintained at 34±1ºC under continuous superfusion with the oxygenated physiological solution.

In vitro whole cell recordings

For all recordings, slices were bathed in 34±1˚C aCSF (bubbled with 95% O_2 and 5% CO_2). Whole-cell patch-clamp recordings were performed using an EPC-10 amplifier (HEKA Electronics, Lambrecht, Germany) for 20-60 min and digitized at 20 kHz. Whole cell recordings were obtained using borosilicate pipettes (4-6 MΩ) filled with internal solution containing (in mM): 120 K-gluconate, 6 NaCl, 10 HEPES, 1 EGTA-KOH, 0.1 $CaCl_2$, 4 Mg-ATP, 0.4 Na-GTP, 2 KCL, 14 Creatine phosphate TRIS, 2 $MgCl_2$ (pH 7.36, osmolarity 290). After breaking from gigaseal into whole cell configuration, cells were kept at holding potentials more negative than the AP threshold (usually -70 to -80 mV) by injecting up to -300 pA of current. Input resistance were recorded after whole-cell configuration was reached, recordings were excluded if the series resistance (R_s) (assessed by -5 or

-10 mV voltage steps following each test pulse) varied by >25% over the course of the experiment. Recording pipettes were supplemented with 1 mg/ml biocytin to allow histological staining (see below). All recordings were performed in the presence of picrotoxin (100 µM, Sigma-Aldrich) to block $GABA_A$-receptor-mediated IPSCs, NBQX (10µm, Tocris, Bristol, UK) and 10 µM APV (10 µm, Tocris) to block respectively AMPA and NMDA receptors.

Measurement of electrophysiological parameters

Potential traces were acquired using Patchmaster software (HEKA Elektronik Dr. Schulze GmbH, Lambrecht, Germany) and stored for offline analysis. For resting membrane potential (V_{rest}) the value was measured 2 ms before the spontaneous AP peak. For analysis of evoked APs, the first APs fired by each cell in response to a series of increasing depolarizing current steps, was isolated and analyzed using clampfit. For frequency-current (f-I) analysis the average firing frequency evoked with current steps of increasing amplitude was recorded; for frequency adaptation, we selected the trace that contained a response of ~40 Hz and normalized the interspike intervals to the initial interval.

Immunofluorescence for in vitro recordings

To visualize the *in vitro* recorded neurons slices were placed in 4% PFA (in 0.12 M PB) for at least 24 hrs. Subsequently, slices were transferred into 0.1 M PBS and rinsed with PBS 3 times for 10 min. Slices were incubated for 1 hr at RT in blocking solution and were subsequently rinsed 3 times for 10 min and incubated for 2 hrs with Streptavidin-Cy3 (1:200, Jackson Immuno Research Inc., West Grove, Pennsylvania, USA) diluted in PBS containing 2% normal horse serum and 0.4% triton. Sections were rinsed in PBS, mounted with Vectashield (Vector laboratories, Burlingame, CA, USA) and imaged with a LSM 700 confocal microscope (Carl Zeiss Microscopy, LLC, Thornwood, NY, USA).

Fluorescence microscopy for 2D Sholl analysis

Recorded neurons were labeled with biocytin. Epifluorescent tile images were obtained using a 20X/0.30 NA (air) objective and a LSM 700 microscope (Carl Zeiss). The position of labeled neurons was confirmed using a stereotactic atlas. To determine the dendritic arborization of biocytin filled cells, we imaged using a 40X/1.30 NA (oil) objective to acquire a stack of images with 0.5 digital zoom and a voxel size of 313 nm width x 313 nm length x 300 nm depth for a 2D Sholl analysis by a Fiji software macro. For preprocessing, stacks with excessive background signal were excluded from further analysis. Subsequently the dendritic arborization was measured in concentric shells of 10 µm distance starting with 15 µm distance from the center of the soma.

Immunofluorescence for in vivo recordings

At the end of the *in vivo* recordings mice were sacrificed with an overdose of pentobarbital and transcardially pre-rinsed with PBS followed with a solution of 4% paraformaldehyde in 0.1 M phosphate buffer. The brain was removed and post-fixed for two hours at room temperature in this paraformaldehyde solution, and then placed overnight at 4°C in a solution of 10% sucrose in 0.1 M phosphate buffer. Brains were embedded in a 0.1M phosphate buffer with 12% gelatine and 10% sucrose, the embedded brain were fixed for two hours in 10% formaldehyde and 30% sucrose solution of 0.1 M phosphate buffer. Then it was placed in a 0.1 M phosphate buffer with 30% sucrose overnight at 4°C. Brains were sliced in 40 or 100 µm thick slices on a freezing microtome. A standardized immunochemistry protocol was used and all slices were stained with the primary Aldolase-C (goat, 1:1000, Santa Cruz Biotechnology Inc, Dallas, Texas) for four days at 4°C, and for two hours at room temperature for the secondary antibody anti-goat (1:200, Jackson Immuno Research) and streptavidin if there was no Evans Blue used (1:200, Jackson Immuno Research). The EAAT4-eGFP brains where only stained with streptavidin if biocytin was used, because the Aldolase-C staining is complementary with the EAAT4-eGFP expression pattern [12]. All slices received a nuclear DAPI staining for 10 min, and were mounted on cover slips from a Chromium(III) potassium sulfate solution and then covered with a microscope slide with mowiol.

Acquisition of confocal images

Wide-field fluorescent tile scan images where acquired with a LSM 700 (Carl ZeissMicroscopy) or a SP5/SP8 (Leica Microsystems, Wetzlar, Germany) confocal laser scanning microscope. The tile scans of the injection spots were made with a 10X objective, 20% overlap and online-stitched. Only recorded neurons that were located within 300 µm from the centre of the injection area and that were not near a border of a nuclei or Zebrin zone were analysed, all other neurons were discarded.

Spike analysis

For spike analysis of the CN neurons (n=404 cells) we included only cells with a recording length of at least 90 s (duration: 214± 160 s). In our analysis we included only the cells of which we could trace the recording location by the use of the injection spot. We used Matlab (Mathworks, Natick, MA, USA) to detect spikes with a custom-built Matlab code using threshold and principal component analysis. Coefficient of variance (CV) is the variation in inter-spike-intervals (ISI) during firing, $\boldsymbol{CV = standard\ deviton\ ISI mean\ ISI}$. CV2, representing the variance on a spike-to-spike base and is less sensitive for a single outlier, $\boldsymbol{CV2 = 2 * |ISIn + 1 - ISInISIn + 1 - ISIn}$. The mean instantaneous firing frequency (miFF) is the average firing frequency (FF) on a spike-to-spike basis,

$miFF = mean(1ISIn + 1ISIn + 1)$. The burst-index reflects the fraction of all spikes that were part of a 'burst', which we defined by three consecutive spikes at ≥100 Hz.

Statistical analysis

Using Graphpad PRISM and SPSS software packages we ran statistical comparisons between the two groups (Z^+ and Z^-) by a Student's *t*-test or the non-parametric test Mann Whitney as indicated in the main text. Sholl analysis results were statistically assessed by performing Chi-square analysis. We corrected missing values by the last observation carried forward procedure. We defined $p<0.05$ as a significant difference. Throughout the main text we report a subset of the statistical data, the full set can be found in tables that accompany each figure. Summarized data are represented as mean ± standard error of the mean unless stated otherwise.

Results

CN firing frequency differs between Zebrin domains

To confirm the dichotomous labelling of the CN that was shown in the rat[10], we evaluated the presence of a clear separation between CN innervated densely by Z^+ PC axons and by Z^- PC axons by assessing the GFP labelling of the CN in EAAT4-eGFP mice [11]. Indeed, we found that the Z^+ CN encompass the interpositus posterior and the lateral and a portion of the medial nuclei and the Z^- the interpositus anterior and the other portion of the medial nuclei (Figure 1A). To evaluate the average firing frequency in these Z^+ and Z^- CN, we performed extracellular *in vivo* recordings throughout the whole CN in adult mice (>P90). A total of 97 CN neurons were recorded could be located in the CN by histological confirmation (see material and methods) (Figure 1A). The CN cells showed a difference in the firing pattern (Figure 1B; Table 1) as a higher firing frequency was observed in Z^- CN neurons compared to Z^+ CN neurons (Z^+: 53.9±3.5 Hz; Z^-: 68.7±4.7 Hz; $p=0.003$, paired *t*-test; Figure $1C_1$; Table 1). The regularity of action potential firing was quantified by calculating the CV and the CV2 (see methods for calculation); we found that the regularity was not significantly different between CN neurons recorded in Z^+ or Z^- CN (CV: Z^+: 1.24±0.26; Z^-: 1.02±0.29; $p=0.62$, Mann-Whitney test; CV2: Z^+: 0.48±0.02; Z^-: 0.48±0.02; $p=0.99$, Mann-Whitney; Figure $1C_2$ and $1C_3$ respectively; Table 1). Because of the higher firing frequency of Z^- cells, we investigated if the Z^- cells were more prone to burst firing. We found that the fraction of burst firing in Z^- CN neurons is significantly higher (Z^+: 0.09±0.01; Z^-: 0.19 ±0.02; $p=0.004$ Mann-Whitney test; Figure 1D; Table 1). The ISI distribution of Zebrin zones in the CN (Figure 1E) indicates that the firing properties of the neurons between zones are similar apart from the increased firing frequency in Z^- CN neurons.

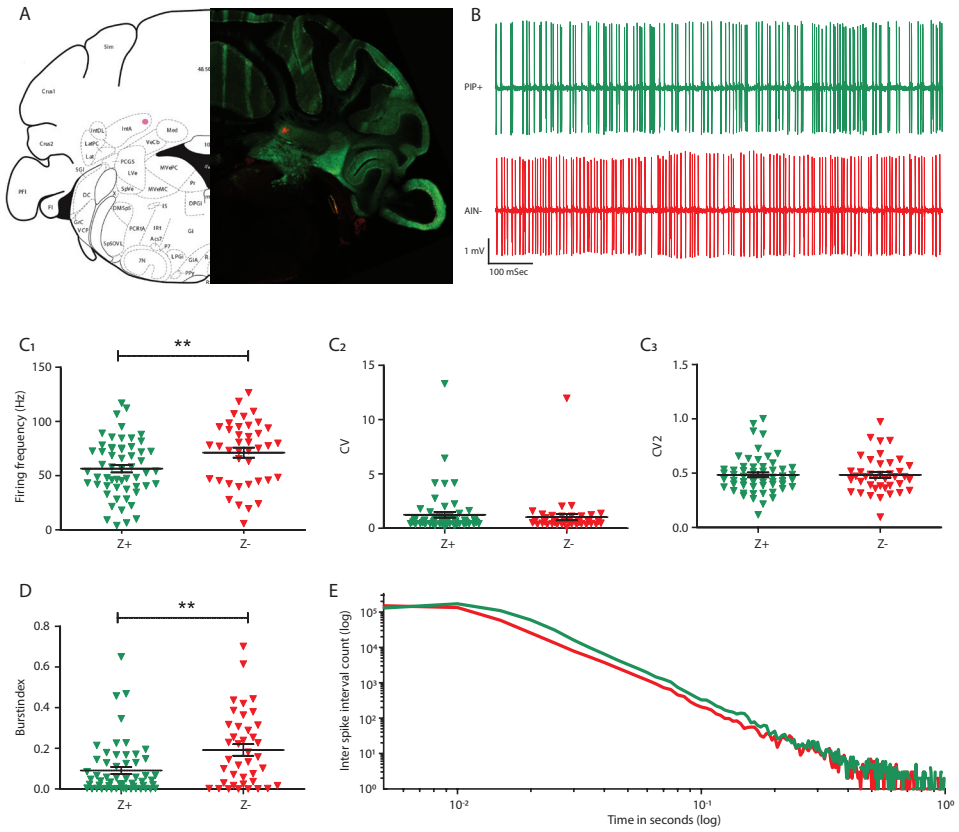

Figure 1. CN firing frequency differs between Zebrin domains *in vivo*. (A) Representative confocal image of a biocytin-labelled injection spot at the recording location of a CN neuron in the interpositus anterior. The injection spots are localized using a stereotactic atlas (Paxinos and Franklin, 2001). **(B)** Two representative example traces of CN neurons recorded in areas densely innervated by Z^+ and Z^- PC axons in adult mice (>P90). **(C)** Quantification of firing frequency **(C1)**, CV **(C2)**, and CV2 **(C3)** for Z^- (n=40) and Z^+ (n=57) CN neurons recorded from 11 mice. **(D)** The fraction of the total population of bursting spikes is displayed as the burst index between Z^- and Z^+ neurons. **(E)** ISI counts of all recorded adult CN neurons binned per 50 ms (max ISI included = 1 s). Green represents ISI's of Z^+ neurons, while red represents the ISI's of Z^- neurons.

Basic CN firing properties and cell excitability are similar in Zebrin domains

As CN cells are known to fire spontaneous action potentials [6] we investigated whether the lower firing frequency of Z^+ CN neurons compared to the Z^- CN neurons is due to a difference in the spontaneous activity of CN neurons in the diverse zebrin domains. In order to do so, we performed whole cell patch clamp of CN neurons from coronal slice of adult (P>90) mice cerebellum. We identified CN neurons with a relatively large

soma as the big glutamatergic cells and recorded the action potential firing patterns in the presence of AMPA receptor (NBQX), NMDA receptor (APV) and GABA receptor (PTX) blockers (Figure 2A). The firing frequency was not significantly different between the two groups (Z^+: 75.9±8.5 Hz; Z^-: 92.9±11.3 Hz; p=0.228, unpaired t-test; Figure 2B; Table 2), nor was the regularity of action potential firing (CV: Z^+: 0.17±0.03; Z^-: 0.12±0.02; p=0.636, Mann Whitney test; CV2: Z^+: 0.05±0.01; Z^-: 0.05±0.01; p=0.511; Mann Whitney test; Figure 2B; Table 2). Also, we did not observe a difference in the resting membrane potential (V_{rest}: Z^+ -41.3±0.8 mV; Z^-: -43.3±0.8 mV, p=0.106: unpaired t-test; Figure 2B; Table 2). Using a depolarizing and hyperpolarizing current steps (Figure 2C; Table 2) we studied AP firing dynamics and focused on the firing frequency versus injected current (f-I) relationship, which provides information related to the excitability of a neuron and how stable the resulting action potential firing pattern is. We found that the rheobase was not different between the two groups as both Z^+ and Z^- showed action potential firing already with 50 pA of current injected. In addition we also analyzed the shape of the first evoked action potential (eAP) fired in response to series of depolarizing current

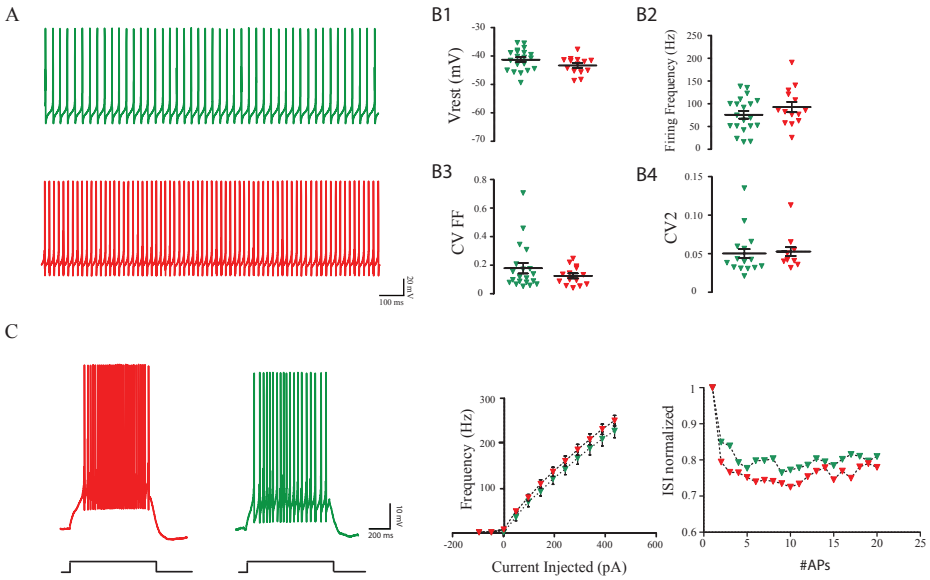

Figure 2. CN firing frequency is similar in spontaneous firing CN neurons. (A) Example traces of neurons recorded by whole cell patch clamp ***in vitro*** without injected holding current in Z^+ and Z^- nuclei. **(B)** Quantification of resting membrane potential (V_{rest}; B1), firing frequency (B2), coefficeints of variance (CV; B3) and CV2 (B4) for 20 Z+ and 14Z- neurons recorded from 38 EAAT4-EGFP mice. **(C)** Example traces of action potential firing evoked by depolarizing current injection (left panel) and the average firing frequency evoked by steps of various current amplitudes (I-F curve; middle panel) and the frequency adaptation (right panel).

steps of increasing amplitudes (from -100 pA to 800 pA) and we did not observe a significant difference between the two groups (Table 3).

We reconstructed the patched neurons to locate them in the Zebrin domains and to assess their morphological characteristics (Figure 3A; Table 4). We found that the average surface of the somata was not different between Z^+ (306.4±16.7 µm^2) and Z^- (342.1±30.2 µm^2; p=0.61, paired t-test; Figure 3B; Table 4). The dendritic branching was investigated using 2D Sholl analysis and revealed that the number of intersections at increasing distance from the soma was not significantly different between Zebrin domains (p=1, Chi square test).

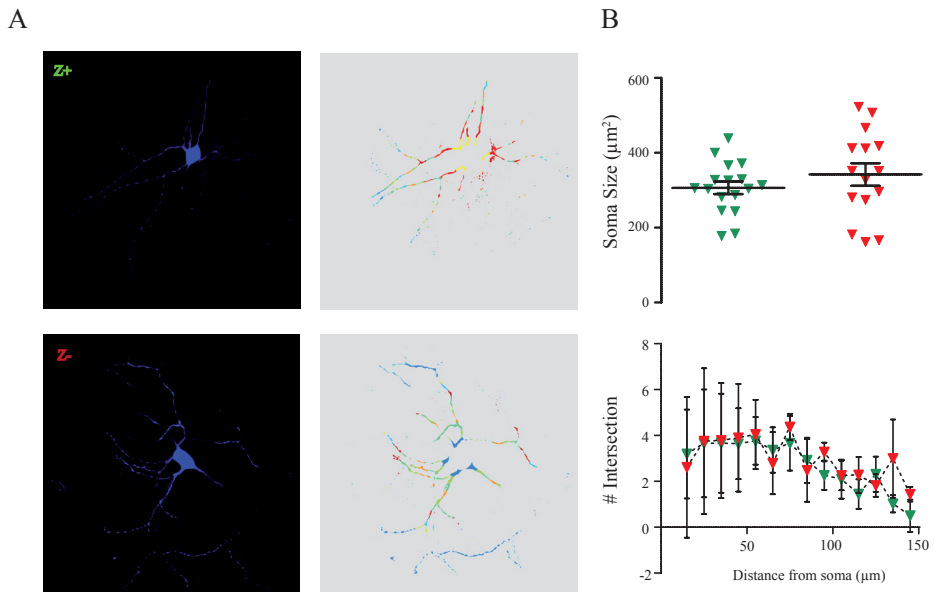

Figure 3. Z^+ and Z^- CN neurons do not differ in somatic and dendritic morphology. (A) Maximum projection of a confocal image stack of two reconstructed neurons (Z^+: top left; Z^-: bottom left) and the correlating Sholl analysis masks (Z^+: top right; Z^-: bottom right). **(B)**. Quantification of soma surface (top) and number of intersections for each concentric circle (bottom) for 17 Z+ and 15 Z- neurons recorded from 22 EAAT4-EGFP mice.

CN in zebrin-negative domain fire faster at early post-natal days

Our *in vitro* results on the intrinsic pacemaking activity of CN neurons indicate that in the adult mice the difference in action potential firing frequency recorded *in vivo* is determined at least partially by the synaptic afferents. Since pharmacological experiments with blockers of inhibitory transmission in vivo are not specifically affecting PC-CN transmission but also affect local inhibitory interneurons, we sought

for other methods to investigate how the PC input from Z^+ and Z^- bands [11] impact on CN neurons in the respective Zebrin domains. In addition to the Zebrin-specific PC firing frequencies, another noticeable aspect of PC and CN firing is that previous reports indicate that both PC and CN firing frequencies increase during postnatal developmental stages [14, 15]. Therefore we investigated the zebrin related firing pattern during postnatal development from the second week and onwards to see if the Zebrin related firing frequency is persistent in development. If the differences in CN firing frequencies recorded in the adult cerebellum are also found during these early stages, this supports our notion on the correlation between increased firing in Z^- compared to Z^+ CN neurons. During development we can see an increase in the firing frequency for the Z^+ and the Z^- groups (Figure 4A,B_1; Table 5). When comparing the firing patterns of Z^+ and Z^- CN neurons during the different developmental stages, we find that already at P12-14 there is a significant difference in firing frequency (Z^+: 7.89±1.66 Hz; Z^-: 19.4±5.1 Hz; p=0.03; Mann Whitney test). Also in the P15-17 age range we found that Z^- CN neurons have a higher firing frequency than Z^+ neurons (Z^+: 17.6±2.4Hz; Z^-: 23.4±3.1 Hz; p=0.04, Mann Whitney test), which matches the difference found in the adult mice (>P90). In the ages between P18 and P40 we found no significant differences between Z^+ and Z^- CN firing frequencies (all p-values >0.05; see also Table 5). In general we observed an increase in regularity, in that CV and CV2 values gradually decreased over age (Figure 4B_2 and 4B_3; Table 5), but also an increased occurrence of burst firing (Figure 4C; Table 5). Solely in the P15-17 age group we found a significant difference between Z^+ and Z^- CN neuron firing patterns (CV: P15-17: Z^+ 1.77±0.20, Z^-: 1.00±0.12: p=0.004, Mann Whitney test; CV2: Z^+: 0.68±0.03; Z^-: 0.54±0.05; p=0.009, Mann Whitney test). These findings indicate that the difference between the firing frequency of Z^+ and Z^- CN neurons that we recorded *in vivo* in adult mice appears already during some of the developmental stages.

So far we solely determined whether there is a difference in CN firing patterns neurons located in CN invaded mostly by Z^+ or Z^- PC axons and our data supports a prominent influence of the afferents in determining the CN firing patterns *in vivo*. Apart from the classification by Zebrin identity the afferents are also specific for the individual nuclei. Therefore we questioned if difference between the firing frequency of Z^+ and Z^- CN neurons is correlated to the location of the recorded CN neurons, and thus by the afferents to the specific nuclei. We found in adult mice that the firing frequency of CN neurons in the interpositus anterior, which is identified as Z^- (see Figure 1 and [10], is higher (75.3±5.0 Hz) than in the Z^+ lateral, interpositus posterior and medial CN regions (52.7±4.4 Hz; p<0.05; Kruskal Wallis test; Figure 5A_1; Table 6). In addition, we also found that interpositus anterior CN neurons have a more 'bursty' firing pattern (Figure 5B: Lat: 0.119±0.04; PIN: 0.129±0.03; Med^+: 0.038±0.01; AIN: 0.22±0.03; Med^-: 0.131±0.05. Med^+ vs Med^- 1.000, Pin vs Med^+ 0.448; Lat vs Med^+ 0.905; Med^+ vs Ain <0.001; Pin vs

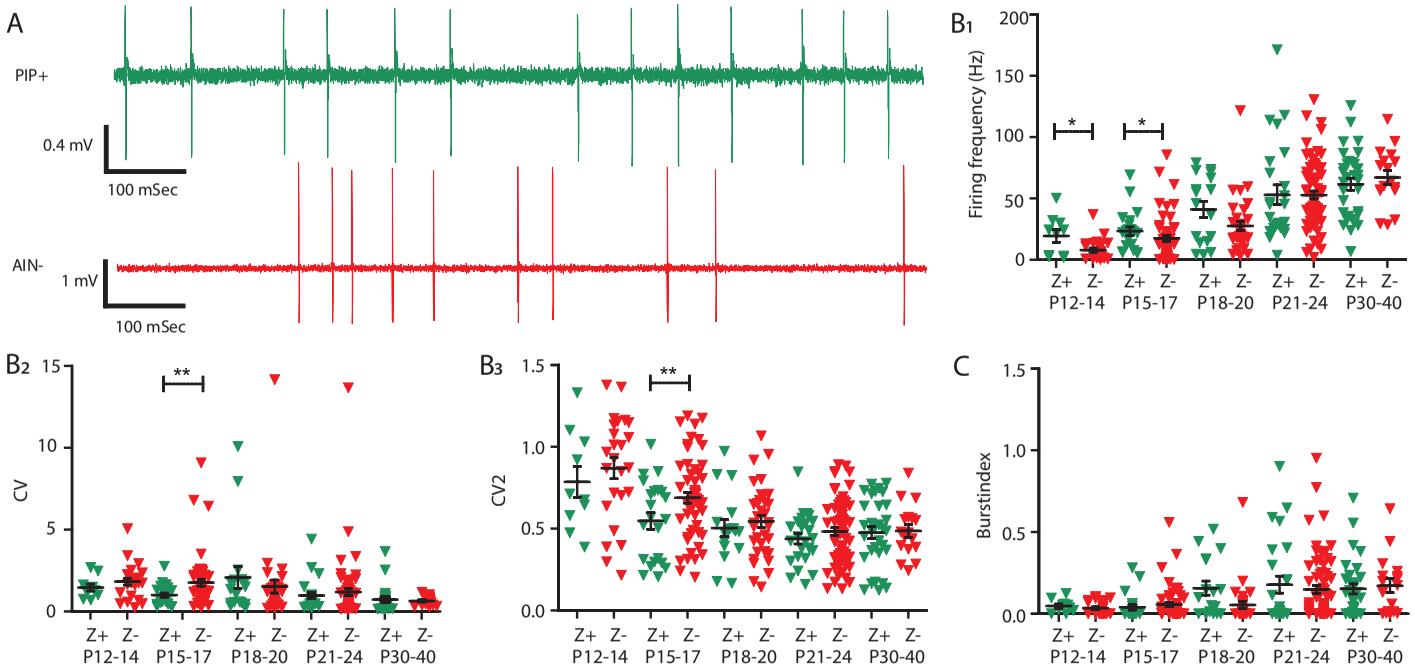

Figure 4. Firing frequency increases with age in both Z+ and Z- CN. (A) (n=307, recorded in 50 mice, age between P12 and P40) Two representative example traces of a Z^+ (green; P13) and a Z^- (red: P14) CN neuron. **(B)** Quantification of the mean firing frequency **(B1)**, CV **(B2)**, and CV2 **(B3)** for each age group (total Z+: n = 201 neurons from 43 mice; total Z^-: n = 106 neurons from 34 mice). **(C)** The fraction of the total population of bursting spikes is displayed as the burst-index for Z^- and Z^+ CN neurons in each age group.

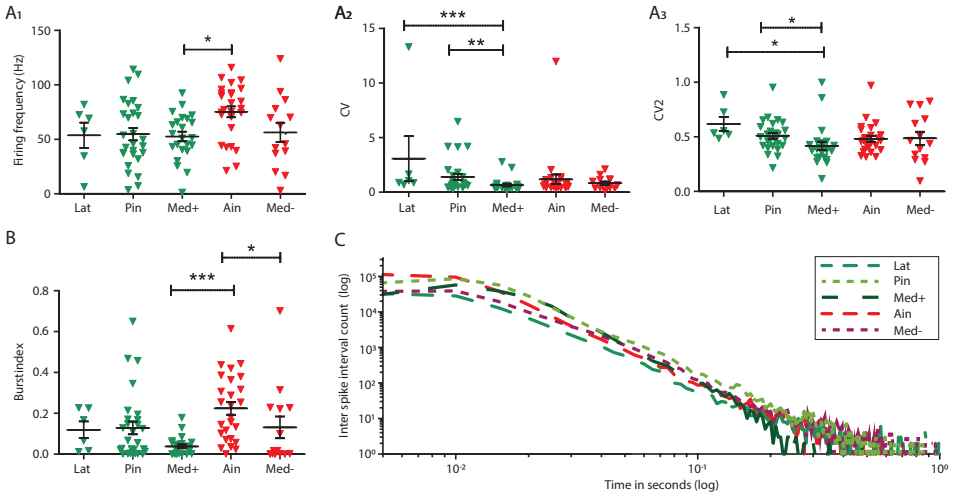

Figure 5. *In vivo* Firing patterns differ per cerebellar nucleus in adult mice. (A) Quantification of the mean firing frequency (A1), CV (A2), and CV2 (A3) CV2 for each sub nucleus (total: n = 97 neurons from 11 mice). **(B)** The fraction of the total population of bursting spikes is displayed as the burst-index between Z^- and Z^+ CN neurons. **(C)** ISI counts of all recorded adult CN neurons binned per 50 ms (max ISI included = 1 s).

Med- 1.000; Lat vs Med- 1.000; Ain vs Med^- 0.050; Lat vs Pin 1.000) and that there was a significant difference in the CV and CV2 values between the three Zebrin+ nuclei (CV: Lat 3.04±2.07; PIN 1.37±0.286; Med^+: 0.621±0.127; AIN: 1.15±0.44; Med-: 0.790±0.152. Lat vs Pin 1.000; Lat vs Med^+ 0.013; Lat vs Ain 0.515; Lat vs Med^- 0.333; Pin vs Med^+ 0.004; Pin vs Ain 1.000; Pin vs Med^- 0.895; Med^+ vs Ain 0.370; Med^+ vs Med^- 1.000; Ain vs Med^- 1.000 Kruskal Wallis; CV2: Lat: 0.619±0.064; Pin 0.511±0.026; Med^+: 0.418±0.039; Ain: 0.483±0.027; Med^-: 0.488±0.060. Lat vs Pin 1.000; Lat vs Med^+ 0.01; Lat vs Ain 0.500; Lat vs Med^- 0.466; Pin vs Med^+ 0.021; Pin vs Ain 1.000; Pin vs Med- 1.000; Med^+ vs Ain 0.320; Med^+ vs Med^- 1.000; Ain vs Med^- 1.000, Kruskal-Wallis; Figure $5A_2$ and $5A_3$ respectively; Table 6). Our recordings also indicate that neurons in the medial CN that is innervated mostly by Z^+ PC axons fire on average more regular than neurons in other CN, which is visualized in the ISI histogram plot (Figure 5C). These data indicate that apart from the Zebrin identity also connectivity of the CN is a relevant factor for setting the firing frequency of CN neurons in the awake mouse cerebellum.

Discussion

PC firing differs between cerebellar modules that are identified with expression of zebrin, but the impact on downstream target neurons in the CN remained to be elucidated. Here we investigated the differences in spiking activity of CN receiving inputs from PCs of different zebrin identity in mice. *In vivo* recordings of AP firing in in the various nuclei showed that the Z^- CN firing frequency was consistently higher than in Z^+ CN. In search for a cause, we performed *in vitro* recordings of the intrinsic activity of big glutamatergic cells, but found no significant difference in the firing frequency between the CN neurons in Z^+ and Z^- nuclei, nor did we find morphological difference in the reconstructed neurons. Further *in vivo* recordings did confirm that already from postnatal day P12 the firing frequency of CN neurons correlates to the zebrin identitiy and that in the adult the neurons in interpositus anterior nucleus fire at the highest frequency. All together these findings showed that overall Z^+ CN neurons fire at a lower frequency than those in Z^- CN and that there is no overt evidence that this difference is solely due a difference in the intrinsic pacemaking activity of CN neurons.

Previous studies showed that PCs with a Z^- identity tend to show a higher firing frequency than Z^+ PCs [11, 16] and given the inhibitory effect of PC afferents on CN neurons, we thus expected to observe a lower firing frequency in the Z^- domain of the CN than in the Z^+ domain.. However, conversely we found that the firing frequency of Z^- CN neurons is higher than that of Z^+ CN neurons. These counterintuitive findings might be at least partially due to: *i)* the mixed population of types of neurons that populate each different nucleus [7, 17, 18]; however, using extracellular recording electrodes we assume to have recorded of the cells with a relatively large soma diameter and continuous action potential firing (see also[19]); *ii*) a potential difference in the number of synaptic inputs between CN neurons in the different zebrin domains, which extends beyond the PC input and that of local inhibitory interneurons to extracerebellar sources of excitatory input from mossy fiber and climbing fiber collaterals ([20]), and *iii*) the potentially different levels of Purkinje cell synchrony in the Z^- and Z^+ domains of the CN, which is of importance since Person and Raman proposed in 2011 that the synchrony of PC firing can be decisive for the timing of action potential firing, in that synchronized phasic inhibitory input can trigger a timed action potential [5, 8, 9, 19, 21, 22]. Based upon these previously published data and our current findings, it is our current hypothesis that Z^- PC inputs are more synchronous compared to the Z^+ PC inputs, which results in a more synchronous inhibition of CN neurons that in turn trigger timed AP firing.

Apart from Purkinje cell synchrony, also the excitatory afferents from mossy and climbing fiber collaterals can have a determining effect on CN spiking patterns. For mossy fiber inputs it was recently shown that selective stimulation can evoke CN action

potential firing [23], a feature that can be modulated by the level of PC synchrony levels [24]. Although the level of synchrony in the numerous mossy fiber sources is likely to be highly variable, it seems likely that an increase in the excitatory input synchronicity will have profound effects on CN spiking. This is also applies to the climbing fiber inputs CN neurons receive. Whereas previous findings indicate that the widely acknowledged anatomical connection is little effective in driving CN action potential firing (e.g. [25]), it has recently been shown that selective optogenetic stimulation of this glutamatergic input depolarizes CN neurons effectively and can readily drive action potential firing [24]. A recent *in vivo* study indicated that in anesthetized mice ~15% of CN action potentials is preceded by climbing fiber inputs [26]. Although it remains to be elucidated how these recording conditions correlate to ours (see below), we assume that also in our *in vivo* dataset a subportion of CN action potential firing is driven by excitatory inputs and thus in principle, the difference in firing frequency between Z^- and Z^+ CN neurons could be at least partially due to a differential input from mossy and/or climbing fiber sources.

The firing frequencies from our *in vivo* awake CN recordings is in the range of previous findings (e.g.,[19]). Although we recorded our subjects a couple of hours after performing surgery, which means that there could be an effect of the used drugs on spontaneous electrophysiological behavior. The most potent and long lasting drug we used is buprenorphine (see materials and methods) which is an opioid receptor modulator. One potential effect of buprenorphine administration can be a decrease of the spontaneous *in vivo* firing, as has been described for the mainolfactory bulb [27],Given that neurons in the cerebellar cortex and CN express low levels of opiate receptors, an similar effect in firing frequency can be a possibility [28]. However, Buprenorphine can also increase the *in vivo* spontaneous firing in dopaminergic neurons in the ventral tegmental area [29], these dopaminergic neurons project directly to multiple cell types in the cerebellar cortex [30], therefore it can cause differential secondary effects in input to the CNn. . Moreover, we are not aware of a differential expression of opioid receptors in Z+ or Z- CN, nor in any afferent and thus the use of buprenorphine does not seem to contribute to the difference in firing rates between Z- and Z+ CN neurons. Another anesthetic we used to sedate the subject for operation purposes was the volatile gas isoflurane. The effect of isoflurane on the firing properties of Purkinje cells is experimentally determined at eight minutes [31], others reported even faster kinetics of releasing the dampening effect on the firing frequency of CNn [19]. We also used Rimadyl cattle, this is a nonsteroidal anit-inflammatory drug which to our knowledge has no effect on electrophysiological properties of neurons. We are convinced that the drugs we used in our *in vivo* experiments do have minimal effects on the neuronal properties. The previous is supported by multiple researches which report lower CNn and PC firing frequencies *in vivo* under influence of anesthesia (CNn: [15, 19, 31, 32]); or

reporting *in vivo* CNn firing frequencies which are comparable with our findings in adult and juvenile animals (adult:[19]; juvenile: [14]). Thus taking into consideration that our in vivo awake recorded firing properties did not deviate from previous *in vivo* awake published word, we conclude that the CNn in our dataset are a good representative for awake spontaneous firing CNn, which are limited influenced by the administered drugs administered for operation purposes.In contrast to the *in vivo* recordings, our *in vitro* data did not show a significant difference in FF between zones. The bath application of AMPA, NMDA and GABA blockers allow us to record only intrinsic activity. All the cells recorded showed high frequency firing rate as previously shown in big glutamatergic neurons [6, 17, 33, 34]. Moreover, we found by histological reconstruction that the recorded neurons had a relatively large soma (figure 3) comparable with data previously shown [17, 32, 34]. As we also found no difference in dendritic branching nor in the action potential half width, the most commonly used electrophysiological discriminator of CN cell types [17], our data indicate that we most likely recorded from a homogeneous cell population that contains glutamatergic projection neurons.

Our current experiments were performed from the second postnatal week, a time span for which it has been shown that GABA-mediated transmission elicits inhibitory responses [35, 36]. We and others found that over the course of the first postnatal months the firing frequency of CN neurons increases over time [14, 37, 38], much alike the increase in PC firing [15]. It remains to be established whether the overt differences in Z- and Z+ PC firing that were recorded in adult mice can also be found in juvenile mice and whether the intrinsic pacemaking activity of PCs differs between zebrin CN.

The striking difference between the CN firing of the individual nuclei remained rather limited, in that solely the difference between the anterior interposed and other nuclei reached a statistically significant level. Although the afferents to the anterior interposed have been studied in several species [39], we are not aware of other publications on the different firing rate of neurons in this nucleus. Several recent studies do pinpoint [40] parts of the interposed nuclei as functionally relevant, in part by its afferents and interconnected loops [23, 41, 42]. For each of these studies it would be of interest to study whether the functional relevance of Z^- or Z^+ innervated CN neurons differs, and thus whether manipulation of the posterior or anterior CN nuclei, differs. In parallel the functional diversification of the other Z- or Z+ domains in CN could be supported by a difference in firing patterns.

Table 1. Statistical data accompanying Figure 1

Panel	Test applied	P-value	Degrees of freedom	Population size	Definition of population
1C Firing Frequency	Paired t-test	*0.0031*	2	97	11 mice
1C CV	Mann-Whitney	0.6208	2	97	11 mice
1C CV2	Mann-Whitney	0.9971	2	97	11 mice
1D Burst index	Mann-Whitney	*0.0040*	2	97	11 mice

Table 2. Statistical data accompanying Figure 2

Panel	Test applied	P-value	Degrees of freedom	Population size	Definition of population
2B V_{rest}	unpaired t-test	0.1067	2	34	28 mice
2B Firing Frequency	unpaired t-test	0.2285	2	34	28 mice
2B CV	Mann-Whitney	0.6366	2	34	28 mice
2B CV2	Mann-Whitney	0.5119	2	34	28 mice
2C I/F	Linear regression	0.1241			18 mice
2C Frequency adaptation	Non-linear Fitting (exponential)	*<0.001* *Plateau different for each dataset*			18 mice

Table 3. Action Potential properties

	Z^+ CN neurons	Z^- CN neurons	*Statistics*
Threshold	-39.3±2.5 mV	-38.7±1.2 mV	M-W *p*=0.56
Peak amplitude (absolute value)	52.1±5.4 mV	45.3±10.3 mV	M-W *p*=0.28
Half width	-13.9±1.2ms	-15.0±2.1ms	M-W *p*=0.80

Table 4. Statistical data accompanying Figure 3

Panel	Test applied	P-value	Degrees of freedom	Population size	Definition of population
3B Soma size	Paired t-test	0.61087	2	32	22 mice
3B Sholl intersections	Chi-square	1.000	2		22 mice

Table 5. Statistical data accompanying Figure 4

Panel	Test applied	P-value	Linear regression- are the line different?	Degrees of freedom	Population size	Definition of population
4A Firing Frequency	Paired *t*-test	P12-14:Z^+ vs Z^-: *0.0391* P15-17:Z^+ vs Z^-: *0.0441* P18-20:Z^+ vs Z^-: 0.1264 P21-24:Z^+ vs Z^-: 0.3207 P30-40:Z^+ vs Z^-: 0.8584	*p*=0.265	2	307	50 mice
CV	Mann-Whitney	P12-14: Z^+ vs Z^-: 0.2814 P15-17: Z^+ vs Z^-: *0.004* P18-20: Z^+ vs Z-: 0.5827 P21-24: Z^+ vs Z^-: 0.7706 P30-40: Z^+ vs Z^-: 0.8418	*p*=0.465	2	307	50 mice
CV2	Mann-Whitney	P12-14: Z^+ vs Z^-: 0.2923 P15-17: Z^+ vs Z^-: *0.0094* P18-20: Z^+ vs Z^-: 0.7319 P21-24: Z^+ vs Z^-: 0.1774 P30-40: Z^+ vs Z^-: 0.5992	*p*=0.655	2	307	50 mice
Burst index	Mann-Whitney	P12-14: Z^+ vs Z^-: 0.3557 P15-17: Z^+ vs Z^-: 0.600 P18-20: Z^+ vs Z^-: 0.0784 P21-24: Z^+ vs Z-: 0.6810 30-40: Z^+ vs Z^-: 0.5766	*p*=0.738	2	307	50 mice
4B1 FF Z+ and Z-	Sperman correlation	Z^+ r=1 Z^- r=1 *p*=*0.0167*		Mean of 307 cells	50 mice	

Table 6. Statistical data accompanying Figure 5

Panel	Test applied	P-value	Degrees of freedom	Population size	Definition of population	Correction
5A FF	Kruskal-Wallis	*0.0191* Lat vs Pin 1.000 Lat vs Med^{+} 1.000 Lat vs Ain 0.828 Lat vs Med^{-} 1.000 Pin vs Med^{+} 1.000 Pin vs Ain 0.050 Pin vs Med^{-} 1.000 Med^{+} vs Ain *0.034* Med^{+} vs Med- 1.000 Ain vs Med^{-} 0.288	4	97	11 mice	Bonferroni
5B CV	Kruskal-Wallis	*0.001* Lat vs Pin 1.000 Lat vs Med^{+} *0.013* Lat vs Ain 0.515 Lat vs Med^{-} 0.333 Pin vs Med^{+} *0.004* Pin vs Ain 1.000 Pin vs Med^{-} 0.895 Med^{+} vs Ain 0.370 Med^{+} vs Med- 1.000 Ain vs Med^{-} 1.000	4	97	11 mice	
5C CV2	Kruskal-Wallis	*0.004* Lat vs Pin 1.000 Lat vs Med^{+} *0.011* Lat vs Ain 0.500 Lat vs Med^{-} 0.466 Pin vs Med^{+} *0.021* Pin vs Ain 1.000 Pin vs Med^{-} 1.000 Med+ vs Ain 0.320 Med+ vs Med^{-} 1.000 Ain vs Med^{-} 1.000	4	97	11 mice	
5D Burst index	Kruskal-Wallis	*0.0000* Med^{+} vs Med^{-} 1.000 Pin vs Med^{+} 0.448 Lat vs Med^{+} 0.905 Med^{+} vs Ain *<0.001* Pin vs Med- 1.000 Lat vs Med- 1.000 Ain vs Med^{-} *0.050* Lat vs Pin 1.000 Pin vs Ain 0.087 Lat vs Ain 1.000	4	97	11 mice	

References

1. Wang, S.S., A.D. Kloth, and A. Badura, *The cerebellum, sensitive periods, and autism.* Neuron, 2014. 83(3): p. 518-32.
2. Strick, P.L., R.P. Dum, and J.A. Fiez, *Cerebellum and nonmotor function.* Annu Rev Neurosci, 2009. 32: p. 413-34.
3. Teune, T.M., et al., *Topography of cerebellar nuclear projections to the brain stem in the rat.* Prog Brain Res, 2000. 124: p. 141-72.
4. Harvey, R.J. and R.M. Napper, *Quantitative studies on the mammalian cerebellum.* Prog Neurobiol, 1991. 36(6): p. 437-63.
5. Person, A.L. and I.M. Raman, *Purkinje neuron synchrony elicits time-locked spiking in the cerebellar nuclei.* Nature, 2011. 481(7382): p. 502-5.
6. Raman, I.M., A.E. Gustafson, and D. Padgett, *Ionic currents and spontaneous firing in neurons isolated from the cerebellar nuclei.* J Neurosci, 2000. 20(24): p. 9004-16.
7. Uusisaari, M. and E. De Schutter, *The mysterious microcircuitry of the cerebellar nuclei.* J Physiol, 2011. 589(Pt 14): p. 3441-57.
8. Gauck, V. and D. Jaeger, *The control of rate and timing of spikes in the deep cerebellar nuclei by inhibition.* J Neurosci, 2000. 20(8): p. 3006-16.
9. De Zeeuw, C.I., et al., *Spatiotemporal firing patterns in the cerebellum.* Nat Rev Neurosci, 2011. 12(6): p. 327-44.
10. Sugihara, I., *Compartmentalization of the deep cerebellar nuclei based on afferent projections and aldolase C expression.* Cerebellum, 2011. 10(3): p. 449-63.
11. Zhou, H., et al., *Cerebellar modules operate at different frequencies.* Elife, 2014. 3: p. e02536.
12. Dehnes, Y., et al., *The glutamate transporter EAAT4 in rat cerebellar Purkinje cells: a glutamate-gated chloride channel concentrated near the synapse in parts of the dendritic membrane facing astroglia.* J Neurosci, 1998. 18(10): p. 3606-19.
13. Ankri, L., Y. Yarom, and M.Y. Uusisaari, *Slice i t hot: acute adult brain slicing in physiological temperature.* J Vis Exp, 2014(92): p. e52068.
14. LeDoux, M.S., D.C. Hurst, and J.F. Lorden, *Single-unit activity of cerebellar nuclear cells in the awake genetically dystonic rat.* Neuroscience, 1998. 86(2): p. 533-45.
15. Arancillo, M., et al., *In vivo analysis of Purkinje cell firing properties during postnatal mouse development.* J Neurophysiol, 2015. 113(2): p. 578-91.
16. Zhou, H., et al., *Differential Purkinje cell simple spike activity and pausing behavior related to cerebellar modules.* J Neurophysiol, 2015. 113(7): p. 2524-36.
17. Uusisaari, M., K. Obata, and T. Knopfel, *Morphological and electrophysiological properties of GABAergic and non-GABAergic cells in the deep cerebellar nuclei.* J Neurophysiol, 2007. 97(1): p. 901-11.
18. Uusisaari, M.Y. and T. Knopfel, *Diversity of neuronal elements and circuitry in the cerebellar nuclei.* Cerebellum, 2012. 11(2): p. 420-1.
19. Hoebeek, F.E., et al., *Differential olivo-cerebellar cortical control of rebound activity in the cerebellar nuclei.* Proc Natl Acad Sci U S A, 2010. 107(18): p. 8410-5.
20. Pugh, J.R. and I.M. Raman, *Potentiation of mossy fiber EPSCs in the cerebellar nuclei by NMDA receptor activation followed by postinhibitory rebound current.* Neuron, 2006. 51(1): p. 113-23.
21. Tang, T., et al., *Synchrony is Key: Complex Spike Inhibition of the Deep Cerebellar Nuclei.* Cerebellum, 2016. 15(1): p. 10-3.

22. Dykstra, S., et al., *Determinants of rebound burst responses in rat cerebellar nuclear neurons to physiological stimuli.* J Physiol, 2016. 594(4): p. 985-1003.
23. Beitzel, C.S., et al., *Rubrocerebellar Feedback Loop Isolates the Interposed Nucleus as an Independent Processor of Corollary Discharge Information in Mice.* J Neurosci, 2017. 37(42): p. 10085-10096.
24. Wu, Y. and I.M. Raman, *Facilitation of mossy fibre-driven spiking in the cerebellar nuclei by the synchrony of inhibition.* J Physiol, 2017. 595(15): p. 5245-5264.
25. Lu, H., B. Yang, and D. Jaeger, *Cerebellar Nuclei Neurons Show Only Small Excitatory Responses to Optogenetic Olivary Stimulation in Transgenic Mice: In Vivo and In Vitro Studies.* Front Neural Circuits, 2016. 10: p. 21.
26. Yarden-Rabinowitz, Y. and Y. Yarom, *In vivo analysis of synaptic activity in cerebellar nuclei neurons unravels the efficacy of excitatory inputs.* J Physiol, 2017. 595(17): p. 5945-5963.
27. Mast, T.G. and E.R. Griff, *The effects of analgesic supplements on neural activity in the main olfactory bulb of the mouse.* Comp Med, 2007. 57(2): p. 167-74.
28. Pert, C.B., A. Pert, and J.F. Tallman, *Isolation of a novel endogenous opiate analgesic from human blood.* Proc Natl Acad Sci U S A, 1976. 73(7): p. 2226-30.
29. Grant, S.J. and G. Sonti, *Buprenorphine and morphine produce equivalent increases in extracellular single unit activity of dopamine neurons in the ventral tegmental area in vivo.* Synapse, 1994. 16(3): p. 181-7.
30. Ikai, Y., et al., *Dopaminergic and non-dopaminergic neurons in the ventral tegmental area of the rat project, respectively, to the cerebellar cortex and deep cerebellar nuclei.* Neuroscience, 1992. 51(3): p. 719-28.
31. Schonewille, M., et al., *Purkinje cells in awake behaving animals operate at the upstate membrane potential.* Nat Neurosci, 2006. 9(4): p. 459-61; author reply 461.
32. Canto, C.B., L. Witter, and C.I. De Zeeuw, *Whole-Cell Properties of Cerebellar Nuclei Neurons In Vivo.* PLoS One, 2016. 11(11): p. e0165887.
33. Aizenman, C.D., E.J. Huang, and D.J. Linden, *Morphological correlates of intrinsic electrical excitability in neurons of the deep cerebellar nuclei.* J Neurophysiol, 2003. 89(4): p. 1738-47.
34. Najac, M. and I.M. Raman, *Synaptic excitation by climbing fibre collaterals in the cerebellar nuclei of juvenile and adult mice.* J Physiol, 2017. 595(21): p. 6703-6718.
35. Gardette, R., et al., *Electrophysiological studies on the postnatal development of intracerebellar nuclei neurons in rat cerebellar slices maintained in vitro. I. Postsynaptic potentials.* Brain Res, 1985. 351(1): p. 47-55.
36. Gardette, R., et al., *Electrophysiological studies on the postnatal development of intracerebellar nuclei neurons in rat cerebellar slices maintained in vitro. II. Membrane conductances.* Brain Res, 1985. 352(1): p. 97-106.
37. Alvina, K., et al., *Questioning the role of rebound firing in the cerebellum.* Nat Neurosci, 2008. 11(11): p. 1256-8.
38. Alvina, K., E. Tara, and K. Khodakhah, *Developmental change in the contribution of voltage-gated Ca(2+) channels to the pacemaking of deep cerebellar nuclei neurons.* Neuroscience, 2016. 322: p. 171-7.
39. Ruigrok, T.J., *Ins and outs of cerebellar modules.* Cerebellum, 2011. 10(3): p. 464-74.
40. Sarnaik, R. and I.M. Raman, *Control of voluntary and optogenetically perturbed locomotion by spike rate and timing of neurons of the mouse cerebellar nuclei.* Elife, 2018. 7.
41. Gao, Z., et al., *Excitatory Cerebellar Nucleocortical Circuit Provides Internal Amplification during Associative Conditioning.* Neuron, 2016. 89(3): p. 645-57.
42. Houck, B.D. and A.L. Person, *Cerebellar Premotor Output Neurons Collateralize to Innervate the Cerebellar Cortex.* J Comp Neurol, 2015. 523(15): p. 2254-71.

3

"The thalamus is like the Flying Dutchman: many heard of it, some believe in it, but few actually seen it"

J.E. Rose

Chapter 4

Differentiating cerebellar impact on thalamic nuclei

Simona V. Gornati*
Carmen B. Schäfer*
Oscar H.J. Eelkman Rooda
Alex Nigg
Chris I. De Zeeuw
Freek E. Hoebeek

*These authors contributed equally

Cell Reports

Summary

The cerebellum plays a role in coordination of movements and possibly also non-motor functions. Cerebellar nuclei (CN) axons connect to various parts of the thalamo-cortical network, but detailed information on the characteristics of cerebello-thalamic connections is lacking. Here, we assessed the cerebellar input to the ventrolateral (VL), ventromedial (VM) and centrolateral (CL) thalamus. Confocal and electron microscopy showed an increased density and size of CN axon terminals in VL compared to VM or CL. Electrophysiological recordings *in vitro* revealed that optogenetic CN stimulation resulted in enhanced charge transfer and action potential firing in VL neurons compared to VM or CL neurons, despite that the paired-pulse ratio was not significantly different. Together these findings indicate that the impact of CN input onto neurons of different thalamic nuclei varies substantially, which highlights the possibility that cerebellar output differentially controls various parts of the thalamo-cortical network.

Introduction

Cerebellar best-known functions are involved in coordinating motor activities. It contributes for example to learning new motor skills and prediction of the sensory consequences of action [1-3]. However anatomical, physiological and neuroimaging studies provide compelling evidence of the cerebellar involvement in various non-motor functions, like cognitive processes, language and emotion, which became established in both animal models and patients [4-8]. For instance, it was recently shown that manipulating the cerebellar output affects sensorimotor integration by somatosensory and motor cortices and thereby could direct voluntary movements [9, 10]. The anatomical connections that underlie such wide impact of cerebellar activity on thalamo-cortical information processing do not only include cerebellar axons that innervate the premotor centers in the brainstem, like the red nucleus, but also a variety of nuclei within the thalamic complex, each of which has reciprocal connections with the cerebral cortex [11-18].

The glutamatergic projection neurons located in the cerebellar nuclei (CN) connect to primary thalamic relay nuclei, like the ventrolateral (VL) nucleus, thalamic motor-associated nuclei such as the ventromedian (VM) nucleus and additionally to intralaminar nuclei such as centromedian, parafascicular and centrolateral (CL) nuclei [16, 19]. Historically the thalamic relay neurons have been divided in two fundamentally different sets: parvalbumin-positive 'core' neurons, which form topographically organized projections to middle layers of patches of cerebral cortex; and calbindin-positive 'matrix' neurons, which send more diffuse projections to the cortices and layers [20, 21]. Provided that CN axons project to thalamic nuclei with high densities of core neurons, like VL and with high densities of matrix neurons, like VM and CL, this connectivity of cerebellar-recipient thalamic nuclei suggests that the cerebellar impact differentially affects cortical information processing. Moreover, single axon reconstructions of cerebellar-recipient zones within VL, VM and CL reveal that their axons also spread throughout other regions [22-24] further highlighting that the cerebellar input can affect a wide range of thalamo-cortical networks and functions.

Apart from their connectivity to the cortex, the heterogeneity of cerebellar recipient thalamic nuclei also extends into the dendritic morphology. For instance, the cerebellar-recipient zones of the VL and VM have been shown to contain neurons with 'bushy' dendrites [22, 23, 25-27] and thereby have a different appearance than CL neurons that show polarized dendritic branching [24]. This variability in the morphological aspects of thalamic neurons in the cerebellar-recipient nuclei corroborates the differential axonal projection patterns and suggests that the impact of cerebellar output on thalamic neurons varies for each target nucleus. Yet, the anatomical and electrophysiological data

on the cerebello-thalamic projections lack an in-depth comparison of the cerebellar impact on the various thalamic targets.

So far, the electrophysiological studies that investigated the cerebello-thalamic projections focused on the VL nucleus. Intracellular recordings in this nucleus in anesthetized rats and cats revealed that electrical microstimulation of the CN neurons or the brachium conjunctivum triggered action potential firing [28-31], which matches the cerebellar-evoked responses in motor cortex [32-34]. Likewise, also single-pulse optogenetic stimulation in CN in the mouse brain has been proven to effectively control thalamo-cortical network activity [10, 35]. Morphological and ultrastructural analysis of the CN axon terminals in VL revealed that they typically synapse perisomatically on large diameter dendrites and form large terminals with various mitochondria and release sites [13, 19, 36, 37]. These findings function as a frame of reference, but a thorough understanding of the cerebellar impact on thalamo-cortical information processing is hampered by the lack of detailed *in vitro* cell physiological analysis and morphological characterization of the CN axonal projections throughout the various thalamic nuclei.

In order to elucidate how the cerebellar impact on thalamic neurons correlates to the specific nuclei, we studied the postsynaptic responses of thalamic relay neurons to selective stimulation of CN axons using *in vitro* whole cell recordings. We focused on neurons in the VL, VM and CL and correlated the electrophysiological data to the morphological details of the target neurons. Our results show that both pre- and post-synaptic aspects of the cerebello-thalamic transmission vary between these thalamic nuclei and thereby provide the first evidence for the functional diversification of the cerebellar impact on thalamo-cortical networks.

Results

Thalamic nuclei receive various densities of CN axons and terminals

To assess the innervation of VL, VM and CL thalamic nuclei by cerebellar axons in the mouse brain, we transfected CN neurons located mostly, but not limited to the interposed CN with a virally encoded ChR2-YFP-expressing construct (Figure 1A). In several mice we found that the medial and lateral CN also contained ChR2-YFP-expressing neurons. In the thalamus we found the level of intensity of this membrane-bound fluorophore to be highest in the VL (55.9±8.0 a.u.) compared to VM (38.7±3.9 a.u.) and CL (25.8±2.3 a.u.) (p=0.529 for VL *vs* VM; p=0.002 for VL *vs* CL, p=0.136 for VM *vs* CL, K-W tests, Dunn's correction; Figure 1B and Table S1).

To dissociate between the active CN terminals and passing axons, we chose to stain for vesicular glutamate transporter 2 (vGluT2), which has previously been shown

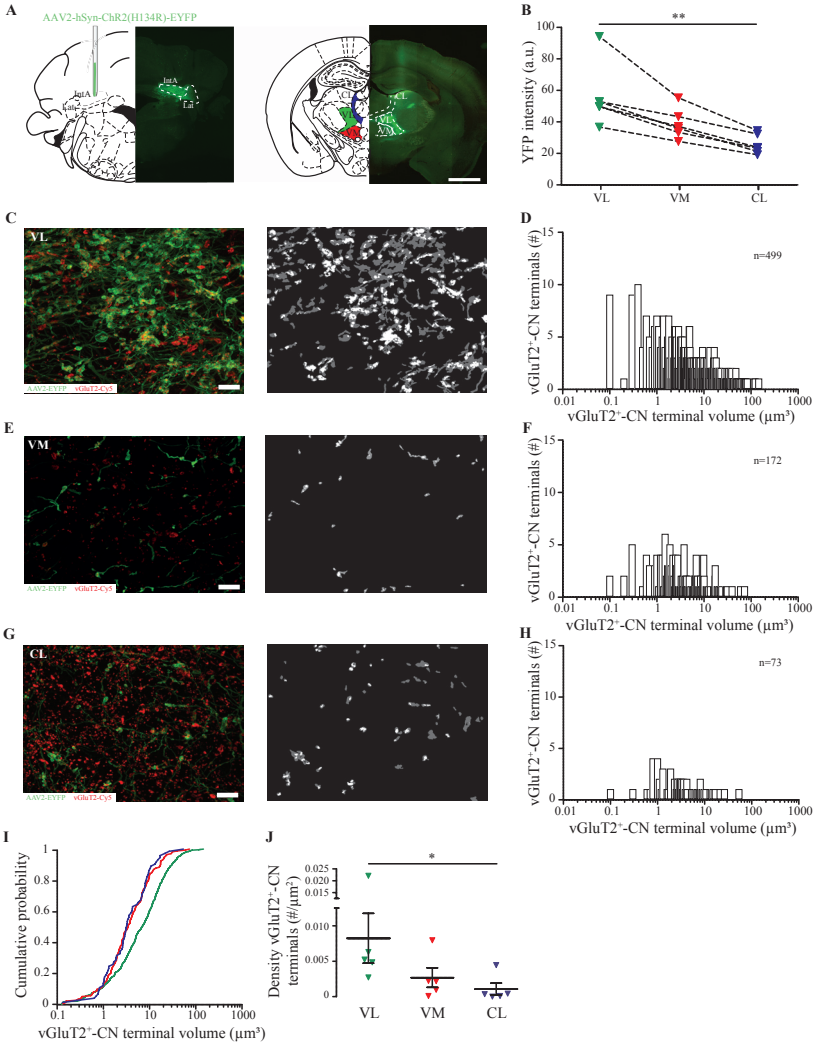

Figure 1. Variable innervation of VL, VM and CL nuclei by CN axons. A schematic representation of the experiment. *Left* AAV-injection in the interposed nucleus and (right) fluorescent (ChR2-EYFP) CN axons throughout the thalamic complex (3 weeks post-injection) of the same mouse. The nuclei of interest are highlighted in green (VL), red (VM) and blue (CL). This color code will be applied throughout all the figures. Scale bar indicates 1 mm. **B** YFP signal intensity in the three nuclei of interest (N = 6 mice) normalized to fluorescence in VL. **C**,**E**,**G** *Left*: maximum intensity projection of *Z-stack* (14 µm thick) showing in green ChR2-EYFP stained CN axons, in red vGluT2 staining and *right* the result of the colocalization mask; gray indicates ChR2-EYFP-stained axons and white vGluT2$^+$ and EYFP **D,F,H** histograms showing vGluT2$^+$-CN terminal volume and number for VL, VM and CL (N=5 mice). **I** cumulative plot of the terminal volume (green: VL; red: VM; blue: CL). (VL vs CL $p<0.001$: VL vs VM $p<0.001$ and VM vs CL $p=0.966$; N=5 mice, K-S test). **J** average density of vGluT2$^+$-CN terminals (VL vs CL $p=0.024$). Data are presented as mean ± S.E.M; * $p<0.05$, *** $p<0.001$. K-W test was used. For full statistical report see Table S1.

to label CN axon terminals [22, 38], and solely quantify the double-labelled vGluT2-positive (vGluT2$^+$) ChR2-EYFP-expressing CN terminals. When we assessed these vGluT2$^+$-CN terminals using stacks of high–magnification images acquired with confocal microscopy and subsequently applied custom-written image analysis scripts, we found that the VL nucleus was most densely populated by vGluT2$^+$-CN terminals (total count 499 vGluT2$^+$-CN terminals; N=5 mice; Figure 1C-D) with a mean volume of 12.45±0.74 µm^3. As previously reported [13], VM encompasses CN axons passing through, some of which send some branches in the most medial part of the nucleus (Figure 1E). The number of vGluT2$^+$-CN terminals in VM was lower compared to VL and their volume was significantly smaller (6.65±0.71 µm^3; n=172 terminals, $p<0.001$, K-S test; Figure 1F,I and Table S1). The CL nucleus showed the lowest number of vGluT2$^+$-CN terminals and their volume was statistically different from VL but not from VM (5.85±0.9 µm^3; n=73 terminals; $p=0.002$ for VL vs CL and p=0.966 for VM vs CL, K-S test; Figure 1G-I and Table S1). We observed a significantly higher density of vGluT2$^+$-CN terminals in VL compared to CL ($p=0.024$; K-W test), whereas the differences in density between VL-VM and VM-CL were not significantly different ($p=0.334$ and $p=0.865$, respectively; K-W tests; Figure 1J and Table S1). These data demonstrate that the cerebellar projection innervates preferentially VL and that these terminals are also bigger compared to VM and CL.

Basic transmission properties of cerebello-thalamic synapses differ across thalamic nuclei

It has been shown by sharp electrode recordings in anesthetized cats and rats that electrical stimulation of CN axons could elicit monosynaptic excitatory post-synaptic potentials (EPSPs) from which a fast spike could arise in VL relay cells [28, 29]. To our knowledge, no data have been published about the postsynaptic currents underlying these changes in VL potentials, or about the postsynaptic responses of thalamic VM or CL cells. To gather these data we performed whole cell patch-clamp recordings of VL, VM and CL neurons in acutely prepared thalamic slices of mice that received bilateral CN injections with ChR2-EYFP-encoding AAV-vectors, which transfected neurons located mostly, but not exclusively, in the interposed nuclei (see material and methods section). We selected the recorded neurons based on their position in the slice, i.e. surrounded by ChR2-EYFP encoding CN axons, their monosynaptic responses to 470 nm optical stimulation (see below) and their anatomical location. Overall, we found that the resting membrane potential of VL (-71.6±0.9 mV), VM (-72.2±2.0 mV) and CL (-70.0±1.4 mV) neurons was not significantly different ($p=0.736$, one-way ANOVA), but that the input resistance of CL neurons was significantly higher than in VL neurons ($p=1$ for VL *vs* VM, $p=0.012$ for VL *vs* CL and $p=0.175$ for VM *vs* CL; n=49; K-W test). In all three thalamic nuclei single light pulses (1 ms, 470 nm, applied through the objective) elicited an EPSC

(Figure 2A). These events were reliably blocked by bath-application of the voltage-gated Na^+-channel blocker tetrodotoxin (TTX) (n=5 cells; >99% decrease in charge transfer), which indicates that the postsynaptic events were triggered by action potential-driven release of glutamate from CN terminals (data not shown). The mean EPSC amplitude that we could maximally evoke was significantly higher in VL than in VM and CL (VL: -847.7±109.5 pA; VM: -165.0±40.2 pA; CL: -210.8±89.2 pA; p=0.001 for VL *vs* VM, p<0.001 for VL *vs* CL and p=1 for VM *vs* CL; K-W tests), which was also represented in the evoked charge (VL: -3820±595 pA*ms; VM: -862±235 pA*ms; CL: -1284±542 pA*ms; p=0.002 for VL *vs* VM; p=0.001 for VL *vs* CL, p=1 for VM *vs* CL; K-W tests; Figure 2B and Table S2). The variability in optically stimulated EPSC amplitude and charge was quantified by calculating the coefficient of variation (CV) (Figure 2C). We found significant differences in the CV of EPSC amplitudes (VL: 0.13±0.02; VM: 0.25±0.04; CL: 0.38±0.07; p=0.031 for VL *vs* VM, p=0.001 for VL *vs* CL; p=1 for VM *vs* CL, K-W tests, Dunn's correction; Figure 2D and Table S2) and of EPSC charge (VL: 0.13±0.02; VM: 0.28±0.04; CL: 0.47±0.12; p=0.03 for VL *vs* CL, p=0.025 for VL *vs* VM, p=1 for VM *vs* CL, K-W tests, Dunn's correction and Table S2). We found no significant correlation of the incubation time to the EPSC amplitude, nor to the CV of the EPSC amplitude (p=0.470, r_s=0.116 for EPSCs and p=0.269, r_s=0.161 for CV, Spearman correlation), which supports the notion that the difference in postsynaptic responses is actually due to a difference in the charge transfer between CN axons in VL, VM and CL neurons.

To establish the impact of neurotransmitter release from CN terminals on thalamic neurons' membrane potential we also recorded a subset of cells in current clamp (Figure 2E). When stimulated at maximum light intensity most VL neurons fired action potentials (9 cells out of 10) whereas most VM (3 out of 3) and CL neurons (4 out of 5; Figure 2F) did not. The probability to elicit an action potential was not related to the resting membrane potential of the cell (p=0.628; r_s=-0.127, Spearman correlation). As we expected from the EPSC amplitudes, neurons in VL fired action potentials more readily than those in VM and CL.

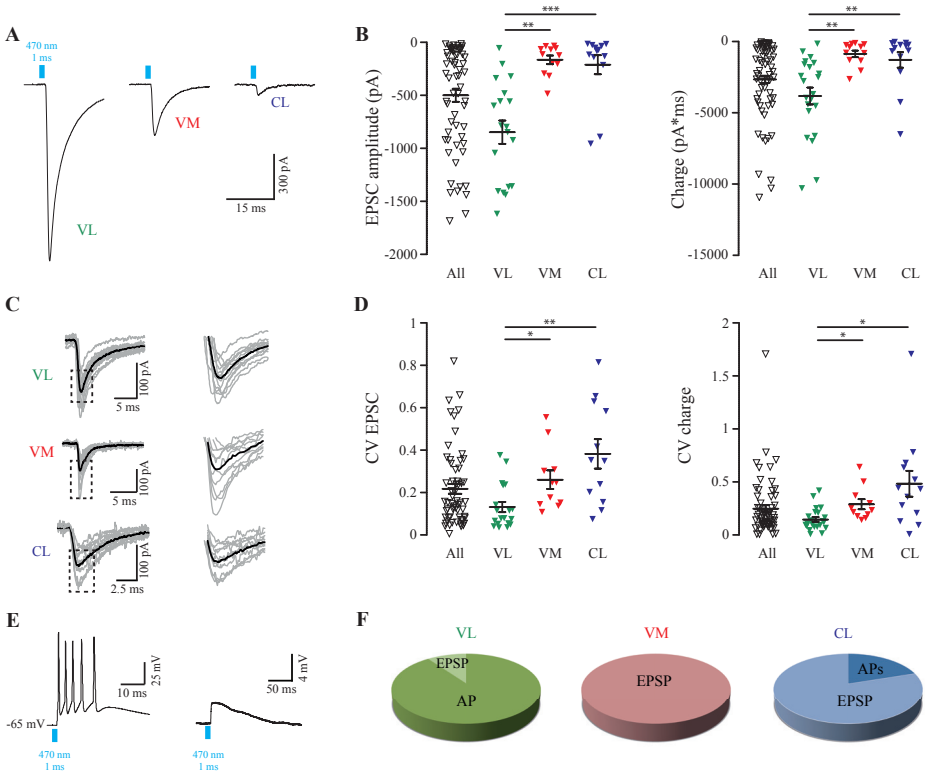

Figure 2. Charge transfer between CN axons and thalamic neurons differs for VL, VM and CL. **A** optical wide field stimulation of CN terminals (470 nm, 1 ms pulse length) evoked EPSCs of variable amplitude in VL, VM and CL. **B** quantification of EPSCs amplitude and charge for all recorded cells (n=63 for EPSC amplitude and n = 65 for charge) and for the nuclei of interest (EPSC: VL: n=19; VM: n=12; CL: n=13; charge: VL: n=22; VM: n=12; CL: n=13, respectively; 'All' category represents all cells recorded, of which some were not recovered by histology and therefore were not classified to a specific nucleus – note that all cells in VL, VM and CL are also represented in 'All'). **C** example traces of EPSCs amplitude in gray and average trace in black. Note the variability in EPSC amplitude of individual responses. **D** coefficient of variation (CV) for (left) EPSCs amplitude and (right) EPSC charge. **E** example traces of (left) action potential (AP) firing or (right) excitatory postsynaptic potential (EPSP) evoked by single pulse CN stimulation. **F** pie charts representing responses to CN stimulation recorded in current-clamp mode (VL: n=9 AP, n=1 EPSP; VM: n=3 EPSP; CL: n=1 AP, n=4 EPSP). Data are presented as mean ± S.E.M; * $p<0.05$, ** $p<0.01$, *** $p<0.001$. K-W was used. For full statistical report see Table S2.

Thalamic responses show paired-pulse depression and are predominantly sensitive to ionotropic glutamate receptor blockers

Thalamic afferents are often categorized as 'driver' or 'modulator' [39, 40]. This classification is partially determined by the response to repetitive stimulation of presynaptic terminals: driver synapses are thought to show paired-pulse depression

(PPD) whereas modulator synapses evoke paired-pulse facilitation (PPF) [41-43]. Although cerebellar input to motor thalamus has been listed as driver input [39], short-term synaptic dynamics of thalamic responses following repetitive CN stimulation in VL, VM and CL still need to be evaluated. Here we performed voltage-clamp recordings while stimulating the CN terminals repetitively with trains of light pulses at 10, 20 and 50 Hz (Figure 3A-C). To evaluate the time course of the depression we normalized EPSC amplitudes to the first peak amplitude (Figure 3D-F).

In general, we found that the ratio between the amplitudes of the first two EPSCs showed a PPD at all frequencies tested (Figure 3G). At 50 Hz the second EPSC showed a ~twofold reduction in amplitude compared to the initial one (VL: 0.52±0.06; VM: 0.72±0.12; CL: 0.41±0.08), whereas lower frequency stimulations showed a smaller effect on the paired-pulse depression. At 20 Hz the depression was around 30% of the first EPSC in all the nuclei (VL 0.70±0.02, VM 0.77±0.10, CL 0.73±0.07) whereas at 10 Hz only VL (0.80±0.03) and VM (0.88±0.04) neurons showed on average PPD but CL did not (1.08±0.25) (Figure 3H). When we compared the paired-pulse depression across all nuclei for each frequency, we found that the ratio between the first two responses did not show any significant difference between the nuclei (10 Hz: p=0.344; 20 Hz: p=0.168; 50 Hz: p=0.137, K-W tests, Dunn's correction; Figure 3H and Table S3).

Next, we analyzed the subsequent responses to the train stimulation to determine the average sustained release of presynaptic terminals during high frequency steady-state synaptic transmission (Figure 3A-C). For this analysis, the average phasic EPSC amplitude within the train was normalized to the average first EPSC amplitude for each frequency and each nucleus. Across all recorded cells, we find normalized steady state amplitudes of 64.4±3.1% (VL), 71.3±6.9% (VM) and 81.4±8.9% (CL) at 10 Hz: 53.1±3.6% (VL), 70.1±11.1% (VM) and 85.2±28.0% (CL) at 20 Hz and 44.4±5.0% (VL) 41.9±6.5% (VM) and 39.1±7.7% (CL) at 50 Hz (Figure 3I and Table S3). We found no significant differences between the values recorded per nucleus, but did find that in VL the steady-state depression was significantly higher at 50 Hz than at 10 Hz (p=0.005, K-W test, Figure 3I and Table S3). These data indicate that the general tendency for transmission at cerebello-thalamic synapses in VL, VM and CL is to show a depression of neurotransmitter release in response to repetitive stimulation.

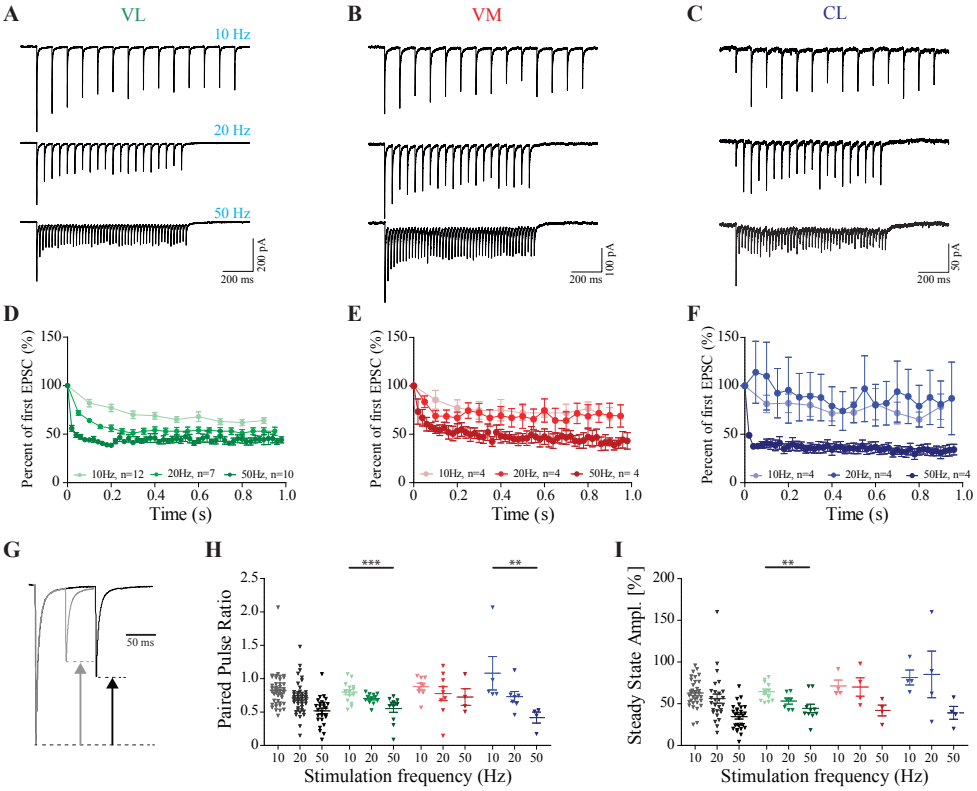

Figure 3. High-frequency stimulation results in paired-pulse depression of EPSC. A,B,C averaged responses of VL, VM and CL neurons (of 5 repeats) to 1 sec trains of 10 Hz, 20 Hz or 50 Hz stimuli. **D,E,F** average normalized EPSC amplitudes for 10, 20 and 50 Hz stimulus trains. **G** superimposed example responses (average of 5 repeats) to paired-pulse stimulation at 10 Hz (black) and 20 Hz (grey). **H** average paired pulse ratio at 10, 20 and 50 Hz for each recorded cell in each nucleus. **I** average normalized steady state response amplitude during the last 5 stimuli of the train for each cell in each nucleus. (For panels H VL: n=39; VM: n=22; CL: n=16 and I VL: n=29; VM: n=12; CL: n=12). ** p<0.01, *** p<0.001. K-W test was used. For full statistical report see Table S3.

Our results indicate that the synaptic transmission at cerebello-thalamic synapses in VL, VM and CL are glutamatergic, which matches previous *in vivo* findings on the excitatory responses of VL neurons evoked by microstimulation of the brachium conjunctivum or the neurons in CN [28-31]. To elucidate whether these excitatory postsynaptic responses where mediated by ionotropic and/or metabotropic receptors we next tested the effects of their selective blockage on the responses to 50 Hz stimulus trains. Upon wash-in of AMPAR-antagonist NBQX the EPSC charge decreased from -74.6±2.4 nA*ms to -28.0±8.3 nA*ms and following the wash-in of NMDAR-antagonist APV the EPSC charge decreased even further to -13.5±4.3 nA*ms (p<0.001, Friedman test; Figure

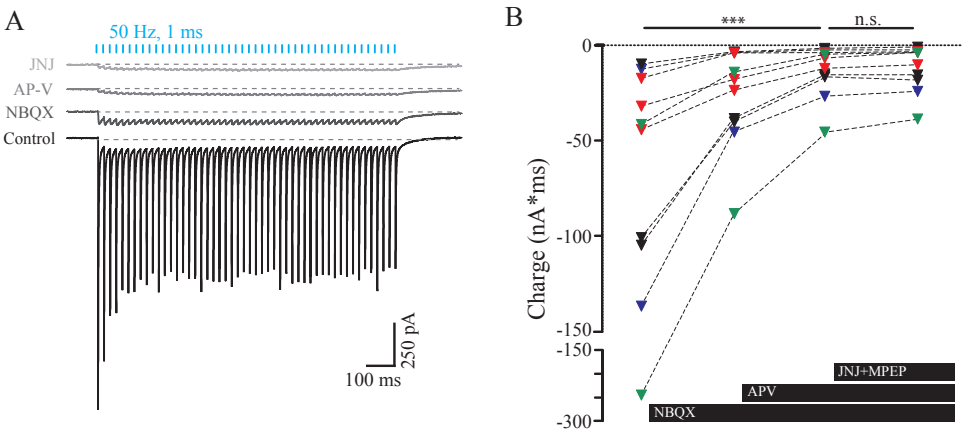

Figure 4. Thalamic responses to CN-stimulation are sensitive to ionotropic receptor blockers. **A** example traces of averaged EPSCs evoked by 1 sec train of 1 ms pulses at 50 Hz in control (aCSF) conditions and following application of NBQX, APV and JNJ to block AMPA, NMDA and mGluR1 and 5 receptors, respectively. **B** summary data showing the decrease of charge after drug application (VL in green, VM in red, CL in blue, undefined location in black; n=10 in total). *** $p<0.001$. For full statistical report see Table S4.

4A,B and Table S4). Further application of blockers for the mGluRs most abundantly expressed in thalamic neurons (JNJ for mGluR1 and MPEP for mGluR5 [41, 44]) did not affect the remaining current (-12.1±3.9 nA*ms; Friedman test, $p=1$; Figure 4B and Table S4), suggesting the absence of a substantial mGluR1- or mGluR5-mediated component in cerebellar transmission on thalamic neurons.

Postsynaptic determinants of variable CN-impact in thalamic cells

Next we evaluated whether the electrophysiological characteristics described above could be linked to the morphology of the thalamic neurons, bearing in mind that in rat thalamus the neuronal morphology in VL, VM and CL neurons varies [22-25, 45-47]. By reconstructing biocytin-filled neurons throughout the VL, VM and CL nuclei (Figure 5A) and analyzing their dendritic branching using a 3D-Sholl analysis (Figure 5B) we found that 23 VL neurons on average show a more elaborate branching pattern than the 14 CL neurons at 55 µm distance from the soma ($p<0.05$, 2-way ANOVA; Mann Whitney comparison, Figure 5C,D and Table S5). The number of proximal dendrites (VL: 8.13±0.47; VM: 7.83±0.83; and CL: 6.83±0.34) was not significantly different between nuclei ($p=0.115$, K-W test; Figure 5E and Table S5). To better illustrate the dendritic architecture of cells in each of the three defined nuclei we also quantified the angular distance between dendrites at 15 µm from the soma. We found no significant difference in the angular distance (VL: 40.2±2.6°; VM: 41.1±3.5°; CL: 47.0±2.8°; $p=0.14$, K-W test;

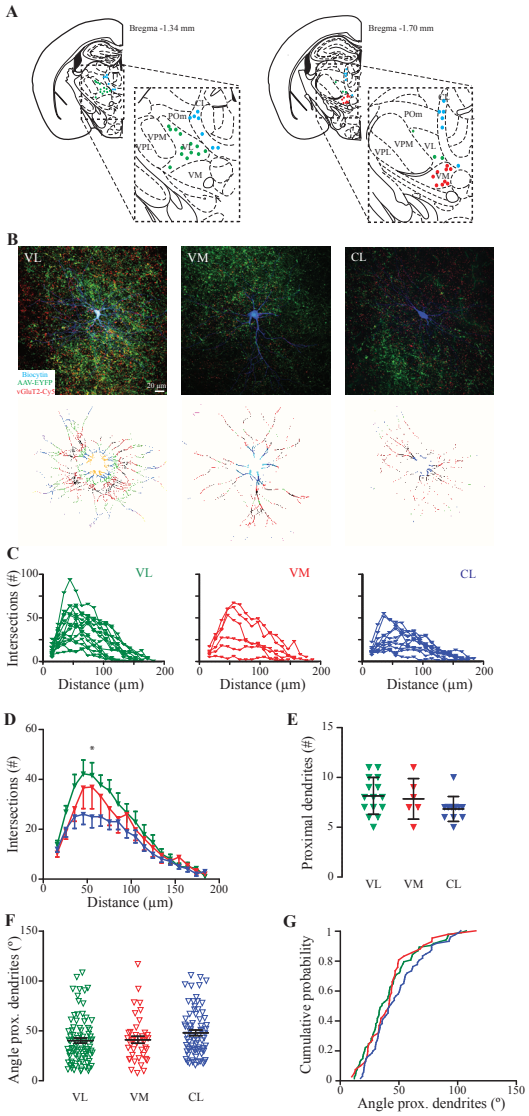

Figure 5. Morphological characterization of thalamic cells recorded in VL, VM and CL. A location of all recorded cells in VL, VM and CL projected on two coronal planes [78]. **B** *Top* maximum projections of the somatodendritic morphology of biocytin-filled cells (blue), surrounding ChR2-EYFP labelled CN axons (green) and vGluT2-staining (red) for VL (left), VM (middle) and CL (right). *Bottom*: maximum projections of 10 µm-thick 3D-spheres surrounding an example neuron from VL, VM and CL (as indicated by the different colors along dendritic trees). **C** Sholl analysis shows dendritic arborisation by the number of intersections of the concentric spheres for VL (left), VM (middle) and CL (right) (VL: n=15; VM: n=6; CL: n=11). **D** average number of dendritic intersections is shown in 10 µm steps from the soma and each nucleus. **E** number of proximal dendrites as quantified at 15 µm distance from soma for VL, VM and CL (VL: n=15; VM: n=6; CL: n=11). **F** directionality of proximal dendrites (at 15 µm from soma center) is determined by the angle between individual dendrites. Note that the angle is proportional to the angular distance between two neighboring dendrites. **G** cumulative distribution of data represented in panel *F*. * $p<0.05$, ** $p<0.01$. For full statistical report see Table S5.

Figure 5F,G and Table S5). Although limited, these morphological distinctions between cerebellar-recipient neurons possibly corroborate the distinct electrophysiological characteristics, which together suggest a differential impact of cerebellar input to thalamic neurons.

Distribution and morphology of reconstructed CN terminals

Previous structural studies in rats suggested that in VL cerebellar terminals are larger than those in intralaminar nuclei [19]. To further characterize the identity of cerebellar terminals for each recorded neuron, we stained the tissue slices containing the patched neurons for vGluT2 and assessed the morphology of the vGluT2^{+}-CN terminals using high magnification confocal microscopy (Figure 6A). The number of vGluT2^{+}-CN terminals on the recorded cells did not vary significantly between the nuclei (VL: 4.5±0.7; VM: 3.66±1.17; CL: 3.08±0.83; p=0.37, K-W test, Figure 6C, Table S6) neither their distance from soma (VL: 26.7±1.9 µm; VM: 33.8±5.7 µm; CL: 26.6±2.5 µm; p=0.58, K-W test, Figure 6D; Table S6). To enhance the *x-y* resolution and reduce the blurring caused by the point spread function, we deconvolved the images and selected the virus-labeled vGluT2^{+}-CN terminals to measure their volume (Figure 6B). We found that terminals onto recorded VL neurons had a larger volume (11.67±1.30 µm^3) than those onto recorded CL neurons (CL: 7.23±1.57 µm^3) (p=0.02, K-W test, Figure 6E-F and Table S6), whereas no significant differences were found comparing VM terminals (9.26±1.93 µm^3) to VL and CL (p=1.00 and p=0.35, respectively, K-W tests, Figure 6E-F and Table S6).

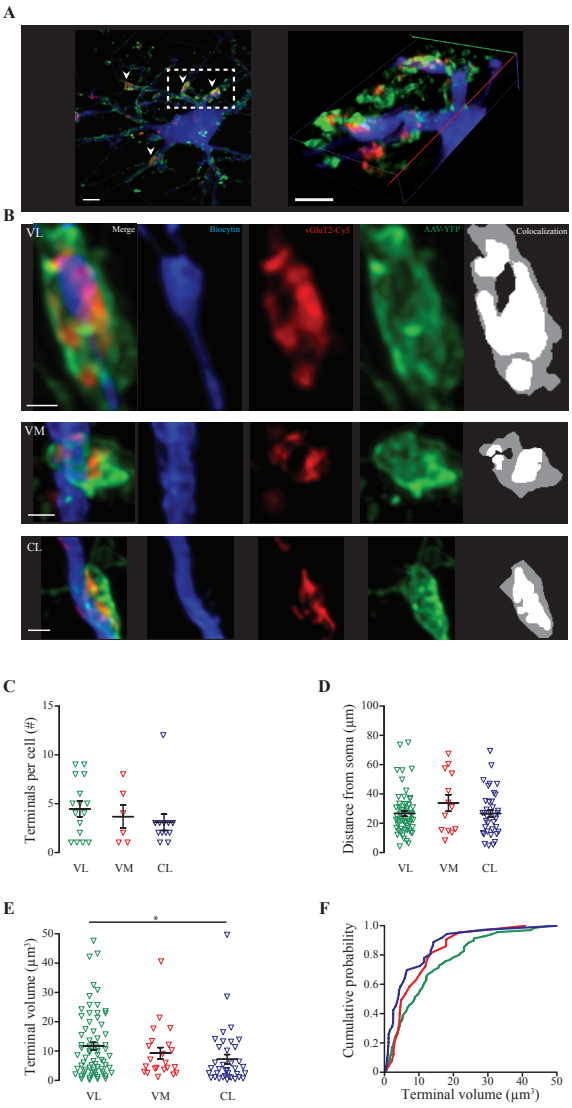

Figure 6. CN terminals of variable volume are similarly positioned along dendrites of recorded thalamic neurons. A maximum intensity projection of Z-stack image (22 µm thick) of biocytin filled neuron (blue: streptavidin-Cy3; green: ChR2-YFP terminals; Red: vGluT2-Cy5). Arrowheads indicate the vGluT2^{+}-CN terminals onto proximal thalamic dendrites. Scale bar 10 µm. *Right:* 3D reconstruction of inset in A. Scale bar 2.5 µm. **B** *Left four panels:* example of vGluT2^{+}-CN terminals in VL, VM and CL (blue: thalamic dendrite; red: vGluT2; green: CN terminal). *Right panel*: colocalization of ChR2-EYFP and vGluT2-staining to identify active terminals and calculate their volume based on ChR2-EYFP signal. Scale bar 1 µm. **C** summary data of the number of reconstructed vGluT2^{+}-CN terminals (VL: n=16; VM: n=6; CL: n=12). **D** summary data of distance of reconstructed terminals from soma (VL: n=60; VM: n=13; CL: n=37. **E-F** terminal volume (VL: n=71; VM n=22; CL n=37) and cumulative distribution. * p<0.05. For full statistical report see Table S6.

To further investigate CN axon terminal dimensions and characteristics of the post-synaptic structures we studied synaptic contacts at the ultrastructural level. To identify CN axon terminals in electron micrographs we collected VL, VM and CL tissue from mice which we injected with biotin dextran amine (BDA) in CN, which spread mostly, but not exclusively, in the interposed CN. Representative examples of the synaptic profiles formed by BDA- stained CN terminals and thalamic neurons are shown in figure 7A. Measurements made from the profiles included terminal surface, number and size of mitochondria, dendritic diameter, PSD length and number of release sites per terminal (Figure 7B). Although we observed in the fluorescent images that the terminal size was significantly different between VL and CL, at the ultrastructural level the difference was not significant even though on average VL terminals appeared to be bigger (VL: n = 42 terminals; 2.35±0.38 μm^2; VM: n = 27 terminals; 2.07±0.31 μm^2; CL: n = 28 terminals; 1.23±0.11 μm^2 p=0.099, K-W test). We did observe a significant difference in the mitochondrial surface between VL and CL (VL: 0.13±0.01 μm^2; VM: 0.10±0.01 μm^2; CL: 0.06±0.01 μm^2; VL vs VM p=0.034; VL vs CL p<0.001; VM vs CL p< 0.001; K-W test; Figure 7B and Table S7), which correlated significantly with the total surface of the terminals (r_s=0.7156; p<0.001, Spearman correlation; Figure 7C and Table S7). Another characteristic of cerebello-thalamic synapses we could observe in all three nuclei is that most terminals contained several release sites (VL: 2.97±0.38; VM: 3.08±0.47; CL: 2.96±0.29; p=0.667; K-W test) [13]. The axon terminals in VL and VM also showed a more complex interaction with the postsynaptic structures than in CL, in that we found dendritic protrusions inside the majority of the VL (24 out of 42 terminals) and VM (17 out of 27) terminals, whereas this was less common in CL (4 out of 28) terminals. No significant differences were found in the surface of the dendritic protrusions between the thalamic nuclei (VL: 0.23±0.16 μm^2; VM: 0.29±0.18 μm^2; CL: 0.13±0.12 μm^2; p=0.1723; K-W test). The surface area of the dendritic protrusions showed a significant correlation with the terminals surface (r_s=0.6146; p<0.001, Spearman correlation; Figure 7C and Table S7). At the post-synaptic side we found that although the dendritic diameter opposing CN terminals did not show any difference between the nuclei (VL: 0.97±0.13 µm; VM: 1.18±0.12 µm; CL: 0.84±0.08 µm; p=0.08; K-W test), we did find that the length of post-synaptic densities (PSD) was longer in VL (0.17±0.01 µm) compared to VM (0.14±0.01 µm) and CL (0.15±0.01 µm; VL vs VM: p=0.024; VL vs CL: p=0.055; VM vs CL: p=1; K-W test). Altogether, these ultrastructural findings support the notion that CN axons tend to synapse on proximal dendrites in all three studied nuclei, but that there may be a structural difference in the constellation of the pre- and post-synaptic sites which could correlate to the difference in transmission at CN-synapses throughout the thalamic complex.

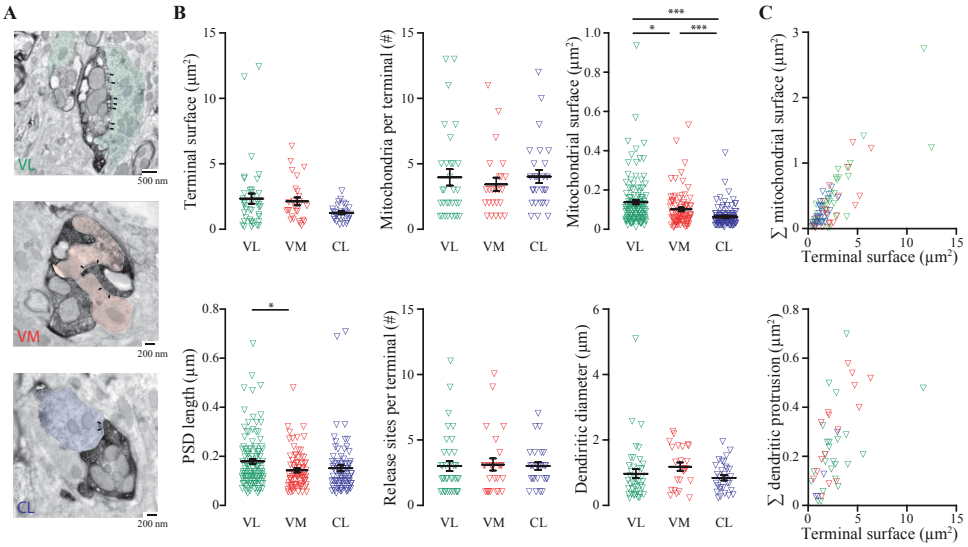

Figure 7. Ultrastructure of CN terminals in VL, VM and CL reveals pre- and post-synaptic specialization. A pseudo-colored ultramicrographs of CN terminal in VL (top), VM (middle) and CL (bottom). Note the complex structure of these terminals. Arrowheads indicate synapses. **B** quantification of terminal surface (top left; VL: n=48; VM: n=28; CL: n=27), number of mitochondria (top middle; VL: n=32; VM: n=27; CL: n=24), mitochondrial surface (top right; VL: n=124; VM: n=109; CL: n=82; VL vs VM p=0.034; VL vs CL p<0.001; VM vs CL p<0.001, K-W tests), length of post-synaptic density (PSD) (bottom left; VL: n=114; VM: n=81; CL: n=80; VL vs VM p=0.024; VL vs CL p=0.055; VM vs CL p=1; K-W test), release sites per terminal (bottom middle; VL: n=37; VM: n=27; CL: n=26; p=0.667, K-W test) and diameter of the contacted dendrite (bottom right; VL: n=40; VM: n=31; CL: n=25; p=0.080, K-W test). **C** *Top* correlation of the terminal surface with the sum of the surface occupied by mitochondria for each given terminal (VL: green; VM: red; CL: blue). *Bottom* Correlation of the terminal surface with the sum of the surface occupied by dendritic protrusions for each given terminal. Note that terminals without a mitochondria or dendritic protrusion are not represented in these correlation plots. * p<0.05, *** p<0.001. For full statistical report see Table S7.

Discussion

Our data show that in mouse brain CN neurons innervate the VL thalamic nucleus more densely compared to VM and CL. Although the distribution matches that in other species [11-14, 16, 17, 19, 48] our study does provide one of the first quantitative comparisons of active CN axon terminals in VL, VM and CL, since we exclusively quantified the vGluT2^{+}-CN terminals that expressed ChR2-EYFP. Our density values of these CN terminals per nucleus (Figure 1) may very well be an underestimate of the total proportion of CN axons that innervate VL, VM and CL nuclei given that i) the injections of viral particles did not transfect the complete CN population projecting to these nuclei and ii) the use of vGluT2-antibodies most likely resulted in a limited penetrance into the slices, leaving those ChR2-expressing CN terminals located deeper into the slice unstained. These aspects possibly also confound the number and location of CN axon terminals on a single thalamic neuron (Figure 6) in that there may have been more CN terminals that contributed to the evoked charge transfer, but that due to their location, i.e., depth in the slice, some were identified as vGluT2-negative. Still, we would like to emphasize that the difference in the number of CN terminals between VL, VM and CL is likely to be independent from viral transfection rates or antibody penetrance since these data have been gathered from the same tissue samples.

A potential source for the variability of CN-evoked responses in thalamic neurons and the difference in CN-terminal morphology throughout the thalamic nuclei may be the location of the transfected CN neurons. According to previous anatomical studies that used classical neurotracers, glutamatergic projection neurons from the lateral, interposed and medial CN all innervate VL, VM and CL neurons with a clear preference for the contralateral thalamic complex, but not excluding ipsilateral projections [12, 14, 16]. Whereas we aimed for centering our bilateral viral injections in the interposed nuclei, we also found ChR2-EYFP transfected CN neurons in the lateral and/or medial CN in several mice. Although in principle it is possible that the variability in the recorded responses and terminal morphology is due to the transfection of glutamatergic CN neurons in various nuclei in both sides of the cerebellum, there are currently no data available supporting such notion. In fact, the few data available on the direct comparison between axon terminals from the various nuclei reveal that the dimensions and ultrastructural morphology in thalamic nuclei is comparable between axons originating from interposed and lateral CN [13]. These anatomical data are corroborated by the previous *in vivo* electrophysiological experiments using intracellular and extracellular recordings in anesthetized cats that revealed that electrical stimulation of both the interposed and lateral CN can evoke postsynaptic responses in single VL thalamic neurons [28, 30, 31, 49, 50]. A set of dedicated *in vitro* experiments using tissue with

small injections in the single CN will provide further insight in the potential role of the various CN in the differentiation of the cerebellar impact on thalamic nuclei.

The electrophysiological characterization of thalamic responses to CN stimulation revealed that on average VL neurons showed larger EPSCs than those in VM or CL. As expected, these voltage-clamp results translated to a higher chance of action potential firing upon stimulation for VL than for VM and CL when recorded in current-clamp. Our data from VL and VM match earlier reports about faithful action potential firing by VL neurons upon CN or brachium conjunctivum stimulation [28-31, 34, 51] and provide the first detailed insights for synaptic transmission at CN-CL synapses (cf. [52, 53]). Using 10, 20 and 50 Hz stimulus trains, we were able to sample the responses of thalamic neurons to physiologically relevant cerebellar input, since the firing rates reported for CN projections recorded *in vivo* range from ~30-100 Hz (as reviewed by [54]). We consistently found that the responses in VL, VM and CL neurons showed paired-pulse depression, which is suggested to play an important role in information processing by helping the system to adapt to ongoing levels of activity [41, 55, 56]. In our current experiments the ChR2 off-kinetics limited us to stimulus frequencies well below the maximal CN firing rates, which may also have prevented us from recording a significant effect of mGluR-receptor blockage, in that the total mGluR-mediated currents in thalamic neurons evoked by a stimulus frequency of 50 Hz tends to be limited (see also [57]). Therefore, we cannot rule out that the activation of either pre- or postsynaptic modulatory mechanisms have affected the responses we recorded *in vitro*.

Referring to intracellular *in vivo* recordings, the cerebellar input on VL neurons has been classified as a driver input to neurons in the motor domain of the thalamus [28, 29, 39]. However, several recent papers classify thalamic inputs in more than two categories: in addition to the 'driver' and 'modulator' inputs, a third category of 'driver-like' input has been defined [58, 59]. In the tecto-geniculate system the driver-like inputs have also been identified at the anatomical level by medium-sized terminals that contain round vesicles and innervate proximal dendrites, and at the electrophysiological level stable response amplitudes to trains of stimuli of up to 20 Hz [60, 61]. Our *in vitro* data showed that responses in VL neurons to stimulation of CN terminals meet a number of criteria used to define driver inputs [40]: *i*) CN stimulation evokes a large post-synaptic current that *ii*) is solely mediated by ionotropic receptors and *iii*) depresses upon higher-frequency stimulation, *iv*) CN axons form large synaptic boutons that *v*) contact proximal thalamic dendrites. For CN terminals in VM and CL the categorization is less clear, since these only show some of the 'driver' characteristics. They lack mGluR-mediated transmission and proximal terminal location and their terminal volume is smaller. Moreover, the responses of VM and CL neurons to CN stimulation are significantly smaller, and CL neurons tend to show a stable paired-pulse ratio in response to 10 Hz stimulus trains.

At the ultrastructural level, we also found a trend, although not significant, to a reduced terminal surface in CL compared to VL and a significantly smaller CL mitochondrial surface. Given that previous studies revealed that terminals with larger surface have a higher chance to release neurotransmitter compared to smaller terminals [62-64], our data may at least partially explain why the evoked response amplitude and charge in CL were smaller and more variable (Figure 2).

Further explanation for the difference in post-synaptic responses to CN stimulation between VL and the other nuclei may come from the difference in PSD length, which previously has been linked to neurotransmission efficacy [65]. Our ultrastructural analysis of CN terminals further revealed that the characteristics described earlier for VL in the rat brain, i.e., large terminal surface, presence of multiple mitochondria, fragmented release sites and large diameter of opposing dendritic structure [13, 36, 37], are also found in mouse brain. The complexity of the cerebello-thalamic contacts in the VL and VM seemed more prominent, in that CN terminals in these nuclei were found to contain dendritic protrusions more often than in CL. This typical structure, found also in other large terminals in thalamus, such as those formed by the piriform cortex in medial thalamus [66], enlarge the contact surface between axon terminals and the dendrite. However, in our current dataset we found no significant difference between the number of release sites for VL, VM or CL. Future experiments on the release properties of single CN terminals, alike those performed for 'giant' corticothalamic synapses in the sensory system [42, 43] should elucidate how the morphological characteristics can translate into the clear differentiation between postsynaptic responses in VL, VM and CL.

Our current findings provide new building blocks to construct the frame of reference for the impact of the cerebellar output on thalamic neurons. Given that mouse thalamus VL, VM and CL are free of interneurons, we argue that all our recordings are from thalamic relay neurons that synapse throughout the various regions of the cerebral cortex. By adapting the classification of relay neurons from rat thalamus (reviewed by [25]), our VL recordings are from a mix of core (C)-type and matrix (M)-type neurons, VM recordings are from matrix (M)-type neurons and CL recordings from intralaminar (IL)-type neurons, which to some extent is supported by the reduced dendritic branching of CL neurons (Figure 6). If we assume that the axonal branching of C-, M- and IL-neurons in mouse brain indeed shows lamina-specific termination as described for rat [18, 22-24, 67], our data indicate that the information conveyed by C- and M-type neurons in VL to manipulate activity of the middle and output layers of motor cortices [22] that contribute to initiation of movement [68]. In contrast, M-type VM neurons projections are more dense in layer 1 of widespread cortical areas, including the motor-associated, orbital, cingulate and visual areas in the rat [23]. Direct activation of cerebellar afferents to VM neurons indeed resulted in a widespread change of cortical activity to the

gamma-band range [34], which in these VM-projection regions have been linked to cognitive processes. Indeed, a recent study indicates that the cerebellar-recipient zone in mouse VM has a reciprocal connection with the prefrontal anterior lateral motor cortex that determines the ability to prepare a correct motor response to a sensory cue [69]. For IL-type CL neurons it has been shown that their axons excite striatal, but also cortical neurons affecting motor, premotor, parietal, prelimbic and anterior cingulate processing, as well as regulating behavioral arousal levels [53, 70, 71].

Although it remains to be investigated how in *in vivo* conditions thalamic responses may differ between the different types of neurons, our study provides new insights into the diversity of the cerebellar impact on thalamo-cortical networks. Thalamo-cortical activity exhibits two distinct states, i.e., tonic and burst firing, which are related to different conditions such as waking, non-REM state, slow-wave sleep or even epileptogenic activity [72]. Thalamic afferents, like CN axons, are likely to modulate the activity of thalamo-cortical relay neurons from tonic to burst firing and vice versa. Indeed, single-pulse stimulation of CN neurons efficiently stops thalamo-cortical oscillations in epileptic mutant mice [35]. The underlying mechanism may at least partially depend on the variable impact of CN axons on thalamic neurons, as we showed for VL, VM and CL. For instance, a brief pause in the firing of CN neurons, which can occur following synchronized activity in the cerebellar cortex [54] will most likely result in a recovery of synaptic PPD for all nuclei, but the first postsynaptic response in VL will be notably larger than in VM or CL. Such differential effects on thalamic action potential firing may potentially be modulated by cortical input, as well as glycinergic or cholinergic projections arising from brainstem [73, 74] or GABAergic projections from substantia nigra [75], all of which may synergistically diversify the cerebellar impact on thalamo-cortical processes throughout the various (non-) motor domains.

Experimental procedures

Animals

All experiments were performed in accordance with the European Communities Council Directive. Protocols were reviewed and approved by the Dutch national experimental animal committees (DEC) and every precaution was taken to minimize stress, discomfort and the number of animals used. Data were collected from 21-56 day old C57BL/6NHsd mice of both sexes, which were purchased from Envigo laboratories (Horst, Netherlands).

Virus injections

We performed stereotaxic injections of adeno-associated virus carrying Channelrhodopsin2 AAV2-hSyn-ChR2(H134R)-EYFP into CN at 2 mm anterior-posterior and 1.5-2 mm medial-lateral to lambda. For localization of the injection sites 40 µm thick horizontal sections were obtained on a freezing microtome. The tissue was incubated with DAPI (300nM). Sections where rinsed and mounted on glass.

Electrophysiological recordings in slices and optogenetics

Electrophysiological recordings in coronal or horizontal slices were performed at 34 ± 1˚C aCSF 40 min after dissection. Internal solution was supplemented with biocytin for morphological reconstruction. Full-field optogenetic stimulation (1 ms, 470 nm peak excitation, 0.1 to 6.65 mW/mm^2) was generated using a Polygon4000 (Mightex, Toronto, Canada) or a pE2 (CoolLED, Andover, UK). Pharmacology experiments were assessed adding AMPA- (10 µM NBQX), NMDA- (10 µM APV), mGluR1- (10 µM JNJ-16259685) and mGluR5- (50 µM MPEP) blockers to the aCSF.

Immunofluorescence and reconstruction

To visualize the recorded neurons and CN terminals, slices were stained for Streptavidin-Cy3 (Jackson Immunoresearch) and vGluT2 anti Guinea pig Cy5 (Millipore Bioscience Research Reagent). Using custom-written Fiji-scripts (ImageJ) we identified putative synaptic contacts that were isolated and morphologically studied using a LSM 700 microscope (Carl Zeiss). Stack's subsets of the connection were deconvolved using Huygens software (Scientific Volume Imaging) and the volume measured using a custom-written Fiji macro. To quantify the distance from soma for vGluT2-positive CN terminals we calculated the distance in 3 dimensions (using x-, y-, z-coordinates) between the center of the terminal and the center of the soma by Pythagorean Theorem. To determine the dendritic arborization of biocytin filled cells, we used the 3D Sholl analysis macro implemented in Fiji software [76].

Electron microscopy

Ultrastructural morphology was analyzed using electron microscope (CM 100, Philips). Staining for DAB and preparation of ultrathin section was performed as previously described [77].

Data analysis and statistics

All numerical values are given as means and error bars are SEM. Parametric and non-parametric tests were chosen as appropriate and were reported in figure legends. Data analyses were performed using SPSS 22.0 software package.

Detailed experimental procedures and statistical analyses for each experiment can be found in Supplemental Experimental Procedures.

References

1. De Zeeuw, C.I., and Ten Brinke, M.M. (2015). Motor Learning and the Cerebellum. Cold Spring Harb Perspect Biol *7*, a021683.
2. Manto, M., Bower, J.M., Conforto, A.B., Delgado-Garcia, J.M., da Guarda, S.N., Gerwig, M., Habas, C., Hagura, N., Ivry, R.B., Marien, P., et al. (2012). Consensus paper: roles of the cerebellum in motor control--the diversity of ideas on cerebellar involvement in movement. Cerebellum *11*, 457-487.
3. Brooks, J.X., Carriot, J., and Cullen, K.E. (2015). Learning to expect the unexpected: rapid updating in primate cerebellum during voluntary self-motion. Nature neuroscience *18*, 1310-1317.
4. Peter, S., Ten Brinke, M.M., Stedehouder, J., Reinelt, C.M., Wu, B., Zhou, H., Zhou, K., Boele, H.J., Kushner, S.A., Lee, M.G., et al. (2016). Dysfunctional cerebellar Purkinje cells contribute to autism-like behaviour in Shank2-deficient mice. Nature communications *7*, 12627.
5. Wang, S.S., Kloth, A.D., and Badura, A. (2014). The cerebellum, sensitive periods, and autism. Neuron *83*, 518-532.
6. Stoodley, C.J., D'Mello, A.M., Ellegood, J., Jakkamsetti, V., Liu, P., Nebel, M.B., Gibson, J.M., Kelly, E., Meng, F., Cano, C.A., et al. (2017). Altered cerebellar connectivity in autism and cerebellar-mediated rescue of autism-related behaviors in mice. Nature neuroscience *20*, 1744-1751.
7. Bodranghien, F., Bastian, A., Casali, C., Hallett, M., Louis, E.D., Manto, M., Marien, P., Nowak, D.A., Schmahmann, J.D., Serrao, M., et al. (2016). Consensus Paper: Revisiting the Symptoms and Signs of Cerebellar Syndrome. Cerebellum *15*, 369-391.
8. Tsai, P.T., Hull, C., Chu, Y., Greene-Colozzi, E., Sadowski, A.R., Leech, J.M., Steinberg, J., Crawley, J.N., Regehr, W.G., and Sahin, M. (2012). Autistic-like behaviour and cerebellar dysfunction in Purkinje cell Tsc1 mutant mice. Nature *488*, 647-651.
9. Popa, D., Spolidoro, M., Proville, R.D., Guyon, N., Belliveau, L., and Lena, C. (2013). Functional role of the cerebellum in gamma-band synchronization of the sensory and motor cortices. The Journal of neuroscience : the official journal of the Society for Neuroscience *33*, 6552-6556.
10. Proville, R.D., Spolidoro, M., Guyon, N., Dugue, G.P., Selimi, F., Isope, P., Popa, D., and Lena, C. (2014). Cerebellum involvement in cortical sensorimotor circuits for the control of voluntary movements. Nature neuroscience *17*, 1233-1239.
11. Cohen, D., Chambers, W.W., and Sprague, J.M. (1958). Experimental study of the efferent projections from the cerebellar nuclei to the brainstem of the cat. The Journal of comparative neurology *109*, 233-259.
12. Haroian, A.J., Massopust, L.C., and Young, P.A. (1981). Cerebellothalamic projections in the rat: an autoradiographic and degeneration study. The Journal of comparative neurology *197*, 217-236.
13. Aumann, T.D., Rawson, J.A., Finkelstein, D.I., and Horne, M.K. (1994). Projections from the lateral and interposed cerebellar nuclei to the thalamus of the rat: a light and electron microscopic study using single and double anterograde labelling. The Journal of comparative neurology *349*, 165-181.
14. Angaut, P., Cicirata, F., and Serapide, F. (1985). Topographic organization of the cerebellothalamic projections in the rat. An autoradiographic study. Neuroscience *15*, 389-401.
15. Daniel, H., Billard, J.M., Angaut, P., and Batini, C. (1987). The interposito-rubrospinal system. Anatomical tracing of a motor control pathway in the rat. Neuroscience research *5*, 87-112.
16. Teune, T.M., van der Burg, J., van der Moer, J., Voogd, J., and Ruigrok, T.J. (2000). Topography of cerebellar nuclear projections to the brain stem in the rat. Prog Brain Res *124*, 141-172.

17. Bentivoglio, M., and Kuypers, H.G. (1982). Divergent axon collaterals from rat cerebellar nuclei to diencephalon, mesencephalon, medulla oblongata and cervical cord. A fluorescent double retrograde labeling study. Experimental brain research *46*, 339-356.
18. Herkenham, M. (1979). The afferent and efferent connections of the ventromedial thalamic nucleus in the rat. The Journal of comparative neurology *183*, 487-517.
19. Aumann, T.D., and Horne, M.K. (1996). Ramification and termination of single axons in the cerebellothalamic pathway of the rat. The Journal of comparative neurology *376*, 420-430.
20. Jones, E.G., and Hendry, S.H. (1989). Differential Calcium Binding Protein Immunoreactivity Distinguishes Classes of Relay Neurons in Monkey Thalamic Nuclei. The European journal of neuroscience *1*, 222-246.
21. Jones, E.G. (1998). Viewpoint: the core and matrix of thalamic organization. Neuroscience *85*, 331-345.
22. Kuramoto, E., Furuta, T., Nakamura, K.C., Unzai, T., Hioki, H., and Kaneko, T. (2009). Two types of thalamocortical projections from the motor thalamic nuclei of the rat: a single neuron-tracing study using viral vectors. Cerebral cortex *19*, 2065-2077.
23. Kuramoto, E., Ohno, S., Furuta, T., Unzai, T., Tanaka, Y.R., Hioki, H., and Kaneko, T. (2015). Ventral medial nucleus neurons send thalamocortical afferents more widely and more preferentially to layer 1 than neurons of the ventral anterior-ventral lateral nuclear complex in the rat. Cerebral cortex *25*, 221-235.
24. Deschenes, M., Bourassa, J., and Parent, A. (1996). Striatal and cortical projections of single neurons from the central lateral thalamic nucleus in the rat. Neuroscience *72*, 679-687.
25. Clasca, F., Rubio-Garrido, P., and Jabaudon, D. (2012). Unveiling the diversity of thalamocortical neuron subtypes. The European journal of neuroscience *35*, 1524-1532.
26. Yamamoto, T., Noda, T., Samejima, A., and Oka, H. (1985). A morphological investigation of thalamic neurons by intracellular HRP staining in cats. The Journal of comparative neurology *236*, 331-347.
27. Monconduit, L., and Villanueva, L. (2005). The lateral ventromedial thalamic nucleus spreads nociceptive signals from the whole body surface to layer I of the frontal cortex. The European journal of neuroscience *21*, 3395-3402.
28. Uno, M., Yoshida, M., and Hirota, I. (1970). The mode of cerebello-thalamic relay transmission investigated with intracellular recording from cells of the ventrolateral nucleus of cat's thalamus. Experimental brain research *10*, 121-139.
29. Sawyer, S.F., Young, S.J., Groves, P.M., and Tepper, J.M. (1994). Cerebellar-responsive neurons in the thalamic ventroanterior-ventrolateral complex of rats: in vivo electrophysiology. Neuroscience *63*, 711-724.
30. Rispal-Padel, L., and Grangetto, A. (1977). The cerebello-thalamo-cortical pathway. Topographical investigation at the unitary level in the cat. Experimental brain research *28*, 101-123.
31. Bava, A., Cicirata, F., Giuffrida, R., Licciardello, S., and Panto, M.R. (1986). Electrophysiologic properties and nature of ventrolateral thalamic nucleus neurons reactive to converging inputs of paleo- and neocerebellar origin. Experimental neurology *91*, 1-12.
32. Rispal-Padel, L., and Latreille, J. (1974). The organization of projections from the cerebellar nuclei to the contralateral motor cortex in the cat. Experimental brain research *19*, 36-60.
33. Yoshida, M., Yajima, K., and Uno, M. (1966). Different activation of the 2 types of the pyramidal tract neurones through the cerebello-thalamocortical pathway. Experientia *22*, 331-332.

34. Steriade, M. (1995). Two channels in the cerebellothalamocortical system. The Journal of comparative neurology *354*, 57-70.
35. Kros, L., Eelkman Rooda, O.H., Spanke, J.K., Alva, P., van Dongen, M.N., Karapatis, A., Tolner, E.A., Strydis, C., Davey, N., Winkelman, B.H., et al. (2015). Cerebellar output controls generalized spike-and-wave discharge occurrence. Annals of neurology *77*, 1027-1049.
36. Sawyer, S.F., Tepper, J.M., and Groves, P.M. (1994). Cerebellar-responsive neurons in the thalamic ventroanterior-ventrolateral complex of rats: light and electron microscopy. Neuroscience *63*, 725-745.
37. Aumann, T.D., and Horne, M.K. (1996). A comparison of the ultrastructure of synapses in the cerebello-rubral and cerebello-thalamic pathways in the rat. Neurosci Lett *211*, 175-178.
38. Rovo, Z., Ulbert, I., and Acsady, L. (2012). Drivers of the primate thalamus. The Journal of neuroscience : the official journal of the Society for Neuroscience *32*, 17894-17908.
39. Sherman, S.M. (2014). The function of metabotropic glutamate receptors in thalamus and cortex. The Neuroscientist : a review journal bringing neurobiology, neurology and psychiatry *20*, 136-149.
40. Sherman, S.M., and Guillery, R.W. (1998). On the actions that one nerve cell can have on another: distinguishing "drivers" from "modulators". Proceedings of the National Academy of Sciences of the United States of America *95*, 7121-7126.
41. Reichova, I., and Sherman, S.M. (2004). Somatosensory corticothalamic projections: distinguishing drivers from modulators. Journal of neurophysiology *92*, 2185-2197.
42. Groh, A., de Kock, C.P., Wimmer, V.C., Sakmann, B., and Kuner, T. (2008). Driver or coincidence detector: modal switch of a corticothalamic giant synapse controlled by spontaneous activity and short-term depression. The Journal of neuroscience : the official journal of the Society for Neuroscience *28*, 9652-9663.
43. Seol, M., and Kuner, T. (2015). Ionotropic glutamate receptor GluA4 and T-type calcium channel Cav 3.1 subunits control key aspects of synaptic transmission at the mouse L5B-POm giant synapse. The European journal of neuroscience *42*, 3033-3044.
44. Liu, X.B., Munoz, A., and Jones, E.G. (1998). Changes in subcellular localization of metabotropic glutamate receptor subtypes during postnatal development of mouse thalamus. The Journal of comparative neurology *395*, 450-465.
45. Rubio-Garrido, P., Perez-de-Manzo, F., Porrero, C., Galazo, M.J., and Clasca, F. (2009). Thalamic input to distal apical dendrites in neocortical layer 1 is massive and highly convergent. Cerebral cortex *19*, 2380-2395.
46. Ohno, S., Kuramoto, E., Furuta, T., Hioki, H., Tanaka, Y.R., Fujiyama, F., Sonomura, T., Uemura, M., Sugiyama, K., and Kaneko, T. (2012). A morphological analysis of thalamocortical axon fibers of rat posterior thalamic nuclei: a single neuron tracing study with viral vectors. Cerebral cortex *22*, 2840-2857.
47. Deschenes, M., Bourassa, J., Doan, V.D., and Parent, A. (1996). A single-cell study of the axonal projections arising from the posterior intralaminar thalamic nuclei in the rat. The European journal of neuroscience *8*, 329-343.
48. Asanuma, C., Thach, W.T., and Jones, E.G. (1983). Distribution of cerebellar terminations and their relation to other afferent terminations in the ventral lateral thalamic region of the monkey. Brain research *286*, 237-265.

49. Smith, A.M., Massion, J., Gahery, Y., and Roumieu, J. (1978). Unitary acitvity of ventrolateral nucleus during placing movement and associated postural adjustment. Brain research *149*, 329-346.
50. Shinoda, Y., Futami, T., and Kano, M. (1985). Synaptic organization of the cerebello-thalamo-cerebral pathway in the cat. II. Input-output organization of single thalamocortical neurons in the ventrolateral thalamus. Neuroscience research *2*, 157-180.
51. Steriade, M., Apostol, V., and Oakson, G. (1971). Control of unitary activities in cerebellothalamic pathway during wakefulness and synchronized sleep. Journal of neurophysiology *34*, 389-413.
52. Bava, A., Manzoni, T., and Urbano, A. (1967). Effects of fastiginal stimulation on thalamic neurones belonging to the diffuse projection system. Brain research *4*, 378-380.
53. Chen, C.H., Fremont, R., Arteaga-Bracho, E.E., and Khodakhah, K. (2014). Short latency cerebellar modulation of the basal ganglia. Nature neuroscience *17*, 1767-1775.
54. De Zeeuw, C.I., Hoebeek, F.E., Bosman, L.W., Schonewille, M., Witter, L., and Koekkoek, S.K. (2011). Spatiotemporal firing patterns in the cerebellum. Nature reviews. Neuroscience *12*, 327-344.
55. Chung, S., Li, X., and Nelson, S.B. (2002). Short-term depression at thalamocortical synapses contributes to rapid adaptation of cortical sensory responses in vivo. Neuron *34*, 437-446.
56. Mease, R.A., Krieger, P., and Groh, A. (2014). Cortical control of adaptation and sensory relay mode in the thalamus. Proceedings of the National Academy of Sciences of the United States of America *111*, 6798-6803.
57. Viaene, A.N., Petrof, I., and Sherman, S.M. (2013). Activation requirements for metabotropic glutamate receptors. Neuroscience letters *541*, 67-72.
58. Bickford, M.E. (2015). Thalamic Circuit Diversity: Modulation of the Driver/Modulator Framework. Frontiers in neural circuits *9*, 86.
59. Bickford, M.E., Zhou, N., Krahe, T.E., Govindaiah, G., and Guido, W. (2015). Retinal and Tectal "Driver-Like" Inputs Converge in the Shell of the Mouse Dorsal Lateral Geniculate Nucleus. The Journal of neuroscience : the official journal of the Society for Neuroscience *35*, 10523-10534.
60. Kelly, L.R., Li, J., Carden, W.B., and Bickford, M.E. (2003). Ultrastructure and synaptic targets of tectothalamic terminals in the cat lateral posterior nucleus. The Journal of comparative neurology *464*, 472-486.
61. Masterson, S.P., Li, J., and Bickford, M.E. (2009). Synaptic organization of the tectorecipient zone of the rat lateral posterior nucleus. The Journal of comparative neurology *515*, 647-663.
62. Rollenhagen, A., and Lubke, J.H. (2006). The morphology of excitatory central synapses: from structure to function. Cell and tissue research *326*, 221-237.
63. Zikopoulos, B., and Barbas, H. (2007). Parallel driving and modulatory pathways link the prefrontal cortex and thalamus. PloS one *2*, e848.
64. Zikopoulos, B., and Barbas, H. (2012). Pathways for emotions and attention converge on the thalamic reticular nucleus in primates. The Journal of neuroscience : the official journal of the Society for Neuroscience *32*, 5338-5350.
65. Geinisman, Y. (1993). Perforated axospinous synapses with multiple, completely partitioned transmission zones: probable structural intermediates in synaptic plasticity. Hippocampus *3*, 417-433.
66. Pelzer, P., Horstmann, H., and Kuner, T. (2017). Ultrastructural and Functional Properties of a Giant Synapse Driving the Piriform Cortex to Mediodorsal Thalamus Projection. Frontiers in synaptic neuroscience *9*, 3.

67. Herkenham, M. (1980). Laminar organization of thalamic projections to the rat neocortex. Science *207*, 532-535.
68. Goldberg, J.H., Farries, M.A., and Fee, M.S. (2013). Basal ganglia output to the thalamus: still a paradox. Trends in neurosciences *36*, 695-705.
69. Guo, Z.V., Inagaki, H.K., Daie, K., Druckmann, S., Gerfen, C.R., and Svoboda, K. (2017). Maintenance of persistent activity in a frontal thalamocortical loop. Nature *545*, 181-186.
70. Gummadavelli, A., Motelow, J.E., Smith, N., Zhan, Q., Schiff, N.D., and Blumenfeld, H. (2015). Thalamic stimulation to improve level of consciousness after seizures: evaluation of electrophysiology and behavior. Epilepsia *56*, 114-124.
71. Berendse, H.W., and Groenewegen, H.J. (1991). Restricted cortical termination fields of the midline and intralaminar thalamic nuclei in the rat. Neuroscience *42*, 73-102.
72. McCormick, D.A., and Bal, T. (1997). Sleep and arousal: thalamocortical mechanisms. Annual review of neuroscience *20*, 185-215.
73. Miller, J.W., Gray, B.C., and Bardgett, M.E. (1992). Characterization of cholinergic regulation of seizures by the midline thalamus. Neuropharmacology *31*, 349-356.
74. Giber, K., Diana, M.A., Plattner, V., Dugue, G.P., Bokor, H., Rousseau, C.V., Magloczky, Z., Havas, L., Hangya, B., Wildner, H., et al. (2015). A subcortical inhibitory signal for behavioral arrest in the thalamus. Nature neuroscience *18*, 562-568.
75. Buee, J., Deniau, J.M., and Chevalier, G. (1986). Nigral modulation of cerebello-thalamo-cortical transmission in the ventral medial thalamic nucleus. Experimental brain research *65*, 241-244.
76. Ferreira, T.A., Blackman, A.V., Oyrer, J., Jayabal, S., Chung, A.J., Watt, A.J., Sjostrom, P.J., and van Meyel, D.J. (2014). Neuronal morphometry directly from bitmap images. Nature methods *11*, 982-984.
77. Hoebeek, F.E., Khosrovani, S., Witter, L., and De Zeeuw, C.I. (2008). Purkinje cell input to cerebellar nuclei in tottering: ultrastructure and physiology. Cerebellum *7*, 547-558.
78. Franklin, K., and Paxinos, G. (2001). The mouse brain in stereotactic coordinates, Compact, 2nd Edition, (Academic Press).

Supplementary Experimental Procedures

Experimental Procedures

All experiments were performed in accordance with the European Communities Council Directive. Protocols were reviewed and approved by the Dutch national experimental animal committees (DEC) and every precaution was taken to minimize stress, discomfort and the number of animals used.

Animals

Data were collected from 21-56 day old C57BL/6NHsd mice of both sexes, which were purchased from Envigo laboratories (Horst, Netherlands).

Viral injections

Mice were anesthetized with isoflurane, (4% in 0.5 L/min O_2 for induction and 1.5% in 0.5 L/min O_2 for maintenance), carprofen (5 mg/kg), buprenorphine (50 µg/kg) and lidocaine (10%, local application). For optogenetic stimulation we stereotactically delivered adeno-associated virus (AAV) encoding Channelrhodopsin2 (ChR2) coupled with a EYFP fluorophore (AAV2-hSyn-ChR2(H134R)-EYFP) to the CN. Following bilateral craniotomies of ~0.5 mm above the interparietal bone (-2 mm anterior-posterior and 1.5-2 mm medial-lateral to lambda), 150-200 nl (at a rate of ~20 nl/min) of AAV was injected to the CN in both hemispheres. The viral vector was kindly provided by Prof. K. Deisseroth (Stanford University) through the UNC and UPENN vector cores.

Preparation of acute brain slices

Following 3-6 weeks of incubation isoflurane-anesthetized mice were decapitated, their brains were quickly removed and placed into ice-cold slicing medium containing (in mM): 93 NMDG, 93 HCl, 2.5 KCl, 1.2 $NaHPO_4$, 30 $NaHCO_3$, 25 Glucose, 20 HEPES, 5 Na-ascorbate, 3 Na-pyruvate, 2 Thiourea, 10 $MgSO_4$, 0.5 $CaCl_2$, 5 N-acetyl-L-Cysteine (osmolarity 310 ± 5; bubbled with 95% O_2 / 5% CO_2) [1]. Next, 250-300 µm thick horizontal or coronal slices were cut using a Leica vibratome (VT1000S). For the recovery, brain slices were incubated for 5 min in slicing medium at 34 ± 1˚C and subsequently for ~40 min in ACSF (containing in mM: 124 NaCl, 2.5 KCl, 1.25 Na_2HPO_4, 2 $MgSO_4$, 2 $CaCl_2$, 26 $NaHCO_3$, and 20 D–glucose, osmolarity 310 ± 5; bubbled with 95% O_2 / 5% CO_2) at 34 ± 1˚C. After recovery brain slices were stored at room temperature (RT) before the experiments started. The accompanying hindbrain was post-fixed in 4% paraformaldehyde (PFA), for histological confirmation of the viral injection location (see below).

In vitro whole cell recordings

For all recordings, slices were bathed in 34 ± 1˚C ACSF (bubbled with 95% O_2 and 5% CO_2). Whole-cell patch-clamp recordings were performed using an EPC-9 or EPC-10 amplifier (HEKA Electronics, Lambrecht, Germany) for 20-60 min and digitized at 20 kHz. Resting membrane potential (V_{rest}) and input resistance were recorded after whole-cell configuration was reached. Recordings were excluded if the series resistance (R_S) (assessed by -5 or -10 mV voltage steps following each test pulse) varied by >25% over the course of the experiment. Voltage and current clamp recordings were performed using borosilicate glass pipettes with a resistance of 3-5 MΩ when filled with K^+-based internal (in mM: 124 K-Gluconate, 9 KCl, 10 KOH, 4 NaCl, 10 HEPES, 28.5 Sucrose, 4 Na_2ATP, 0.4 Na_3GTP (pH 7.25-7.35; osmolarity ~290)). Recording pipettes were supplemented with 1 mg/ml biocytin to allow histological staining (see below). Current clamp recordings were corrected offline for the calculated liquid junction potential of -10.2 mV. All recordings were performed in the presence of picrotoxin (100 µM, Sigma-Aldrich) to block $GABA_A$-receptor-mediated IPSCs.

Full-field optogenetic stimulation (470 nm peak excitation) was generated using a Polygon4000 (Mightex, Toronto, Canada) or a pE2 (CoolLED, Andover, UK), that were controlled using TTL-pulses generated by the HEKA amplifier. Light intensities at 470 nm were recorded using a photometer (Newport 1830-C equipped with an 818-ST probe, Irvine, CA) at the level of the slice. Typically the light intensities sufficient to trigger the maximal response amplitude in thalamic cells ranged from 0.1 to 6.65 mW/mm^2. To trigger neurotransmitter release from transfected CN axons we delivered 1 ms light pulses at 0.1 Hz and an intensity resulting in the maximally evoked response, unless stated otherwise. To characterize the postsynaptic receptors we sequentially bath-applied AMPA- (10 µM NBQX), NMDA- (10 µM APV), mGluR1- (10 µM JNJ-16259685) and mGluR5- (50 µM MPEP) blockers. Each drug was added only after the EPSC amplitude stabilized. All drugs were purchased from Tocris (Bristol, UK). To ensure that we recorded action potential-driven neurotransmitter release most experiments were concluded by bath application of 10 µM tetrodotoxin (TTX), which blocked all post-synaptic responses in the recorded thalamic neurons. The responses evoked in thalamic neurons by optogenetic stimulation of CN axons were solely of monosynaptic origin, which matches the known absence of local interneurons and of local axon collaterals [2].

Immunofluorescence

To visualize the recorded neurons and CN axons, slices were placed in 4% PFA (in 0.12 M PB) for at least 24 hrs [3]. Subsequently, slices were transferred into 0.1 M PBS and rinsed with PBS 3 times for 10 min. Slices were incubated for 1 hr at RT in blocking solution (containing 10% normal horse serum (NHS) and 0.5% triton diluted in PBS), which

was followed by over-night incubation with primary antibody for vesicular glutamate transporter type 2 (vGluT2) (anti Guinea Pig; Millipore Bioscience Research Reagent; 1:2000 diluted in PBS containing 2% NHS and 0.4% Triton). Slices were subsequently rinsed 3 times for 10 min and incubated for 2 hrs with Streptavidin-Cy3 (1:200, Jackson Immunoresearch) and anti-guinea pig Cy5 (1:200, Jackson Immunoresearch) diluted in PBS containing 2% normal horse serum and 0.4% triton. Sections were rinsed in PBS, mounted with Vectashield (Vector laboratories) and imaged with a LSM 700 confocal microscope (Carl Zeiss Microscopy, LLC, USA).

For localization of the injection sites, the cerebellum was removed from forebrain and fixed with PFA 4% for 5 to 10 days on a shaker at 4°C. Serial 40 µm thick horizontal sections were obtained on a freezing microtome. The tissue was rinsed in PBS solution and then transferred in blocking solution for 1 hr at RT and subsequently incubated for 10 min with DAPI (300nM). Sections where rinsed with 0.01M PB and mounted on glass.

Fluorescence microscopy and reconstruction

Guided by calbindin D28-K staining (primary: Calbindin α-rabbit 1:7000, Swant Inc, #CB-38a; secondary: 405 nm rabbit-α-donkey 1:400, Jackson Immunoresearch #A421) and a reference atlas [4] we outlined the thalamic nuclei of interest. For each nucleus the expression pattern of ChR2-YFP was quantified with RGB measure function of Fiji (ImageJ) in order to have the mean intensity among the region of interest (ROI).

Recorded neurons were labeled with biocytin. Epifluorescent tile images were obtained using a 20X/0.30 NA (air) objective and a LSM 700 microscope (Carl Zeiss). The position of labeled neurons was confirmed using a stereotactic atlas [4]. Terminals positive to VGluT2 staining were identified and morphologically studied using confocal images that were captured using the following excitation wavelengths: 488 nm (YFP), 555 nm (Cy3) and 639 nm (Cy5). Terminals were imaged using a 40X/1.30 NA (oil) objective by acquiring a stack of images with 0.5 digital zoom and a voxel size of 313 nm width x 313 nm length x 300 nm depth. Using custom-written Fiji-scripts (ImageJ) we identified putative synaptic contacts, i.e. YFP-positive varicosities that colocalized with vGluT2-staining that are within 1 µm distance from the recorded neurons. Once synaptic contacts were isolated high resolution image stacks were acquired using a 63X1.4 NA oil objective with 1X digital zoom, a pinhole of 1 Airy unit and significant oversampling for deconvolution (voxel dimension is: 46 nm width x 46 nm length x 130 nm depth calculated according to Nyquist factor; 8-bit per channel; image plane 2048 x 2048 pixels). Signal-to-noise ratio was improved by 2 times line averaging. Stack's subsets of the connection were deconvolved using Huygens software (Scientific Volume Imaging). Further analysis was performed using a custom-written Fiji macro. The color channels (YFP, Cy3 and Cy5) of the images were split to get separate stacks. The YFP and Cy3

channels were Gaussian blurred (sigma = 1) and selected by a manually set threshold. A binary open function was done on both images (iterations = 4, count = 2) and objects were removed if their size was <400 pixels (YFP) or <120 pixels (Cy3). A small dilatation was done on the red image (iteration = 1, count = 1). With the image calculator an 'and-operation' was done using the binary red and green image. The values 255 (white) of the binary YFP image were set to 127. This image and the result of the AND-operation were combined by an OR-operation. The resulting image was measured with the 3D-object counter plugin for volumes and maximum intensities. Only objects containing pixels with an intensity of 255 (overlap) are taken in account for analysis. Estimation of synapse density (number of terminals/area μm^2) was obtained for each nucleus by dividing the number of terminals by the image area [5]. To quantify the distance from soma for vGluT2-positive CN terminals on reconstructed neurons we used a custom-written macro in Fiji software (ImageJ). Briefly, we calculated the distance in 3 dimensions (using x-, y-, z-coordinates) between the center of the terminal and the center of the soma by Pythagorean Theorem.

3D Sholl analysis

To determine the dentritic arborization of biocytin filled cells, we used the 3D Sholl analysis macro implemented in Fiji software [6]. For preprocessing, image stacks over a z-volume of 18.5 - 87.5 µm were binarized. Stacks with excessive background signal were excluded from further analysis. Subsequently the dendritic arborization was measured in concentric shells of 10 µm distance starting with 15 µm distance from the center of the soma. At this first sphere we manually counted the number of primary dendrites and assessed their directionality by calculating the radial angle between the primary dendrites.

Electron microscopy

Four mice were injected with anterograde neuronal tract tracer biotinylated dextran–amine (10% BDA in 0.1 M PB, pH 7.4, molecular weight 10,000) by iontophoresis (pulses of 4 µA, 10 min) with a glass micropipette (tip opening, 8–10 µm) in the interpositus and lateral CN. After 5 days mice were anesthetized with an overdose of nembutal (i.p.) and transcardially perfused with 4% PFA and 1% glutaraldehyde in phosphate buffer. Brains were removed, kept overnight in 4% PFA, and cut into 60 µm thick coronal sections using a vibratome. Sections were subsequently washed in PBS, incubated for 20 min in 3% H_2O_2 (in PBS) to remove endogenous peroxidase activity of blood, washed again, placed for 1 hr in 10% NHS and finally incubated for 24 hrs in ABC-HRP (Vector). At the end of the immunostaining, the sections were stained with 0.5% 3,3-diaminobenzidine tetrahydrochloride (DAB) and 0.01% H_2O_2 for 15 min at RT. Ultimately, the sections

were osmicated with 1% osmium in 8% glucose solution, dehydrated in propyleen oxide, and embedded in araldite (Durcupan, Fluka, Germany). Guided by staining levels in semithin sections (0.5 µm thick), we made pyramids of the VL, VM and CL nuclei. Ultrathin sections (60 nm) were cut using an ultramicrotome (Leica, Germany), mounted on nickel grids, and counterstained with uranyl acetate and lead citrate. CN axon terminals were photographed at various magnifications (range 3900X-25500X) using an electron microscope (CM 100, Philips, Eindhoven, Netherlands) and analyzed off-line using standard measurement functions in Fiji (ImageJ). To limit the possibility that our electron micrographs contained various images of the same pre- and postsynaptic structures we separated our ultrathin sections by various semi-thin sections.

Data analysis and statistics

Current and potential traces were acquired using Pulse and Patchmaster software (HEKA) and stored for offline analysis. Single stimulus data was analyzed using Clampfit software (Molecular Devices), while trains of stimuli were analyzed with custom written routines in Igor Pro 6.1 (Wavemetrics, Lake Oswego, Oregon). To evaluate the variability of EPSC amplitude and charge transfer we calculated the coefficient of variation (CV): the ratio between standard deviation and mean. For trains of stimuli, the peak amplitude of each evoked postsynaptic current (EPSC) was detected relative to baseline. All EPSC amplitudes within the train were normalized to the first EPSC. The total charge during train stimulation was calculated by determining the area under the curve between the first and the last stimulus relative to baseline. For all recordings averages of at least 5 sweeps per cell were calculated. The steady state amplitude was calculated by averaging the amplitude of responses to the last 5 stimuli.

Using GraphPad PRISM and SPSS software packages we ran statistical comparisons between the thalamic nuclei (VL, VM and CL) by one-way ANOVA, Kruskal-Wallis (K-W) or Kolmogorov-Smirnov (K-S) tests as indicated in the main text. Statistical difference for pharmacology data was assessed using Friedman test. For Sholl analysis a two-way ANOVA was used with Bonferroni Multiple comparison test. We corrected missing values by the Last observation carried forward (LOCF) method. Correlation coefficients were calculated using Spearman. We defined $p<0.05$ as a significant difference. Throughout the main text we report a subset of the statistical data; all details are provided in the Supplemental data tables that accompany each figure. Summarized data are represented as mean ± standard error. Throughout the figures data from VL are indicated in green, VM in red and CL in blue, unless stated otherwise.

References

1. Ting, J.T., Daigle, T.L., Chen, Q., and Feng, G. (2014). Acute brain slice methods for adult and aging animals: application of targeted patch clamp analysis and optogenetics. Methods in molecular biology *1183*, 221-242.
2. Jones, E.G. (2007). principles of thalamic organization. In The thalamus, Volume 1. (Cambridge: Cambridge university press), p. 97.
3. Marx, M., Gunter, R.H., Hucko, W., Radnikow, G., and Feldmeyer, D. (2012). Improved biocytin labeling and neuronal 3D reconstruction. Nature protocols *7*, 394-407.
4. Franklin, K., and Paxinos, G. (2001). The mouse brain in stereotactic coordinates, Compact, 2nd Edition, (Academic Press).
5. DeKosky, S.T., and Scheff, S.W. (1990). Synapse loss in frontal cortex biopsies in Alzheimer's disease: correlation with cognitive severity. Annals of neurology *27*, 457-464.
6. Ferreira, T.A., Blackman, A.V., Oyrer, J., Jayabal, S., Chung, A.J., Watt, A.J., Sjostrom, P.J., and van Meyel, D.J. (2014). Neuronal morphometry directly from bitmap images. Nature methods *11*, 982-984.

Figure 1

Panel	Test applied	P-value	Degrees of freedom	Population size	Definition of population	Correction
1B	Kruskal Wallis	*0.003* -VL-VM 0.529 -VM-CL 0.136 *-VL-CL 0.002*	2	18	6 mice	Dunn-Sidak
1I	Kolmogorov Smirnov	*VL-VM <0.001* VM-CL 0.966 *VL-CL <0.001*		671 terminals 245 terminals 572 terminals	5 mice	Bonferroni
1J	Kruskal Wallis	*0.028* VL-VM 0.334 VM-CL 0.865 *VL-CL 0.024*	2	15	5 mice	Dunn-Sidak

Figure 2

Panel	Test applied	P-value	Degrees of freedom	Population size	Definition of population	Correction
2B *EPSC Amplitude*	Kruskal Wallis	*<0.001* *VL-VM 0.001* VM-CL 1 *VL-CL <0.001*	2	44 cells	40 mice	Dunn-Sidak
2B EPSC Charge	Kruskal Wallis	*<0.001* *VL-VM 0.002* VM-CL 1 *VL-CL 0.001*	2	47 cells	40 mice	Dunn-Sidak
2D EPSC CV	Kruskal Wallis	*0.001* *VL-VM 0.031* VM-CL 1 *VL-CL 0.001*	2	42 cells	40 mice	Dunn-Sidak
2D Charge CV	Kruskal Wallis	*0.001* *VL-VM 0.025* VM-CL 1 *VL-CL 0.03*	2	46 cells	40 mice	Dunn-Sidak

Figure 3

Panel 3H	Test applied	P-value	Degrees of freedom	Population size	Definition of population	Correction
VL	Kruskal Wallis	*0.002* 10-20 Hz 0.492 *10-50 Hz 0.001* 20-50 Hz 0.111	2	39 cells	29 mice	Dunn-Sidak
VM	Kruskal Wallis	0.496	2	22 cells	9 mice	
CL	Kruskal Wallis	*0.006* 10-20 Hz 0.234 *10-50 Hz 0.004* 20-50 Hz 0.230	2	16 cells	9 mice	Dunn-Sidak

Panel 3H	Test applied	P-value	Degrees of freedom	Population size	Definition of population	Correction
10 Hz	Kruskal Wallis	0.344	2	29 cells	18 mice	
20 Hz	Kruskal Wallis	0.168	2	27 cells	13 mice	
50 Hz	Kruskal Wallis	0.137	2	20 cells	16 mice	

Panel 3I	Test applied	P-value	Degrees of freedom	Population size	Definition of population	Correction
VL	Kruskal Wallis	*0.007* 10-20 Hz 0.464 *10-50 Hz 0.005* 20-50 Hz 0.529	2	29 cells	29 mice	Dunn-Sidak
VM	Kruskal Wallis	*0.037* 10-20 Hz 1 10-50 Hz 0.056 20-50 Hz 0.118	2	12 cells	9 mice	Dunn-Sidak
CL	Kruskal Wallis	0.077	2	12 cells	9 mice	

Panel 3I	Test applied	P-value	Degrees of freedom	Population size	Definition of population	Correction
10 Hz	Kruskal Wallis	0.167	2	20 cells	18 mice	
20 Hz	Kruskal Wallis	0.321	2	18 cells	13 mice	
50 Hz	Kruskal Wallis	0.867	2	15 cells	16 mice	

Figure 4

Panel 4B	Test applied	P-value	Degrees of freedom	Population size	Definition of population	Correction
Control *vs* NBQX	Friedman	0.500	3	10 cells	9 mice	
NBQX *vs* NBQX+APV	Friedman	0.146	3	10 cells	9 mice	Dunn-Bonferroni
Control *vs* NBQX+APV	Friedman	*<0.001*	3	10 cells	9 mice	Dunn-Bonferroni
NBQX+APV *vs* NBQX-AP5-MPEP+JNJ	Friedman	1.000	3	10 cells	9 mice	Dunn-Bonferroni
NBQX *vs* NBQX+APV+ MPEP+JNJ	Friedman	*0.019*	3	10 cells	9 mice	Dunn-Bonferroni

Figure 5

Panel	Test applied	P-value	Degrees of freedom	Population size	Definition of population	Correction
5D *Intersection 55 µm*	2-way ANOVA	VL-VM 0.733 VM-CL 0.350 *VL-CL 0.018*		26 cells	26 mice	
5E	Kruskal Wallis	0.015	2	33 cells	26 mice	Dunn-Sidak
5F	Kruskal Wallis	0.141	2	164	26 mice	
5G	Kolmogorov-Smirnov	VL-VM 0.831 VM-CL 0.136 VL-CL 0.343		93 123 112	26 mice	Bonferroni

Figure 6

Panel	Test applied	P-value	Degrees of freedom	Population size	Definition of population	Correction
6B	Kruskal Wallis	0.373	2	34 cells	24 mice	Dunn-Sidak
6C	Kruskal Wallis	0.586	2	110 cells	24 mice	Dunn-Sidak
6E	Kruskal Wallis	*0.027* VL-VM 1.00 VM-CL 0.353 *VL-CL 0.023*	2	130 terminals	24 mice	Dunn-Sidak
6F	Kolmogorov Smirnov	VL-VM 0.834 VM-CL 0.080 *VL-CL 0.044*		93 terminals 59 terminals 108 terminals	24 mice	Bonferroni

Figure 7

Panel 7B	Test applied	P-value	Degrees of freedom	Population size	Definition of population	Correction
Terminal surface	Kruskal Wallis	0.099	2	97 terminals	4 mice	Dunn Sidak
Number of Mitochondria	Kruskal Wallis	0.468	2	83 terminals	4 mice	Dunn Sidak
Mitochondria Surface	Kruskal Wallis	*<0.001* *VL-VM 0.034* *VM-CL 0.000* *VL-CL <0.001*	2	315 mitochondria	4 mice	Dunn Sidak
PSD length	Kruskal Wallis	*0.012* *VL-VM 0.024* VM-CL 1.000 VL-CL 0.055	2	275 PSD	4 mice	Dunn Sidak
Number of Release sites	Kruskal Wallis	0.667	2	90 terminals	4 mice	Dunn Sidak
Dendritic diameter	Kruskal Wallis	0.080	2	97 dendrites	4 mice	Dunn Sidak

"Alle miserie sue, l'uomo incolpando

Del suo dolor, ma dà la colpa a quella

Che veramente è rea, che de' mortali

Madre è di parto e di voler matrigna"

La Ginestra – Giacomo Leopardi

Chapter 5

Single-pulse stimulation of cerebellar nuclei stops cortical oscillations by desynchronizing epileptic thalamic activity

Oscar H.J. Eelkman Rooda*
Lieke Kros*
Sade J. Faneyte
Peter J. Holland
Simona V. Gornati
Huub J. Poelman
Nico A. Jansen
Else A. Tolner
Arn M.J.M. van den Maagdenberg
Chris I. De Zeeuw
Freek E. Hoebeek

*These authors contributed equally

Submitted to Curr Biol

Summary

Reorganization of local networks in the cerebral cortex following focal insults can facilitate the induction of more widespread hypersynchronized activity [1-5] and thereby lead to generalized seizures [6]. Directly restoring the activity of the cortical networks themselves forms a promising therapeutic strategy [7, 8], but manipulating the activity of upstream brain regions that provide prominent and specific synaptic inputs to these networks may be an interesting alternative. Here, we investigated how optogenetic stimulation of the cerebellar nuclei (CN) or their efferents affects the neuronal spiking patterns during seizures in the thalamus, which forms the major upstream hub of the cerebral cortex [7]. We show that single-pulse stimulation of CN neurons, which provide not only mono-synaptic but also multi-synaptic inputs to the thalamic nuclei [9, 10], is highly effective in stopping generalized absence seizures in tottering mice [11, 12] by instantly reducing synchronicity and rhythmicity in the thalamus. Notably, optogenetic stimulation of CN axons in the thalamic nuclei alone was less effective in stopping seizures than direct stimulation of CN neurons, supporting that the putative relevance of the upstream multi-synaptic cerebello-thalamic pathway is relevant. In between the seizures, thalamic responses to CN stimulation varied from short-latency increases to bimodal, inhibitory and delayed network effects. Our data show that single-pulse stimulation of CN neurons can stop epileptic seizures by desynchronizing thalamic neuronal firing, and they highlight the importance of cerebellar activity for controlling thalamo-cortical information processing in general.

Results

Cerebellar nuclei stimulation desynchronizes thalamic spiking activity

To examine the effects of CN stimulation on seizure-related thalamo-cortical neuronal activity patterns we recorded neuronal multi-unit activity (MUA) throughout the thalamic complex while monitoring cortical activity by ECoG in awake, freely behaving *tottering* mice (**Fig. 1A-C**). We observed that cortical generalized spike-and-wave discharges (GSWDs) were accompanied by rhythmic neuronal firing, i.e., characteristic for synchronized firing, in the thalamic complex. During interictal periods, however, thalamic MUA was relatively arrhythmic, i.e., characteristic for desynchronized firing (**Fig. 1C**). Termination of seizure activity by optogenetic CN stimulation (single-pulse, 50 ms, 470 nm) (see also [12]) instantly reverted the phase-locked thalamic MUA to a desynchronized state, as shown by a reduction of the MUA autocorrelation (**Fig. 1C,D** and **Suppl. Table 1**).

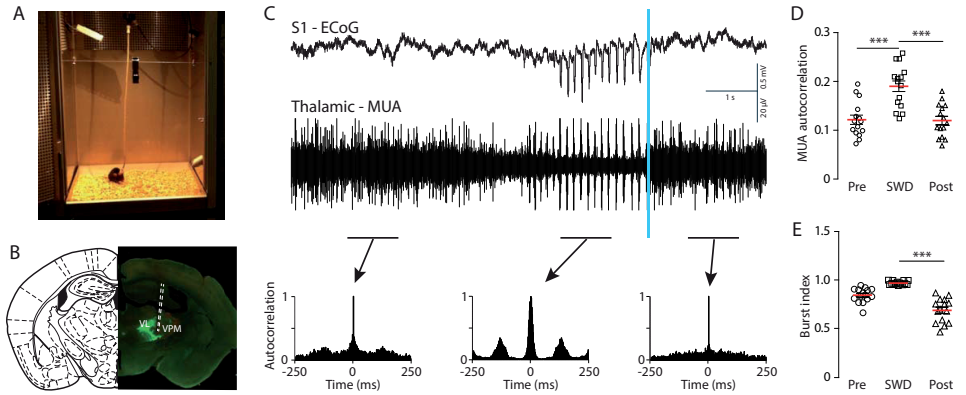

Figure 1. Single-pulse optogenetic CN stimulation stops rhythmic thalamic spiking. (**A**) Tethered recording system for optogenetic stimulation in CN and thalamic neuronal multi-unit activity (MUA) and ECoG recordings from primary motor (M1) and sensory (S1) cortices in freely behaving *tottering* mice. (**B**) ChR2-EYFP-expressing CN axons in the thalamus complex with the location of the MUA electrode indicated by white-dashed lines. (**C**) (*Top - middle*) Example of spike-and-wave discharges (SWDs) in S1-ECoG (*top*) in synchrony with thalamic MUA (*middle*), during which mice developed behavioral arrest. Single-pulse optogenetic stimulation (vertical blue line; 50 ms, 470 nm, 0.5 mW/mm^2) in CN stopped synchronous burst firing in thalamic neurons and ended the SWDs, upon which behavioral arrest was typically ended. On average, SWDs occurred every 72.6 ± 19.8 s (N = 8 mice, 1-hour recording per mouse). (*Bottom*) Accompanying normalized autocorrelograms of MUA in 1-second periods of the pre-SWD, SWD and post-SWD phase. (**D**) Average MUA autocorrelation for pre-SWD, SWD and post-SWD multi-unit recordings. (**E**) As (D) but for burst index. Data are represented as mean ± SEM. * indicates $p < 0.05$, *** indicate $p < 0.001$ (see **Suppl. Table 1** for statistics).

We also found that upon ictal CN stimulation the MUA burst index reverted to baseline levels (**Fig. 1E**). These findings indicate that single-pulse CN stimulation can consistently desynchronize seizure-related rhythmic thalamic MUA.

Thalamic responses to single-pulse cerebellar nuclei stimulation is variable

Our MUA recordings of thalamic neurons suggest that single-pulse stimulation in CN, which was shown to promote synchronous action potential firing [12], may have a differential effect on thalamic neurons. To further investigate the thalamic responses to CN stimulation, we recorded single-unit responses during interictal periods in head-fixed *tottering* mice (see STAR experimental procedures). Out of the 201 recorded neurons 165 neurons were responsive to single-pulse CN stimulation (50 ms pulse of 470 nm and 0.5 mW/mm^2 at 0.2 Hz) (**Fig. 2A**). Both the response latency and the type of response were variable (**Fig. 2B-D**) (see also **Suppl. Fig. 1** and **Suppl. Table 2**). We observed a significant negative correlation between the pre-stimulus firing frequency and the number of spikes during the pulse (**Fig. 2C**). Most thalamic neurons increased their firing rate during CN stimulation (group 'increased'; 114 out of 165 neurons; 69.1%). Other thalamic neurons responded in a bi-phasic manner, i.e. following the initial excitatory response the firing rate was significantly reduced (group 'bi-phasic'; 17 out of 165; 10.3%). Again other thalamic neurons only showed a reduction of their firing rate upon CN stimulation (group 'decreased'; 15 out of 165; 9.1%). Finally we recorded neurons that did not show a significant response during the 50-ms stimulus, but only thereafter (group 'delayed'; 19 out of 165; 11.5%). Given that in a mouse brain the CN projection neurons that synapse onto thalamic neurons are known to be glutamatergic [13, 14], these recordings of bi-phasic-, decreased- and delayed-responses are most likely representing a combination of direct CN-input and additional afferent input possibly gated via CN-afferents to pre-thalamic nuclei [9]. To investigate the impact single-pulse CN stimulation has on cortical activity we analyzed M1 and S1 ECoG activities. As shown in the ECoG traces single-pulse CN stimulation resulted in a clear change of frequency and amplitude (**Fig. 2E,F**). A broadband decrease in power was observed lasting ~1 s; the most prominent suppression was found within in the seizure-related θ*-band (7-10 Hz) across the recording sites. We found that this response was reliably evoked, as can be seen from the averaged responses and power spectrogram (**Fig. 2G,H** and **Suppl. Table 3**).

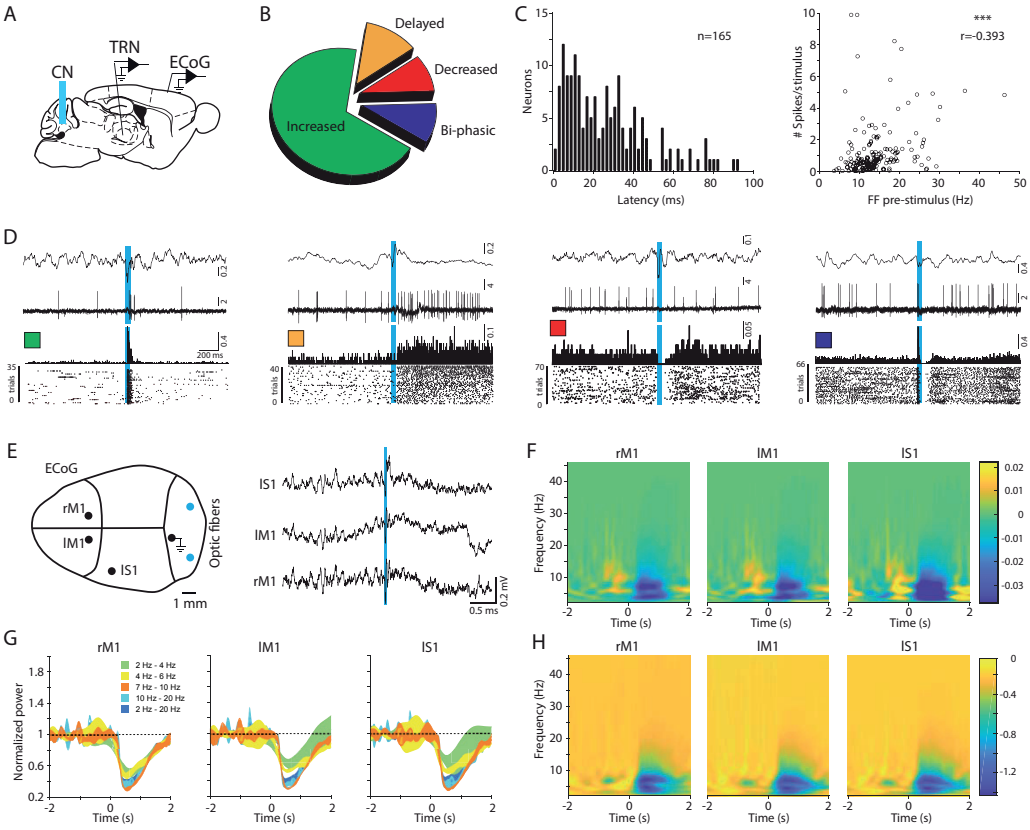

Figure 2. CN stimulation induces variable changes in interictal thalamic firing and cortical activity. (**A**) Schematic outline of head-fixed experiment in *tottering* mice for CN optogenetic stimulation, single-unit extracellular recordings from thalamic relay neurons (TRN) and multi-site ECoG recordings from M1 and S1 regions. (**B**) Distribution of response types for the 165 thalamic neurons that showed a significant response to CN stimulation (as determined by Z-score based diagnostics; see STAR methods). See main text for number of cells per type of response. (**C**) (*Left*) Cumulative histogram of response latencies of thalamic neurons (n = 165 neurons) to single-pulse (50 ms) CN stimulation. (*Right*) Scatterplot for the correlation between the pre-stimulus firing frequency (FF) and the number of spikes recorded during the CN stimulus (Pearson's correlation coefficient: r = -0.393; p < 0.001). (**D**) Example traces of ECoG (*top traces*) and simultaneously recorded TRN (*bottom traces*) with accompanying per-stimulus histograms and scatterplots for each type of response. Green: 'increased' (see also **Suppl. Fig. 1B**); orange: 'delayed' (see also **Suppl. Fig. 1D**); red: 'decreased' (see also **Suppl. Fig. 1E**); and blue: 'bi-phasic' (see also **Suppl. Fig. 1C**). Vertical blue lines indicate time of optogenetic CN stimulation (50 ms). (**E**) (*Left)* Placement of craniotomies for ECoG recording electrodes and optic fibers in CN. (*Right*) Example ECoG trace from left S1 (lS1), left M1 (lM1) and right M1 (rM1) suggesting widespread effect of single-pulse optogenetic stimulation to bi-lateral CN (50 ms). (**F**) Normalized ECoG spectrogram from a single mouse (n = 246 stimuli) calculated following the masking of the large-amplitude ECoG response directly following the CN stimulation – to accurately analyze the post-

stimulus response in all frequency bands (see STAR methods). This procedure is also applied to panels G and H. Note the clear drop in all frequency bands. (**G**) Normalized power in the separate frequency bands, indicating that in all recorded cortices a single-pulse CN stimulation resulted in a significant decrease in all channels, or in rM1 θ (4–7 Hz), θ* (7–10 Hz), β (10–20 Hz), and the broadband 2–20 Hz, but not in rM1 δ- (2–4 Hz) and γ (25–40 Hz) bands (N = 7 mice) (see **Suppl. Table 3** for statistics). (**H**) Normalized spectrogram accompanying panel G.

Pharmacological intervention of CN activity affects firing patterns of thalamic neurons

We previously showed that infusing $GABA_A$-receptor blocker gabazine (SR-95531) into the CN of *tottering* mice blocked GSWD occurrence and increased the frequency and regularity of CN spike firing [12]. To assess whether such long-term increases in CN firing had differential effects on interictal thalamic firing, as opposed to single-pulse CN stimulation, we recorded the effect of gabazine infusions into CN and found that the firing pattern of thalamic neurons was affected (**Suppl. Fig. 2A-C**). Comparison of the interictal activity recorded before and after gabazine infusion revealed that thalamic spiking contained less bursts and an increased level of regularity, while the average firing frequency was not significantly altered (**Suppl. Fig. 2D** and **Suppl. Table 4**). These alterations in thalamic firing indicate that upon gabazine infusion in CN, thalamic neurons shifted from the characteristic burst-pause firing pattern (related to a down-state of the membrane potential) to a more regular firing pattern (related to an up-state of the membrane potential) [15]. In parallel, the power of most ECoG frequency bands was changed (**Suppl. Fig. 2E-G**). Most notably, the power in the seizure-related θ*-band (7–10 Hz) was significantly decreased (**Suppl. Fig. 2H,I** and **Suppl. Table 5**). Together these data indicate that pharmacological interventions at the level of the CN affect the interictal firing pattern of thalamic neurons.

Factors contributing to the variability of thalamic responses to CN stimulation

Our current data indicate that single-pulse stimulation at a millisecond timescale and long-lasting pharmacological interventions, both of which increase CN firing [12], have a profound but variable effect on thalamic firing patterns and cortical network activity during interictal periods. This wide range of thalamic responses to optogenetic CN stimulation (**Fig. 2**) may have various causes. It may be that we recorded from different cell types [16]. Hereto we evaluated the firing pattern of thalamic neurons during GSWDs. We observed that 56.6% (69 out of 122 thalamic neurons) of the neurons revealed firing associated with GSWD patterns, i.e. 'GSWD-modulated' (**Fig. 3A-C**) (see also **Suppl. Fig. 3** and **Suppl. Table 6**), with a variable level of rhythmic spiking (**Fig. 3C**). To assess whether the location of the recordings and thereby the afferent connections related to the rhythmic firing could contribute to the wide range of responses to

CN stimulation we labelled the recording sites of 70 thalamic neurons (from 8 mice) using iontophoretic injections of biocytin (**Fig. 3D**). We found that a subpopulation of neurons throughout the various nuclei showed firing patterns directly associated with ECoG GSWDs. For these neurons the periodicity with the ECoG spikes was remarkably consistent per nucleus, ranging between 16.7 and 23.5 ms (**Fig. 3E**). In sharp contrast to these consistent firing patterns recording during ECoG GSWDs, we found that interictally

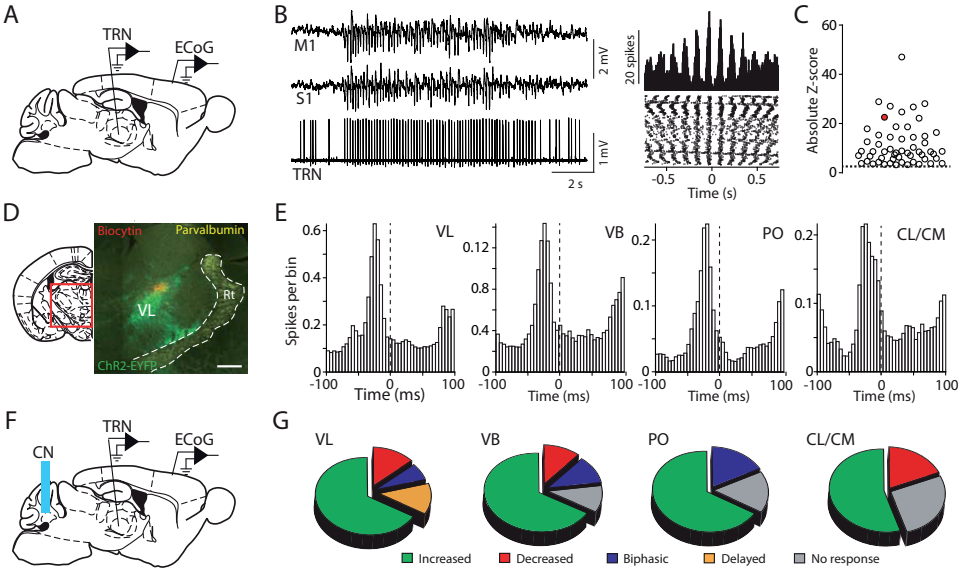

Figure 3. Varying thalamic responses to CN stimulation, but constant modulation by GSWDs. (**A**) Schematic outline of head-fixed experiment for single-unit extracellular recordings from thalamic relay neurons (TRN) and multi-site ECoG recordings from M1 and S1 regions. (**B**) (*Left*) Typical example of TRN from which the firing becomes strongly associated with M1- and S1-recorded GSWDs. (*Right*) Accompanying per-ECoG-spike-histogram and scatterplot. (**C**) Absolute Z-score range for GSWD-modulated TRN recordings (Z-score = 9.97 ± 0.99; range 1.74 – 47.17; n = 69 cells from 8 mice). Note that all recordings (n = 53) with a Z-score < 1.96 are not represented in this panel for clarity of representation. The red circle indicates the neuron shown in (**B**). (**D**) Schematic and example image of immunohistological staining indicating the thalamic recording location (biocytin, red) in the VL nucleus that is innervated by ChR2-EYFP expressing CN axons (green). Reticular nucleus neurons are stained by parvalbumin (yellow). (**E**) Per-ECoG-spike histogram for all GSWD-modulated neurons recorded in VL (n = 15 cells; 7138 ECoG spikes from 3284 GSWD episodes), VB (n = 4 cells, 2064 ECoG spikes from 1369 GSWD episodes), PO (n = 5 cells, 2342 ECoG spikes from 1149 GSWDs) and CL/CM (n = 7 cells, 1645 ECoG spikes from 1066 GSWD episodes). Note that the time lag between histogram peaks only differs marginally (VL 23.1 ms, VB 16.0 ms, PO 16.2 ms, CL/CM 20.4 ms). (**F**) As (**A**) including optogenetic CN stimulation. (**G**) Proportions of neurons in VL (n = 20 neurons), VB (n = 9 neurons), PO (n = 6 neurons) and CL/CM (n = 11 neurons) that showed an 'increase', 'decrease', 'bi-phasic' or 'delayed' response upon single-pulse CN stimulation.

the responses to single-pulse CN stimulation ranged widely throughout thalamic nuclei (**Fig. 3F**). In VL neurons we found that all recorded neurons changed their firing pattern upon CN stimulation. Most VL neurons increased the firing frequency, but the other response types (decreased, bi-phasic and delayed), which putatively can be linked to a multi-synaptic effect of CN stimulation, were also readily recorded (**Fig. 3G**).
Likewise, in the VB, PO and the intralaminar CL/CM nuclei we found several types of responses to CN firing, albeit that in these nuclei we also recorded several neurons the firing pattern of which did not change (**Fig. 3G**). These findings highlight not only that the various response types are not restricted to a particular thalamic nucleus, but also that throughout the various thalamic nuclei CN stimulation evokes a variety of changes in spiking patterns.

CN neuron stimulation is more effective than activation of cerebellar efferents inside thalamus

To determine whether controlling the activity of a portion of CN axonal input to thalamic neurons is sufficient to stop GSWDs, we implanted optic fibers directly in nuclei of the thalamic complex. We initially focused on VL and VM since the density of CN axons, as evidence by the level of fluorescence from AAV-ChR2-EYFP transfected CN axons, in these nuclei was highest (VL: 47.5 ± 11.2 a.u.; VM: 54.5 ± 14.0 a.u.; N = 5 mice) (see also [10]). Given that VL and VM not only innervate M1, but also prefrontal, sensory and associative cortical regions [17, 18], we reasoned that stimulating only the CN axons in these nuclei may be sufficient to stop the widespread cortical oscillations underlying absence seizures. To test this premise, we implanted optic fibers bilaterally in VL and VM and ensured that the level of light intensity was sufficient to in principle activate ChR2-expressing CN axons throughout the thalamic nuclei (see STAR Methods). Surprisingly, optogenetic stimulation of these regions stopped only a proportion of seizures, regardless of whether we stimulated uni- or bilaterally (**Fig. 4A-C**). In an attempt to increase the efficacy of seizure termination we activated all thalamic optic fibers simultaneously, but 50-ms pulses applied bilaterally to both VL and VM still only stopped a proportion of seizures (**Fig. 4B** and **Suppl. Table 7**). In the same mice, we also implanted optic fibers in the CN. In contrast to VL/VM stimulation bilateral CN stimulation stopped nearly all seizures (98.7 ± 1.3%); significantly more than in any of the VL/VM stimulation conditions. Even when we decreased the pulse length to 10 ms the efficacy of stopping GSWDs by direct CN stimulation (71.4 ± 6.8%) was at least as effective as applying 50 ms pulses to the VL and VM optic fibers simultaneously (**Fig. 4D** and **Suppl. Table 7**). To evaluate whether selective activation of CN axons in other thalamic nuclei is more effective in stopping seizures, we also implanted fibers in the zona incerta and in the intralaminar CL and CM nuclei, for which unilateral electrical or optogenetic stimulation was shown to dampen

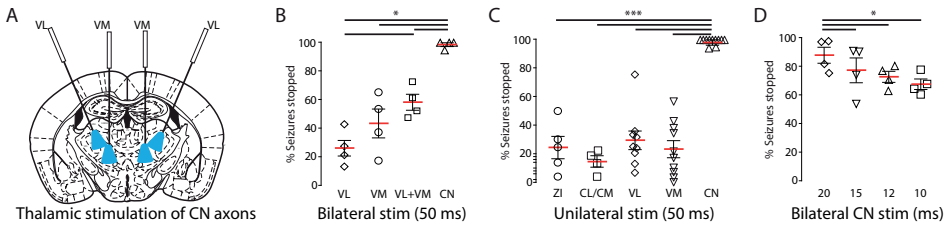

Figure 4. Activation of cerebellar afferents in thalamic nuclei is less sufficient in stopping GSWDs compared with direct cerebellar nuclei neuron stimulation. (**A**) Experimental setup with four optic fibers implanted in thalamic nuclei. (**B**) Proportion of the seizures that stopped following bilateral VL (bilateral VL 25.8 ± 1.8% N = 4 animals; 244 seizures), bilateral VM (56.2 ± 6.0% N = 4 animals; 185 seizures), quadruple VL/VM (57.3 ± 3.9%, N = 4 mice, 250 seizures) or bilateral CN stimulation (98.7 ± 1.3% N = 4 animals; 3,254 seizures). (**C**) Proportion of the seizures that stopped following unilateral zona incerta (ZI) (24.4 ± 7.8 %; N = 5 sites; 302 seizures), CL/CM (16.8 ± 2.2 %, N = 4 animals; 205 seizures), VL (31.7 ± 2.7 %, N = 5 mice, 281 seizures), VM (32.9 ± 5.0%, N = 6 mice, n = 417 seizures) or CN stimulation (98.0 ± 1.9%, N = 11 sites; 199 seizures). (**D**) Proportion of the seizures that stopped following bilateral CN stimulation with varying pulse lengths. Data from the same mice as reported in **B**. Note that at 10-ms pulse length, CN stimulation is still effective in stopping most seizures. Data are represented as mean ± SEM. * indicates $p < 0.05$, *** indicate $p < 0.001$ (see **Suppl. Table 7** for statistics).

cortical seizure activity [19, 20]. However, neither unilateral stimulation of CN terminals in zona incerta nor in CL/CM was as effective as unilateral stimulation of CN neurons (**Fig. 4C** and **Suppl. Table 7**). Collectively these data reveal that direct optogenetic CN stimulation has a more reliable effect in GSWD termination than activating proportions of cerebellar axons throughout the thalamic complex.

Discussion

Using a combination of *in vivo* electrophysiological and optogenetic techniques we could show that single-pulse stimulation of CN has a varying effect on neuronal spiking patterns throughout the thalamic complex, causing desynchronization of thalamic activity that disrupts epileptogenic GSWDs. Controlling the activity in CN for a fraction of a second was sufficient to desynchronize thalamic neurons for a prolonged period of time. Thereby our findings unveil a previously unknown function of cerebellar output in potentially directly affecting information processing in thalamo-cortical networks. We suggest that both under healthy and pathological conditions CN firing can direct the extent of thalamic synchronization and thereby contribute to neuronal network patterns encoded in various cerebral regions.

In freely behaving *tottering* mice thalamic neuronal activity recordings showed phase-locked action potential firing during GSWDs, which parallels earlier reports on

cellular excitability and hypersynchronicity in thalamo-cortical networks in this model [21-23], and other rodent models of absence epilepsy [24]. Our single-cell recordings showed that ~50% of neurons recorded in primary, associative and intralaminar thalamic nuclei fire most of their action potentials ~20 ms prior to the peak of the ECoG spikes during GSWD episodes. In the other rodent models this delay in thalamo-cortical activity ranged from 9 ms in GAERS to 28 ms in Long-Evans rats [15, 25]. In contrast to a rather fixed periodicity in thalamic firing, cerebellar firing is known to be far more variable when compared to cortical GSWDs [12, 26, 27]. Although it is not known whether CN neurons show increased levels of synchrony during GSWDs and thus could contribute to driving synchronous thalamic firing [28, 29], our findings indicate that CN output has a rather opposite effect: synchronizing CN firing by direct CN stimulation desynchronizes thalamic firing. Our previous pharmacological interventions confirm this anti-seizure effect of cerebellar output, and showed that GSWD occurrence was prevented by enhancing CN firing, whereas dampening of CN action potential firing strongly increased the seizure load [12]. Also in refractory epilepsy dentate CN stimulation has such dual effect, which was recognized to have therapeutic value [30-32].

Increasing cerebellar output resulted in a variable effect on thalamic nuclei. Anatomical connections between cerebellum and thalamus and the impact on cerebral cortical activity revealed that in various species CN axonal projections to VL neurons and the interconnected motor cortex are excitatory [10, 33-46]. However, early reports indicated bi-modal responses following electrical stimulation of the cerebellar nuclei in cats [45, 47, 48]. Although such responses may be easily caused by intra-thalamic inhibitory projections that run through the reticular thalamic nucleus, we speculate that axonal connections from CN to other pre-thalamic nuclei, such as the middle and deeper layers of the superior colliculus, the zona incerta and the anterior pretectal nucleus, contribute to the differential thalamic responses to CN stimulation (see also [9, 49]). Other sources that could contribute to a desynchronizing effect of CN stimulation on thalamic firing come from: *i*) inhibitory afferents that manipulate thalamic responses [50] to CN stimulation, as has been shown for substantia nigra pars reticulata input to VM neurons [51]; *ii*) an increased contribution of $Ca_V2.2$ (N-type) voltage-gated Ca^{2+} channels to neurotransmitter release to compensate the loss of $Ca_V2.1$ (P/Q-type) channel function in *tottering* mice, which may increase the asynchronous release of neurotransmitter (as discussed by [52]); *iii*) excitation of pre-motor CN that do not project to the thalamus but rather to premotor nuclei in the brainstem and thereby drive behavioral motor responses [53, 54]; such behavioral responses are likely to affect thalamo-cortical synchrony through the coding of proprioceptive input (see for instance ref [55]).

In conclusion, our data show that targeted stimulation of CN neurons results in desynchronization of thalamic firing in line with termination of GSWDs in *tottering* mice. We thereby suggest CN as an important node in the neuronal network underlying generalized seizures. Stimulating this node can not only acutely stop hypersynchrony in the thalamo-cortical networks during seizures, but may also have more general effects. For example, cerebellar output has been implicated in cognitive processes, like social interaction [56, 57], sensory coding [39, 40], and language [58, 59], all of which have also been linked to the integrity of the thalamic structure and its activity [60-66]. Therefore, we argue that cerebellar stimulation may also have important effects on cognitive functioning in epilepsy patients (as reviewed by [67]).

5

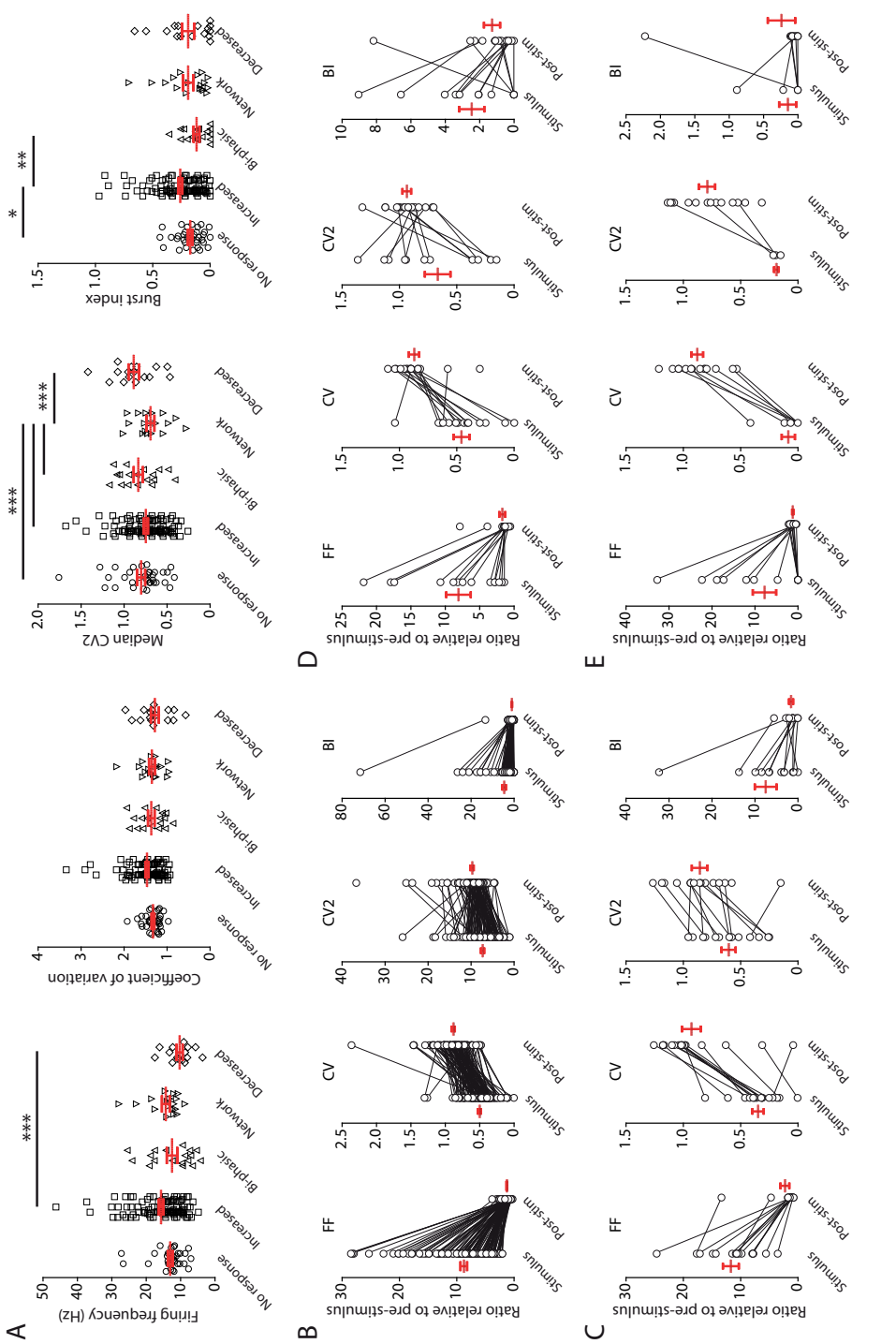
A
B
C
D
E
Firing frequency (Hz)
Coefficient of variation
Median CV2
Burst index
Ratio relative to pre-stimulus
FF
CV
CV2
BI
Stimulus
Post-stim
No response
Increased
Bi-phasic
Network
Decreased
*
**
***

Supplemental Figure 1: Spiking pattern characteristics of thalamic relay neurons in relation to CN stimulation. (**A**) Pre-stimulus firing frequency, coefficient of variation, median CV2 and burst index recorded from neurons that did not respond with a significantly altered spiking pattern to CN stimulation ('no response'; n = 36 neurons) and from neurons that responded with increased firing patterns during the 50-ms CN stimulation pulse ('increased'; n = 114 neurons), a bi-phasic modulation of spiking during the stimulus and post-stimulus period ('bi-phasic'; n = 17 neurons), a delayed response, i.e., no significant change in firing rate during the CN but only during the post-stimulus period ('delayed'; n = 15 neurons) or solely a decreased firing rate during the stimulus and/or post-stimulus periods ('decreased'; n = 19 neurons). See **Fig. 2D** for typical examples of each type of response. (**B-E**) Relative difference in firing frequency (FF), CV, CV2 and burst index (BI) during the stimulus and the post-stimulus period compared to the pre-stimulus period for all 'increased' (**B**), 'bi-phasic' (**C**), 'delayed' (**D**) and 'decreased' neurons (**E**). Only when the number of spikes allowed a calculation of all parameters the data points of the individual recordings are connected. Red markers indicate mean ± SEM. * indicates $p < 0.05$, ** $p < 0.01$ and *** $p < 0.001$. (see **Suppl. Table 2** for statistics).

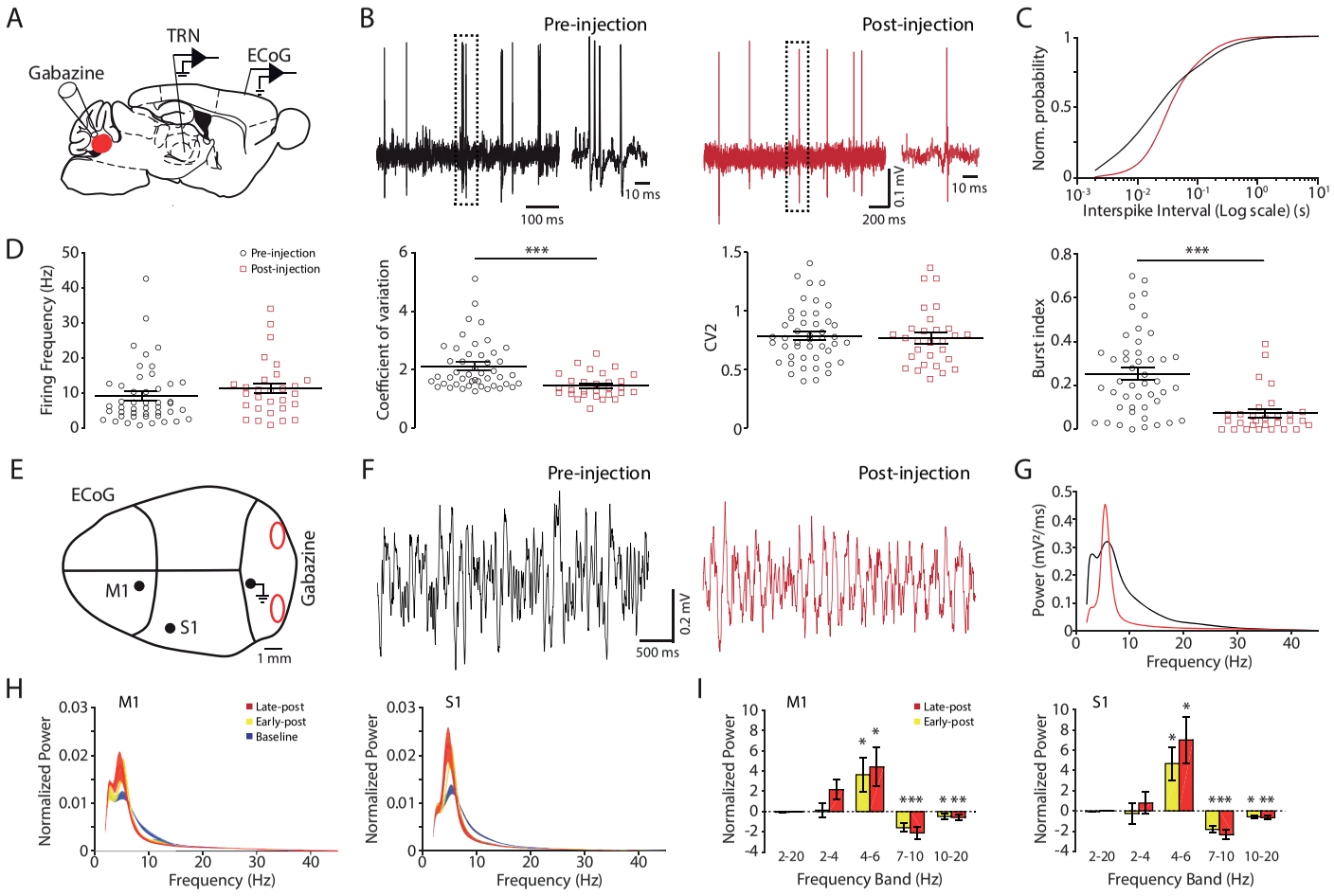
A
TRN
ECoG
Gabazine
B
Pre-injection
Post-injection
100 ms
10 ms
0.1 mV
200 ms
C
Norm. probability
Interspike Interval (Log scale) (s)
D
Pre-injection
Post-injection
Firing Frequency (Hz)
Coefficient of variation
***
CV2
Burst index
E
ECoG
M1
S1
Gabazine
1 mm
F
Pre-injection
Post-injection
0.2 mV
500 ms
G
Power (mV²/ms)
Frequency (Hz)
H
M1
S1
Late-post
Early-post
Baseline
Normalized Power
Frequency (Hz)
I
M1
S1
Late-post
Early-post
Normalized Power
2-20
2-4
4-6
7-10
10-20
Frequency Band (Hz)

Supplemental Figure 2. Long-term modulation of cerebellar output by bilateral gabazine injections. (**A**) Schematic outline of head-fixed experiment for CN injection of gabazine, single-unit extracellular recordings from thalamic relay neurons (TRN) and multi-site ECoG recordings from M1 and S1 regions. (**B**) Example traces of two single-unit TRNs: one in the absence (pre-injection; black) and one in the presence (post-injection; red) of gabazine in the bilateral CN. Note the presence (left trace) and absence (right) of burst-firing. (**C**) Normalized cumulative distribution for the interspike interval of thalamic neurons pre-injection (black) and post-injection of gabazine in the bilateral CN. (**D**) Average firing frequency, coefficient of variation (CV), CV2 and burst-index calculated for neurons recorded pre-gabazine (n = 46 neurons, N = 4 mice) and another set of neurons post-gabazine (n = 29 neurons, N = 4 mice). ** indicate $p < 0.01$. (**E**) Placement of craniotomies for ECoG recording electrodes and gabazine injections into the CN. (**F**) Four seconds of M1 ECoG recording pre-gabazine (*left*, black) and post-gabazine (*right*, red) from a single mouse. (**G**) Result of fast-Fourier transform of pre-gabazine (black) and post-gabazine (red) M1 ECoG. (**H**) Normalized ECoG power in M1 (*left*) and S1 (*right*) recordings from 4 mice, comparing pre-gabazine (baseline), ~5–20 min after gabazine (early-post) and ~1 hour after gabazine (late-post). (**I**) Relative change in ECoG power (normalized to pre-gabazine condition) showing an increase in θ- (4–7 Hz) power and a significant decrease in the β-band (10–20 Hz) and the θ*-band (7–10 Hz). The power in δ- (2–4 Hz), γ (25–40 Hz) and broadband 2–20 Hz activity was not affected. Note that there was no difference between M1 and S1 responses (see also [68]). * indicates $p < 0.05$, ** indicate $p < 0.01$ and ** indicate $p < 0.001$. See **Suppl. Tables 4 and 5** for statistics.

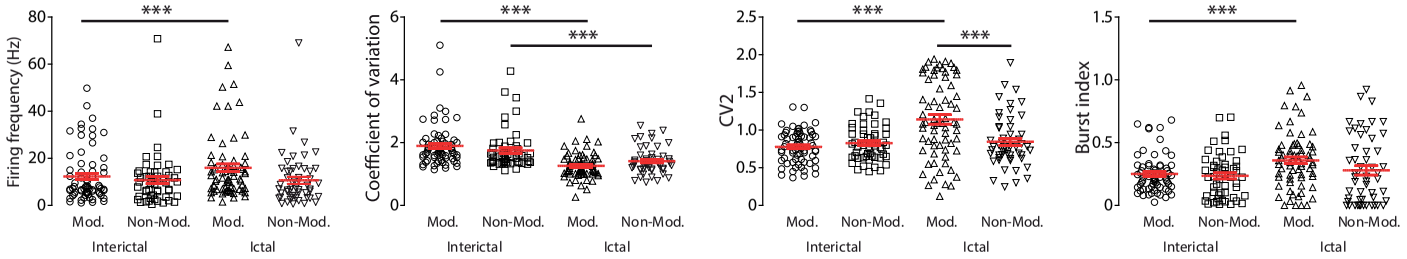

Supplemental Figure 3: Spiking pattern characteristics of thalamic relay neurons in relation to ECoG spike-and-wave discharges. Firing frequency, coefficient of variation, CV2 and burst index for thalamic relay neurons that revealed spike-and-wave discharge (GSWD)-modulated or non-modulated spiking. Each firing parameter is represented for the interictal and ictal phases (determined by the occurrence of SWDs; see STAR methods section). Red markers indicate mean ± SEM. *** indicate $p < 0.001$ (see **Suppl. Table 6** for statistics).

STAR* Methods

*Key resource table

Reagents	Source	Identifier
Antibodies		
Parvalbumin	SWANT	PV-235
Cy5	Jackson Immunoresearch	715-175-150
DAPI	Invitrogen	D3571
Bacterial and viral strains		
AAV vector	UNC – vector core	AAV2-hSyn-Chr2(H134R)-EYFP
Chemicals, peptides, recombinant proteins		
Biocytin	Sigma-Aldrich	B4261
Gabazine (SR-95531)	Tocris	1262
Evans Blue	Sigma-Aldrich	E2129
DNA primer for tottering mutation 5′-TTCTGGGTACCAGATACAGG-3′ 5′-AAGTGTCGAAGTTGGTGCGC-3′	Eurogentech	N/A
Essential experimental equipment		
borosilicate glass capillaries	World Precision Instruments	PG52165-4
Micromanipulator	Luigs&Neumann	SM-7
Cyberamp 380	Molecular Devices	N/A
Neurodata	Cygnus technology	IR183A and IR283A
CED AD/DA converter	Molecular Devices	Power 1401-3
Digidata digitizer	Molecular Devices	1322/A
Multiclamp	Molecular Devices	700B
Experimental models: Organisms/ Strains		
Mouse: natural $Ca_V2.1$ mutant *'Tottering'*	Originally purchased from Jax Laboratories	Maintained colony with C57BL/6-NHsd
Software and Algorithms		
SPSS 22.0	SPSS	https://www.ibm.com/products/spss-statistics
Matlab	Mathworks Inc	https://www.mathworks.com/
Fieldtrip software	*Open Source*	doi:10.1155/2011/156869
Labview	National Instruments	http://www.ni.com/en-us/shop/labview.html
Spiketrain	Neurasmus B.V.	http://www.neurasmus.com/spiketrain.php
Fiji	ImageJ	https://fiji.sc

***Contact for reagent and resource sharing**

Further information and requests for resources and reagents should be directed to and will be fulfilled by the lead contact, Freek E. Hoebeek (f.hoebeek@erasmusmc.nl)

***Experimental model and subject details**

Data were collected from male and female homozygous *tottering* mice (4- to 30-weeks-old) and their wild-type littermates, which were bred using heterozygous mice. The colony, originally purchased from Jackson laboratory (Bar Harbor, ME, USA), was maintained using C57BL/6NHsd mice obtained from Envigo laboratories (Horst, the Netherlands). PCR was used to confirm the presence of the tottering mutation in the *Cacna1a* gene using 5′-TTCTGGGTACCAGATACAGG-3′ (forward) and 5′-AAGTGTCGAAGTTGGTGCGC-3′ (reverse) primers (Eurogentech, Seraing, Belgium) and subsequent digestion using restriction enzyme *Nsb*I at the age of P9 - P12. All surgical and experimental procedures were performed in accordance with the European Communities Council Directive. Protocols were reviewed and approved by the institutional experimental animal committee (DEC).

***Method Details**

Viral infection

Stereotactic viral injections were performed as previously described [12]. Briefly, the mice were kept under anesthesia in a custom made stereotactic frame. Craniotomies in the sagittal bone allowed us access to the cerebellar surface. We bilaterally injected virus-containing solutions (100 to 120 nL at a rate of ~20 nL/min) to transfect neurons in the interposed and lateral CN with Channelrhodopsin-2 (AAV2-hSyn-Chr2(H134R)-EYFP) [69]. After 10 minutes the injection pipette was slowly retracted and optic fibers were implanted ~200 µm above the injection site. Stereotaxic coordinates for CN injections were 2.5 mm posterior to lambda, 2.2 mm lateral to the midline and 2.2 mm below the pial surface. Viral vectors were originally designed by Dr. K. Deisseroth and were acquired from the University of North Carolina vector core.

Preparation for freely behaving recordings

Chronic electrode implantation was performed under isoflurane anesthesia (induction 4%; maintenance 1.5% in oxygen-enriched air) at the following coordinates (mm to bregma): -1.0 AP; +3.5 ML; -0.6 DV (right S1; single 75 µm platinum (Pt)/iridium (Ir) electrodes, PT6718; Advent Research Materials, Oxford, UK); or 1.0 mm AP; -1.5 mm ML; -0.6 mm V (right M1; single Pt/Ir electrodes) for LFP recordings; -1.3 mm AP; +1.25 mm ML; -3.1 mm DV (right VL; paired Pt/Ir); or -1.8 mm AP; +0.75 mm ML; -3.0 mm V (right

CL; paired Pt/Ir); or -1.8 mm AP; +1.6 mm ML; -3.0 mm V (right VPL/VPM; paired Pt/Ir) for MUA recordings; two ball-tip electrodes (Ag, 75 µm) were positioned just posterior from lambda above cerebellum to serve as reference and ground electrodes. To enable optogenetic control of neuronal activity in CN, mice received 2 craniotomies in the interparietal bone for viral vector injection and placement of two optical fibers (200 µm diameter; CFML22L05, Thorlabs, Newton, NJ, USA) (-2.5 mm relative to lambda; 2.0 ML; 2.0 DV). CN were stereotactically injected bilaterally with 100-150 nl of the AAV2-hSyn-ChR2(H134R)-EYFP vector (kindly provided by Dr K. Deisseroth from Stanford University through the Vector Core at the University of North Carolina). Electrodes were connected to a 7-channel pedestal (E363/0 socket contacts and MS373 pedestal; Plastics One, Roanoke, VA, USA) and secured to the skull together with the optic fibers using light-activated bonding primer and dental cement (Kerr optibond / premise flowable, DiaDent Europe, Almere, the Netherlands) Carprofen (5 mg/kg, s.c.) and Temgesic (0.1 mg/kg, s.c.) was administered for post-operative pain relief.

Preparation for head-fixed in vivo recording

Male and female mice were anesthetized with a mixture of isoflurane (2% mixed with O_2. Body temperature was supported by a heating pad (FHC, Bowdoin, ME, USA). ECoG electrode implantation in M1 and S1 cortices was performed as previously described [12]. To enable extracellular recordings from thalamic neurons, a subset of mice received bilateral craniotomies (~ 1.5 mm diameter) in the parietal bone and great care was taken to preserve the dura mater. In another subset of mice the thalamic complex was implanted with optic fibers. These fibers were positioned using the following coordinates (in degrees (°) relative to the interaural axis and in mm relative to bregma): VL: 22° roll angle, -1.2 AP, -3.0 ML, -3.1 depth; VM: 2° roll angle, -1.2 AP, -1.1 ML, 3.3 depth; CL/CM: 0° roll angle, -1.3 AP, -0.75 ML, -3.0 depth; zona incerta: 0° roll angle, -2.5 AP, -1.75 ML, -3.6 depth). The positioning of the optic fibers was confirmed using immunofluorescent staining (see below). The exposed tissue was surrounded by a recording chamber, covered with tetracycline-containing ointment (Terra-cortril; Pfizer, New York, NY, USA) and sealed with silicon wax (Twinsil speed; Picodent, Wipperfurth, Germany). To allow the use of precise stereotactic coordinates during recording sessions we marked the position of bregma. After surgery, the mice recovered for at least five days in their home cage before experiments were performed.

In vivo extracellular electrophysiology

Following ~2-hour daily accommodation session in the setup on the first two days we performed recordings in awake, head-fixed mice on the third day lasting no longer than 4 hours. Although being head-fixed, the mice were able to move all limbs freely. The

recording sessions typically were between 9:00 and 17:00, i.e., during the light period. Body temperature was supported using a heating pad (FHC). For extracellular single-unit recordings, custom-made, borosilicate glass capillaries (OD 1.5 mm, ID 0.86 mm; resistance 8–12 MΩ; taper length ~5 µm; tip diameter 0.5 µm) (Harvard Apparatus, Holliston, MA, USA) filled with 2 M NaCl were positioned stereotactically using an electronically driven pipette holder (SM7; Luigs & Neumann, Ratingen, Germany). Stereotactic coordinates for the thalamic recordings were tailored to the different thalamic nuclei. Thalamic neurons were localized by stereotactic location and a subset of recording sites was identified using iontophoretic injections of biocytin (1.5%, ~ 1 min, 4 sec on/off, 50% duty cycle, 4 µA), which was present in the NaCl-filled recording pipette.

ECoG recordings were filtered online using a 1–100 Hz band pass filter and a 50 Hz notch filter, sampled at 500 Hz and amplified before being stored for off-line analysis. Single-unit extracellular recordings were filtered online using a 30 Hz high pass filter and a 50 Hz notch filter, sampled at 20 kHz and stored for off-line analysis. All electrophysiological recordings were performed using either a combination of CyberAmp 380 (Molecular Devices, LLC, Sunnyvale, Ca, USA), Neurodelta IR 183A or IR283A (Cygnus Technology Inc., Delaware Water Gap, PA, USA) and CED power 1401-3 (Cambridge England), or the combination of Multiclamp 700B and Digidata 1322A (Molecular Devices).

Optogenetics and electrophysiology in head-fixed in vivo preparation

For extracellular recordings combined with optogenetic CN or thalamic stimulation brief pulses (50 ms) of blue (470 nm) light were used to activate ChR2-infected CN neurons. Optic fibers (for CN stimulation: inner diameter = 200 µm, numerical aperture (NA) = 0.39; for thalamic stimulation: inner diameter = 105 µm, NA = 0.22; Thor Labs, Newton, NJ, USA) were placed ~200 µm from the injection site and connected to 470 nm LED sources (Thor Labs). Light intensity at the tip of the implantable fiber was 550 ± 50 µW/mm^2. We chose these optic fiber diameters following estimation of the light intensity in the brain [70] so as to ensure that in CN sufficient neurons would be activated and that in thalamus a sufficient number of CN axons were activated. LEDs were activated for 50 ms at 0.2 Hz or by a closed-loop GSWD-detection system [12, 71].

Freely behaving electrophysiological recordings and optogenetic stimulation

After a 2-3 weeks recovery period, electrophysiological recordings were performed in freely behaving animals as described previously [72]. Electrophysiological signals were 3x pre-amplified and fed into separate ECoG (0.5-500 Hz, 800x gain) and MUA amplifiers (500-5,000 Hz; 12,000X gain). Signals were digitized (Power1401 and Spike2

software; CED) at 5,000 Hz (ECoG) or 25,000 Hz (MUA). Synchronized video-recordings made using a digital CCD camera at 30 frames/s (acA1300-60gmNIR; Basler, Ahrensburg, Germany). Optic fibers were connected to 470 nm LEDs (Thor Labs). Manual stimulation was performed to test efficacy of single pulse stimulation (0.5 mW/mm^2, 50 ms) for the disruption of GSWDs using a pulse generator (Prizmatix, Givat-Shmuel, Is) as previously described [12].

Pharmacological modulation of CN neurons

Procedure to increase CN action potential firing was performed as described previously ([12]. Briefly, we located CN neurons after which we recorded one hour of 'baseline' ECoG. After this an injection was made with 100 µM gabazine ($GABA_A$-antagonist; Tocris) dissolved in 1 M NaCl combined with fluorescence of Evans Blue (1% in 1 M NaCl) for histological verification. Next, we recorded during 20-50 min after the injection thalamic activity. The data on GSWD-occurrence following gabazine injection from 4 out of the 6 mice have been reported previously (Fig. 2 in ref [12]).

Immunohistochemistry

Animals were anesthetized with pentobarbital (0.15 mL, intraperitoneal) immediately after acquiring the postinjection ECoG and perfused transcardially with saline followed by 4% paraformaldehyde (Sigma-Aldrich) in 0.1 M phosphate buffer (Sigma-Aldrich, pH = 7.4). Brains were removed and postfixed for 1–3 hours in 4% phosphate-buffered paraformaldehyde at room temperature, placed overnight in 10% sucrose in 0.1 M PB at 4°C and subsequently embedded in gelatine with 30% sucrose. We serially collected 50-µm-thick coronal sections for immunofluorescent staining. Cerebellar sections were incubated for 10 min with DAPI (300 nM) to verify the locations of viral injections and diencephalic sections were processed for parvalbumin staining (primary staining: 1:7,000 α-mouse, Swant #Pv-235; secondary staining: 1:200 mouse-α-donkey, Jackson Immunoresearch #715-175-150 (Westgrove, PA, USA) to locate thalamic nuclei and for biocytin staining to locate the recording sites. We confirmed the correct localization of the injections of gabazine and biocytin with images captured using a confocal laser scanning microscope (LSM 700; Zeiss, Lambrecht, Germany) at 555 nm (Evans Blue, Sigma), 488 (ChR2-EYFP) and 647 nm (parvalbumin).

***Quantification and statistical analysis**

Offline GSWD and extracellular action potential analysis

Both analysis of extracellular recordings and spontaneous GSWD characteristics were performed using previously described offline statistical analysis [12]. In brief, action

potential analysis was performed using custom-written Matlab-based program SpikeTrain (Neurasmus, Erasmus MC Holding, Rotterdam, the Netherlands). Extracellular recordings were included if activity was stable and well isolated for at least 100 s. GSWD analysis was performed using a custom-written GSWD detection algorithm (LabVIEW, National Instruments, Austin, TX, USA). Co-efficient of variance (CV) was calculated as the ratio between the average and standard deviation of the interspike intervals (σ_{ISI}/μ_{ISI}), CV2 as ($2|ISI_{n+1} - ISI_n|/(ISI_{n+1} + ISI_n)$) [73] and burst index as (BI = number of action potentials within bursts / total number of action potentials) for which we defined 'burst' as a sequence of ≥3 spikes within 100 ms.

Offline MUA analysis

MUA data were analyzed using the template-matching method for spike sorting with an optimal spike threshold of 3 times SD from a 60-sec baseline recording. Sorted spikes were exported and analyzed following a custom-written algorithm in MATLAB to generate spike histograms. The spike-to-spike correlation (autocorrelation) was plotted based on a previous method [74]. Data points (x) were normalized (X_s) in a [0,1] range using the maximum spike count (x_{max}) and the minimum spike count (x_{min}): $X_s = x - x_{min} / x_{max} - x_{min}$. Mean correlation values were calculated by taking the ratio of the greatest correlation peak and the peak at t=0. The same time range was used to determine the greatest correlation in baseline and post-stimulation. Trials were included when the seizure ended 10 ms before stimulation and 150 ms after stimulation.

Assessment of modulation of TRN units

GSWD triggered rasterplots and peri-stimulus-time-histograms (PSTHs; 5 ms bin width) were used to calculate the modulation amplitude and frequency. ISIs of the data used for the rasterplots were subsequently shuffled randomly 500 times to create a normal distribution of modulation amplitudes. Cells were considered GSWD-modulated if the modulation amplitude was significantly higher than expected by chance, as indicated by a Z-score ($Z = (X-\mu)/\sigma$; $Z \geq 1.96$, $p \leq 0.05$) using the shuffled data as described previously [12], and if cells modulated at seizure frequency (6–9 Hz). The phase difference between the occurrence of the most negative deflection of a GSWD-episode and the time of the peak in thalamic activity was calculated by dividing this time difference by the median time difference between two GSWDs in that particular seizure.

Response of optogenetic stimulation

To determine if thalamic single units were significantly modulated following optogenetic CN stimulation we performed a random permutation calculation following a Monte-Carlo Bootstrap method, using 2 ms bin width PSTHs. For every recording we calculated

the ISIs of action potentials 4 s prior to every pulse and combined them in a single ISI distribution, which was randomly permutated 250 times. We created PSTHs from these 'fake' spike times and calculated the average and standard deviation. If the PSTH of the 'true' spiking response to optogenetic stimuli breached the mean + 2SD threshold we noted the recording to have an increased firing response. For a subset of neurons we noticed a compelling inhibition. We marked the recording to have a decreased firing response if at any time during the post-stimulus period (5 s in total) 25 consecutive bins, i.e., 50 ms, the spike count was zero.

Assessment of fluorescence in thalamic nuclei

Guided by a reference atlas [75] we outlined the thalamic nuclei of interest. For each nucleus the expression pattern of ChR2-YFP was quantified with RGB measure function of Fiji (ImageJ) to calculate the mean intensity (in arbitrary units; a.u.) among the region of interest (ROI).

Interictal ECoG analysis

Analysis of EcoG data was performed with the fieldtrip toolbox (http://www.fieldtriptoolbox.org) [76] in MATLAB. For the optogenetic data, stimuli that occurred during manually identified inter-ictal periods were extracted and subsequently any found to contain artefacts or short periods of increased oscillatory activity were removed from further analysis. Extracted epochs contained 4 s of activity both before and after the stimulus and data was bandpass filtered between 2 and 125 Hz prior to further analysis. Replacement of the stimulus artefact was performed by removing the section of data 700 ms prior to the stimulus to 300 ms after the stimulus and replacing it with a section of data extracted from 3 s prior to the stimulus on a trial by trial basis the ends of the replaced section were then smoothed to reduce edge effects. Spectrograms were calculated using Morlet wavelets with a width of 7 and evaluated at every sample.

For the Gabazine injection data, 100 epochs of 10 s were extracted from inter-ictal periods prior to injection (Baseline), immediately following injection (Early Post) and after ~1 hr (Late Post). Epochs with artefacts were rejected on the same basis as for the optogenetic data. The frequency content of the signals was calculated using Morlet Wavelets and normalized to the total power in the 2 to 115 Hz frequency band.

Statistical analysis

We examined the variance in each group using Kolmogorov-Smirnov and Shapiro-Wilk's test for normality. We analyzed the data using parametric (two-samples, one/two-tailed Student's *t*-test or (repeated measures) (M)ANOVA) or non-parametric (one/two-tailed Mann-Whitney U) depending on whether data was normally distributed. For

the ECoG data statistical analysis of the power in each frequency band was carried out via repeated measures ANOVA with time point (Baseline, Early Post and Late Post) as the within-subject factor and recording location as the between subject factor. Only frequency bands which displayed a significant main effect of time point were subjected to post-hoc paired sample *t*-tests, Bonferroni-corrected *p*-values are reported in the figure legends. $P < 0.05$ is considered significantly different. A single asterisk indicates $p < 0.05$, two asterisks indicate $p < 0.01$, three asterisks indicate $p < 0.001$.

Acknowledgements

The authors thank Elize Haasdijk, Erika Sabel-Goedknegt, Mandy Rutteman, Marloes Adank, Jinne Geelen, Beerend Winkelman, Maarten Schenke and Farnaz Nassirinia for excellent technical and analytical support and Thijs Houben, Bas van Hoogstraten, Daniël Dumas, Carmen Schäfer, Sander Lindeman, Zhenyu Gao, Saša Peter and for their practical and insightful comments. This research was supported by funding from ERC-Adv, ERC-PoC to CIDZ, various ZonMw and NWO-ALW grants to A.M.J.M.v.d.M., C.I.D.Z. and F.E.H, FP7 "EUROHEADPAIN" and EU IAPP "BRAINPATH" to A.M.J.M.v.d.M. and E.A.T., EU Marie Curie Career Integration Grant to E.A.T. and the Dutch National Epilepsy Foundation to A.M.J.M.v.d.M. and E.A.T.

Contributions:

O.H.J.E.R. performed all experiments with help of L.K, H.J.P. and N.A.J. for recordings and stimulations in head-fixed animals, of S.J.F. and E.A.T. for the data recorded in freely moving animals, of L.K. for the analyses of seizure detection and spike modulation, of P.H. for analysis of ECoG activity, and of S.V.G. for axonal projection analyses; E.A.T., A.M.J.M.v.d.M. and C.I.D.Z. contributed experimental setups, supervised the project and provided financial support; O.H.J.E.R. L.K. and F.E.H. conceived and designed experiments; O.H.J.E.R. and F.E.H. wrote the manuscript with help from all co-authors.

References

1. Aarabi, A., Wallois, F., and Grebe, R. (2008). Does spatiotemporal synchronization of EEG change prior to absence seizures? Brain research *1188*, 207-221.
2. Beenhakker, M.P., and Huguenard, J.R. (2009). Neurons that fire together also conspire together: is normal sleep circuitry hijacked to generate epilepsy? Neuron *62*, 612-632.
3. Cressman, J.R., Ullah, G., Ziburkus, J., Schiff, S.J., and Barreto, E. (2009). The influence of sodium and potassium dynamics on excitability, seizures, and the stability of persistent states: I. Single neuron dynamics. Journal of Computational neuroscience *26*, 159-170.
4. Danober, L., Deransart, C., Depaulis, A., Vergnes, M., and Marescaux, C. (1998). Pathophsyiological mechanisms of genetic absence epilepsy in the rat. Progress in neurobiology *55*, 27-57.
5. Stam, C.J. (2014). Modern network science of neurological disorders. Nat Rev Neurosci *15*, 683-695.
6. Adebimpe, A., Aarabi, A., Bourel-Ponchel, E., Mahmoudzadeh, M., and Wallois, F. (2015). Functional Brain Dysfunction in Patients with Benign Childhood Epilepsy as Revealed by Graph Theory. PLoS One *10*.
7. Paz, J.T., and Huguenard, J.R. (2015). Microcircuits and their interactions in epilepsy: is the focus out of focus? Nature Neuroscience *18*, 351-359.
8. Krook-Magnuson, E., and Soltesz, I. (2015). Beyond the hammer and the scalpel: selective circuit control for the epilepsies. Nat Neurosci *18*, 331-338.
9. Schafer, C.B., and Hoebeek, F.E. (2017). Convergence of primary sensory cortex and cerebellar nuclei pathways in the whisker system. Neuroscience *Epub ahead of print*.
10. Teune, T.M., Van der Burg, J., Van der Moer, J., and Ruigrok, T.J. (2000). Topography of cerebellar nuclear projections to the brain stem in the rat. Prog. Brain Res. *124*, 141-172.
11. Noebels, J.L., and Sidman, R.L. (1979). Spike-Wave and focal motor seizures in the mutant mouse tottering. Science *204*, 1334-1336.
12. Kros, L., Eelkman Rooda, O.H.J., Spanke, J.K., Alva, P., Van Dongen, M.N., Karapatis, A., Tolner, E.A., Strydis, C., Davey, N., Winkelman, B.H.J., et al. (2015). Cerebellar output controls generalized spike-and-wave discharge occurrence. Annals of Neurology *77*, 1027-1049.
13. Gao, Z., Proietti-Onori, M., Lin, Z., Ten Brinke, M.M., Boele, H.J., Potters, J.W., Ruigrok, T.J., Hoebeek, F.E., and De Zeeuw, C.I. (2016). Excitatory Cerebellar Nucleocortical Circuit Provides Internal Amplification during Associative Conditioning. Neuron *89*, 645-657.
14. Houck, B.D., and Person, A.L. (2015). Cerebellar Premotor Output Neurons Collateralize to Innervate the Cerebellar Cortex. J Comp Neurol *523*, 2254-2271.
15. Polack, P.O., and Charpier, S. (2006). Intracellular activity of cortical and thalamic neurones during high-voltage rhythmic spike discharge in Long-Evans rats in vivo. J. Physiol. *571*, 461-476.
16. Clasca, F., Rubio-Garrido, P., and Jabaudon, D. (2012). Unveiling the diversity of thalamocortical neuron subtypes. The European journal of neuroscience *35*, 1524-1532.
17. Kuramoto, E., Ohno, S., Furuta, T., Unzai, T., Tanaka, Y.R., Hioki, H., and Kaneko, T. (2015). Ventral medial nucleus neurons send thalamocortical afferents more widely and more preferentially to layer 1 than neurons of the ventral anterior-ventral lateral nuclear complex in the rat. Cereb Cortex *25*, 221-235.
18. Kuramoto, E., Furuta, T., Nakamura, K.C., Unzai, T., Hioki, H., and Kaneko, T. (2009). Two types of thalamocortical projections from the motor thalamic nuclei of the rat: a single neuron-tracing study using viral vectors. Cereb Cortex *19*, 2065-2077.

19. Chen, J., and Kriegstein, A.R. (2015). A GABAergic projection from the zona incerta to cortex promotes cortical neuron development. Science *350*, 554-558.

20. Valentin, A., Garcia Navarrete, E., Chelvarajah, R., Torres, C., Navas, M., Vico, L., Torres, N., Pastor, J., Selway, R., Sola, R.G., et al. (2013). Deep brain stimulation of the centromedian thalamic nucleus for the treatment of generalized and frontal epilepsies. Epilepsia *54*, 1823-1833.

21. Zhang, Y., Mori, M., D.L., B., and Noebels, J.L. (2002). Mutations in high-voltage activated calcium channel genes stimulate low-voltage-activated currents in mouse thalamic relay neurons. Journal of Neuroscience *22*, 6362-6371.

22. Song, I., Kim, D., Choi, S., Sun, M., Kim, Y., and Shin, H.S. (2004). Role of the A1G T-type calcium channel in spontaneous absence seizures in mutant mice. Journal of Neuroscience *24*, 5249-5257.

23. Sasaki, S., Huda, K., Inoue, T., Miyata, M., and Imoto, K. (2006). Impaired feedforward inhibition of the thalamocortical projection in epileptic Ca2+ channel mutant mice, tottering. J Neurosci *26*, 3056-3065.

24. Depaulis, A., and Charpier, S. (2017). Pathophysiology of absence epilepsy: Insights from genetic models. Neuroscience letters.

25. Polack, P.O., Mahon, S., Chavez, M., and Charpier, S. (2009). Inactivation of the somatosensory cortex prevents paroxysmal oscillations in cortical and related thalamic neurons in a genetic model of absence epilepsy. Cerebral Cortex *19*, 2078-2091.

26. Kandel, A., and Buzsáki, G. (1993). Cerebellar neuronal activity correlates with spike and wave EEG patterns in the rat. Epilepsy Res. *16*, 1-9.

27. Kros, L., lindeman, S.L., Eelkman Rooda, O.H.J., De Zeeuw, C.I., and Hoebeek, F.E. (in press). Synchronicity and rhythmicity of Purkinje cell firing during generalized spike-and-wave discharges in a natural mouse model of absence epilepsy. Frontiers in cellular neuroscience.

28. Maejima, T., Wollenweber, P., Teusner, L., Noebels, J.L., Herlitze, S., and Mark, M.D. (2013). Postnatal loos of P/Q-type channels confined to rhombic-lip-derived neurons alters synaptic transmission at the parallel fiber to Purkinje cell synapse and replicates genomic Cacna1a mutation phenotype of ataxia and seizures in Mice. J. Neurosci. *33*, 5162-5174.

29. Mark, M.D., Maejima, T., Kuckelsberg, D., Yoo, J.W., Hyde, R.A., Shah, V., Gutierrez, D., Moreno, R.L., Kruse, W., Noebels, J.L., et al. (2011). Delayed postnatal loss of P/Q-type calcium channels recapitulates the absence epilepsy, dyskinesia, and ataxia phenotypes of genomic Cacna1a mutations. J. Neurosci. *31*, 4311-4326.

30. Chkhenkeli, S.A., Šramka, M., Lortkipanidze, G.S., Rakviashvili, T.N., Bregvadze, E.S., Magalashvili, G.E., Gagoshidze, T.S., and Chkhenkeli, I.S. (2004). Electrophysiological effects and clinical results of direct brain stimulation for intractable epilepsy. Clin. Neuro.l Neurosurg. *106*, 318-329.

31. Sramka, M., and Chkhenkeli, S.A. (1990). Clinical experience in intraoperational determination of brain inhibitory structures and application of implanted neurostimulators in epilepsy. Stereotact Funct Neurosurg *54-55*.

32. Šramka, M., Fritz, G., Galanda, M., and Nádvorník, P. (1976). Some observations in treatment stimulation of epilepsy. Acta Neurochir. (Suppl.) *23*, 257-262.

33. Asanuma, C., Thach, W.T., and Jones, E.G. (1983). Distribution of cerebellar terminations and their relation to other afferent terminations in the ventral lateral thalamic region of the monkey. Brain research *286*, 237-265.

34. Sasaki, K., Matsuda, Y., and Mizuno, N. (1973). Distribution of cerebellar-induced responses in the cerebral cortex. Exp Neurol *39*, 342-354.

35. Aumann, T.D., and Horne, M.K. (1996). Ramification and termination of single axons in the cerebellothalamic pathway of the rat. J. Comp. Neurol. *376*, 420-430.
36. Bentivoglio, M., and Kuypers, H.G. (1982). Divergent axon collaterals from rat cerebellar nuclei to diencephalon, mesencephalon, medulla oblongata and cervical cord. A fluorescent double retrograde labeling study. Exp Brain Res *46*, 339-356.
37. Cohen, D., Chambers, W.W., and Sprague, J.M. (1958). Experimental study of the efferent projections from the cerebellar nuclei to the brainstem of the cat. J Comp Neurol *109*, 233-259.
38. Haroian, A.J., Massopust, L.C., and Young, P.A. (1981). Cerebellothalamic projections in the rat: an autoradiographic and degeneration study. J Comp Neurol *197*, 217-236.
39. Popa, D., Spolidoro, M., Proville, R.D., Guyon, N., Belliveau, L., and Léna, C. (2013). Functional role of the cerebellum in gamma-band synchronization of the sensory and motor cortices. J. Neurosci. *33*, 6552-6556.
40. Proville, R.D., Spolidoro, M., Guyon, N., Dugué, G.P., Selimi, F., Isope, P., Popa, D., and Léna, C. (2014). Cerebellum involvement in cortical sensorimotor circuits for the control of voluntary movements. Nature Neuroscience *17*, 1233-1239.
41. Rispal-Padel, L., and Grangetto, A. (1977). The cerebello-thalamo-cortical pathway. Topographical investigation at the unitary level in the cat. Exp Brain Res *28*, 101-123.
42. Rispal-Padel, L., and Latreille, J. (1974). The organization of projections from the cerebellar nuclei to the contralateral motor cortex in the cat. Exp Brain Res *19*, 36-60.
43. Sawyer, S.F., Young, S.J., Groves, P.M., and Tepper, J.M. (1994). Cerebellar-responsive neurons in the thalamic ventroanterior-ventrolateral coplex of rats: in vivo electrophysiology. Neuroscience *63*, 711-724.
44. Steriade, M., and Contreras, D. (1995). Relations between cortical and thalamic cellular events during transition from sleep patterns to paroxysmal activity. Journal of Neuroscience *15*, 623-642.
45. Uno, M., Yoshida, M., and Hirota, I. (1970). The mode of cerebello-thalamic relay transmission investigated with intracellular recording from cells of the ventrolateral nucleus of cat's thalamus. Exp Brain Res *10*, 121-139.
46. Yoshida, M., Yajima, K., and Uno, M. (1966). Different activation of the 2 types of the pyramidal tract neurones through the cerebello-thalamocortical pathway. Experientia *22*, 331-332.
47. Bava, A., Cicirata, F., Giuffrida, R., Licciardello, S., and Panto, M.R. (1986). Electrophysiologic properties and nature of ventrolateral thalamic nucleus neurons reactive to converging inputs of paleo- and neocerebellar origin. Exp Neurol *91*, 1-12.
48. Bava, A., Manzoni, T., and Urbano, A. (1967). Effects of fastiginal stimulation on thalamic neurones belonging to the diffuse projection system. Brain research *4*, 378-380.
49. Halassa, M.M., and Acsady, L. (2016). Thalamic Inhibition: Diverse Sources, Diverse Scales. Trends in neurosciences *39*, 680-693.
50. Paz, J.T., Chavez, M., Saillet, S., Deniau, J.M., and Charpier, S. (2007). Activity of ventral medial thalamic neurons during absence seizures and modulation of cortical paroxysms by the nigrothalamic pathway. Journal of Neuroscience *27*, 929-941.
51. Buee, J., Deniau, J.M., and Chevalier, G. (1986). Nigral modulation of cerebello-thalamo-cortical transmission in the ventral medial thalamic nucleus. Exp Brain Res *65*, 241-244.
52. Bomben, V.C., Aiba, I., Qian, J., Mark, M.D., Herlitze, S., and Noebels, J.L. (2016). Isolated P/Q Calcium Channel Deletion in Layer VI Corticothalamic Neurons Generates Absence Epilepsy. J Neurosci *36*, 405-418.

53. Witter, L., Canto, C.B., Hoogland, T.M., de Gruijl, J.R., and De Zeeuw, C.I. (2013). Strength and timing of motor responses mediated by rebound firing in the cerebellar nuclei after Purkinje cell activation. Frontiers in neural circuits *7*, 133.

54. Hoogland, T.M., De Gruijl, J.R., Witter, L., Canto, C.B., and De Zeeuw, C.I. (2015). Role of Synchronous Activation of Cerebellar Purkinje Cell Ensembles in Multi-joint Movement Control. Current biology : CB *25*, 1157-1165.

55. Yu, C., Derdikman, D., Haidarliu, S., and Ahissar, E. (2006). Parallel thalamic pathways for whisking and touch signals in the rat. PLoS biology *4*, e124.

56. Tsai, P.T., Hull, C., Chu, Y., Greene-Colozzi, E., Sadowski, A.R., Leech, J.M., Steinberg, J., Crawley, J.N., Regehr, W.G., and Sahin, M. (2012). Autistic-like behaviour and cerebellar dysfunction in Purkinje cell Tsc1 mutant mice. Nature *488*, 647-651.

57. Peter, S., Ten Brinke, M.M., Stedehouder, J., Reinelt, C.M., Wu, B., Zhou, H., Zhou, K., Boele, H.J., Kushner, S.A., Lee, M.G., et al. (2016). Dysfunctional cerebellar Purkinje cells contribute to autism-like behaviour in Shank2-deficient mice. Nature communications *7*, 12627.

58. Marien, P., Ackermann, H., Adamaszek, M., Barwood, C.H., Beaton, A., Desmond, J., De Witte, E., Fawcett, A.J., Hertrich, I., Kuper, M., et al. (2014). Consensus paper: Language and the cerebellum: an ongoing enigma. Cerebellum *13*, 386-410.

59. Lesage, E., Hansen, P.C., and Miall, R.C. (2017). Right Lateral Cerebellum Represents Linguistic Predictability. J Neurosci *37*, 6231-6241.

60. Lin, J.J., Siddarth, P., Riley, J.D., Gurbani, S.G., Ly, R., Yee, V.W., Levitt, J.G., Toga, A.W., and Caplan, R. (2013). Neurobehavioral comorbidities of pediatric epilepsies are linked to thalamic structural abnormalities. Epilepsia *54*, 2116-2124.

61. Wolf, R., Dobrowolny, H., Nullmeier, S., Bogerts, B., and Schwegler, H. (2017). Effects of neonatal excitotoxic lesions in ventral thalamus on social interaction in the rat. European archives of psychiatry and clinical neuroscience.

62. Bruno, R.M. (2011). Synchrony in sensation. Current opinion in neurobiology *21*, 701-708.

63. Poulet, J.F., Fernandez, L.M., Crochet, S., and Petersen, C.C. (2012). Thalamic control of cortical states. Nat Neurosci *15*, 370-372.

64. Whitmire, C.J., Waiblinger, C., Schwarz, C., and Stanley, G.B. (2016). Information Coding through Adaptive Gating of Synchronized Thalamic Bursting. Cell reports *14*, 795-807.

65. Craig-McQuaide, A., Akram, H., Zrinzo, L., and Tripoliti, E. (2014). A review of brain circuitries involved in stuttering. Frontiers in human neuroscience *8*, 884.

66. Ehlen, F., Vonberg, I., Kuhn, A.A., and Klostermann, F. (2016). Effects of thalamic deep brain stimulation on spontaneous language production. Neuropsychologia *89*, 74-82.

67. van Diessen, E., Diederen, S.J., Braun, K.P., Jansen, F.E., and Stam, C.J. (2013). Functional and structural brain networks in epilepsy:What have we learned? Epilepsia *54*, 1855-1865.

68. Sorokin, J.M., Davidson, T.J., Frechette, E., Abramian, A.M., Deisseroth, K., Huguenard, J.R., and Paz, J.T. (2017). Bidirectional Control of Generalized Epilepsy Networks via Rapid Real-Time Switching of Firing Mode. Neuron *93*, 194-210.

69. Mattis, J., Tye, K.M., Ferenczi, E.A., Ramakrishnan, C., O'Shea, D.J., Prakash, R., Gunaydin, L.A., Hyun, M., Fenno, L.E., Gradinaru, V., et al. (2012). Principles for applying optogenetic tools derived from direct comparative analysis of microbial opsins. Nature Methods *9*, 159-172.

70. university, s. (2017). Predicted irradiance values: model based on direct measurements in mammalian brain tissue Volume 2016, D. lab, ed.

71. van Dongen, M.N., karapatis, A., Kros, L., Eelkman Rooda, O.H.J., seepers, R.M., Strydis, C., De Zeeuw, C.I., hoebeek, F.E., and Serdijn, W.A. (2014). An implementation of a wavelet-based seizure detection filter suitable for realtime closed-loop epileptic seizure suppression. In BioCAS. (Lausanne), pp. 504-507.

72. Houben, T., Loonen, I.C., Baca, S.M., Schenke, M., Meijer, J.H., Ferrari, M.D., Terwindt, G.M., Voskuyl, R.A., Charles, A., van den Maagdenberg, A.M., et al. (2017). Optogenetic induction of cortical spreading depression in anesthetized and freely behaving mice. Journal of cerebral blood flow and metabolism : official journal of the International Society of Cerebral Blood Flow and Metabolism *37*, 1641-1655.

73. Holt, G.R., Softky, W.R., Koch, C., and Douglas, R.J. (1996). Comparison of discharge variability in vitro and in vivo in cat visual cortex neurons. J. Neurophys. *75*, 1806-1814.

74. Kundishora, A.J., Gummadavelli, A., Ma, C., Liu, M., McCafferty, C., Schiff, N.D., Willie, J.T., Gross, R.E., Gerrard, J., and Blumenfeld, H. (2016). Restoring conscious arousal during focal limbic seizures with deep brain stimulation. Cerebral Cortex *Epub ahead of Print*.

75. Franklin, K., and Paxinos, G. (2001). The mouse brain in stereotactic coordinates, Compact, 2nd Edition, (Academic Press).

76. Oostenveld, R., Fries, P., Maris, E., and Schoffelen, J.M. (2011). FieldTrip: Open source software for advanced analysis of MEG, EEG, and invasive electrophysiological data. Computational intelligence and neuroscience *2011*, 156869.

"Hände, lasst von allem Tun,

Stirn vergiss du alles Denken,

Allen meine Sinne nun,

Wollen sich in Schlummer senken"

Beim Schlafengehen – Herman Hesse

Chapter 6

Consensus Paper: Experimental Neurostimulation of the Cerebellum

Lauren N. Miterko
Kenneth B. Baker
Jaclyn Beckinghausen
Alim L. Benabid
Lynley V. Bradnam
Michelle Y. Cheng
Jessica Cooperrider
Mahlon DeLong
Simona V. Gornati
Mark Hallett
Detlef H. Heck
Freek E. Hoebeek
Abbas Z. Kouzani
Sheng-Han Kuo
Elan D. Louis
Andre Machado
Mario Manto
Alana B. McCambridge
Michael Nitsche
Nordeyn Oulad Ben Taib
Traian Popa
Masaki Tanaka
Dagmar Timmann
Gary K. Steinberg
Eric H. Wang
Thomas Wichmann
Tao Xie
Roy V. Sillitoe

Abstract

The cerebellum is best known for its role in controlling motor behaviors. However, recent work supports the view that it also influences non-motor behaviors. The contribution of the cerebellum toward different brain functions is underscored by its involvement in a diverse and increasing number of neurological and neuropsychiatric conditions including ataxia, dystonia, tremor, stroke, epilepsy, Parkinson's disease, multiple sclerosis, autism spectrum disorders, dyslexia, ADHD, and schizophrenia. Although there are no cures for these conditions, cerebellar stimulation is quickly gaining attention, as cerebellar circuitry has arisen as a potentially powerful target for invasive and non-invasive neuromodulation. This consensus paper brings together experts from the fields of neurophysiology, neurology, and neurosurgery to discuss recent efforts in using the cerebellum as a therapeutic inroad. We report on the most advanced techniques for manipulating cerebellar circuits in humans and animal models and define key hurdles and questions for moving forward.

Introduction (L.N. Miterko, J. Beckinghausen, R.V. Sillitoe)

The cerebellum has emerged as a potentially powerful target for neurostimulation in different diseases. Experimental animal models show exciting possibilities for invasive cerebellar stimulation while work in patients not only solidifies the animal studies but provides major hopes for conditions that are severe and respond poorly to drug treatment. Non-invasive cerebellar stimulation likewise has provided new treatment possibilities, but importantly these strategies also serve to uncover the fundamental mechanisms for how the human brain might be modulated by exogenous stimulation. In this consensus paper, we discuss recent animal and human stimulation paradigms, and as a group we attempt to identify key successes and failures, which are both critical for improvements in human therapy. We outline important hurdles and suggest possible ways to overcome them. We start by introducing the normal structure, connectivity, and function of the mammalian cerebellum before each section considers various stimulation approaches.

The basic cellular composition of the cerebellum was worked out well over a century ago [1] with the details expanded upon in recent years by more modern techniques [2,3]. The firing properties of the different classes of cerebellar neurons have been disentangled by *in vitro* and *in vivo* recording approaches [4–6], and its finer connectivity unveiled at the level of microcircuits [7–14], patterns [15–18] and individual types of electrical and chemical synapses using genetics, molecular biology, anatomy, and electrophysiology [19–22]. It is therefore safe to say that the cerebellum is amongst the most well understood of all structures in the entire nervous system.

There have also been marked advances in how we think about cerebellar-dependent behaviors [23]. We are in unanimous and firm agreement that the cerebellum is required for motor behaviors ranging from coordination, posture, and balance, to learning and adaptation [24–27] – although the exact mechanisms are far from clear. However, we are now beginning to appreciate the role of the cerebellum in behaviors previously thought to be strictly dedicated to brain regions that process higher order functions, including emotion, language, and cognition [28–31]. This is an important issue to raise here because all of the paradigms that are used for cerebellar neurostimulation must consider the large variety of behaviors that could be, and are likely, affected. But before discussing the experimental and therapeutic cerebellar manipulations that are employed in human conditions and mimicked in animal models, we first revisit the basic anatomical plan of the mammalian cerebellum in order to fully appreciate the outcomes of its stimulation in health and disease.

Viewed from the surface, the outer structure of the cerebellum can be grossly divided into three main regions [2]. The middle portion is called the vermis and is named for its worm-like appearance. On either side of the vermis is a region called the paravermis, which is not structurally distinct, but does contain dedicated circuits for executing specific behaviors. The most lateral portions of the cerebellum are adjacent to each paravermis and are known as the hemispheres. Surface examination also reveals what is perhaps the most recognizable feature of the cerebellum in mammals, its highly folded architecture. The adult cerebellum is anatomically segmented into distinct folds called lobules [32]. There are ten primary lobules that are separated from one another by a series of fissures [2]. Because each fissure extends to a specific depth in the cerebellum, each lobule develops with a unique shape. However, all lobules contain the same canonical microcircuit.

The connectivity within the cerebellum is largely repeated through the structure, with each cell type forming stereotypical connections with its neighbors [1,2,33]. The cerebellum has three distinct layers, and each layer is comprised of distinct cell types (Fig. 1). The most superficial layer contains inhibitory stellate and basket cell interneurons and excitatory climbing fibers. All three of these interneuron classes project onto Purkinje cells, which make up the middle layer called the Purkinje cell layer. The Purkinje cell layer also contains interneurons called candelabrum cells as well as specialized astrocytes called Bergmann glia. The Purkinje cells perform the main computations in the cerebellum. The deepest layer is called the granular layer and it contains billions of small excitatory neurons called granule cells in addition to inhibitory Golgi cells, inhibitory Lugaro cells, mossy fibers that deliver sensory signals to the cerebellum, and a peculiar excitatory cell type called the unipolar brush cell. Unlike all other cell types that are found in all regions of the cerebellum, the unipolar brush cells are localized mainly to the vermis of lobules IX and X [9]. There are also modulatory "beaded" fibers that terminate in all layers of all lobules. Below the three layers is the white matter that contains a dense network of fiber tracts. Embedded in this network are three pairs of cerebellar nuclei that are located on each side of the cerebellar midline. These nuclei contain specialized neurons that transmit the final output of the cerebellum, albeit that some types have been shown to provide axon collaterals to the cerebellar cortex (Houck and Person, 2015, J Comp Neurol; Ankri et al., 2015, Elife; Gao et al 2016, Neuron). From medial to lateral, they are the fastigial, interposed, and dentate nuclei, all of which link the cerebellum to the rest of the brain and spinal cord [33]. The interposed nuclei can be divided into the anterior and posterior portions, which in primates, are referred to as the emboliform and globose nuclei, respectively.

At the behavioral level, it is the output connections of the cerebellar nuclei that are pertinent to our discussion of cerebellar stimulation in health and disease. The cerebellar nuclei project monosynaptic connections to the thalamus, red nucleus, vestibular nuclei, and inferior olive. The cerebellar nuclei were also recently shown to project directly to the locus coeruleus [34]. However, there are also polysynaptic short latency connections with critical structures such as the basal ganglia [35,36] in addition to other poorly defined, but likely functionally very important connections, to the hypothalamus [37] and hippocampus [38]. There are also several other underappreciated cerebellar afferent pathways (e.g. cerebellar connections with the brainstem nuclei - 38) and efferent connections (e.g. from the periaqueductal gray - 39) that we will not discuss here, but suffice it to say that cerebellar stimulation almost certainly affects many more circuits than just the well-known output pathways that project directly to the thalamus.

This consensus paper comprises 13 brief sections. The topics range from the different methods of neurotherapeutic brain stimulation such as deep brain stimulation (DBS), transcranial magnetic stimulation (TMS), theta burst stimulation, and transcranial direct current stimulation (tDCS), through to experimental methods of stimulation such as optogenetics, near-infrared, and magnetothermal DBS. Importantly, two of the sections are dedicated to the systems level impact of electrical stimulation on the basic activity of the cerebellar cortex and cerebellar nuclei. Diseases such as ataxia, dystonia, tremor, stroke, and Parkinson's disease are considered in the context of cerebellar motor (coordination, balance, posture, learning) and non-motor function (language, social cognition, emotion, literacy acquisition, attention). Over the past two decades, thanks to the advances in device engineering and technology, powerful pre-clinical animal models, and cutting-edge surgical methods, our view of the cerebellum in disease therapy has changed dramatically. Given that the future of brain stimulation holds enormous promise for treatment, we think this consensus paper is timely as the cerebellum finds itself at the center of many disorders. However, although we think deeply towards the refinement of current approaches and techniques, as well as towards the potential for future applications, we draw heavily upon the initial findings in this modern era of DBS and the pioneering discoveries of authors Alim L. Benabid and Mahlon DeLong.

The Non-Human Primate as a Disease Model and its Role in the Development of Functional Surgery (T. Wichmann, M. DeLong)

Starting in the 1960s, widely used ablative procedures, such as pallidotomy and thalamotomy for movement disorders, were rapidly replaced by medication treatments (e.g., the use of levodopa in the treatment of Parkinson's disease (PD)), which seemed more effective and safe. Over time, however, it became clear that medications such as levodopa can produce significant side effects that limit their use. In the 1990s, functional surgery re-emerged as a major treatment modality, initially for patients with tremor and shortly thereafter, for patients with PD, dystonia and other conditions. The return to surgery was strongly influenced by knowledge gained through studies in non-human primates (NHPs). We present five examples of the impact of this work.

1. Segregated basal ganglia thalamocortical circuits.

One of the key insights from research in NHPs was the finding that the basal ganglia, thalamus, and cerebral cortex are components of anatomical circuits that remain largely segregated throughout their subcortical course, with separate territories for 'motor,' 'associative,' and 'limbic' functions [41,42]. This knowledge has helped us to better understand both the normal physiology and the pathophysiology of specific signs and symptoms of neurologic and psychiatric disorders of basal ganglia disorders. For example, both hypo- and hyperkinetic *movement* disorders arise from specific disruptions in the basal ganglia *motor* circuit, while psychiatric conditions may arise from disruptions of the limbic circuitry [43]. The concept of functional specificity of segregated basal ganglia circuits provides a clear rational for the neurosurgical targeting of interventions used for such network disorders: Selective targeting of different nodes of the motor circuit is used for movement disorders, with few limbic or cognitive side effects [44], while targeting of specific non-motor circuits can be used for psychiatric disorders such as Obsessive-Compulsive Disorder [44–48].

2. The role of the subthalamic nucleus in movement and movement disorders.

Systematic exploration of the effects of lesions, affecting the primate subthalamic nucleus (STN) by Mettler and Carpenter in the 1940s and 1950s, as well as subsequent electrophysiologic recording studies in NHPs laid the groundwork for our understanding that the STN is part of brain circuits that are strongly involved in limiting excessive movement. Transient or permanent interruption of STN activity was found to lead to involuntary movements of the contralateral limbs [49,50]. Later rodent and NHP studies showed that basal ganglia output to the thalamus and other targets is inhibitory, and that it is regulated by cortical inputs. These studies identified 2 separate pathways ('direct'

and 'indirect') between the primary basal ganglia input station (the striatum) and the basal ganglia output structures (the internal pallidal segment, GPi, and the substantia nigra pars reticulata; 42, 50). While activation of the inhibitory 'direct' pathway leads to a reduction of basal ganglia output and a facilitation of movement, activation of the excitatory 'indirect' pathway strengthens inhibitory basal ganglia output leading to an inhibition of movement (see, e.g., ref.51). The STN is a key component of the 'indirect' pathway of the basal ganglia.

3. Studies in the NHP MPTP (1-methyl-4-phenyl-1,2,3,6-tetrahydropyridine) model of Parkinsonism.

NHP research had a particularly important role in the development of current functional neurosurgical treatments of Parkinsonism because of the availability of an NHP model of Parkinsonism, the MPTP-treated monkey, a species whose brain is anatomically and functionally very close to that of humans [53]. NHPs, treated with the dopaminergic toxin MPTP, develop Parkinsonian signs that closely mimic those found in humans. Studies in this model have led to multiple discoveries relevant for our current understanding of the pathophysiology of this disorder, showing profound changes in neuronal activity in the basal ganglia and in associated brain regions such as the brainstem, thalamus and cortex [54]. Abnormal activity in the STN appears to drive many of the pathologic activity patterns in the basal ganglia output structures. The subsequent discovery in the NHP that lesioning [55] or electrical DBS of the STN [56] has strong anti-Parkinsonian properties soon led to the use of DBS as treatment for patients with PD [57,58]. Since then, DBS of either, the STN or the GPi, have become mainstays in the treatment of patients with PD with refractory tremor or medication-induced motor side effects [59,60], and are also increasingly used for the treatment of dystonia and other movement disorders.

4. Studies of DBS mechanisms.

Studies of the mechanism of action of DBS in various disease states are needed for the optimization of DBS strategies, the definition of new DBS targets, and the development of 'on demand' DBS, i.e., dynamic adjustments of DBS parameters based on biomarkers of disease severity. Since the mid-1990s, studies of DBS mechanisms, particularly in the field of PD research, have strongly relied on investigations in NHPs. Early studies in Parkinsonian monkeys demonstrated that DBS effects are complex mixtures of activation and inactivation effects that involve activity changes downstream and upstream from the stimulated brain area [61,62]. Since STN- and GPi-DBS are effective in hypo- and hyperkinetic movement disorders, it appears that these interventions do not counteract specific aspects of the pathophysiology of different movement disorders, but, rather, they non-specifically block the different types of abnormal basal ganglia output to the

relatively intact downstream portions of the motor circuitry [63–65].

More recent studies have shown that coupling of the amplitude of DBS to the occurrence of beta band oscillatory activity (one of the presumed biomarkers for PD) results in greater anti-Parkinsonian benefits than uncoupled stimulation [66]. This result, the first example of on-demand DBS for the treatment of Parkinsonism, was quickly translated to use in human patients, using different methodologies, and is being further optimized through newly engineered programmable pulse generators [67,68].

5. Interactions between basal ganglia and cerebellar networks.

Movement disorders are commonly viewed as originating in either the basal ganglia or the cerebellum. Anatomical studies in primates showed, however, that there are strong bidirectional subcortical connections between the subnuclei of basal ganglia and cerebellum which appear to be of significant functional and pathophysiological importance [26,69,70]. Physiologically, the two may interact with the cerebral cortex as part of an integrated distributed learning system (among other functions), where the cerebellum plays a key role in supervised learning (through plasticity at parallel fiber-Purkinje cell synapses), the precentral motor fields in unsupervised (Hebbian) learning, and the basal ganglia in reinforcement learning [26]. Pathophysiologically, the cerebellum and the basal ganglia may interact in some of the dystonias [71–74], and in the generation of Parkinsonian tremor [26,75–78].

These findings not only raise questions about viewing movement disorders as purely "cerebellar" or "basal ganglia" disorders, but also present unforeseen opportunities for treating dystonia and other movement disorders, targeting the cerebellum and its output targets. It is noteworthy that such approaches were attempted earlier with some success, but later abandoned. The long history of functional surgery is characterized by periodic waves of exploration, application, and replacement, of which even more can be anticipated as technology and our understanding of the pathophysiology of neuropsychiatric disorders advances.

Cerebellar DBS: Technology and Implementation in Animal Models

(L.N. Miterko, J. Beckinghausen, A.Z. Kouzani, A.L. Benabid, R.V. Sillitoe)

We recently used the *Cre/LoxP* genetic approach to develop a new mouse model for testing the role of the cerebellum in dystonia [79]. By selectively silencing the glutamatergic output of olivocerebellar fibers we were able to successfully induce a severe dystonia that initiated during development and continued throughout the life

of the mice [79]. These data raised the possibility that perhaps our mice could serve as an ideal model for examining whether the cerebellar circuits for ongoing motion were optimal targets for DBS. For this reason, we targeted the interposed nuclei (Fig. 2), which project to several areas, such the red nucleus and thalamus, through which they modulate movement. We used bilaterally implanted twisted bipolar electrodes, and in general the approach was inspired by the paradigms used for pre-clinical non-human primatestudies and the treatment of human Parkinson's disease [80]. We reported immediate improvement in motor behavior with the alleviation of twisting postures and rigidity [79]. We also implanted DBS electrodes into the centrolateral nucleus of the thalamus, a region implicated in mediating the communication between the cerebellum and basal ganglia in dystonia [36]. In accordance with the idea of a "dystonia circuit," high frequency stimulation of the centrolateral nucleus also improved movement in our mouse model of dystonia [79].

DBS is in fact widely used to treat human dystonia, and in the USA, the Food and Drug Association (FDA) have approved its use in the disease. The internal segment of the globus pallidus is typically the target [81]. Our motivation for asking whether the cerebellum could be considered as an alternate target was based on the hypothesis that perhaps the reason for unresponsive surgeries could be due to the stimulation site rather than efficacy of DBS itself [82]. Moreover, based on previous and recent experimental data, there is a compelling argument that the cerebellum should be considered as a bonafide locus that participates in dystonia [71,72,83]. Our DBS results in rodent dystonia are promising for human therapy, but there are many questions that should be addressed if the cerebellum is to make it onto a shortlist of targets for motor disease. In the specific case of dystonia, in what circumstances should the cerebellum be considered for therapy? An alternative question, and perhaps not mutually exclusive, is when should globus pallidus stimulation not be the primary choice? Certainly, the neurologist and neurosurgeon have to assess each patient and their history, but even armed with an evaluation, these questions are still not trivial to address. A major consideration in this regard is what type of dystonia the patient has, and if it is a genetic form, is there any indication that the mutant gene and its effects involve the cerebellum? This problem has yet to be solved, although for *Dyt1* at least there is some indication that the genetic pathway in the cerebellum is at fault [84].

There is a long history of cerebellar stimulation for dystonia-related behaviors [85–90], although due to much needed regulations, progress was unfortunately turbulent [91]. Still, much optimism has remained [92]. In accordance with this, our results showing that multiple motor features that are indicative of human dystonia are convincingly alleviated

in our mouse model of dystonia support cerebellar stimulation for human therapy [79]. In addition, although we showed a specific utility of interposed stimulation in dystonia-like behavior, our study was not the first demonstration of using the cerebellar nuclei for motor repair in pre-clinical models. Elegant work from the Machado group (see section by Cooperrider and colleagues in this Consensus) consisted of inducing stroke in rats and then stimulating the dentate nucleus to improve motor outcome [93]. These studies are supported by optogenetic stimulation of the dentate, which also provides motor benefits (92; see section by Cheng and colleagues in this Consensus). With the resurgence of cerebellar nuclei stimulation as a potential therapy, come many questions. The most pressing question is, what is the mechanism of action? From a general perspective, the cellular, circuit, and network effects of DBS have been debated at length [63,95], and there are several different aspects of a potential "cerebellar mechanism" that could be discussed.

Here, we would like to consider a possible mechanism from the view of the normal internal organization of the cerebellum. All aspects of cerebellar development, function, behavior, and in many cases disease, are organized around a striking array of parasagittal stripe domains, or zones as they are often called [3,33,96,97]. At the center of each stripe are the Purkinje cells, the sole output of the cerebellar cortex. Remarkably, more than 30 years ago it was recognized that stimulating adjacent regions of the cerebellar cortex –or the stripes – resulted in different behavioral outcomes in cerebral palsy patients that showed symptoms of dystonia [98]. These neurosurgical data are supported by electrophysiology studies in non-human primates showing that the normal cerebellum controls co-contractions of agonist and antagonist muscle activity [99] as well as transynaptic retrograde tracing of the muscles all the way back to Purkinje cell stripes in rats [100]. The key to this architecture is that the Purkinje cell stripes and their associated climbing fiber inputs operate as synchronous units [101,102]. The synchronous activity is processed within the deep nuclei, but here the signals from Purkinje cells must converge [10]. So, what type of activity are we tapping into when we stimulate the cerebellar nuclei using DBS? There are likely retrograde effects within the cerebellar cortex itself, but it would be interesting to test whether the responses within the thalamus and other downstream targets operate according to the topography that originates from within the cerebellum. If this is true, one must reconsider the possibility that cerebellar DBS could have incredibly variant effects depending on which specific sets of cerebellar zonal modules are recruited. These effects could manifest at the levels of cells, molecules, and circuits, which all contribute to the cerebellar zonal map. The use of conditional mouse genetics combined with optogenetics and DREADD approaches lend themselves to testing these possibilities in different disease models. There is already

mounting evidence that different methods of cerebellar modulation are effective in a wide number of motor diseases [103].

The largest hurdle to overcome will be to solve the mechanism of action in DBS, for each circuit, in each disease. The use of optogenetics is already proving invaluable. Creed and co-workers adjusted their DBS parameters to mimic an optogenetic stimulation protocol to treat a mouse model of cocaine addiction [104]. Perhaps similar logic could be applied to disorders affecting the cerebellum. We already know that cerebellar DBS [93] and optogenetics [94] are both effective in stroke, the question now is whether the effective output in stroke can teach us how best to tackle classic cerebellar diseases such as ataxia, which have been difficult to treat with drugs and stimulation. Other technological advances will have to be employed. Closed-loop DBS [105] as well as closed-loop optogenetics [106] methods could be very effective in experimental studies of cerebellum. As the techniques become more integrated and sophisticated, one could consider approaches such as near-infrared light technology alone or combined with optogenetics [107]. The complexity of the zonal cerebellar circuitry as well as its wide-spread connectivity in motor and non-motor behavior necessitates an equal level of sophistication in examining the responses to cerebellar stimulation. It will be imperative that single-unit electrophysiology approaches are used to analyze the cell-specific details of neuronal responses downstream of stimulation, but also population level responses will have to be collected using tools such as tetrodes, array electrodes, silicone probes, or even fiber photometry and deep tissue endoscopy.

Cerebellar DBS in Stroke: Human and Rodent Models (J. Cooperrider, Kenneth B. Baker, A. Machado)

Post-stroke motor disability presents a substantial burden to the population, both in terms of individual quality of life and in the social and economic resources required to care for these patients. Current treatment for patients with motor sequelae is largely limited to physical therapy, however, with many patients retaining long-term disabling deficits despite best efforts. As such, there has been substantial interest in the development of new, more effective therapies to enhance post-stroke recovery, including the use of electrical or magnetic stimulation of the cerebral cortex to promote post-stroke functional recovery. Unfortunately, the efficacy of such approaches has, thus far, been variable or limited [108]. To this end, our group was the first to propose, research, test, and translate a novel neuromodulatory stimulation approach targeting the ascending dentatothalamocortical (DTC) pathway for post-stroke motor rehabilitation. This approach involves stimulation of the cerebellar dentate nucleus, the origin of the

DTC pathway, in order to enhance activity along this natural excitatory fiber tract and augment thalamocortical interactions across multiple prefrontal, frontal, and parietal cortical regions (Fig. 3). We proposed stimulation of the DTC as part of a neuromodulation-based rehabilitation strategy for several reasons. First, single pulse stimulation of the dentate nucleus had been previously shown to modulate cerebral cortical excitability [109–111]. We extended those findings by showing that continuous stimulation of the dentate nucleus produces sustained, frequency-dependent modulation of cortical excitability in both naïve and post-stroke rodents [112,113]. These results enabled our group to conclude that low-frequency beta band stimulation might optimally enhance cortical excitability and create an ideal environment for further promoting functional reorganization and recovery. Second, we hypothesized that chronic, exogenous activation of this excitatory pathway could reverse the crossed cerebellar diaschisis, and possibly even atrophic changes, that occur following contralateral cortical ischemia and contribute to loss of function [114–116].

Initial studies in our lab investigated the effect of chronic stimulation of the lateral cerebellar nucleus (LCN, i.e. the homologue of the primate dentate nucleus) in rats with large, ischemic strokes of the middle cerebral artery, revealing significant enhancement of motor recovery with lower frequency stimulation [117]. Subsequent work examined whether stimulation combined with simultaneous motor training promotes recovery following small, cortical lesions [93,118]. We found that dentate stimulation at 30 Hz produced significant gains in motor function compared to control animals and significantly enhanced the expression of synaptophysin in the perilesional cortex [93,118]. Recently, a Stanford group has replicated the neurorestorative effect of DTC stimulation utilizing optogenetic stimulation instead of electrical stimulation in the mouse model [94].

In parallel with our optimization and behavioral work, we have sought to uncover the mechanisms through which DTC stimulation-induced recovery occurs. We have demonstrated that post-stroke stimulation is associated with significant synaptic changes in the perilesional cortex, including increased expression of PSD95, a marker of synaptogenesis, as well as an increase in the number of perilesional synapses [93]. DTC stimulation has also been associated with perilesional upregulation of markers of LTP, including CAMKII and the NMDA receptor [93]. In addition, stroked rats who received DTC stimulation with LCN leads have altered cortical motor maps, with increased representation of distal and proximal forelimb and decreased representation of the unaffected limb [93]. Furthermore, stimulation has recently been shown to be associated with increased neurogenesis in the perilesional cortex, as well as in the mediodorsal and

ventrolateral thalamic relay nuclei, providing another mechanism through which the facilitative effects of stimulation may occur. Interestingly, stimulation was associated with greater glutamatergic and less GABAergic neurogenesis compared to control animals [119]. These data indicate that there are a number of associated microstructural, cellular, and potentially even neuroregenerative changes associated with DTC stimulation that may provide the mechanistic underpinnings of this neuromodulatory therapy.

Based on these promising preclinical data, a first-in-human phase I trial (Electrical Stimulation of the Dentate Nucleus Area (EDEN) for Improvement of Upper Extremity Hemiparesis Due to Ischemic Stroke: A Safety and Feasibility Study) has recently received approval and is actively enrolling. This study will evaluate the safety and feasibility of dentate nucleus stimulation in conjunction with physical therapy in patients with moderate to severe upper-extremity hemiparesis following middle cerebral artery ischemia. Although significant differences exist between the formative rodent work and human application, initial results from the first implanted patient are promising and have inspired an extension of the original study timeline in order to examine not-yet-plateaued motor recovery.

The dentate stimulation-associated microstructural and neural excitability changes are currently only correlative; future work will evaluate the causal mechanisms underlying its therapeutic effect. Additionally, whether the functional recovery achieved in preclinical studies is a result of stable reorganization of the cortex or whether the facilitatory effects of DTC stimulation will require continual stimulation to maintain benefits also needs to be examined. Future work in rodent and non-human primate models, as well as human studies, will also focus on optimization of stimulation timing and parameters. Finally, we postulate that stimulation of the DTC pathway may be beneficial in improving recovery from other types of cortical injury, including traumatic brain injury. Results of the first-in-human trial will soon be available and will drive future investigation.

DBS in Essential Tremor (S-H Kuo, T. Xie, E.D. Louis)

ET is a progressive disease, and with time, the tremor becomes larger in amplitude and slower in frequency [120]. DBS of the ventrointermediate (VIM) nucleus of the thalamus is one of the most effective surgical options for the treatment of essential tremor (ET). It can decrease tremor amplitude up to 50%-80% [121] and has become the standard therapy for medication-refractory ET [122,123]. The VIM nucleus receives extensive cerebellar outflow fibers from the cerebellar nuclei [70], and specific neuromodulation

by VIM DBS can eliminate tremor, supporting the role of the cerebellum in tremor. Furthermore, intra-operative recordings from the VIM nucleus showed that neurons are firing rhythmically at the same frequency as the tremor [124], indicating that VIM neurons are likely entrained by abnormal cerebellar activity in the setting of structural alterations to the Purkinje cell axons and dendrites [125,126], possible Purkinje cell loss [127], and/or abnormal Purkinje cell synaptic organization [128,129] observed in the postmortem ET cerebellum, which have been postulated to be responsible for tremor generation. In the experimental animal models with harmaline-induced tremor, enhanced coupling of the inferior olivary neurons can produce rhythmic discharges of the downstream cerebellum that drive tremor [130], which can be effectively eliminated by VIM DBS in a frequency and voltage dependent manner [131]. Although there is no clear evidence of enhanced neuronal coupling in the inferior olives of ET patients [132], animal models of harmaline-induced tremor indicate that the abnormal physiology within the cerebello-thalamo-cortical loop can produce ET-like tremor; thus, neuromodulation such as DBS in this brain circuitry can suppress tremor.

ET is characterized by bilateral kinetic, postural and intention tremors in the arms and hands, which often respond to VIM DBS. A subset of ET patients will also have voice tremor and head (i.e., neck) tremor, which can be reduced by VIM DBS and is more effective under bilateral stimulation [122], although the responsiveness of these tremors to VIM DBS seems to be less than that of arm and hand tremor. VIM DBS might even cause dysarthria and dysphagia, more when under bilateral stimulation [122]. Collectively, the differential effects of VIM DBS on tremor of different body parts might be related to the somatotopic organization of the VIM nucleus. Another relevant question that can arise from VIM DBS in ET patients is related to the role of the cerebello-thalamo-cortical loop in tremor and ataxia, two clinical signs that might involve similar brain circuitry. ET patients often have subtle cerebellar ataxia manifested by difficulty in tandem gait [133], and a subset of ET patients will eventually develop frank ataxia [134]. With VIM DBS, effective tremor suppression can sometimes come with the price of worsening gait ataxia, a clinical observation that suggests different neuronal coding mechanisms for tremor and ataxia within the same cerebello-thalamo-cortical loop [135].

Although DBS can achieve region-specific modulation of neuronal activities in the VIM nucleus, it also can lead to wide-spread activity changes in the brain network, including the cerebellum [136]. For example, differential cerebellar synaptic reorganization has been observed in ET cases with and without DBS [137], suggesting that DBS might have some disease-modifying effects. Degenerative changes within the cerebellum have been found in the postmortem ET cerebellum, including Purkinje cell loss [127]

and Purkinje cell axonal pathology [125]. It remains unclear whether early intervention with DBS could modulate the cerebellar activity, which might alter these structural and degenerative changes in the ET cerebellum, but is considered as an appealing therapeutic approach regardless due to the progressive and wide-spread nature of this disease. These important questions will need to be further tested in animal models of tremor and confirmed in detailed postmortem human studies.

Another issue related to VIM DBS in ET is the development of tolerance over time. Although VIM DBS continues to be effective in ET over 7 years of follow-up [138], it is estimated that 73% of ET patients will need to gradually increase DBS settings in order to achieve satisfactory tremor control [139]. This tolerance phenomenon is likely due to a compensatory mechanism within the cerebello-thalamo-cortical loop [140]. The alternative possibility is disease progression in ET over time [140]. The mechanism of tolerance is not well-understood, and it deserves further study.

Besides VIM, other emerging targets for DBS in ET are the caudal zona incerta (cZi) and prelemniscal radiation (Rsprl) in posterior subthalamic area (PSA), which also receive innervations from the cerebellum and other brain regions such as the midbrain and basal ganglia as well. The cZi DBS seems to be as effective in tremor suppression and perhaps with fewer side effects of dysarthria, disequilibrium, or ataxia, or better tolerance than VIM DBS [141]; however, a long-term study with bilateral DBS placed across the cZi and VIM is required to compare the efficacy and adverse effects of these targets. In addition, the neuroanatomy and the mechanism as to why cZi or Rsprl in PSA might be superior targets to VIM for neuromodulation in tremor will need to be explored.

Since tremor is a very unique movement disorder and can be characterized by phase, frequency, and amplitude, VIM stimulation can be optimized to these dynamic, but objectively measurable parameters, while these other targets are being investigated for their efficacy. For example, phase-specific VIM DBS could effectively modulate ET frequency and amplitude [142], which opens a new window for the development of adaptive DBS according to the tremor characteristics in *real time*. In fact, phase-specific VIM DBS has been shown to achieve tremor suppression with much less energy requirement [143]. Recently available directional lead would also help us to reserve the battery, avoid side effects related to high DBS settings, and make more precise stimulation possible. Overall, future adaptive DBS would deliver stimulation on demand based on the reliable biomarker to guide automatic adjustments of stimulation, which would also lead to a better understanding of the brain circuitry of ET.

In summary, ET is a brain disorder with rhythmic movements, possibly originating from the abnormal activities of the cerebellum. The clinical effectiveness of thalamic DBS for ET suggests that the disruption of these abnormal activities within the cerebello-thalamo-cortical loop can suppress the consequent tremor. Studies on how DBS could modulate tremor will advance our knowledge in the neurophysiology of tremor and how the brain can generate movement rhythm in both the physiological state (such as physiological tremor) and pathological states (such as ET).

Cerebellar Stimulation: Optogenetic and Experimental and Therapeutic Approaches for Epilepsy (S.V. Gornati, F.E. Hoebeek)

Epilepsy is a neurological disorder characterized by episodes of dysfunctional neuronal network activity. The seizures, which often come about due to hyper-synchronous neuronal firing [144], can be the result of many different causes: brain injury, stroke, genetic mutations, and birth defects [145]. Approximately ~30% of epilepsy patients do not respond adequately to anti-epileptic drugs and thus may need surgical resection of the seizure focus, or neurostimulation. Whereas vagal nerve stimulation is commonly used in refractory epilepsy patients [146], an increasing number of patients receive intracranial DBS [147]. The first brain region that was selected for DBS in epilepsy patients was the cerebellum [148].

Already since the 1940s it was known that electrical stimulation of cerebellum could control motor seizures [149]. Partially driven by the experimental findings that the output of the cerebellar cortex is purely inhibitory [150], several investigators explored how cerebellar cortical stimulation can be used to control seizures, which were known to be driven by cerebral hyperexcitability. The efficacy of cerebellar cortical and cerebellar nuclei (CN) stimulation has been tested for therapeutic value in a wide variety of animal models in various species (mouse, rat, cat and monkey) in which seizures had been evoked by genetic manipulations, chemical infusions or neurostimulation approaches [151,152]. Driven by the positive outcome of the experimental studies on cerebellar stimulation, in the 1970s the first epilepsy patients with refractory seizures were implanted with electrical stimulation peddles, which were positioned on the anterior cerebellar hemisphere. These initial patients mostly received chronic low-frequency (10 Hz) cerebellar stimulation alternating between the left- and right-side, which led to a marked reduction of seizure incidence for up to three years [153]. However, the first double-blind controlled studies on cerebellar stimulation in five patients of refractory seizures revealed no consistent benefit from the actual activation of the implanted

stimulation device to dampen the epileptogenic thalamo-cortical networks [154].

Landmark studies on the origin of (excessive) thalamo-cortical burst firing revealed that the balance between inhibition and excitation in thalamo-cortical networks is effective in setting the firing pattern of thalamo-cortical relay neurons by controlling the activation of low-threshold voltage-gated Ca^{2+}-channels (as reviewed by [155]). Thus, by increasing the excitatory drive onto thalamic neurons, the burst-firing of thalamic relay neurons can be prevented. A recent study showed in epileptic mouse and rat models that membrane depolarization of thalamic relay neurons prevented burst-firing and thereby stopped generalized absence seizures [156]. Likewise, it has also been shown in various mouse models that by pharmacological manipulation of the cerebellar nuclei (CN) neurons, which form numerous glutamatergic synapses throughout the thalamic complex, that increasing CN firing frequency dampens the occurrence of generalized absence seizures. Notably, decreasing CN firing potently increased such seizures [157]. These findings underline the importance of gaining precise control over the cerebellar output for optimal therapeutic effects.

To ensure a temporally precise activation of inhibitory or excitatory inputs, optogenetic stimulation is a seemingly ideal tool. Optogenetics avoid the weakness of a-specific effects by electrical stimulation and the temporal resolution is sufficient to mimic endogenous activity patterns in most types of neurons [158]. Moreover, by expressing light-activated proteins like channelrhodopsin (ChR2) or halorhodopsin (HR) in specific cell types, optogenetics allow full control over action potential firing patterns. For instance, the expression of ChR2 in Purkinje cells, which can be induced using transgenic mutant mice, by *in utero* electroporation or by viral injections [159], allows precise control over action potential firing in their downstream target the CN [160] and thereby over cerebellar-evoked excitation or inhibition in the thalamus.

Optogenetic stimulation of the cerebellar cortex has so far been tested in two experimental studies. Krook-Magnuson and colleagues investigated the impact of on-demand optogenetic stimulation or inhibition of cerebellar Purkinje cells on seizures induced by intrahippocampal kainic acid injections [161]. The authors found that the seizure duration can be shortened upon activation of ChR2- or HR- channels in both laterally and medially localized Purkinje cells, but that the seizure occurrence could only be dampened when the midline Purkinje cells were optogenetically excited. These findings indicate that the cerebellar cortical stimulation, which putatively stopped action potential firing in CN neurons, revealed therapeutic effects on limbic seizures. In contrast, absence seizures occur more frequently upon pharmacological inhibition of

CN activity [157]. Instead, optogenetic excitation of CN neurons consistently resulted in an abrupt stop of cerebral seizure activity. These findings on the impact of cerebellar manipulations on the various types of seizures indicate that cerebellar stimulation can have a widely varying effect on the seizure occurrence. Indeed, also in the earlier reports on the effects of low- or high-frequency stimulation (10 – 200 Hz), it was noted that seizure occurrence was either dampened or enhanced (e.g., [153]).

One potential source for the variability in effects of cerebellar stimulation comes from the diverse anatomical connections that may be stimulated. Even though the cerebello-thalamic projections is mono-synaptic and purely glutamatergic [162], many CN axons also project to inhibitory neurons in the zona incerta and anterior pretectal nucleus, which provide dense inhibitory input to thalamic nuclei [163,164]. Thereby, the cerebellar impact on thalamic nuclei is most likely multi-phasic, in that an optogenetically induced increase in glutamate release from CN axons in the thalamus may be followed by an increase in GABA. Although the impact of such feed-forward connections is currently unknown, we postulate that these speculative multi-phasic responses in thalamus evoked by CN stimulation aid to stop thalamo-cortical oscillations by increasing the excitatory drive onto thalamic relay neurons and by desynchronizing thalamo-cortical activity. It remains to be investigated whether the impact of chronic, non-responsive stimulation paradigms are as effective as the responsive cerebellar cortical or CN stimulation [157,161]. Further research is also warranted to elucidate whether cerebellar DBS has a broad therapeutic effect against a variety of seizures.

Cerebellar Optogenetics in Stroke Research (M.Y. Cheng, E.H. Wang, G.K. Steinberg)

Stroke is a devastating neurological event that disrupts brain function and causes neuronal death. Most stroke survivors suffer long-term deficits that range from motor and/or sensory dysfunction to speech or memory loss, depending on infarct site and injury severity. After stroke the brain has a remarkable capacity for plasticity, in areas adjacent to the infarct, the peri-infarct, but also in remotely connected regions [165]. Recovery from stroke likely requires re-mapping of lost function onto surviving neural circuitry through structural and functional plasticity [165,166]. Extensive studies have focused on changes in the peri-infarct, including activation of an axonal sprouting program, cellular composition changes (astrocyte and microglia proliferation/migration), and neurophysiological properties [167,168]. While some of these adaptations may exacerbate injury such as pro-inflammatory microglia activation [169], other changes

such as increased neural excitability are positively correlated with good functional outcomes [170].

As stroke can disrupt neuronal function within minutes and extend this effect to connected areas, increasing research efforts have focused on stroke-induced changes in the remotely connected regions, including cortical areas in the contralesional hemisphere, thalamus, and the cerebellum [171,172]. In particular, stroke can cause changes in the cortico-cerebellar system, resulting in depression of brain metabolism and function in the cerebellum; this is known as crossed cerebellar diaschisis (CCD) [173]. In turn, this leads to dysfunction in both motor and non-motor functions, including balance, coordination and visuospatial perception [173,174]. CCD has been reported as a potential prognosis indicator for stroke recovery [173].

Various strategies have been used to improve functional outcomes after stroke such as stem cell therapies, pharmacological interventions, and brain stimulation [175,176]. While cell therapy and drugs may catalyze endogenous repair processes, these approaches lack the necessary spatial resolution to precisely target specific areas. On the other hand, conventional brain stimulation techniques such as electrical stimulation, transcranial magnetic stimulation (TMS) and transcranial direct current stimulation (tDCS) allows direct manipulation of a region's excitability and have been shown to enhance recovery after stroke [177,178]. Increasing brain activity can lead to the release of trophic factors, axonal sprouting, and myelination – all of which are beneficial for brain repair [179,180]. However, these techniques may also induce undesirable side effects in addition to the potential functional gains. To circumvent this, our laboratory employed optogenetics as a tool to selectively stimulate specific cell populations after stroke, enabling further targeting precision and the ability to disentangle heterogeneous stimulation effects.

Data from our laboratory and others have shown that increasing excitability of the ipsilesional primary motor cortex (iM1) after stroke is beneficial for recovery [176,181]. Using optogenetic neuronal stimulation, we showed that repeated neuronal stimulations in iM1 promotes behavioral recovery in a stroke mouse model, with an associated increase in cerebral blood flow, neurovascular coupling response, and an increase in neurotrophins and the plasticity marker, GAP43 [181]. Within the cerebellum, the lateral cerebellar nucleus (LCN) has emerged as a promising brain stimulation target. LCN is the largest of the four CN in primates and sends major excitatory output to the motor, premotor, and somatosensory cortex via the dentatothalamocortical pathway [182]. Post-stroke chronic electrical stimulations in the rat LCN have been shown to enhance stroke recovery, with an increased expression of markers for synaptogenesis

and long-term potentiation [93]. Chronic LCN stimulations also increased neurogenesis selectively in glutamatergic neurons of the motor cortex [116].

We have recently demonstrated that selective neuronal stimulation in the contralesional LCN using optogenetic approaches resulted in robust and persistent recovery after stroke, as mice maintained their improved performance even after cessation of stimulation for 2 weeks [94]. The persistent recovery suggests that repeated LCN stimulations may enhance structural plasticity. Our plasticity marker GAP43 data further supports this speculation, as LCN stimulations significantly increased the axonal growth protein, GAP43, in the ipsilesional somatosensory cortex, and its expression was positively correlated with improved functional outcomes [94]. The mechanisms of LCN stimulation-enhanced recovery likely involve multiple mechanisms, including activity-dependent molecules such as cfos and CREB, which are transcription factors that mediate an array of downstream genes involved in cell survival and synaptic plasticity [183]. High throughput next generation sequencing in LCN stimulation-induced axonal sprouted neurons can reveal major biological pathways underlying stimulation-induced recovery, which may provide potential drug targets for enhancing stroke recovery.

The cerebellar brain stimulation studies have highlighted LCN as a promising brain stimulation target. It is an anatomically small brain region that contains widespread projections to multiple brain regions; thus activating this single site has the potential to result in widespread brain activation [182]. Indeed, our indirect comparison suggests that stimulating the LCN can potentially be more efficacious than stimulating the motor cortex, as LCN-stimulated mice exhibited fast and robust recovery. Several clinical studies support the use of LCN stimulation in stroke patients. A recent study used probabilistic tractography to demonstrate that the dentate-thalamo-cortical tract was positively correlated to both general motor output and fine motor skills in chronic stroke patients, further highlighting the importance of the cerebellar dentate-thalamo-cortical circuit [184]. A recent case study reported that a woman with a cerebellar stroke exhibited improvements in cerebellar ataxia after DBS in the cerebellar LCN, further supporting the feasibility of LCN stimulation for stroke patients [185]. While using optogenetics to enhance stroke recovery is highly dependent on exogenous gene therapy being approved for use in clinical trials, the Cleveland Clinic had started a clinical study to evaluate the safety and patient outcomes of electrical stimulation of the LCN for the management of chronic, moderate to severe upper extremity hemiparesis due to ischemic stroke (ClinicalTrials.gov Identifier: NCT02835443). Taken together the cerebellar brain stimulation studies are encouraging, and specific stimulations in the cerebellar circuit have tremendous translational potential to facilitate treatments for stroke recovery.

tDCS of the Cerebellum in Healthy Subjects and Cerebellar Patients

(M. Manto, N. Oulad Ben Taib)

The cerebellum is a major player for movement execution and motor control in numerous species, including human [186]. Its roles extend beyond the field of voluntary motion, including cognitive and behavioral functions. Interestingly, the human cerebellum is easily accessible to non-invasive stimulation due to its anatomical location [187]. The technique of transcranial direct current stimulation (tDCS) is a non-invasive method, which is gaining in popularity to probe and modulate cerebellar functions, both in healthy subjects and in cerebellar disorders [188]. The recently described anatomical communications between the cerebellum and basal ganglia extend the potential applications of tDCS to extra-pyramidal disorders, especially Parkinson's disease and dystonia [189]. Pathological modifications in the cerebellum circuitry, both neuropathological and functional, have been reported in Parkinson's disease and likely reflect a compensatory response to the hypofunction of the striato-thalamo-cortical pathway [190–192].

tDCS consists of the administration of a low-intensity current (0.5 – 2.5 mAmp) over the scalp with sponge electrodes. One electrode (cathode or anode) is applied in front of the cerebellum on the back of the skull, with a reference electrode either on the skull (in particular: motor cortex, prefrontal cortex or in front of the buccinator muscle) or on the shoulder. Cerebellar tDCS modifies the excitability of the cerebellar cortex with minor side effects (mainly burning or itching sensation). Polarity of the electrodes dictates the effects on the cerebellum [187]. Anodal tDCS excites the cerebellar cortex, whereas cathodal tDCS exerts an inhibitory effect. Interestingly, the technique allows the application of a sham current. Modelling studies provide a strong support for a direct effect of the tDCS upon the cerebellar circuitry, without current spreading to the brainstem or the occipital cortex [189].

Cerebellum tunes the excitability of the motor cortex via the dentato-thalamo-cortical pathway. Purkinje neurons exert an inhibition over cerebellar nuclei. This cerebellum-brain inhibition (CBI) can be assessed by TMS. [194]. Basically, a first magnetic pulse over a cerebellar hemisphere reduces the amplitude of the motor evoked potential (MEP) resulting from stimulation of the contralateral motor cortex 5-7 msec later. tDCS has been shown to modulate CBI in healthy subjects [195]. However, there is no consensus regarding the impact of cerebellar tDCS on CBI. Some authors have found a reduction of CBI following anodal stimulation of the cerebellum [196]. Possible explanations are a direct effect upon the inhibitory interneurons of the cerebellar cortex or an effect of

the cerebello-thalamo-projections upon the inhibitory interneurons of M1. Cerebellum is also a major structure for adaptive learning and motor adaptation. Cerebellar tDCS improves postural control following perturbations induced by Achilles tendon vibration [197]. Other evidence of a physiological effect of cerebellar tDCS upon brain circuitry is provided by EEG studies [198]. Unlike cathodal or sham stimulation of the cerebellum, anodal tDCS induces (1) a lateralized synchronization over the sensorimotor area in the gamma band and (2) an increase of the network segregation in sensori-motor rhythms with a greater communication between left-right hemispheres in the gamma band [199]. The plastic modifications induced by cerebellar tDCS are particularly relevant given the numerous forms of plasticity encountered in the cerebellar circuitry [189]. Cerebellar tDCS influences also the perception of pain [200].

tDCS of the cerebellum reduces the amplitudes of long-latency stretch reflexes in cerebellar ataxias, without effect upon short-latency stretch reflexes [201]. This suggests that tDCS strengthens the inhibitory effect of Purkinje neurons upon cerebellar nuclei. tDCS over the cerebellum immediately followed by tDCS over the contralateral motor cortex (tCCDCS: transcranial cerebello-cerebral DC stimulation) reduces the amplitude of postural tremor and action in tremor in SCA2 [202]. In addition, tDCS reduces hypermetric movements and improves the abnormal timing of agonist-antagonist EMG bursts. However, a confirmatory study on a large sample of cerebellar patients is currently missing. Postural tremor in cerebellar ataxia can also respond to tCCDCS with a return electrode located on the contralateral motor cortex [203]. The 2 studies of Benussi et al. (a: single session, b: two weeks' administration; double-blind, randomized, sham-controlled study) have shown a symptomatic benefit on the ataxia scores and quantified measurements [204,205]. In particular, anodal cerebellar tDCS exerts a favourable effect upon SARA score, ICARS score, and 9-hole peg test (9HPT) testing. A two-weeks' treatment with anodal cerebellar tDCS improves cerebellar symptoms and restores CBI as compared to the sham condition.

Essential tremor is associated with cerebellar pathology, especially at the level of the cerebellar cortex [206]. Whereas a first randomized, double blind, cross-over study with bilateral cathodal cerebellar stimulation showed no effect [207], a second study in which tDCS was applied over the dorsolateral prefrontal cortex (DLPFC) showed an improvement in ADL scores and TETRAS scores [208]. A recent systematic review and meta-analysis provides evidence for a positive effect of non-invasive brain stimulation on motor symptoms [209]. Both the motor cortex and the cerebellum are the main targets.

Cerebellum infuences also (1) prefrontal, parietal, and temporal lobes via multiple loops running in parallel, and (2) the striatum via a disynaptic circuit, with a projection back from the subthalamic nucleus to the cerebellar cortex [69]. Cerebellar tDCS has been applied in basal ganglia disorders, in particular Parkinson's disease and dystonia. Anodal tDCS applied during five consecutive days over the motor cortical areas and the cerebellum improves the levo-dopa induced dyskinesias in Parkinson's disease [210]. Cerebellar anodal tDCS improves the kinematics of handwriting and circle drawing tasks in patients with writing dystonia [211]. However, the effects of cerebellar tDCS upon dystonia remain controversial [212]. Cerebellar tDCS is promising to promote the rehabilitation for language deficits, in particular aphasia following a stroke [213], but the optimal location of stimulation requires to be defined. Anodal tDCS of the right cerebellum coupled with behavioural therapy is more efficient than behavioural therapy alone to improve spelling and dictation [196]. Interestingly, the resting state functional connectivity MRI data show that improved spelling is associated with an increase in cerebello-cerebral network connectivity. Cathodal tDCS enhances verb generation without modifying verb naming in post-stroke aphasia [214].

Together, these preliminary results open the door for a tDCS-based symptomatic management of cerebellar ataxias. A few studies have indeed shown that cerebellar tDCS is promising, but clear improvements are required in terms of the identification of the montage that needs to be used, a better definition of the intensity of the current delivered, and an optimization of the intervals between sessions and the number of sessions. It remains also unclear which patients might benefit from on-line versus off-line assessments. Whereas on-line effects might reflect a direct action upon Purkinje neurons, long-lasting changes might result from an action upon Golgi cells [215,216]. The polarity of the after-effects of cerebellar tDCS might be influenced by both the task-induced activity and the pre-existing excitability state [217,218]. There is a prevailing opinion in the clinical community that tDCS might potentiate the effects of motor rehabilitation in cerebellar ataxias, but sound demonstration is required. Large randomized controlled studies are necessary to establish the efficacy. The type of cerebellar ataxia, the duration of the disease, and the concurrent treatments might have interfering factors [219]. A careful phenotypic characterization appears as a pre-requisite given the very high heterogeneity of cerebellar disorders. Efforts are also required to better quantify the cerebellar reserve, another factor which might influence the response to tDCS. Severe cerebellar atrophy with a major loss of neurons above a threshold is unlikely to respond. Regarding pediatric applications, studies remain limited. The simplicity of the technique, the excellent tolerance, and its low cost should encourage methodologically sound experimental and clinical works. More data are definitely needed in this regard

and there is also a clear need to assess the effects of multi-site stimulation with similar or distinct modes of stimulation [218]. Whereas lesions of cerebellar nuclei (edema, tumor, stroke,…) cause a depression of the excitability of the contralateral motor cortex, lesions of the cerebellar cortex (cerebellitis, cerebellar cortical atrophy,…) lead to a disinhibition of cerebellar nuclei and overactivity of contralateral motor cortex. This will impact on the selection of the polarity of DCS. We should also consider that tDCS could become a complementary tool to classical pharmacotherapy [188].

Cerebellar tDCS and Motor Learning (D. Timmann, M.A. Nitsche)

A hallmark of cerebellar disease is motor incoordination and disordered balance. As of yet, there is no medication, which ameliorates the signs and symptoms of cerebellar ataxia. The mainstay of treatment is physical therapy, that is motor training, accompanied by occupational and speech therapy [220]. Although the cerebellum is an essential part of the motor learning network, evidence has grown that training improves cerebellar dysfunction in patients [221,222]. Neuromodulatory interventions are highly desirable which foster respective learning abilities in cerebellar disease, and thus enhance therapeutic efficacy. Non-invasive brain stimulation has been shown to induce and enhance plasticity, a physiological process relevant for learning and memory formation, and is therefore a likely candidate to enhance cerebellar-dependent learning processes [223,224]. Because of its easy application and low costs, transcranial direct current stimulation (tDCS) of the cerebellum has gained most interest in recent years [187]. Initial results were very promising. Firstly, cerebellar tDCS likely modulates excitability of the cerebellar cortex. In accordance, cathodal tDCS reduces cerebellar brain inhibition (CBI), whereas anodal tDCS leads to increased CBI, at least at low intensities of the conditioning cerebellar TMS pulse [195]. Hereby CBI explores the inhibitory impact of cerebellar cortex activity on primary motor cortex excitability. These results are in line with supposed direct neuroplastic effects of tDCS on the cerebellar cortex. Because neuroplasticity is essential for learning and memory formation, and plasticity induced by tDCS over other cortical areas has been shown to improve learning [225,226], there are reasons to assume that tDCS may modulate also cerebellar-dependent learning. Initial findings in reach adaptation and eyeblink conditioning support this assumption.

For example, Galea et al. (2011) found that anodal tDCS resulted in faster visuomotor reach adaptation compared to sham stimulation in young and healthy subjects [227]. Herzfeld et al. (2014) showed that anodal cerebellar tDCS improved force field reach adaptation whereas cathodal tDCS disrupted this learning ability [228]. Similarly,

locomotor adaptation has been found to improve with anodal cerebellar tDCS and decline with cathodal tDCS [229]. Furthermore, the acquisition of conditioned eyeblink responses was fostered using anodal tDCS, but deteriorated with cathodal tDCS [230]. These results do not only imply that cerebellar tDCS can improve learning, but deliver also relevant mechanistic information. Since anodal tDCS induces long-term potentiation (LTP)-like plasticity, and improved learning, the results provide further evidence against the long-standing view that long-term depression (LTD) at the parallel fiber-Purkinje cell synapse is the only and the essential kind of plasticity underlying learning in the cerebellar cortex [231]. In accordance, a recent study in mice found that anodal tDCS effects depend on LTP and the intrinsic plasticity of Purkinje cells in VOR habituation [232]. This has been further supported in recent years by Johansson et al. (2015) and Gutierres-Castellanos et al. (2017) [233,234].

Despite the promising initial results of cerebellar anodal tDCS on motor learning, recent studies showed that at least some of these findings are difficult to replicate. Firstly, Hulst et al. (2017) found no effects of neither cerebellar cathodal nor anodal tDCS on force field reach adaptation in young controls, elderly controls, and in patients with cerebellar degeneration [235]. Maybe most importantly, Galea and colleagues (2017) were unable to reproduce their initial findings in visuomotor reach adaptation using a very similar set-up and paradigm [236]. They found positive effects of anodal tDCS only for adaptation of movements of the right index finger, but not of movement of a digitizing pen (as in the original study conducted by Galea et al. 2011) [227]. They were unable, however, to reproduce the respective positive finding in a second group of young and healthy subjects. Inconsistent findings have also been observed in eyeblink conditioning. Timmann and colleagues (2017) were unable to reproduce their initial strong tDCS effects in studies using the same conditioning set-up [237]. Thus, prior to clinical applications, one needs to understand the reasons for these inconsistent findings. One important factor may be that effect sizes are much smaller than expected based on the initial positive findings, because of a bias towards publishing positive, but not negative, results [236]. Furthermore, directionality, and the amount of tDCS effects, critically depend on the orientation of the nerve fibers, and the highly convoluted cerebellar cortex may be a reason that it is difficult to predict tDCS effects in an individual subject [238]. To make things even more difficult, zebrin positive and zebrin negative zones of the cerebellar cortex appear to be involved in different forms of motor learning (e.g. VOR adaptation vs. eyeblink conditioning), and use different learning-related plasticity mechanisms, that is LTP in zebrin positive zones, and LTD (and other mechanisms to suppress simple spike firing in Purkinje cells) in zebrin negative zones [239]. Thus, for cerebellar tDCS, it might be necessary to shape stimulation protocols to allow targeted

and efficient intervention in future studies, including clinical applications.

To this aim, it may be helpful to develop predictors of tDCS efficacy. Here, sensitivity for CBI might be a promising candidate. Similar to the effects of tDCS on the primary motor cortex, which correlate with the sensitivity to TMS effects [240,241], there may be a relationship between CBI and tDCS effects at least for certain motor learning tasks. Furthermore, systematic optimization of stimulation protocols, regarding stimulation intensity, duration, repetition rate, targeting, electrode arrangement, and computational modeling based on individual MRI scans to optimize stimulation protocols at the level of the individual might be helpful to increase efficacy of the intervention [241,242] . For improving the understanding of the mechanisms of action of tDCS, and thus shape stimulation protocols on a physiology-based foundation, animal experiments are needed to comprehend tDCS effects on the level of different cerebellar layers, cell types including inhibitory interneurons, zebrin positive and negative zones, and the cerebellar nuclei. Finally, cerebellar tDCS effects likely depend on disease stage and ataxia type in patients with cerebellar degeneration, thus individual adaptation of stimulation protocols due to the physiological and structural state of the cerebellum might be required. These multi-level activities are needed to systematically explore the utility of this intervention tool beyond small-sized pilot studies.

Cerebellar Non-invasive Stimulation in Human Dystonia (T. Popa, M. Hallet)

The cerebellum is linked to the pathophysiology of numerous movement disorders, such as ataxia, essential tremor, and levodopa-induced dyskinesia, as well as dystonia [103] . Dystonia stands out in the complex mosaic of movement disorders because of its heterogeneity regarding both the etiology and expression. As described in the previous sections of this Consensus, animal models strongly support the involvement of the cerebellum in the generation of dystonic phenomena. In humans, neuroimaging and non-invasive stimulation are powerful tools to explore similar associations. However, while neuroimaging has been widely used to describe structural and functional abnormalities of the cerebellum in dystonia, non-invasive brain stimulation studies are scarce and mostly limited to those dystonia types in which it is possible to have EMG recordings uncontaminated by muscle contractions; that is, focal/segmental dystonia and dystonic contractions in the setting of levodopa-induced dyskinesia.

The first electrophysiological parameter quantifying the communication within the

cerebello-thalamo-cortical path in humans was cerebellar-brain inhibition (CBI), characterized by a reduction in the amplitude of the motor-evoked potential (MEP) from the primary motor cortex (M1) with the magnetic pulse following a conditioning magnetic pulse delivered over the cerebellum [194]. The CBI was decreased in 8 subjects with focal hand dystonia [243].

Further insight into cerebello-cortical interaction comes from studies using repetitive transcranial magnetic stimulation (rTMS) or transcranial direct current stimulation (tDCS) to induce plastic changes. In healthy subjects, rTMS and tDCS can bidirectionally change the cerebellar cortex output for at least 30 minutes: 1Hz rTMS, continuous theta burst stimulation (cTBS), or cathodal tDCS decreases CBI, while iTBS and anodal tDCS strengthen it [195,244]. When the same stimulation is applied prior to paired associative stimulation (PAS) with a 25 ms interval, which is a protocol to induce long-term potentiation-like plasticity in M1, PAS can be bidirectionally modulated: $cTBS_{cerebellum}$ and cathodal $tDCS_{cerebellum}$ lead to significant enhancement of PAS-induced M1 plastic effect above the $ShamTBS_{cerebellum}+PAS_{M1}$ level, while $iTBS_{cerebellum}$ and anodal $tDCS_{cerebellum}$ lead to its abolition [245,246]. Interestingly, the enhancement of M1 excitability in the target muscle of healthy volunteers with median nerve stimulation, i.e., APB, following $cTBS_{cerebellum}+PAS_{M1}$ is accompanied by a non-specific excitability increase in an ulnar muscle, i.e., ADM [246] – a pattern of increased plastic response and loss of cortical map specificity similar to that described in focal dystonia explored with PAS_{M1} alone [247]. When this combined $TBS_{cerebellum}+PAS_{M1}$ paradigm was explored in patients with writer's cramp, cerebellar cortex excitation and inhibition were both ineffective in modulating PAS-induced plasticity, suggesting a functional disconnection [248]. When this paradigm was explored in patients with cervical dystonia, cerebellar cortex excitation and inhibition induced the exact opposite modulatory effect on PAS-induced plasticity – a pattern observed also in healthy controls voluntarily maintaining a turned head or maintaining the head straight and having the sternocleidomastoid muscle vibrated [249]. This discrepancy suggests that the apparently common alterations in cortical excitability, sensory processing, susceptibility to undergo plastic changes, and wide-scale cortico-subcortical interactions do not have the same pathophysiology in different types of dystonia.

This conclusion emerges also from the several attempts made to use non-invasive stimulation of the cerebellum as therapy for focal dystonia; all trials addressing cervical dystonia obtained clinically positive, albeit modest, outcomes, while the trials addressing focal hand dystonia did not. A study using ten consecutive days of sham-controlled cTBS (600 pulses) delivered bilaterally over the posterior cerebellum of 20 patients with

cervical dystonia led to a small (15%) improvement of the Toronto Western Spasmodic Torticollis Rating Scale (TWSTRS) and the recovery of the motor map responsiveness measured as a reduction of the heterotopic PAS_{M1} potentiation, i.e., only APB and not FDI excitability was responsive to PAS post-intervention[250]. In this study, no changes were found in Burke-Fahn-Marsden Dystonia Rating Scale, cortical silent period, intracortical inhibition/facilitation, or cerebellar-brain inhibition. The changes were found significant immediately after the 10 therapeutic sessions, but not at the 2- or 4-week follow-up post-intervention. Another study using an identical sham-controlled design, but with $iTBS_{cerebellum}$, in 16 patients found a small but significant improvement in the severity and quality of life scores, but no changes in the cortical neurophysiological parameters [251]. While the $cTBS_{cerebellum}$ study normalizing the exaggerated PAS_{M1} effect is in line with the reversed modulation finding [249], the $iTBS_{cerebellum}$ study can appear counterintuitive. Both studies need further confirmation on larger cohorts. However, if the results of both studies are reproduced, it might suggest that any perturbation of the cerebellar cortex might be beneficial for cervical dystonia. A single-case, proof-of-concept study combined botulinum toxin with anodal tDCS in a cervical dystonia patient, applying the stimulation for 30 minutes, twice a week, over the right cerebellum (5 sessions), left cerebellum (5 sessions), and right M1+left cerebellum (10 sessions), switching the stimulation site when patient reported no benefit for two consecutive sessions [252]. There was a 39% improvement in the TWSTRS score and about 40% improvement in the quality of life questionnaires from one toxin injection to the other (12 weeks, 20 mixed-site stimulation sessions) without any other neurophysiological change. Another study reported that a single-session of cTBS over the right cerebellum paradoxically normalized the abnormal eyeblink classical conditioning in 10 patients with cervical dystonia [253]. This was opposite to the degradation of eyeblink conditioning observed in healthy subjects [254].

None of four studies using non-invasive cerebellar stimulation as therapy in focal hand dystonia found any significant clinical effect or a correlation between the neurophysiological parameters and the arm kinematics [211,212,255,256]. This absence of acute clinical effects is not surprising especially after only a single session of cerebellar stimulation [257]. A common feature of deep brain stimulation of the globus pallidus, an emerging efficient treatment for certain types of dystonia [258], is that it often takes weeks to months for the alleviation of symptoms to occur [259,260]. One possible explanation for this phenomenon is that dystonia is a network and/or plasticity disorder [261], and the delay represents the time necessary for the plastic changes to spread throughout the concerned networks. What is surprising is to have other types of dystonia respond acutely with clinical improvements to any kind of stimulation

[250]. This behooves us to carefully consider generalizations of neurophysiological observations from one form of dystonia to another, and to not discount the idea that similar abnormalities (like an impaired CBI or exaggerated plastic response to PAS_{M1}) might stem from different causes.

No explorations of the cerebellar output were attempted with non-invasive brain stimulation in other forms of dystonia. This leaves a big gap in our knowledge of the dystonic syndromes still to be characterized from an electrophysiologic point of view.

Anodal Transcranial Direct Current Stimulation (L.V. Bradnam, A. McCambridge)

Over the past decade, transcranial direct current stimulation (tDCS) has advanced the understanding of the cerebellum in health and disease. Cerebellar tDCS (ctDCS) has primarily been used as a research tool to study the motor system, but also non-motor processes such as cognitive and verbal functions. Although the exact neurophysiological mechanisms and resultant behavioral effects of ctDCS are not fully understood, there are several practical advantages that make ctDCS an attractive tool in cerebellar research and potential clinical intervention for motor and non-motor dysfunction.

The proposed mechanisms underlying anodal ctDCS-induced neuromodulation are derived from direct current findings in animal slices and primary motor cortex (M1) tDCS in humans[262,263]. Current research suggests anodal tDCS induces a subthreshold, polarity-dependent membrane polarization that induces neural plasticity via N-methyl-D-aspartate, gamma-Aminobutyric acid, brain-derived neurotrophic factor, and calcium-dependent mechanisms [179,264–266]. The neural circuitry underlying anodal ctDCS-induced effects on motor and non-motor function are not yet known, but are thought to involve the modulation of the cerebellar-thalamo-cortical route (see review [187]). Anodal ctDCS may facilitate cerebellar excitability by enhancing the inhibitory activity of Purkinje cells onto the deep cerebellar nuclei, thereby exerting less facilitatory drive to contralateral thalamic nuclei and the cerebral cortex [187]. The cerebellar-thalamo-cortical projections can be investigated in humans using transcranial magnetic stimulation (TMS). The dual-coil TMS technique, termed cerebellar brain inhibition (CBI), delivers a conditioning TMS pulse to the cerebellum, followed by a test pulse to M1 to infer inhibition [194]. Studies have found that anodal ctDCS can influence activity in the cerebellar-thalamo-cortical pathway of healthy subjects and patient populations using dual coil TMS [195,196,204,211].

A key study by Galea and colleagues (2009) revealed polarity-dependent modulation of cerebellar excitability after ctDCS[195], which formed the basis for future studies. Anodal ctDCS increased CBI, whereas cathodal ctDCS suppressed inhibition in healthy adults [195]. Increased inhibitory drive from the cerebellum was also noted in patients with cerebellar ataxia who underwent multiple ctDCS sessions [204]. However the opposite result was reported by others, whereby anodal ctDCS suppressed cerebellar brain inhibition in healthy [196] and focal hand dystonia [211] participants.

Another method to infer cerebellar function in humans is delayed eyeblink conditioning. Based on findings in animals and support from neuroimaging and patient evidence, the cerebellum plays a key role in the acquisition, timing, and retention of conditioned eyeblink responses [267]. In this method, a reflexive eyeblink is acquired in response to a given stimuli (e.g., air puff) and repeatedly paired with a conditioning stimulus (e.g., loud tone). In comparison to sham ctDCS, the acquisition and retention of conditioned eyeblink responses after the conditioning stimulus alone was enhanced following anodal and reduced following cathodal stimulation[230]. Unfortunately, the same group were unable to replicate these findings using either a cephalic or extracephalic electrode montage [237], highlighting the poor understanding of the optimal stimulation parameters for ctDCS and issues with the replicability and reliability of ctDCS findings.

Another neurophysiological technique shown to be partially cerebellar-dependent is paired associative stimulation [245]. This technique involves repetitively pairing peripheral nerve stimuli and M1 TMS at distinct inter-stimulus intervals to induce long-term potentiation (LTP)-like effects [268]. Anodal ctDCS blocked the induction of LTP, therefore indicating that human associative plasticity is influenced by the cerebellum [245]. Computational models show, as expected, that the cerebellum is the primary structure stimulated during ctDCS [269]. Yet further investigation of the after-effect of ctDCS on the cerebello-thalamo-cortical pathway and whole brain activity using various other methods such as neuroimaging is required.

Behavioral studies of anodal ctDCS commonly deliver stimulation concurrently with motor training. This idea is based on the hypothesis that increased cerebellar excitability induced by anodal ctDCS will facilitate motor performance, and concurrent training will enhance the functional specificity of tDCS to the neural circuits involved [270]. Several studies have found that anodal ctDCS can enhance the acquisition and/or consolidation of simple motor tasks by reducing movement errors [271,272]. Interestingly, when performing a force field reaching task, anodal ctDCS increased the ability to learn from

errors, plus form, and retain motor memory [228]. In contrast, there was no effect of anodal ctDCS on similar motor tasks in patients with cerebellar degeneration [235,273]. This may indicate the importance of an anatomically functional cerebellum to mediate ctDCS effects. The latter idea is supported by findings of performance improvements following anodal ctDCS in other small patient studies. For instance, anodal ctDCS improved dyskinesia scores in Parkinson's disease [210], and timing of agonist commands and tremor in cerebellar ataxia [202,204,205].

The cerebellum is known to have a broad influence and makes a strong contribution to non-motor domains such as cognition [274]. Thus, it would be expected that anodal ctDCS would also modulate non-motor processes. Several preliminary studies have reported positive effects of anodal ctDCS on verbal fluency [275] and pain perception [276] in healthy subjects and cognitive symptoms in Parkinson's patients [210]. Whilst other studies have observed no effect on cognitive learning [277] or memory [278], for example. A meta-analysis of cognition studies found cognitive processes were influenced by anodal ctDCS but to a lesser extent than motor-related effects [279]. Whether this disparity is due to the sensitivity of assessments or a weaker influence of the cerebellum on cognitive processes is still uncertain.

Overall, emerging evidence provides some support for anodal ctDCS as a neuromodulatory tool for motor and non-motor functions. But the lack of replication is a significant concern that must be addressed. As recommended for tDCS research in general, the factors that underlie inter-individual variability must first be determined, as substantial variability will pose an additional challenge when exploring tDCS-induced effects in inherently heterogeneous patient groups. Nevertheless, there are several practical advantages of ctDCS in comparison to other therapeutic techniques and brain stimulation protocols that make tDCS a promising tool. For example, tDCS is painless, has minimal side effects [280,281], the devices are low cost, portable, and require minimal training or supervision. The feasibility of delivering semi-supervised home-based neuromodulation is currently being trialed [282] and considering the dosage for inducing meaningful clinical effects is likely to involve repeated sessions, there are obvious practical advantages for home-based therapy programs. Furthermore, there is still much to be explored with regards to determining the optimal stimulation parameters for ctDCS, including high-definition montages and dual-site stimulation (i.e., cerebellum-M1 tDCS). Future research must establish the underlying mechanisms of action and neuronal circuitry that mediate reliable neurophysiological and behavioral effects, before large clinical trials of the efficacy of ctDCS can implemented.

Electrical Stimulation of the Cerebellar Cortex (D.H. Heck)

Electrical stimulation of the cerebellar cortex was an early, versatile method for manipulating cerebellar neuronal activity with high temporal and spatial precision. Only a small selection of the vast body of knowledge created with this method can be reviewed here, and an attempt has been made to focus on findings that had lasting impact.

Electrical stimulation of the cerebellar cortex provided first insights into basic principles of cerebellar network function *in vivo* [283–286] and *in vitro*[287,288], was used in elucidating key principles of cerebellar cortical interactions with the cerebellar nuclei [10], allowed the generation of early cerebellar motor maps (particularly oculomotor maps) [289–294]and promised therapeutic potential in reducing the frequency and severity of epileptic seizures [295–297].

Before discussing the research in more detail, it is important to mention a key limitation of electrical brain stimulation that is often overlooked: electrical stimulation will not primarily activate the cell bodies of neurons surrounding the tip of the stimulation electrode, but instead activates predominantly axons [298,299]. This, of course, includes axons passing through the target area and will result in a mix of antidromic and orthodromic activation of fibers of passage as well as fibers that do originate in the target area. This is particularly problematic when small nuclei are embedded in white matter, such as the cerebellar nuclei, are the target. But this problem is also relevant for cerebellar cortical stimulation if the electrode tip is placed at a depth where stimulation could cause the antidromic activation of mossy fiber axons. Stimulation of the surface of the cerebellar cortex minimizes the risk of activating mossy fibers and will instead mostly activate parallel fibers which will in turn provide excitatory input to Purkinje cells and molecular layer interneurons [285].

In experiments where electrical stimuli were directly applied to the surface of the cerebellar cortex but also at various depths below the surface, John Eccles and a group of pioneering cerebellar electrophysiologists (1966) observed an excitatory response that propagated along the parallel fibers and was flanked on either side by inhibitory responses [285]. From these findings emerged the concept of the "beam" of activated parallel fibers as a geometric representation of a possible principle of neuronal computation in the cerebellar cortex [285,300]. The "beam" concept emphasized the potential functional significance of the orthogonal arrangement of excitatory (parallel

fiber) and inhibitory (stellate and basket cell) axonal projections, a unique characteristic of the cerebellar cortical network [19]. The combination of the unusual geometrical network architecture and the characteristic simple spike/complex spike waveforms that readily identified Purkinje cells [301] were likely responsible for the fact that most of the early electrophysiological investigations of cerebellar function focused on the cerebellar cortex, neglecting the role of the cerebellar nuclei. However, understanding cerebellar function requires understanding how the cerebellar cortex, hence Purkinje cell activity, modulates the activity of the cerebellar output neurons in the cerebellar nuclei. Electrical stimulation of the cerebellar cortex *in vivo* combined with *in vitro* experiments was used by Person and Raman (2011) to show that synchrony in Purkinje cell firing causes synchronized spike firing in cerebellar nuclear cells time-locked to that of the Purkinje cells [10].

Gordon Holmes' studies of cerebellar deficits in WWI veterans (1917) had firmly established the cerebellum as a key player in the coordination of movements, including eye movements[302]. Later, electrical stimulation of the cerebellar cortex (mostly in cats) was employed to determine whether motor representation in the cerebellar cortex was topographically organized, or whether a cerebellar motor map existed. Whoever expected a map similar to the motor homunculus in the primary motor cortex must have been disappointed. The results were rather complex. Cerebellar stimulation could elicit both simple movements and complex motor sequences, depending on stimulation site, stimulus amplitude and frequency (e.g. [289,290]). But, while results on body and extremity movements were quite variable, these experiments most prominently identified cerebellar cortical sites whose stimulation reliably elicited eye movements [291–293]. Those sites are now considered to jointly constitute to the widely studied "oculomotor" cerebellum [303].

In the 1950s, DBS was explored as a potential treatment for epilepsy [148]. Interestingly, the cerebellar cortex and thalamus were the first two targets chosen for DBS treatment of epilepsy (reviewed in [148]). Initial studies of cerebellar stimulation produced promising outcomes in reducing seizure severity and frequency [295,296]. Later, however, closely controlled double-blind studies failed to show significant therapeutic effects [154,304] and other studies showed variable results [297], which caused interest in cerebellar cortical stimulation for epilepsy treatment to wane. But recently the approach has received renewed attention, albeit with a focus on stimulating the cerebellar nuclei rather than the cerebellar cortex, which is believed to be more efficient and likely to reduce the variability of outcomes [152].

Finally, most applications of electrical cerebellar cortical stimulation used single-site stimulation techniques and varied the temporal characteristics and amplitude of the stimulus applied to the site. If bipolar electrodes are used the polarity can be switched to move the stimulus to the other pole, but stimulation is always at one site at a time. If multiple electrodes are used, it becomes possible to generate spatio-temporal activity patterns that allow the investigation of cerebellar network responses to dynamic events that cannot be studied with single site stimulation. Such a multi-electrode arrangement was, for example, used to demonstrate the ability of the cerebellar cortical parallel fiber system to transform sequential inputs to the granule cell layer into synchronous inputs to postsynaptic Purkinje cells [288,305].

In summary, electrical stimulation of the cerebellar cortex has been a powerful tool with a broad spectrum of uses. The introduction of optogenetic tools overcame the problem of stimulating fibers of passage and, of course, allows the stimulation of specific subset of neurons[306]. However, because optogenetic tools are not (yet) available in all animal models and in all structures electrical stimulation will continue to be an important technique.

Non-human Primates: Physiology, Lesion, and Stimulation of Cerebellar Nuclei (M. Tanaka)

Neurons in the CN usually show high baseline firing rate and exhibit a transient activity during limb, hand, eye, and eyelid movements [307]. The CN outputs directly regulate movement signals in the brainstem and spinal cord, boost motor commands in the cerebral cortex via the thalamus, and modulate signals for adaptive learning through inhibitory projections to the inferior olive. Besides the transient activity during movements, a subset of neurons in the interposed and dentate nuclei also exhibit sustained, preparatory activity preceding movements [308], indicating the roles for the lateral cerebellum in motor planning [309]. Consistent with this, cerebellar lesions attenuate cortical readiness potentials [310], and the regional blood flow in the cerebellum correlates with the magnitude of contingent negative variation (CNV) which predicts the occurrence of relevant events [311]. Recent studies in non-human primates demonstrated that neurons in the cerebellar dentate nucleus exhibited a gradual buildup of activity before self-initiated saccadic eye movements [312,313], and that electrical stimulation applied to them facilitated self-timed, but not reactive, saccades [313]. Similar ramping neuronal activities were also found in the ventrolateral (VL)

thalamus [314], and inactivation of the thalamus delayed self-timing [315], suggesting that the preparatory signals in the cerebellar nuclei might be sent through the thalamus to the cortex and regulate the timing of movement decisions. Irrespective of the length of the delay period, neurons in the dentate nucleus always started firing approximately a half-second before self-timed movements [313]. The neuronal mechanism for the triggering of preparatory activity in the cerebellar nuclei needs to be elucidated in future studies.

The cerebellum also plays a role in predicting sensory consequences of movements to compute prediction errors that eventually alter subsequent movements. It has been well established that the cerebellum is essential for adaptive motor learning, which optimizes the force and timing of individual muscle contractions for accurate movements. Recent studies also suggest a role for the cerebellum in higher-order adaptive control of actions [316]. For example, it has been shown that the error-related cortical potentials during anti-saccades are reduced in subjects with focal cerebellar lesions [317] and that the magnitudes of the potentials correlate with the volume of Crus I and II in patients with cerebellar degeneration [318]. The other study used the stop-signal reaction time task and demonstrated causal relationships between cerebellar activity and error-related activation in the thalamus and the supplementary motor area, which in turn correlated with activation in the lateral prefrontal cortex during post-error slowing [319]. These results suggest that the cerebello-thalamo-cortical pathways may play roles in error detection and subsequent behavioral adjustment. In monkeys, neurons in the cerebellar dentate nucleus showed enhanced activity during both correct and erroneous anti-saccades [320]. Inactivation of them shortened the latency and deteriorated the accuracy of anti-saccades, while the proportion of error trials modestly increased [320]. During the tasks requiring deliberate control, the cerebellum may predict error in advance of sensory feedback and may activate frontal cortical network to alter behavioral strategy for subsequent movements [319], while the cortico-basal ganglia pathways execute proactive inhibition for the difficult tasks [321].

Many recent studies in humans also show that the cerebellum is involved in non-motor cognitive functions [322]. Evolutionally, the lateral cerebellum is well developed in primates, and the associated dentate nucleus in humans comprises approximately 92% of total neurons in the cerebellar nuclei while this proportion is 26% in cats [309]. Anatomical data show that the ventral portion of the dentate nucleus provides signals to the association areas in the cerebral cortex through the thalamus, suggesting that these pathways are crucial for higher-order cognitive functions [174]. To date, only a few studies have explored the neuronal correlates of non-motor functions in the lateral cerebellum in experimental animals. In cats, Purkinje cells in the cerebellar Crus I have

been shown to exhibit sustained activity for a moving object even when the object was temporarily removed, indicating that these neurons represent an internal model of external objects [323]. In monkeys, neurons in the dentate nucleus have been shown to exhibit a gradual increase of sensory gain when the animals attempt to detect a single omission of isochronously presented visual stimulus (Fig. 4A) [324,325]. For these neurons, the inter-stimulus interval appears to be represented by the magnitude of firing modulation for each stimulus, and the time course of neuronal activity during each inter-stimulus interval accurately predicts timing of the next stimulus. Inactivation of these neurons delayed [324], and electrical stimulation promoted (Fig. 4B) [325] the detection of stimulus omission, suggesting that they may provide temporal prediction of stimulus occurrence, which is needed to compute prediction error for the absence of regular stimuli [326]. Similar to the time course of neuronal activity in the cerebellar nuclei, temporally specific periodic signals predicting event timing have also been reported in the beta-band coherence of neuromagnetic activity between the cerebellum and the cerebral cortex when listening to an auditory beat [327], suggesting that such signals may provide a basis for the perception of rhythms. For temporal information processing, another line of evidence also suggests that the cerebellum might play a role in Bayesian inference of event timing [328,329], although the underlying neuronal mechanism needs to be clarified in future studies in experimental animals

The Molecular Mechanisms Underlying the Efficacy of Cerebellar Stimulation (L.N. Miterko, R.V. Sillitoe)

The various mechanisms by which neurostimulation elicits large-scale, behavioral responses range from inducing plasticity to modulating local and global neural network activity, as previously discussed by Bradnam, McCambridge, Heck, Tanaka and colleagues, and regardless of the paradigm (i.e. tDCS, electrical stimulation, lesioning, optogenetics). While changes in plasticity and local or systems-level electrophysiological properties depend on what is being activated (axons vs. somata) and the region-specific functions that are being capitalized on by neurostimulation, there are common molecular threads that underlie learning and neural communication. For example, learning is a process shared among neurons throughout different brain regions and involves an increase in the influx of intracellular Ca^{2+} so that receptors involved in learning (e.g. mGluR1) can be activated. In turn, the activation of learning receptors can induce ultrastructural changes in the neuron, especially at the synapse (e.g. greater spine density), to promote sustained activity. Also common among neurons, is their ability to communicate with one another. The release of neurotransmitters are a critical feature of action potential

propagation and can be specific to the behavior by facilitating communication between cells in particular neural circuits. For instance, dopamine and serotonin can regulate emotion and support feelings of addiction and reward. Furthermore, cholinergic signaling is commonly associated with satiating hunger and glutamatergic signaling is commonly associated with learning and memory. While the roles of neurotransmitters are dynamic, and can switch depending on age and circumstance, the fact that neurotransmitter classes are well-elucidated, and we are learning more and more about their contributions to health and disease, creates optimism that we can uncover the molecular mechanism(s) of neurostimulation. However, it is still not clear whether neurostimulation approaches simply piggy back on the endogenous molecular pathways or whether stimulation in fact highjacks one or more pathways to shape neural activity for behavioral improvement.

Efforts to elucidate the molecular mechanisms of neurostimulation approaches transcend methods and brain regions. Of much interest to scientists and clinicians alike is how electrical stimulation works since this is an FDA-approved method that is already readily employed in humans. Early studies on the molecular mechanisms of Parkinson's Disease entailed a combination of fast cyclic voltammetry (FSCV), microdialysis, high performance liquid chromatography electrochemical detection (HPLC-ECD), and functional imaging (PET) [330,331]. Increased tyrosine hydroxylase (TH) expression accompanied increased dopamine in the striatum of Parkinsonian rats after STN stimulation [330,331]. Furthermore, behavioral improvements were documented after STN stimulation increased dopamine metabolism [331,332]. However, these results were not reproducible in humans [333] and even if they were, it would not explain why DBS works despite patient resistance to dopaminergic drugs. Fluctuating serotonin levels have recently been implicated in the after-effects of STN DBS due to data reporting that (1) cognitive and depressive symptoms develop after stimulation and (2) anti-Parkinsonian drugs reduce serotonin in the prefrontal cortex and hippocampus, and (3) selective serotonin reuptake inhibitors (SSRIs) such as fluoxetine enhances responsiveness to neurostimulation [334–336].

While measuring neurotransmitter concentration and imaging its release gave insight into possible molecular mechanisms of DBS, more sophisticated methods have been developed to analyze molecular and genetic changes that occur on the single-cell level. Forniceal DBS is one example where quantitative PCR, RNA-sequencing, bisulfite sequencing, and proteomics were performed to address how electrical stimulation improves learning, memory, and promotes neurogenesis, as previously found by and Hao, Shirvalker, and colleagues [337–339]. Through a combination of these molecular

and stimulation techniques, Pohodich et al. (2018) found that forniceal DBS in mouse upregulates genes involved in cell survival, synaptic function, and neurogenesis, specifically through Jun signaling [337]. These data are particularly interesting since earlier stimulation studies support the role of DBS in promoting neurogenesis through findings that electrical fields can (1) selectively direct the migration of stem cells [340–342], (2) increase blood flow [343], and (3) modulate neural networks (see sections by Cooperrider, Manto and Oulad Ben Taib, Bradnam and McCambridge, Popa and Hallet, and Timmann and Nitsche).

Are the molecular insights we have gained from studying STN and forniceal DBS applicable to cerebellar stimulation? There is a breadth of evidence suggesting that there may be some similarities. Not only does stimulating the cerebellum result in increased plasticity (see section by Cooperider and colleagues), it has also been found to be associated with dopamine release [344], increased blood flow [345,346], non-motor relief [347], and modulatory effects on global neural networks [193,348,349]. Despite these shared properties, it is likely that molecular profiles diverge, especially as the paradigm changes. For instance, different locations (e.g. dentate vs. interposed vs. fastigal nuclei), frequencies (e.g. low vs. high), and pathologies most likely elicit different molecular changes in order to achieve improvements in varied behaviors.

Understanding the molecular underpinnings of neurostimulation will greatly advance the treatment of diseases originating from or involving the cerebellum. Expanding studies to simultaneously address the effects of chronically implanting electrodes into the cerebellum will also deepen our knowledge of how to best treat diseases. It is already known that metal electrodes can promote gliosis, scarring, and prolonged inflammation, but can chronic implantation have any benefit [350]? Electrical stimulation may counter some of the negative effects of implantation, such as it can modulate inflammatory responses [351], but can implantation itself be additive and positively alter gene expression? It will be interesting to discover what stimulation versus implantation does, in addition to resolving whether stimulation at different frequencies and locations have distinct benefits. Solving these challenging problems will promote the design and implementation of treatments and therapies for targeting the many disorders with cerebellar involvement.

Consensus and Summary

We present 13 different sections reviewing data for what is currently known about cerebellar stimulation in humans, non-human primates, and rodent models. Based on studies of electrical stimulation in the normal brain and in disease (human and animal models), there is a general consensus that stimulating the cerebellum has profound effects on behavior. Still, from a therapeutic perspective, one has to ask (and perhaps re-ask) the most direct and fundamental questions: does cerebellar neurostimulation *actually* work? If yes, how does it work?

Clearly, stimulating the cerebellar cortex has a powerful influence on the circuit, and the response conforms to the structural framework within the cerebellar layers as well as their interaction with the cerebellar nuclei (see section by D.H. Heck). Cerebellar nuclei stimulation has similarly convincing effects, particularly in the behavioral domain in which motor and non-motor responses are modulated (see section by M. Tanaka). But does this mean that placing stimulating electrodes into a cerebellar region alters the activity within that region? This has been a challenging problem to address since most often the stimulating current creates enough noise that *in vivo* recording of the responses at the stimulation site are masked. However, based on analysis of neuronal activity in mice that are genetically modified to exhibit dystonia, it is suggested that stimulation indeed could have local effects on the output properties of cerebellar neurons [79]. Although, is it really enough just to modulate cerebellar activity? Might there be additional long-distance changes that occur after cerebellar stimulation? The result of cerebellar stimulation in stroke certainly argues that cerebellar stimulation can induce plasticity in regions as distant as the cerebral cortex (see section by Cooperrider and colleagues) and these changes may be dependent on specific molecular mechanisms (see section by Cheng and colleagues). Even with this apparent specificity, it is hard to rule out the possibility that stimulation could induce several anterograde and retrograde effects, and they could be local or long-distance [352]. For DBS, this leads us back to the question that remains unanswered: what is the mechanism of DBS? The general concept of DBS is that high-frequency stimulation modulates erroneous neural activity and entrains it to a pattern that normalizes behavior. There are a number of possible mechanisms [353], but one perspective is that the pulses produce inhibitory neuronal effects on somata that are proximal to the location of the electrode. The inhibitory action could be the direct result of a depolarization block through a mechanism involving sodium channel inactivation and potassium current potentiation. However, DBS might also increase and regularize the output of the stimulated region by activating local axons—this is certainly an appealing hypothesis in cerebellar

disorders since much of electrophysiological defects could stem from changes in the firing regularity of the cerebellar nuclear neurons. At the network level, the end result is that the entrainment overrides pathological oscillatory activity. Again, given the potential dependence of cerebellar function on neuronal synchrony, it could be that DBS ultimately serves to normalize activity within an existing internal framework that packages cerebellar circuits into distinct functional modules.

Is the purpose of cerebellar stimulation to correct cerebellar functional itself, or is it more important that it improves its functional connectivity with the rest of the brain? There is also a third possibility that the most critical outcome of cerebellar stimulation is to enhance connectivity between other brain regions. Testing between these ideas could be carried out using modern optogenetics approaches (see section by Gornati and Hoebeek), but human non-invasive stimulation has provided some important clues. Long-lasting changes in motor and non-motor functions and the potential benefits in ataxia, dystonia, and tremor would suggest that cerebellar rTMS and tCDS approaches also induce changes in connected brain regions (see sections by Manto and Oulad Ben Taib, Bradnam and McCambridge, Popa and Hallet, and Timmann and Nitsche). While there is a consensus that cerebellar non-invasive stimulation is practical, relatively easy to implement in most medical institutions, and is relatively safe, there is also a consensus on several matters that must be addressed. Blind, and perhaps double-blind, studies will have to be performed to solve the lack of reproducibility across some studies. As for DBS, the mechanism of action(s) is poorly understood, and the full impact on global brain networks remain unclear.

We have argued that the cerebellum should be considered as a target for neurostimulation, especially when other brain regions are, for whatever reason, not ideal. However, being in its infancy as a therapeutic neurosurgical target, perhaps to play devil's advocate for a moment, we could ask why the cerebellum should not (yet) be considered. There is a need to understand what regions of the cerebellar cortex are best suited for different disease conditions, should stimulation paradigms take into account zones, and when should the cerebellar nuclei be considered instead? If the cerebellum is a better target in particular cases, which nucleus should be targeted? We have to consider that stimulating a given nucleus might not only result in a specific outcome because of its circuit connectivity, but also because each nucleus could have a very different composition of glutamatergic, GABAergic, and glycinergic neurons. It should also be noted that diseases such as ataxia can have developmental rearrangements in the circuitry [354], which means that stimulating a certain target might not yield the predicted outcome. Even if a desired location is theoretically the most ideal, what is

the evidence that the electrode, in the case of DBS, will remain in place? We know from experimental studies in rodents that while tetrodes maintain stability in regions such as the hippocampus, there can be considerable drift in cerebellum. This could be due to several factors such as curvature of the cerebellum, shape of the overlying, bone, sinuses, and tissue density, which all could affect the proper anchoring of electrodes to the targeted region. Current ongoing studies in human stroke patients (see section by Cooperrider and colleagues) could help address many of these concerns, in addition to determining the types of electrodes that are most suitable for the cerebellum, and what the long-term impact on the tissue is. That is, what type of damage response is initiated locally within the cerebellum – or by the cerebellum and then communicated to connected regions – and are there any contraindications that arise, and how might they be dealt with by troubleshooting and modifying the approach?

Another major consideration, with its own hurdles, is if and when to use brain stimulation in pediatric patients. The sheer number of neurons and glia in the cerebellum, and its protracted developmental timetable all contribute to its high level of susceptibility to injury and disease. The diseases that affect cerebellar development are many, including well known disorders such as ataxia (several forms), hydrocephalus, medulloblastoma, cerebral palsy, and ASD. Interactions and expression in gene networks are significantly altered, and as a consequence the normal dynamics of morphogenesis are abnormal. The normal dynamics of typical cerebellar development are already a challenge for predicting when it might be safe and effective to intervene with stimulation, and with the added complexity of disease-induced changes, the need for determining when and where the best stimulation targets are, becomes even greater. That is, a reasonable target at one time point during development may be inappropriate at another time point because of structural and functional changes based on neuronal migration, circuit connectivity, synaptic plasticity, and gene expression. These biological properties of the cerebellum (and for that matter, all brain regions) are core features for asking what ethical standards must be in place in order to consider stimulation in children, especially for invasive approaches such as DBS.

Although cerebellar stimulation arose from controversial work starting in the 1950s, there has been a major overhaul in ethical standards throughout medical practice around the world. Even though cerebellar neuromodulation has its origins in what some researchers are now describing as a dark era of neurosurgery [355], there are many important scientific findings and ethical lessons to draw upon. Although this consensus focusses on relatively recent advances, the idea of stimulating the cerebellum, especially as it relates to non-motor diseases, dates far back to the work

of Robert G. Heath published in the 1970s but initiated in the 1950s [356, 357, see also ref. 148]. Advances in our understanding of cerebellar development, genetics, anatomy, and electrophysiological properties provide an ever-growing number of ideas to be enthusiastic about, especially given the range of motor and non-motor functions that are now attributed to normal cerebellar function. Perhaps the firmest consensus that we have come to is that studies of cerebellar neurostimulation should proceed, but only with the sharpest critical eye for experimental and ethical standards, alternate explanations, and the mechanisms of action for each stimulation paradigm.

Concluding Remarks (R.V. Sillitoe)

As we continue to unravel the many functions of the cerebellum, including its unexpected roles in non-motor function, its utility as a target for therapeutic neurostimulation will expand. As a field, we should proceed with cautious optimism that the cerebellum could be a much-needed source of corrective signals in a number of diseases. We look forward to further experimentally testing whether cerebellar cortical, cerebellar nuclear, or even cerebellar peduncular stimulation could be beneficial in ataxia, dystonia, tremor, epilepsy, stroke, and a growing list of disorders. Whatever clinical successes are achieved, we must continue to ask, how does neurostimulation work?

Acknowledgements

Miterko, Beckinghausen, Sillitoe: This work was supported by funds from Baylor College of Medicine (BCM) and Texas Children's Hospital, BCM IDDRC Grant U54HD083092 from the Eunice Kennedy Shriver National Institute of Child Health and Human Development (The IDDRC Neuropathology and Neurobehavior Sub-Cores were used for anatomy and behavior), and by National Institutes of Neurological Disorders and Stroke (NINDS) R01NS089664 and R01NS100874 to RVS.

Wichmann, DeLong: We acknowledge support from NIH grants R01-NS062876 (TW) and P50-NS098685, as well as support from the American Parkinson's Disease Foundation (TW and MRD). The work was also supported by a grant from the NIH Office of Research Infrastructure Programs OD P51-OD011132 to the Yerkes National Primate Research Center (TW).

Kuo, Xie, Louis: Dr. Kuo has received funding from the National Institutes of Health: NINDS #K08 NS083738, the Louis V. Gerstner Jr. Scholar Award, the Parkinson's Foundation, and the International Essential Tremor Foundation. Dr. Xie has received

research support from the Parkinson's Foundation, the Michael J Fox Foundation for Parkinson's Research, AbbVie, Bristol-Myers Squibb, Biogen, and Bucksbaum Institute of Clinical Excellence (University of Chicago). Dr. Louis has received research support from the National Institutes of Health: NINDS #R01 NS094607 (principal investigator), NINDS #R01 NS085136 (principal investigator), NINDS #R01 NS073872 (principal investigator), NINDS #R01 NS085136 (principal investigator) and NINDS #R01 NS088257 (principal investigator). He has also received support from the Claire O'Neil Essential Tremor Research Fund (Yale University).

Manto, Oulad Ben Taib: MM is supported by the FNRS Belgium

Timmann, Nitsche: Supported by Mercur Pr-2015-0019 and SFB1280 (TP A05, A06)

Conflicts of Interest:

LN Miterko, J Beckinghausen, RV Sillitoe: None

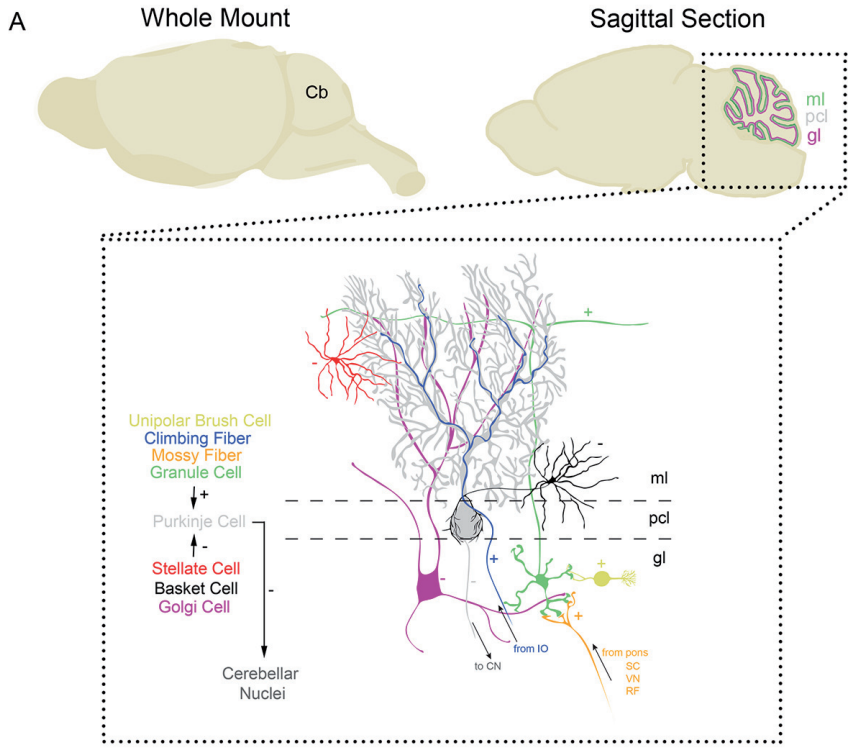

Fig. 1. Schematic of the canonical cerebellar cortical circuit. A Cartoon drawing of the mouse brain (left) and a sagittal section illustrating the three layers of the cerebellar cortex (right). Schematic of the neurons in the cerebellar cortex (bottom, blown up) illustrating the repeating basic circuitry that is comprised of Purkinje cells (gray), granule cells (green, with parallel fiber axons that bifurcate in the ml), climbing fiber afferents (blue), mossy fiber afferents (orange), stellate cell interneurons (red) and basket cell interneurons (black), Golgi cell interneurons (magenta), and unipolar brush cell interneurons (yellow). The excitatory synapses are labeled with a "+" and the inhibitory synapses with a "-" sign. The main output of the Purkinje cells is to the cerebellar nuclei, climbing fibers derive from inferior olive neurons, and mossy fibers come from a number of regions including the pontine nuclei, spinal cord, vestibular nuclei, and reticular formation. For simplicity, we have not shown the Lugaro cells or the candelabrum cells. Abbreviations: Cb = cerebellum, ml = molecular layer, pcl = Purkinje cell layer, gl = granular layer, cn = cerebellar nuclei, IO = inferior olive, SC = spinal cord, VN = vestibular nuclei, RF = reticular formation.

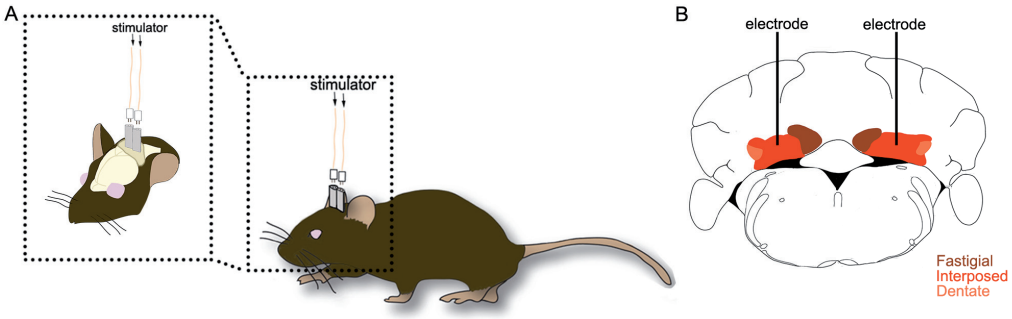

Fig. 2. Deep brain stimulation of the mouse cerebellum. A Cartoon schematic of a mouse implanted with deep brain stimulation electrodes into the cerebellum. Even though this approach uses wires to connect the stimulator to the electrode port, there is enough flexibility for analysis in behaving animals. **B** Schematic of a tissue section cut through the mouse cerebellum illustrating the bilateral targeting of the bipolar stimulating electrodes to the interposed (middle) nucleus (red).

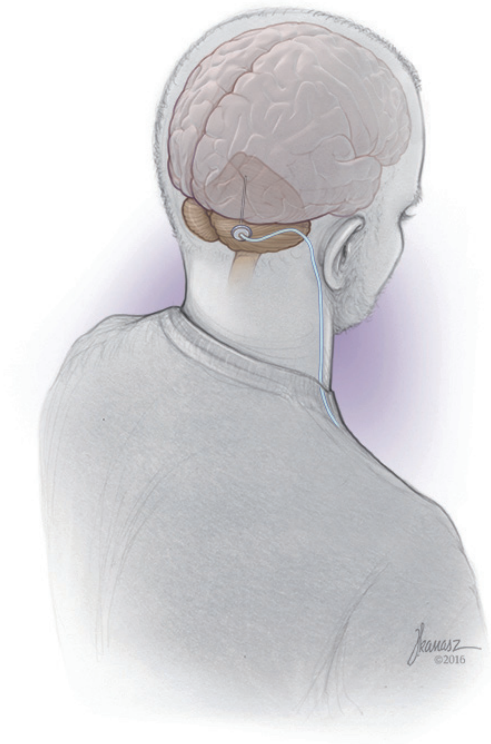

Fig. 3. Deep brain stimulation of the human cerebellum. Cartoon drawing illustrating the general approach of deep brain stimulation targeting the dentate (lateral) nucleus in human.

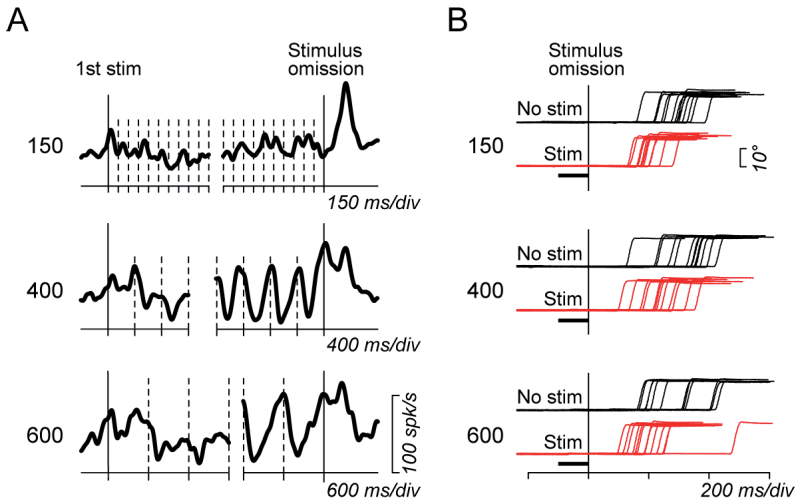

Fig. 4. Electrical stimulation to the dentate nucleus advances sensory prediction. A Neurons in the dentate nucleus exhibited firing modulation when the monkey attempted to detect a single omission of periodic visual stimuli. **B** Electrical stimulation applied to the recording site shortened the reaction time for the stimulus omission. Adapted with permission from [324].

References

1. Santiago Ramón y Cajal. Nerf trigemeau ou de la Ve paire. Maloine. Histol. du Syst. Nerv. L'Homme des vertébrés. Paris; 1909.
2. Voogd J, Glickstein M. The anatomy of the cerebellum. Trends Cogn Sci. 1998;21(9):370-5..
3. Cerminara NL, Lang EJ, Sillitoe RV, Apps R. Redefining the cerebellar cortex as an assembly of non-uniform Purkinje cell microcircuits. Nat Rev Neurosci. 2015;16(2):79-93.
4. Eccles JC. The plasticity of the mammalian central nervous system with special reference to new growths in response to lesions. Naturwissenschaften. 1976;63(1):8-15.
5. Barmack NH, Yakhnitsa V. Functions of interneurons in mouse cerebellum. J Neurosci. 2008;28(5):1140-52.
6. Ruigrok TJH, Hensbroek RA, Simpson JI. Spontaneous activity signatures of morphologically identified interneurons in the vestibulocerebellum. J Neurosci. 2011;31(2):712-24.
7. Davie JT, Clark BA, Hausser M. The origin of the complex spike in cerebellar Purkinje cells. J Neurosci. 2008;28(30):7599-609.
8. Watt AJ, Cuntz H, Mori M, Nusser Z, Sjöström PJ, Häusser M. Traveling waves in developing cerebellar cortex mediated by asymmetrical Purkinje cell connectivity. Nat Neurosci. 2009;12(4):463-73.
9. Mugnaini E, Sekerková G, Martina M. The unipolar brush cell: A remarkable neuron finally receiving deserved attention. Brain Res. Rev. 2011;66(1-2):220-45.
10. Person AL, Raman IM. Purkinje neuron synchrony elicits time-locked spiking in the cerebellar nuclei. Nature. 2011;481(7382):502-5.
11. Ankri L, Husson Z, Pietrajtis K, Proville R, Léna C, Yarom Y, et al. A novel inhibitory nucleo-cortical circuit controls cerebellar Golgi cell activity. Elife. 2015;4.
12. Houck BD, Person AL. Cerebellar premotor output neurons collateralize to innervate the cerebellar cortex. J Comp Neurol. 2015;523(15):2254-71.
13. Guo C, Witter L, Rudolph S, Elliott HL, Ennis KA, Regehr WG. Purkinje cells directly inhibit granule cells in specialized regions of the cerebellar cortex. Neuron. 2016;91(6):1330-41.
14. Witter L, Rudolph S, Pressler RT, Lahlaf SI, Regehr WG. Purkinje cell collaterals enable output signals from the cerebellar cortex to feed back to Purkinje cells and interneurons. Neuron. 2016;91(2):312-9.
15. Voogd J. What we do not know about cerebellar systems neuroscience. Front Syst Neurosci. 2014;8:227.
16. Miterko LN, Sillitoe RV, Hawkes R. Zones and stripes: Development of cerebellar topography. Handb Cerebellum Cerebellar Disord. 2nd ed. Dordrecht: Springer Netherlands; 2018. p. 43–59.
17. Xiao J, Cerminara NL, Kotsurovskyy Y, Aoki H, Burroughs A, Wise AK, et al. Systematic regional variations in Purkinje cell spiking patterns. PLoS One. 2014;9(8):e105633.
18. Zhou H, Lin Z, Voges K, Ju C, Gao Z, Bosman LWJ, et al. Cerebellar modules operate at different frequencies. Elife. 2014;3:e02536.
19. Palay SL, Chan-Palay V. Cerebellar cortex: cytology and organization. Springer-Verlag. 1974.
20. Ango F, Di Cristo G, Higashiyama H, Bennett V, Wu P, Huang ZJ. Ankyrin-based subcellular gradient of neurofascin, an immunoglobulin family protein, directs GABAergic innervation at Purkinje axon initial segment. Cell. 2004;119(2):257-72.

21. Huang CC, Sugino K, Shima Y, Guo C, Bai S, Mensh BD, et al. Convergence of pontine and proprioceptive streams onto multimodal cerebellar granule cells. Elife. 2013;2:e00400.
22. White JJ, Arancillo M, Stay TL, George-Jones NA, Levy SL, Heck DH, et al. Cerebellar zonal patterning relies on Purkinje cell neurotransmission. J Neurosci. 2014;34:8231–45.
23. Reeber SL, Loeschel C a, Franklin A, Sillitoe RV. Establishment of topographic circuit zones in the cerebellum of scrambler mutant mice. Front Neural Circuits. 2013;7:122.
24. Manto M, Bower JM, Conforto AB, Delgado-García JM, Da Guarda SNF, Gerwig M, et al. Consensus paper: Roles of the cerebellum in motor control-the diversity of ideas on cerebellar involvement in movement. Cerebellum. 2012;11(2):457-87.
25. Perciavalle V, Apps R, Bracha V, Delgado-García JM, Gibson AR, Leggio M, et al. Consensus paper: Current views on the role of cerebellar interpositus nucleus in movement control and emotion. Cerebellum. 2013;12(5):738-57.
26. Caligiore D, Pezzulo G, Baldassarre G, Bostan AC, Strick PL, Doya K, et al. Consensus paper: Towards a systems-level view of cerebellar function: The interplay between cerebellum, basal ganglia, and cortex. Cerebellum. 2017;16(1):203-29.
27. Lang EJ, Apps R, Bengtsson F, Cerminara NL, De Zeeuw CI, Ebner TJ, et al. The roles of the olivocerebellar pathway in motor learning and motor control. A consensus paper. Cerebellum. 2017;16(1):230-52.
28. Koziol LF, Budding D, Andreasen N, D'Arrigo S, Bulgheroni S, Imamizu H, et al. Consensus paper: The cerebellum's role in movement and cognition. Cerebellum. 2014; 13(1):151-77..
29. Mariën P, Ackermann H, Adamaszek M, Barwood CHS, Beaton A, Desmond J, et al. Consensus paper: Language and the cerebellum: An ongoing enigma. Cerebellum. 2014;13(3):386-410.
30. Baumann O, Borra RJ, Bower JM, Cullen KE, Habas C, Ivry RB, et al. Consensus paper: The role of the cerebellum in perceptual processes. Cerebellum. 2015;14(2):197-220.
31. Adamaszek M, D'Agata F, Ferrucci R, Habas C, Keulen S, Kirkby KC, et al. Consensus paper: Cerebellum and emotion. Cerebellum. 2017;16(2):552-76.
32. Larsell O. The morphogenesis and adult pattern of the lobules and fissures of the cerebellum of the white rat. J Comp Neurol. 1952;97(2):281-356.
33. Sillitoe RV, Joyner AL. Morphology, molecular codes, and circuitry produce the three-dimensional complexity of the cerebellum. Annu Rev Cell Dev Biol. 2007;23:549-77.
34. Schwarz L, Miyamichi K, Gao X, Beier KT, Weissbourd B, DeLoach KE, Ren J, Ibanes S, Malenka RC, Kremer EJ, Luo L. Viral-genetic tracing of the input-output organization of a central noradrenaline circuit. Nature. 2015;524(7563):88-92.
35. Hoshi E, Tremblay L, Féger J, Carras PL, Strick PL. The cerebellum communicates with the basal ganglia. Nat Neurosci. 2005;8(11):1491-3.
36. Chen CH, Fremont R, Arteaga-Bracho EE, Khodakhah K. Short latency cerebellar modulation of the basal ganglia. Nat Neurosci. 2014;17(12):1767-75.
37. Dietrichs E, Haines DE. Interconnections between hypothalamus and cerebellum. Anat Embryol (Berl). 1989;179(3):207-20.
38. Rochefort C, Arabo A, André M, Poucet B, Save E, Rondi-Reig L. Cerebellum shapes hippocampal spatial code. Science. 2011;334(6054):385-9.
39. Tsubota T, Ohashi Y, Tamura K, Sato A, Miyashita Y. Optogenetic manipulation of cerebellar purkinje cell activity in vivo. PLoS One. 2011;6(8):e22400.

40. Cerminara NL, Koutsikou S, Lumb BM, Apps R. The periaqueductal grey modulates sensory input to the cerebellum: A role in coping behaviour? Eur J Neurosci. 2009;29(11):2197-206.
41. Alexander G. Parallel organization of functionally segregated circuits linking basal ganglia and cortex. Annu Rev Neurosci. 1986;9:357-81.
42. Alexander GE, Crutcher MD, Delong MR. Basal ganglia-thalamocortical circuits: Parallel substrates for motor, oculomotor, "prefrontal" and "limbic" functions. Prog Brain Res. 1990;85:119-45.
43. DeLong MR. Primate models of movement disorders of basal ganglia origin. Trends Neurosci. 1990;13(7):281-5.
44. Wichmann T, Delong MR. Youmans & Winn Neurological Surgery. R.H. Winn. Saunders/Elsevier; 2015.
45. Burdick AP, Foote KD. Advancing deep brain stimulation for obsessive-compulsive disorder. Expert Rev Neurother. 2011;11:341–4.
46. De Koning PP, Figee M, Van Den Munckhof P, Schuurman PR, Denys D. Current status of deep brain stimulation for obsessive-compulsive disorder: A clinical review of different targets. Curr Psychiatry Rep. 2011;13(4):274-82.
47. Kisely S, Hall K, Siskind D, Frater J, Olson S, Crompton D. Deep brain stimulation for obsessive-compulsive disorder: A systematic review and meta-analysis. Psychol Med. 2014;44(16):3533-42.
48. Cleary DR, Ozpinar A, Raslan AM, Ko AL. Deep brain stimulation for psychiatric disorders: where we are now. Neurosurg Focus. 2015;38(6):E2.
49. Carpenter MB, Whittier JR, Mettler FA. Analysis of choreoid hyperkinesia in the rhesus monkey. Surgical and pharmacological analysis of hyperkinesia resulting from lesions in the subthalamic nucleus ol luys. J Comp Neurol. 1950;92(3):293-331.
50. Whittier JR, Mettler FA. Studies on the subthalamus of the rhesus monkey. II. Hyperkinesia and other physiologic effects of subthalamic lesions, with special reference to the subthalamic nucleus of Luys. J Comp Neurol. 1949;90(3):319-72.
51. Albin RL, Young AB, Penney JB. The functional anatomy of basal ganglia disorders. Trends Neurosci. 1989;18(2):63-4.
52. Freeze BS, Kravitz AV, Hammack N, Berke JD, Kreitzer AC. Control of basal ganglia output by direct and indirect pathway projection neurons. J Neurosci. 2013;33(47):18531-9.
53. Burns RS, Chiueh CC, Markey SP, Ebert MH, Jacobowitz DM, Kopin IJ. A primate model of parkinsonism: selective destruction of dopaminergic neurons in the pars compacta of the substantia nigra by N-methyl-4-phenyl-1,2,3,6-tetrahydropyridine. Proc Natl Acad Sci U S A. 1983;80(14):4546-50.
54. Galvan A, Wichmann T. Pathophysiology of Parkinsonism. Clin Neurophysiol. 2008;119(7):1459-74.
55. Bergman H, Wichmann T, DeLong MR. Reversal of experimental parkinsonism by lesions of the subthalamic nucleus. Science. 1990;249(4975):1436-8.
56. Benazzouz A, Gross C, Féger J, Boraud T, Bioulac B. Reversal of rigidity and improvement in motor performance by subthalamic high-frequency stimulation in MPTP-treated monkeys. Eur J Neurosci. 1993;5(4):382-9.
57. Pollak P, Benabid AL, Gross CH, Gao, DM, Laurent A, Benazzouz A, Hoffman D, Gentil M, Perret J. Effets de la stimulation du noyau sous-thalamique dans la maladie de Parkinson. Rev Neurol. 1993;149:175–6.

58. Benabid AL, Pollak P, Gross C, Hoffmann D, Benazzouz A, Gao DM, Laurent A, Gentil M, Perret J. Acute and long-term effects of subthalamic nucleus stimulation in Parkinson's disease. Stereotact Funct Neurosurg. 1994;62:76–84.
59. Bronstein JM, Tagliati M, Alterman RL, Lozano AM, Volkmann J, Stefani A, et al. Deep brain stimulation for Parkinson disease an expert consensus and review of key issues. Arch Neurol. 2011;68(2):165.
60. Ramirez-Zamora A, Ostrem JL. Globus pallidus interna or subthalamic nucleus deep brain stimulation for Parkinson disease: A review. JAMA Neurol. 2018;75:367–72.
61. Hashimoto T, Elder CM, Okun MS, Patrick SK, Vitek JL. Stimulation of the subthalamic nucleus changes the firing pattern of pallidal neurons. J Neurosci. 2003;23(5):1916-23.
62. Miocinovic S, Parent M, Butson CR, Hahn PJ, Russo GS, Vitek JL, McIntyre CC. Computational analysis of subthalamic nucleus and LInticular fasciculus activation during therapeutic deep brain stimulation. J Neurophysiol. 2006;96(3):1569-80.
63. Chiken S, Nambu A. Mechanism of Deep Brain Stimulation: Inhibition, Excitation, or Disruption? Neuroscientist. 2015;22(3):313-22.
64. McCairn KW, Iriki A, Isoda M. Common therapeutic mechanisms of pallidal deep brain stimulation for hypo- and hyperkinetic movement disorders. J Neurophysiol. 2015;114(4):2090-104.
65. Johnson MD, Miocinovic S, McIntyre CC, Vitek JL. Mechanisms and targets of deep brain stimulation in movement disorders. Neurotherapeutics. 2008;5(2):294-308.
66. Rosin B, Slovik M, Mitelman R, Rivlin-Etzion M, Haber SN, Israel Z, et al. Closed-loop deep brain stimulation is superior in ameliorating parkinsonism. Neuron. 2011;72(2):370-84.
67. Little S, Pogosyan A, Neal S, Zavala B, Zrinzo L, Hariz M, et al. Adaptive deep brain stimulation in advanced Parkinson disease. Ann Neurol. 2013;74(3):449-57.
68. Malekmohammadi M, Herron J, Velisar A, Blumenfeld Z, Trager MH, Chizeck HJ, et al. Kinematic adaptive deep brain stimulation for resting tremor in Parkinson's disease. Mov Disord. 2016;31(3):426-8.
69. Bostan AC, Dum RP, Strick PL. The basal ganglia communicate with the cerebellum. Proc Natl Acad Sci. 2010;107(18):8452-6.
70. Bostan AC, Dum RP, Strick PL. Cerebellar networks with the cerebral cortex and basal ganglia. Trends Cogn. Sci. 2013;17(5):241-54.
71. Tewari A, Fremont R, Khodakhah K. It's not just the basal ganglia: Cerebellum as a target for dystonia therapeutics. Mov Disord. 2017;32(11):1537-45.
72. Shakkottai VG, Batla A, Bhatia K, Dauer WT, Dresel C, Niethammer M, et al. Current opinions and areas of consensus on the role of the cerebellum in dystonia. Cerebellum. 2017;16(2):577-94.
73. Prudente CN, Hess EJ, Jinnah HA. Dystonia as a network disorder: What is the role of the cerebellum? Neuroscience. 2014;260:23-35.
74. Bologna M, Berardelli A. Cerebellum: An explanation for dystonia? Cerebellum. 2017;4:6.
75. Lewis MM, Galley S, Johnson S, Stevenson J, Huang X, McKeown MJ. The role of the cerebellum in the pathophysiology of Parkinson's disease. Can J Neurol Sci. 2013;40:299–306.
76. Louis ED, Faust PL, Vonsattel J-PG. Purkinje cell loss is a characteristic of essential tremor. Park Relat Disord. 2011;17(6):406-9.
77. Wu T, Hallett M. The cerebellum in Parkinson's disease. Brain. 2013;136(Pt 3):696-709.
78. Helmich RC, Hallett M, Deuschl G, Toni I, Bloem BR. Cerebral causes and consequences of parkinsonian resting tremor: A tale of two circuits? Brain. 2012;135(Pt 11):3206-26.

79. White JJ, Sillitoe RV. Genetic silencing of olivocerebellar synapses causes dystonia-like behaviour in mice. Nat Commun. 2017;8:1-16.
80. DeLong MR, Benabid A-L. Discovery of high-frequency deep brain stimulation for treatment of Parkinson disease. JAMA. 2014;312(11):1093-4.
81. Crowell JL, Shah BB. Surgery for Dystonia and Tremor. Curr. Neurol. Neurosci. Rep. 2016.
82. Franzini A, Cordella R, Messina G, Marras CE, Romito LM, Carella F, et al. Deep brain stimulation for movement disorders. Considerations on 276 consecutive patients. J Neural Transm. 2011;118(10):1497-510.
83. Jinnah HA, Hess EJ. Evolving concepts in the pathogenesis of dystonia. Park Relat Disord. 2018;46:S62–5.
84. Fremont R, Tewari A, Angueyra C, Khodakhah K. A role for cerebellum in the hereditary dystonia DYT1. Elife. 2017;6:e22775.
85. Zervas NT, Horner FA. Pickren KS. The treatment of dyskinesia by stereotxic dentatectomy. Confin Neurol. 1967;29:93–100.
86. Cooper IS, Upton ARM. Use of chronic cerebellar stimulation for disorders of disinhibition. Lancet. 1978;1(8064):595-600.
87. Penn RA, Gottlieb GL, Agarwal GC. Cerebellar stimulation in man: Quantitative changes in spasticity. J Neurosurg. 1978;48:779–86.
88. Galanda M, Hovath S. Different effect of chronic electrical stimulation of the region of the superior cerebellar peduncle and the nucleus ventralis intermedius of the thalamus in the treatment of movement disorders. Stereotact Funct Neurosurg. 1997;69(1-4 Pt 2):116-20.
89. Sokal P, Rudas- M, Harat M, Szylberg Ł, Zieliński P. Deep anterior cerebellar stimulation reduces symptoms of secondary dystonia in patients with cerebral palsy treated due to spasticity. Clin Neurol Neurosurg. 2015;135:62-8.
90. Galanda, M, Mistina L, Zoltan O. Behavioural responses to cerebellar stimulation in cerebral palsy. Acta Neuroschirurgica Suppl. 1989;46:37–8.
91. Rosenow J, Das K, Rovit RL, Couldwell WT. Irving S. Cooper and his role in intracranial stimulation for movement disorders and epilepsy. Stereotact Funct Neurosurg. 2002;78(2):95-112.
92. Elia AE, Bagella CF, Ferre F, Zorzi G, Calandrella D, Romito LM. Deep brain stimulation for dystonia due to cerebral palsy: A review. Eur J Paediatr. 2018;22:308–15.
93. Cooperrider J, Furmaga H, Plow E, Park H-J, Chen Z, Kidd G, et al. Chronic deep cerebellar stimulation promotes long-term potentiation, microstructural plasticity, and reorganization of perilesional cortical representation in a rodent model. J Neurosci. 2014;
94. Shah AM, Ishizaka S, Cheng MY, Wang EH, Bautista AR, Levy S, et al. Optogenetic neuronal stimulation of the lateral cerebellar nucleus promotes persistent functional recovery after stroke. Sci Rep. 2017;7:46612.
95. Agnesi F, Johnson MD, Vitek JL. Deep brain stimulation. how does it work? Handb Clin Neurol. 2013;116:39-54.
96. Apps R, Hawkes R. Cerebellar cortical organization: a one-map hypothesis. Nat Rev. 2009;10:670–81.
97. White JJ, Sillitoe RV. Development of the cerebellum: From gene expression patterns to circuit maps. Wiley Interdiscip Rev Dev Biol. 2013;2(1):149-64.

98. Galanda M, Zoltan O. Motor and psychological responses to deep cerebellar stimulation in cerebral palsy (correlation with organization of cerebellum into zones). Acta Neuroschir Suppl. 1987;39:129–31.

99. Frysinger RC, Bourbonnais D, Kalaska JF, Smith AM. Cerebellar cortical activity during antagonist cocontraction and reciprocal inhibition of forearm muscles. J Neurophysiol. 1984;51:32–49.

100. Ruigrok TJH, Pijpers A, Goedknegt-Sabel E, Coulon P. Multiple cerebellar zones are involved in the control of individual muscles: A retrograde transneuronal tracing study with rabies virus in the rat. Eur J Neurosci. 2008;28(1):181-200.

101. Welsh JP, Lang EJ, Suglhara I, Llinás R. Dynamic organization of motor control within the olivocerebellar system. Nature. 1995; 374(6521):453-7.

102. Tang T, Suh CY, Blenkinsop TA, Lang EJ. Synchrony is key: Complex spike inhibition of the deep cerebellar nuclei. Cerebellum. 2016;15(1):10-3.

103. França C, de Andrade DC, Teixeira MJ, Galhardoni R, Silva V, Barbosa ER, et al. Effects of cerebellar neuromodulation in movement disorders: A systematic review. Brain Stimul. 2017;11(2):249-60.

104. Creed M, Pascoli VJ, Lüscher C. Refining deep brain stimulation to emulate optogenetic treatment of synaptic pathology. Science. 2015;347(6222):659-64.

105. Parastarfeizabadi M, Kouzani AZ, Gibson I, Tye SJ. A miniature closed-loop deep brain stimulation device. Conf Proc IEEE Eng Med Biol Soc. 2016; 2016:1786-89.

106. Edward ES, Kouzani AZ, Tye SJ. Towards miniaturized closed-loop optogenetic stimulation devices. J Neural Eng. 2018;15(2):021002.

107. Chen S, Weitemier AZ, Zeng X, He L, Wang X, Tao Y, et al. Near-infrared deep brain stimulation via upconversion nanoparticle–mediated optogenetics. Science. 2018;359(6376):679-84.

108. Plow EB, Machado A. Invasive neurostimulation in stroke rehabilitation. Neurotherapeutics. 2014;11:572–82.

109. Butler AJ, Wolf SL. Putting the brain on the map: use of transcranial magnetic stimulation to assess and induce cortical plasticity of upper-extremity movement. Phys Ther. 2007;87:719–36.

110. Di Lazzaro V, Molinari M, Restuccia D, Leggio MG, Nardone R, Fogli D, et al. Cerebro-cerebellar interactions in man: neurophysiological studies in patients with focal cerebellar lesions. Electroencephalogr Clin Neurophysiol. 1994;93:27–34.

111. Werhahn KJ, Taylor J, Ridding M, Meyer BU, Rothwell JC. Effect of transcranial magnetic stimulation over the cerebellum on the excitability of human motor cortex. Electroencephalogr Clin Neurophysiol. 1996;101:58–66.

112. Baker KB, Schuster D, Cooperrider J, Machado AG. Deep brain stimulation of the lateral cerebellar nucleus produces frequency-specific alterations in motor evoked potentials in the rat in vivo. Exp Neurol. 2010;226(2):259-64.

113. Park H-J, Furmaga H, Cooperrider J, Gale JT, Baker KB, Machado AG. Modulation of cortical motor evoked potential after stroke during electrical stimulation of the lateral cerebellar nucleus. Brain Stimul. 2015;8:1043–8.

114. Machado A, Baker KB. Upside down crossed cerebellar diaschisis: Proposing chronic stimulation of the dentatothalamocortical pathway for post-stroke motor recovery. Front Integr Neurosci. 2012;6:20.

115. Takasawa M, Watanabe M, Yamamoto S, Hoshi T, Hashikawa K, Matsumoto M, Kinoshita N. Prognostic value of subacute crossed cerebellar diaschisis: single-photon emission CT study in patients with middle cerebral artery territory infarct. AJNR Am J Neuroadiol. 2002;23:189–93.

116. Chan HH, Cooperrider J, Chen Z, Gale JT, Baker KB, Wathen CA, et al. Lateral cerebellar nucleus stimulation has selective effects on glutamatergic and GABAergic perilesional neurogenesis after cortical ischemia in the rodent model. Neurosurgery. 2017.

117. Machado AG, Baker KB, Schuster D, Butler RS, Rezai A. Chronic electrical stimulation of the contralesional lateral cerebellar nucleus enhances recovery of motor function after cerebral ischemia in rats. Brain Res. 2009;1280:107–16.

118. Machado AG, Cooperrider J, Furmaga HT, Baker KB, Park H-J, Chen Z, et al. Chronic 30-Hz deep cerebellar stimulation coupled with training enhances post-ischemia motor recovery and peri-infarct synaptophysin expression in rodents. Neurosurgery. 2013;73:344–53.

119. Chan HH, Cooperrider JL, Park H-J, Wathen CA, Gale JT, Baker KB, et al. Crossed cerebellar atrophy of the lateral cerebellar nucleus in an endothelin-1-induced, rodent model of ischemic stroke. Front Aging Neurosci. 2017;9:10.

120. Louis ED, Agnew A, Gillman A, Gerbin M, Viner AS. Estimating annual rate of decline: Prospective, longitudinal data on arm tremor severity in two groups of essential tremor cases. J Neurol Neurosurg Psychiatry. 2011;82(7):761-5.

121. Flora DE, Perera CL, Cameron AL, Maddern GJ. Deep brain stimulation for essential tremor: A systematic review. Mov. Disord. 2010;25(11):1550-9.

122. Deuschl G, Raethjen J, Hellriegel H, Elble R. Treatment of patients with essential tremor. Lancet Neurol. 2011;10(2):148-61.

123. Zesiewicz TA, Kuo SH. Essential Tremor. BMJ Clin Evid. 2015.

124. Hua SE, Lenz FA, Zirh TA, Reich SG, Dougherty PM. Thalamic neuronal activity correlated with essential tremor. J Neurol Neurosurg Psychiatry. 1998;64(2):273-6.

125. Babij R, Lee M, Cortés E, Vonsattel JPG, Faust PL, Louis ED. Purkinje cell axonal anatomy: Quantifying morphometric changes in essential tremor versus control brains. Brain. 2013;137(Pt 12):3142-8.

126. Louis ED, Lee M, Babij R, Ma K, Cortés E, Vonsattel JPG, et al. Reduced Purkinje cell dendritic arborization and loss of dendritic spines in essential tremor. Brain. 2014;

127. Choe M, Cortés E, Vonsattel JPG, Kuo SH, Faust PL, Louis ED. Purkinje cell loss in essential tremor: Random sampling quantification and nearest neighbor analysis. Mov Disord. 2016;31(3):393-401.

128. Kuo SH, Lin CY, Wang J, Sims PA, Pan MK, Liou J you, et al. Climbing fiber-Purkinje cell synaptic pathology in tremor and cerebellar degenerative diseases. Acta Neuropathol. 2017;133(1):121-38.

129. Lin CY, Louis ED, Faust PL, Koeppen AH, Vonsattel JPG, Kuo SH. Abnormal climbing fibre-Purkinje cell synaptic connections in the essential tremor cerebellum. Brain. 2014;137(Pt 12):3149-59.

130. Cheng MM, Tang G, Kuo S. Brief reports harmaline-induced tremor in mice: Videotape documentation and open questions about the model. Tremor Other Hyperkinet Mov (N Y). 2013;3:tre-03-205-4668-1.

131. Bekar L, Libionka W, Tian GF, Xu Q, Torres A, Wang X, et al. Adenosine is crucial for deep brain stimulation-mediated attenuation of tremor. Nat Med. 2008;14(1):75-80.

132 Louis ED, Lenka A. The olivary hypothesis of essential tremor: Time to lay this model to rest? Tremor Other Hyperkinet Mov (N Y). 2017;7:473.

133. Hoskovcová M, Ulmanová O, Šprdlík O, Sieger T, Nováková J, Jech R, et al. Disorders of balance and gait in essential tremor are associated with midline tremor and age. Cerebellum. 2013;12(1):27-34.

134. Louis ED, Galecki M, Rao AK. Brief reports four essential tremor cases with moderately impaired gait : How impaired can gait be in this disease? Tremor Other Hyperkinet Mov (N Y). 2013;3:tre-03-200-4597-1.

135. Reich MM, Brumberg J, Pozzi NG, Marotta G, Roothans J, Åström M, et al. Progressive gait ataxia following deep brain stimulation for essential tremor: adverse effect or lack of efficacy? Brain. 2016;139(11):2948-56.

136. Paek SB, Min HK, Kim I, Knight EJ, Baek JJ, Bieber AJ, et al. Frequency-dependent functional neuromodulatory effects on the motor network by ventral lateral thalamic deep brain stimulation in swine. Neuroimage. 2015;105:181-8.

137. Kuo SH, Lin CY, Wang J, Liou JY, Pan MK, Louis RJ, et al. Deep brain stimulation and climbing fiber synaptic pathology in essential tremor. Ann Neurol. 2016;80(3):461-5.

138. Zhang K, Bhatia S, Oh MY, Cohen D, Angle C, Whiting D. Long-term results of thalamic deep brain stimulation for essential tremor. J Neurosurg. 2010;112(6):1271-6.

139. Shih, L.C.; LaFaver, K.; Lim, C.; Papavassiliou, E.; Tarsy D. Loss of benefit in VIM thalamic deep brain stimulation (DBS) for essential tremor (ET): How prevalent is it? Park Relat Disord. 2013;19:676–9.

140. Favilla CG, Ullman D, Wagle Shukla A, Foote KD, Jacobson CE, Okun MS. Worsening essential tremor following deep brain stimulation: Disease progression versus tolerance. Brain. 2012;135(Pt 5):1455-62.

141. Xie T, Bernard J, Warnke P. Post subthalamic area deep brain stimulation for tremors: a mini-review. Transl Neurodegener. 2012;1(1):20.

142. Cagnan H, Little S, Foltynie T, Limousin P, Zrinzo L, Hariz M, et al. The nature of tremor circuits in parkinsonian and essential tremor. Brain. 2014;137(Pt 12):3223-34.

143. Cagnan H, Pedrosa D, Little S, Pogosyan A, Cheeran B, Aziz T, et al. Stimulating at the right time: Phase-specific deep brain stimulation. Brain. 2017;140:132-45.

144. Snead OC. Basic mechanisms of generalized absence seizures. Ann. Neurol. 1995;37(2):146-57.

145. Schachter SC, Shafer PO, Sirven J. What causes epilepsy and seizures? [Internet]. 2013.

146 . Englot DJ, Chang EF, Auguste KI. Vagus nerve stimulation for epilepsy: a meta-analysis of efficacy and predictors of response. J Neurosurg. 2011;115(6):1248-55.

147. Boon P, De Cock E, Mertens A, Trinka E. Neurostimulation for drug-resistant epilepsy: A systematic review of clinical evidence for efficacy, safety, contraindications and predictors for response. Curr Opin Neurol. 2018;31(2):198-210.

148. Fisher RS, Velasco AL. Electrical brain stimulation for epilepsy. Nat Publ Gr. 2014;

149. Cooke PM, Snider RS. Some cerebellar influences on electrically-induced cerebral seizures. Epilepsia. 1955; 4:19-28.

150. Ito M, Yoshida M. The origin of cerebral-induced inhibition of Deiters neurones. I. Monosynaptic initiation of the inhibitory postsynaptic potentials. Exp Brain Res. 1966;2(4):330-49.

151. Kandratavicius L, Alves Balista P, Lopes-Aguiar C, Ruggiero RN, Umeoka EH, Garcia-Cairasco N, et al. Animal models of epilepsy: Use and limitations. Neuropsychiatr Dis Treat. 2014.;10:1693-705.

152. Kros L, Eelkman Rooda OHJ, De Zeeuw CI, Hoebeek FE. Controlling cerebellar output to treat refractory epilepsy. Trends Neurosci. 2015;38(12):787-99.

153. Cooper IS, Amin I, Riklan M, Waltz JM, Poon TP. Chronic cerebellar stimulation in epilepsy. Clinical and anatomical studies. Arch Neurol. 1976;33(8):559-70.

154. Van Buren JM, Wood JH, Oakley J, Hambrecht F. Preliminary evaluation of cerebellar stimulation by double-blind stimulation and biological criteria in the treatment of epilepsy. J Neurosurg. 1978;48(3):407-16.

155. McCormick DA, Bal T. Sleep and arousal: Thalamocortical mechanisms. Annu Rev Neurosci. 1997;20:185-215.

156. Sorokin JM, Davidson TJ, Frechette E, Abramian AM, Deisseroth K, Huguenard JR, et al. Bidirectional control of generalized epilepsy networks via rapid real-time switching of firing mode. Neuron. 2017;93(1):194-210.

157. Kros L, Eelkman Rooda OHJ, Spanke JK, Alva P, Van Dongen MN, Karapatis A, et al. Cerebellar output controls generalized spike-and-wave discharge occurrence. Ann Neurol. 2015;77(6):1027-49.

158. Yizhar O, Fenno LE, Davidson TJ, Mogri M, Deisseroth K. Optogenetics in neural systems. Neuron. 2011;71(1):9-34.

159. Eelkman Rooda OHJ, Hoebeek FE. A guide to in vivo optogenetic applications for cerebellar studies. Neuromethods. 2018.

160. Person AL, Raman IM. Synchrony and neural coding in cerebellar circuits. Front Neural Circuits. 2012;6:97.

161. Krook-Magnuson E, Szabo GG, Armstrong C, Oijala M, Soltesz I. Cerebellar directed optogenetic intervention inhibits spontaneous hippocampal seizures in a mouse model of temporal lobe epilepsy. eNeuro. 2014;1(1):e2014.

162. Gornati, SV; Schaefer, CB; Zeeuw, CID; Hoebeek F. Anatomical and physiological aspects of the cerebellar impact on thalamic relay neurons. Poster Abs. San Diego: Society for Neuroscience (SfN); 2016.

163. Teune TM, Van der Burg J, Van der Moer J, Voogd J, Ruigrok T. Topography of cerebellar nuclear projections to the brain stem in the rat. Prog Brain Res. 2000;124:141–72.

164. Halassa MM, Acsády L. Thalamic inhibition: Diverse sources, diverse scales. Trends Neurosci. 2016;39(10):680-93.

165. Murphy TH, Corbett D. Plasticity during stroke recovery: from synapse to behaviour. Nat Rev Neurosci. 2009;10:861–72.

166. Carmichael ST. Plasticity of cortical projections after stroke. Neurosci. 2003;9:64–75.

167. Carmichael ST, Kathirvelu B, Schweppe C a, Nie EH. Molecular, cellular and functional events in axonal sprouting after stroke. Exp Neurol. 2017;287(Pt 3):384-94.

168. Li S, Overman JJ, Katsman D, Kozlov S V, Donnelly CJ, Twiss JL, et al. An age-related sprouting transcriptome provides molecular control of axonal sprouting after stroke. Nat Neurosci. 2010;13:1496–504.

169. Patel AR, Ritzel R, McCullough LD, Liu F. Microglia and ischemic stroke: a double-edged sword. Int J Physiol Pathophysiol Pharmacol. 2013;5:73–90.

170. Clarkson AN, Carmichael ST. Cortical excitability and post-stroke recovery. Biochem Soc Trans. 2009;37:1412–4.

171. Silasi G, Murphy TH. Stroke and the connectome: How connectivity guides therapeutic intervention. Neuron. 2014;83:1354–68.

172. Butefisch CM. Remote changes in cortical excitability after stroke. Brain. 2003;126:470–81.

173. Machado A, Baker KB. Upside down crossed cerebellar diaschisis: proposing chronic stimulation of the dentatothalamocortical pathway for post-stroke motor recovery. Front Integr Neurosci. 2012;6:20.

174. Strick PL, Dum RP, Fiez JA. Cerebellum and nonmotor function. Annu Rev Neurosci. 2009;32:413–34.

175. George PM, Steinberg GK. Novel stroke therapeutics: Unraveling stroke pathophysiology and its impact on clinical treatments. Neuron. 2015;87(2):297-309.

176. Floel A, Cohen LG. Recovery of function in humans: cortical stimulation and pharmacological treatments after stroke. Neurobiol Dis. 2010;37:243–51.

177. Schlaug G, Renga V, Nair D. Transcranial direct current stimulation in stroke recovery. Arch Neurol. 2008;65:1571–6.

178. Webster BR, Celnik PA, Cohen LG. Noninvasive brain stimulation in stroke rehabilitation. NeuroRx. 2006;3:474–81.

179. Fritsch B, Reis J, Martinowich K, Schambra HM, Ji Y, Cohen LG, et al. Direct current stimulation promotes BDNF-dependent synaptic plasticity: potential implications for motor learning. Neuron. 2010;66:198–204.

180. Gibson EM, Purger D, Mount CW, Goldstein AK, Lin GL, Wood LS, et al. Neuronal activity promotes oligodendrogenesis and adaptive myelination in the mammalian brain. Science. 2014;344(6183):1252304.

181. Cheng MY, Wang EH, Woodson WJ, Wang S, Sun G, Lee a. G, et al. Optogenetic neuronal stimulation promotes functional recovery after stroke. Proc Natl Acad Sci. 2014; 111(35):1213-8..

182. Dum RP, Strick PL. An unfolded map of the cerebellar dentate nucleus and its projections to the cerebral cortex. J Neurophysiol. 2003;89:634–9.

183. Benito E, Valor LM, Jimenez-Minchan M, Huber W, Barco a. cAMP Response Element-Binding Protein Is a Primary Hub of Activity-Driven Neuronal Gene Expression. J Neurosci. 2011;31:18237–50.

184. Schulz R, Frey BM, Koch P, Zimerman M, Bönstrup M, Feldheim J, et al. Cortico-Cerebellar Structural Connectivity Is Related to Residual Motor Output in Chronic Stroke. Cereb Cortex. 2015;27(1):635-45.

185. Teixeira MJ, Cury RG, Galhardoni R, Barboza VR, Brunoni AR, Alho E, et al. Deep brain stimulation of the dentate nucleus improves cerebellar ataxia after cerebellar stroke. Neurology. 2015;85:2075–6.

186. Grimaldi G. Deficits of limbs movements. In: Gruol, DL; Koibuchi, N; Manto, M; Molinari, M; Schmahmann, JD; Shen Y, editor. Essentials Cerebellum Cerebellar Disord. Springer Switzerland; 2016. p. 481–8.

187. Grimaldi G, Argyropoulos GP, Bastian A, Cortes M, Davis NJ, Edwards DJ, Ferrucci R, Fregni F, Galea JM, Hamada M, Manto M, Miall RC, Morales-Queza L, Pope PA, Priori A, Rothwell J, Tomlinson SP, Celnik P. Cerebellar transcranial direct current stimulation (ctdcs): a novel approach to understanding cerebellar function in health and disease. Neuroscientist. 2016;22:83–97.

188. Ferrucci R, Bocci T, Cortese F, Ruggiero F, Priori A. Noninvasive cerebellar stimulation as a complement tool to pharmacotherapy. Curr Neuropharmacol. 2017.

189. Ferrucci R, Bocci T, Cortese F, Ruggiero F, Priori A. Cerebellar transcranial direct current stimulation in neurological disease. Cerebellum & Ataxias. 2016;3(1):16.

190. Heman P, Barcia, C, Gómez A, Ros CM, Ros-Bernal F, Yuste JE, ded Pablos V, Fernandez-Villalba E Toledo-Cárdenas MR, Herrero M. Nigral degeneration correlates with persistent activation of cerebellar Purkinje cells in MPTP-treated monkeys. Histol Histopathol. 2012;27:89–94.

191. Rolland AS, Herrero MT, Garcia-Martinez V, Ruberg M, Hirsch EC, François C. Metabolic activity of cerebellar and basal ganglia-thalamic neurons is reduced in parkinsonism. Brain. 2007;130(Pt 1):265-75.

192. Yu H, Sternad D, Corcos DM, Vaillancourt DE. Role of hyperactive cerebellum and motor cortex in Parkinson's disease. Neuroimage. 2007;35(1):222-33.

193. Ugawa Y, Day BL, Rothwell JC, Thompson PD, Merton PA, Marsden CD. Modulation of motor cortical excitability by electrical stimulation over the cerebellum in man. J Physiol. 1991;

194. Ugawa Y, Uesaka Y, Terao Y, Hanajima R, Kanazawa I. Magnetic stimulation over the cerebellum in humans. Ann Neurol. 1995;37(6):703-13.

195. Galea JM, Jayaram G, Ajagbe L, Celnik P. Modulation of cerebellar excitability by polarity-specific noninvasive direct current stimulation. J Neurosci. 2009;29(28):9115-22.

196. Doeltgen SH, Young J, Bradnam LV. Anodal direct current stimulation of the cerebellum reduces cerebellar brain inhibition but does not influence afferent input from the hand or face in healthy adults. Cerebellum. 2016;15(4):466-74.

197. Poortvliet P, Hsieh B, Cresswell A, Au J, Meinzer M. Cerebellar transcranial direct current stimulation improves adaptive postural control. Clin Neurophysiol. 2018;129(1):33-41.

198. Bodranghien FCAA, Langlois Mahe M, Clément S, Manto MU. A pilot study on the effects of transcranial direct current stimulation on brain rhythms and entropy during self-paced finger movement using the epoc helmet. Front Hum Neurosci. 2017;11:201.

199. Petti M, Astolfi L, Masciullo M, Clausi S, Pichiorri F, Cincotti F, et al. Transcranial cerebellar direct current stimulation: Effects on brain resting state oscillatory and network activity. Conf Proc IEEE Eng Med Biol Soc. 2017; 2017:4359-62.

200. Bocci T, Santarcangelo E, Vannini B, Torzini A, Carli G, Ferrucci R, et al. Cerebellar direct current stimulation modulates pain perception in humans. Restor Neurol Neurosci. 2015;33(5):597-609.

201. Grimaldi G, Manto M. Anodal transcranial direct current stimulation (tDCS) decreases the amplitudes of long-latency stretch reflexes in cerebellar ataxia. Ann Biomed Eng. 2013;41(11):2437-47.

202. Grimaldi G, Oulad Ben Taib N, Manto M, Bodranghien F. Marked reduction of cerebellar deficits in upper limbs following transcranial cerebello-cerebral DC stimulation: tremor reduction and re-programming of the timing of antagonist commands. Front Syst Neurosci. 2014;8:9.

203. Bodranghien F, Oulad Ben Taib N, Van Maldergem L, Manto M. A postural tremor highly responsive to transcranial cerebello-cerebral DCS in ARCA3. Front Neurol. 2017;8:71.

204. Benussi A, Dell'Era V, Cotelli MS, Turla M, Casali C, Padovani A, et al. Long term clinical and neurophysiological effects of cerebellar transcranial direct current stimulation in patients with neurodegenerative ataxia. Brain Stimul. 2017;10(2):242-50.

205. Benussi A, Koch G, Cotelli M, Padovani A, Borroni B. Cerebellar transcranial direct current stimulation in patients with ataxia: A double-blind, randomized, sham-controlled study. Mov Disord. 2015;30(12):1701-5.

206. Shin H, Lee DK, Lee JM, Huh YE, Youn J, Louis ED, et al. Atrophy of the Cerebellar Vermis in Essential Tremor: Segmental Volumetric MRI Analysis. Cerebellum. 2016;15(2):174-81.

207. Gironell A, Martínez-Horta S, Aguilar S, Torres V, Pagonabarraga J, Pascual-Sedano B, et al. Transcranial direct current stimulation of the cerebellum in essential tremor: A controlled study. Brain Stimul. 2014;7(3):291-2.

208. Yilmaz, NH; Polat, B; Hangoglu L. Transcranial direct current stimulation in the treatment of essential tremor: an open-label study. Neurologist. 2016;21:28–9.

209. Kang N, Cauraugh JH. Does non-invasive brain stimulation reduce essential tremor? A systematic review and meta-analysis. PLoS One. 2017;12(9):e0185462.

210. Ferrucci R, Cortese F, Bianchi M, Pittera D, Turrone R, Bocci T, et al. Cerebellar and motor cortical transcranial stimulation decrease levodopa-induced dyskinesias in Parkinson's disease. Cerebellum. 2016;15(1):43-7.

211. Bradnam LV, Graetz LJ, McDonnell MN, Ridding MC. Anodal transcranial direct current stimulation to the cerebellum improves handwriting and cyclic drawing kinematics in focal hand dystonia. Front Hum Neurosci. 2015;9:286.

212. Sadnicka A, Hamada M, Bhatia KP, Rothwell JC, Edwards MJ. Cerebellar stimulation fails to modulate motor cortex plasticity in writing dystonia. Mov Disord. 2014;29(10):1304-7.

213. Monti A, Ferrucci R, Fumagalli M, Mameli F, Cogiamanian F, Ardolino G, et al. Transcranial direct current stimulation (tDCS) and language. J. Neurol. Neurosurg Psychiatry. 2013;84(8):832-42.

214. Marangolo P, Fiori V, Caltagirone C, Pisano F, Priori A. Transcranial cerebellar direct current stimulation enhances verb generation but not verb naming in poststroke Aphasia. J Cogn Neurosci. 2018;30(2):188-199.

215. Chan CY, Nicholson C. Modulation by applied electric fields of Purkinje and stellate cell activity in the isolated turtle cerebellum. J Physiol. 1986;371:89-114.

216. Hull CA, Chu Y, Thanawala M, Regehr WG. Hyperpolarization induces a long-term increase in the spontaneous firing rate of cerebellar golgi cells. J Neurosci. 2013;33(14):5895-902.

217. Bortoletto M, Pellicciari MC, Rodella C, Miniussi C. The interaction with task-induced activity is more important than polarization: A tDCS study. Brain Stimul. 2015;8(2):269-76.

218. Oulad Ben Taib N, Manto M. The in vivo reduction of afferent facilitation induced by low frequency electrical stimulation of the motor cortex is antagonized by cathodal direct current stimulation of the cerebellum. Cerebellum & Ataxias. 2016;3(1):15.

219. Ferrucci, R; Priori A. Noninvasive stimulation. In: Manto, M; Huisman T, editor. Handb lin Neurol Cerebellum Child Adults. Elsevier UK; 2018.

220. Ilg W, Bastian AJ, Boesch S, Burciu RG, Celnik P, Claaßen J, Feil K, Kalla R, Miyai I, Nachbauer W, Schöls L, Strupp M, Synofzik M, Teufel J, Timmann D. Consensus paper: management of degenerative cerebellar disorders. Cerebellum. 2014;13:248–68.

221. Ilg W, Synofzik M, Brötz D, Burkard S, Giese MA, Schöls L. Intensive coordinative training improves motor performance in degenerative cerebellar disease. Neurology. 2009;73:1823–30.

222. Burciu RG, Fritsche N, Granert O, Schmitz L, Spönemann N, Konczak J, Theysohn N, Gerwig M, van Eimeren T, Timmann D. Brain changes associated with postural training in patients with cerebellar degeneration: a voxel-based morphometry study. J Neurosci. 2013;33:4594–604.

223. Rioult-Pedotti MS, Friedman D, Donoghue J. Learning-induced LTP in neocortex. Science (80-). 2000;290:533–6.

224. Buch ER, Santarnecchi E, Antal A, Born J, Celnik PA, Classen J, Gerloff C, Hallett M, Hummel FC, Nitsche MA, Pascual-Leone A, Paulus WJ, Reis J, Robertson EM, Rothwell JC, Sandrini M, Schambra HM, Wassermann EM, Ziemann U, Cohen L. Effects of tDCS on motor learning and memory formation: A consensus and critical position paper. Clin Neurophysiol. 2017;128:589–603.

225. Nitsche MA, Schauenburg A, Lang N, Liebetanz D, Exner C, Paulus W, Tergau F. Facilitation of implicit motor learning by weak transcranial direct current stimulation of the primary motor cortex in the human. J Cogn Neurosci. 2003;15:619–26.

226. Reis J, Schambra HM, Cohen LG, Buch ER, Fritsch B, Zarahn E, Celnik PA, Krakauer J. Noninvasive cortical stimulation enhances motor skill acquisition over multiple days through an effect on consolidation. Proc Natl Acad Sci U S A. 2009;106:1590–5.

227. Galea JM, Vazquez A, Pasricha N, de Xivry JJ, Celnik P. Dissociating the roles of the cerebellum and motor cortex during adaptive learning: the motor cortex retains what the cerebellum learns. Cereb Cortex. 2011;21:1761–70.

228. Herzfeld DJ, Pastor D, Haith AM, Rossetti Y, Shadmehr R, O'Shea J. Contributions of the cerebellum and the motor cortex to acquisition and retention of motor memories. Neuroimage. 2014;98:147–58.

229. Jayaram G, Tang B, Pallegadda R, Vasudevan EV, Celnik P, Bastian A. Modulating locomotor adaptation with cerebellar stimulation. J Neurophysiol. 2012;107:2950–7.

230. Zuchowski ML, Timmann D, Gerwig M. Acquisition of conditioned eyeblink responses is modulated by cerebellar tDCS. Brain Stimul. 2014;7:525–31.

231. D'Angelo E, Mapelli L, Casellato C, Garrido JA, Luque N, Monaco J, Prestori F, Pedrocchi A, Ros E. Distributed circuit plasticity: new clues for the cerebellar mechanisms of learning. Cerebellum. 2016;15:139–51.

232. Das S, Spoor M, Sibindi TM, Holland P, Schonewille M, DeZeeuw CI, Frens MA, Donchin O. Impairment of long-term plasticity of cerebellar Purkinje cells eliminates the effect of anodal direct current stimulation on vestibulo-ocular reflex habituation. Front Neurosci. 2017;11:444.

233. Johansson, F, Carlsson, HA, Rasmussen, A, Yeo, CH, Hesslow G. Activation of a temporal memory in Purkinje cells by the mGluR7 receptor. Cell Rep. 2015;13:1741–6.

234. Gutierrez-Castellanos N, Da Silva-Matos CM, Zhou K, Canto CB, Renner MC, Koene LMC, Ozyildirim O, Sprengel R, Kessels HW, De Zeeuw C. Motor learning requires Purkinje cell synaptic potentiation through activation of AMPA-receptor subunit GluA3. Neuron. 2017;93:409–24.

235. Hulst T, John L, Küper M, van der Geest JN, Göricke SL, Donchin O, Timmann D. Cerebellar patients do not benefit from cerebellar or M1 transcranial direct current stimulation during force-field reaching adaptation. J Neurophysiol. 2017;118:732–48.

236. Jalali R, Miall RC, Galea J. No consistent effect of cerebellar transcranial direct current stimulation on visuomotor adaptation. J Neurophysiol. 2017;118:655–65.

237. Beyer L, Batsikadze G, Timmann D, Gerwig M. Cerebellar tDCS Effects on Conditioned Eyeblinks using Different Electrode Placements and Stimulation Protocols. Front Hum Neurosci. 2017;11:23.

238. Rahman, A, Toshev PK, Bikson M. Polarizing cerebellar neurons with transcranial direct current stimulation. Clin Neurophysiol. 2014;125:435–8.

239. De Zeeuw, CI, Ten Brinke M. Motor learning and the cerebellum. Cold Spring Harb Perspect Biol. 2015;7:a021683.

240. Labruna L, Jamil A, Fresnoza S, Batsikadze G, Kuo MF, Vanderschelden B, Ivry RB, Nitsche M. Efficacy of Anodal Transcranial Direct Current Stimulation is Related to Sensitivity to Transcranial Magnetic Stimulation. Brain Stimul. 2016;9:8–15.

241. Jamil A, Batsikadze G, Kuo HI, Labruna L, Hasan A, Paulus W, Nitsche M. Systematic evaluation of the impact of stimulation intensity on neuroplastic after-effects induced by transcranial direct current stimulation. J Physiol. 2017;595:1273–88.

242. Monte-Silva K, Kuo MF, Hessenthaler S, Fresnoza S, Liebetanz D, Paulus W, Nitsche M. Induction of late LTP-like plasticity in the human motor cortex by repeated non-invasive brain stimulation. Brain Stimul. 2013;6:424–32.

243. Brighina F, Romano M, Giglia G, Saia V, Puma A, Giglia F, et al. Effects of cerebellar TMS on motor cortex of patients with focal dystonia: A preliminary report. Exp Brain Res. 2009;192(4):651-6.

244. Popa T, Russo M, Meunier S. Long-lasting inhibition of cerebellar output. Brain Stimul. 2010;3(3):161-9.

245. Hamada M, Strigaro G, Murase N, Sadnicka A, Galea JM, Edwards MJ, et al. Cerebellar modulation of human associative plasticity. J Physiol. 2012;590(10):2365-74.

246. Popa T, Velayudhan B, Hubsch C, Pradeep S, Roze E, Vidailhet M, et al. Cerebellar processing of sensory inputs primes motor cortex plasticity. Cereb Cortex. 2013;23(2):205-14.

247. Quartarone A, Bagnato S, Rizzo V, Siebner HR, Dattola V, Scalfari A, et al. Abnormal associative plasticity of the human motor cortex in writer's cramp. Brain. 2003;126(Pt 12):2586-96.

248. Hubsch C, Roze E, Popa T, Russo M, Balachandran A, Pradeep S, et al. Defective cerebellar control of cortical plasticity in writer's cramp. Brain. 2013;136(Pt 7):2050-62.

249. Popa T, Hubsch C, James P, Richard A, Russo M, Pradeep S, et al. Abnormal cerebellar processing of the neck proprioceptive information drives dysfunctions in cervical dystonia. Sci Rep. 2018;8(1):2263.

250. Koch G, Porcacchia P, Ponzo V, Carrillo F, Cáceres-Redondo MT, Brusa L, et al. Effects of two weeks of cerebellar theta burst stimulation in cervical dystonia patients. Brain Stimul. 2014;7(4):564-72.

251. Bradnam L, McDonnell M, Ridding M. Cerebellar intermittent theta-burst stimulation and motor control training in individuals with cervical dystonia. Brain Sci. 2016;6(4):pii:E56.

252. Bradnam L V., Frasca J, Kimberley TJ. Direct current stimulation of primary motor cortex and cerebellum and botulinum toxin a injections in a person with cervical dystonia. Brain Stimul. 2014;7(6):909-11.

253. Hoffland BS, Kassavetis P, Bologna M, Teo JTH, Bhatia KP, Rothwell JC, et al. Cerebellum-dependent associative learning deficits in primary dystonia are normalized by rTMS and practice. Eur J Neurosci. 2013;38(1):2166-71.

254. Hoffland BS, Bologna M, Kassavetis P, Teo JTH, Rothwell JC, Yeo CH, et al. Cerebellar theta burst stimulation impairs eyeblink classical conditioning. J Physiol. 2012;590(4):887-97.

255. Linssen MW, van Gaalen J, Munneke MAM, Hoffland BS, Hulstijn W, van de Warrenburg BPC. A single session of cerebellar theta burst stimulation does not alter writing performance in writer's cramp. Brain A J Neurol. 2015;138(Pt 6):e355.

256. Bologna M, Paparella G, Fabbrini A, Leodori G, Rocchi L, Hallett M, et al. Effects of cerebellar theta-burst stimulation on arm and neck movement kinematics in patients with focal dystonia. Clin Neurophysiol. 2016;127(11):3472-9.

257. Meunier S, Popa T, Hubsch C, Roze E, Kishore A. Reply: A single session of cerebellar theta burst stimulation does not alter writing performance in writer's cramp. Brain. 2015;138(Pt 6):e356.

258. Balint B, Bhatia KP. Dystonia: An update on phenomenology, classification, pathogenesis and treatment. Curr Opin Neurol. 2014;27(4):468-76.

259. FitzGerald JJ, Rosendal F, De Pennington N, Joint C, Forrow B, Fletcher C, et al. Long-term outcome of deep brain stimulation in generalised dystonia: A series of 60 cases. J Neurol Neurosurg Psychiatry. 2014;85(12):1371-6.

260. Vidailhet M, Vercueil L, Houeto J-L, Krystkowiak P, Benabid A-L, Cornu P, et al. Bilateral deep-brain stimulation of the globus pallidus in primary generalized dystonia. N Engl J Med. 2005;352(5):459-67.

261. Peterson DA, Sejnowski TJ, Poizner H. Convergent evidence for abnormal striatal synaptic plasticity in dystonia. Neurobiol Dis. 2010;37(3):558-73.

262. Bindman LJ, Lippold OCJ, Redfearn JWT. The action of brief polarizing currents on the cerebral cortex of the rat (1) during current flow and (2) in the production of long-lasting after-effects. J Physiol. 1964;172:369-82.
263. Nitsche MA, Paulus W. Excitability changes induced in the human motor cortex by weak transcranial direct current stimulation. J Physiol. 2000;527(Pt 3):633-9.
264. Liebetanz D. Pharmacological approach to the mechanisms of transcranial DC-stimulation-induced after-effects of human motor cortex excitability. Brain. 2002;125(Pt 10):2238-47.
265. Stagg CJ, Best JG, Stephenson MC, O'Shea J, Wylezinska M, Kincses ZT, et al. Polarity-Sensitive modulation of cortical neurotransmitters by transcranial stimulation. J Neurosci. 2009;29(16):5202-6.
266. Nitsche MA, Fricke K, Henschke U, Schlitterlau A, Liebetanz D, Lang N, et al. Pharmacological modulation of cortical excitability shifts induced by transcranial direct current stimulation in humans. J Physiol. 2003;553(Pt 1):293-301.
267. Yeo CH, Hesslow G. Cerebellum and conditioned reflexes. Trends Cogn Sci. 1998;2(9):322-30.
268. Stefan K, Kunesch E, Benecke R, Cohen LG, Classen J. Mechanisms of enhancement of human motor cortex excitability induced by interventional paired associative stimulation. J Physiol. 2002;543(Pt 2):699-708.
269. Parazzini M, Rossi E, Ferrucci R, Liorni I, Priori A, Ravazzani P. Modelling the electric field and the current density generated by cerebellar transcranial DC stimulation in humans. Clin Neurophysiol. 2014;125(3):577-84.
270. Bikson M, name A, Rahman A. Origins of specificity during tDCS: anatomical, activity-selective, and input-bias mechanisms. Front Hum Neurosci. 2013;7:688.
271. Cantarero G, Spampinato D, Reis J, Ajagbe L, Thompson T, Kulkarni K, et al. Cerebellar direct current stimulation enhances on-line motor skill acquisition through an effect on accuracy. J Neurosci. 2015;35(7):3285-90.
272. Wessel MJ, Zimerman M, Timmermann JE, Heise KF, Gerloff C, Hummel FC. Enhancing consolidation of a new temporal motor skill by cerebellar noninvasive stimulation. Cereb Cortex. 2016;26(4):1660-7.
273. John L, Küper M, Hulst T, Timmann D, Hermsdörfer J. Effects of transcranial direct current stimulation on grip force control in patients with cerebellar degeneration. Cerebellum & Ataxias. 2017;4:15.
274. Tedesco AM, Chiricozzi FR, Clausi S, Lupo M, Molinari M, Leggio MG. The cerebellar cognitive profile. Brain. 2011;134(Pt 12):3672-86.
275. Turkeltaub PE, Swears MK, D'Mello AM, Stoodley CJ. Cerebellar tDCS as a novel treatment for aphasia? Evidence from behavioral and resting-state functional connectivity data in healthy adults. Restor Neurol Neurosci. 2016;34(4):491-505.
276. Pereira M, Rafiq B, Chowdhury E, Babayev J, Boo HJ, Metwaly R, et al. Anodal cerebellar tDCS modulates lower extremity pain perception. NeuroRehabilitation. 2017;40(2):195-200.
277. Verhage MC, Avila EO, Frens MA, Donchin O, van der Geest JN. Cerebellar tDCS does not enhance performance in an implicit categorization learning task. Front Psychol. 2017;8:476.
278. Van Wessel BWV, Claire Verhage M, Holland P, Frens MA, Van Der Geest JN. Cerebellar tDCS does not affect performance in the N-back task. J Clin Exp Neuropsychol. 2016;38(3):319-26.
279. Oldrati V, Schutter DJLG. Targeting the human cerebellum with transcranial direct current stimulation to modulate behavior: a meta-analysis. Cerebellum. 2017;17(2):228-36.

280. Bikson M, Grossman P, Thomas C, Zannou AL, Jiang J, Adnan T, et al. Safety of transcranial direct current stimulation: Evidence based update 2016. Brain Stimul. 2016;10(5):983-5.

281. Brunoni AR, Amadera J, Berbel B, Volz MS, Rizzerio BG, Fregni F. A systematic review on reporting and assessment of adverse effects associated with transcranial direct current stimulation. Int J Psychophysiol. 2011;14(8):1133-45.

282. Charvet L, Shaw M, Dobbs B, Frontario A, Sherman K, Bikson M, et al. Remotely supervised transcranial direct current stimulation increases the benefit of at-home cognitive training in multiple sclerosis. Neuromodulation. 2017;21(4):383-9.

283. Eccles JC, Ito M, Szentagothai J. The cerebellum as a neuronal machine. Berlin: Springer; 1967.

284. Granit R, Phillips CG. Excitatory and inhibitory processes acting upon individual Purkinje cells of the cerebellum in cats. J Physiol. 1956;133(3):520-47.

285. Eccles JC, Llinás R, Sasaki K. Parallel fibre stimulation and the responses induced thereby in the Purkinje cells of the cerebellum. Exp Brain Res. 1966;1(1):17-39.

286. Elias SA, Yae H, Ebner TJ. Optical imaging of parallel fiber activation in the rat cerebellar cortex: Spatial effects of excitatory amino acids. Neuroscience. 1993;52(4):771-86.

287. Vranesic I, Iijima T, Ichikawa M, Matsumoto G, Knöpfel T. Signal transmission in the parallel fiber-Purkinje cell system visualized by high-resolution imaging. Proc Natl Acad Sci U S A. 1994;91(26):13014-7.

288. Heck D. Sequential stimulation of guinea pig cerebellar cortex in vitro strongly affects Purkinje cells via parallel fibers. Naturwissenschaften. 1995;82(4):201-3.

289. Koella W. Motor effects from electrical stimulation of the basal cerebellum in unrestrained cat. J Neurophysiol. 1955;18:559–73.

290. Ball GG, Micco DJ, Berntson GG. Cerebellar stimulation in the rat: Complex stimulation-bound oral behaviors and self-stimulation. Physiol Behav. 1974;13(1):123-7.

291. Cohen B, Goto, K, Schanzer S, Weiss A. Eye movements induced by electrical stimulation of the cerebellum in the alert cat. Exp Neurol. 1965;13:145–62.

292. Ron S, Robinson D. Eye movements evoked by cerebellar stimulation in the alert monkey. J Neurophysiol. 1973;36:1004–22.

293. Godschalk M, Van der Burg J, Van Duin B, De Zeeuw CI. Topography of saccadic eye movements evoked by microstimulation in rabbit cerebellar vermis. J Physiol. 1994;480(Pt 1):147-53.

294. Noda H, Fujikado T. Topography of the oculomotor area of the cerebellar vermis in macaques as determined by microstimulation. J Neurophysiol. 1987;58(2):359-78.

295. Cooper IS, Amin I, Gilman S. The effect of chronic cerebellar stimulation upon epilepsy in man. Trans Am Neurol Assoc. 1973;98:192–6.

296. Cooper IS. Effect of chronic stimulation of anterior cerebellum on neurological disease. Lancet. 1973;1(7796):206.

297. Davis R, Emmonds SE. Cerebellar stimulation for seizure control: 17-year study. Stereotact Funct Neurosurg. 1992;118(4):477-88.

298. Nowak LG, Bullier J. Axons, but not cell bodies, are activated by electrical stimulation in cortical gray matter. I. Evidence from chronaxie measurements. Exp Brain Res. 1998;

299. Nowak LG, Bullier J. Axons, but not cell bodies, are activated by electrical stimulation in cortical gray matter. II. Evidence from selective inactivation of cell bodies and axon initial segments. Exp Brain Res. 1998;118(4):489-500.

300. Heck DH, Thach WT, Keating JG. On-beam synchrony in the cerebellum as the mechanism for the timing and coordination of movement. Proc Natl Acad Sci. 2007;104(18):7658-63.
301. Thach WT. Discharge cerebellar neurons related to two maintained postures and two prompt movements. II Purkinje cell output and input. J Neurophysiol. 1970;33(4):537-47.
302. Holmes G. The symptoms of acute cerebellar injuries due to gunshot injuries. Brain. 1917;
303. Voogd J, Barmack NH. Oculomotor cerebellum. Prog. Brain Res. 2005;151:231-68.
304. Wright GDS, McLellan DL, Brice JG. A double-blind trial of chronic cerebellar stimulation in twelve patients with severe epilepsy. J Neurol Neurosurg Psychiatry. 1984;47(8):769-74.
305. Braitenberg V, Heck D, Sultan F, Arbid MA, Spoelstra J, Bjaalie JG, et al. The detection and generation of sequences as a key to cerebellar function: Experiments and theory. Behav Brain Sci. 1997;20(2):229-45.
306. Adamantidis A, Arber S, Bains JS, Bamberg E, Bonci A, Buzsáki G, et al. Optogenetics: 10 years after ChR2 in neurons—views from the community. Nat Neurosci. 2015;18(9):1202-12.
307. Ito M. The cerebellum: Brain for an implicit self. FT Press; 2012.
308. Monzee J. Responses of cerebellar interpositus neurons to predictable perturbations applied to an object held in a precision grip. J Neurophysiol. 2003;91(3):1230-9.
309. Allen GI, Tsukahara N. Cerebrocerebellar communication systems. Physiol Rev. 1974;54(4):957-1006.
310. Ikeda A, Shibasaki H, Nagamine T, Terada K, Kaji R, Fukuyama H, et al. Dissociation between contingent negative variation and Bereitschaftspotential in a patient with cerebellar efferent lesion. Electroencephalogr Clin Neurophysiol. 1994;90(5):359-64.
311. Nagai Y, Critchley HD, Featherstone E, Fenwick PBC, Trimble MR, Dolan RJ. Brain activity relating to the contingent negative variation: An fMRI investigation. Neuroimage. 2004;21(4):1232-41.
312. Ashmore RC, Sommer MA. Delay activity of saccade-related neurons in the caudal dentate nucleus of the macaque cerebellum. J Neurophysiol. 2013;109(8):2129-44.
313. Ohmae S, Kunimatsu J, Tanaka M. Cerebellar roles in self-timing for sub- and supra-second intervals. J Neurosci. 2017;27(44):3511-22.
314. Tanaka M. Cognitive signals in the primate motor thalamus predict saccade timing. J Neurosci. 2007;27(44):12109-18.
315. Tanaka M. Inactivation of the central thalamus delays self-timed saccades. Nat Neurosci. 2006;9(1):20-2.
316. Bellebaum C, Daum I, Suchan B. Mechanisms of cerebellar contributions to cognition in humans. Wiley Interdiscip Rev Cogn Sci. 2012;3(2):171-84.
317. Peterburs J, Gajda K, Koch B, Schwarz M, Hoffmann KP, Daum I, et al. Cerebellar lesions alter performance monitoring on the antisaccade task-An event-related potentials study. Neuropsychologia. 2012;50(3):379-89.
318. Peterburs J, Thürling M, Rustemeier M, Göricke S, Suchan B, Timmann D, et al. A cerebellar role in performance monitoring - Evidence from EEG and voxel-based morphometry in patients with cerebellar degenerative disease. Neuropsychologia. 2015;68:1390-47.
319. Ide JS, Li C, Shan R. A cerebellar thalamic cortical circuit for error-related cognitive control. Neuroimage. 2011;54(1):455-64.
320. Kunimatsu J, Suzuki TW, Tanaka M. Implications of lateral Ccrebellum in proactive control of saccades. J Neurosci. 2016;36(26):7066-74.

321. Wessel JR, Aron AR. On the globality of motor suppression: Unexpected events and their influence on behavior and cognition. Neuron. 2017;93(2):259-80.

322. Stoodley CJ, Schmahmann JD. Evidence for topographic organization in the cerebellum of motor control versus cognitive and affective processing. Cortex. 2010;46(7):831-44.

323. Cerminara NL, Apps R, Marple-horvat DE. An internal model of a moving visual target in the lateral cerebellum. J Physiol. 2009;587(2):429-42.

324. Ohmae S, Uematsu A, Tanaka M. Temporally Specific Sensory Signals for the Detection of Stimulus Omission in the Primate Deep Cerebellar Nuclei. J Neurosci. 2013;33(39):15432-41.

325. Uematsu A, Ohmae S, Tanaka M. Facilitation of temporal prediction by electrical stimulation to the primate cerebellar nuclei. Neuroscience. 2017;346:190-6.

326. Ohmae S, Tanaka M. Two different mechanisms for the detection of stimulus omission. Sci Rep. 2016;6:20615.

327. Fujioka T, Trainor LJ, Large EW, Ross B. Internalized timing of iochronous sounds is represented in neuromagnetic beta oscillations. J Neurosci. 2012;32(5):1791-802.

328. Roth MJ, Synofzik M, Lindner A. The cerebellum optimizes perceptual predictions about external sensory events. Curr Biol. 2013;23(10):930-5.

329. Narain D, Remington ED, Zeeuw CID, Jazayeri M. A cerebellar mechanism for learning prior distributions of time intervals. Nat Commun. 2018;9(1):469.

330. Meissner W, Harnack D, Paul G, Reum T, Sohr R, Morgenstern R, et al. Deep brain stimulation of subthalamic neurons increases striatal dopamine metabolism and induces contralateral circling in freely moving 6-hydroxydopamine-lesioned rats. Neurosci Lett. 2002;328(2):105-8.

331. He Z, Jiang Y, Xu H, Jiang H, Jia W, Sun P, et al. High frequency stimulation of subthalamic nucleus results in behavioral recovery by increasing striatal dopamine release in 6-hydroxydopamine lesioned rat. Behav Brain Res. 2014;263:108-14.

332. Jin D, Muramatsu SI, Shimizu N, Yokoyama S, Hirai H, Yamada K, et al. Dopamine release via the vacuolar ATPase V0 sector c-subunit, confirmed in N18 neuroblastoma cells, results in behavioral recovery in hemiparkinsonian mice. Neurochem Int. 2012;61(6):907-12.

333. Hilker R, Voges J, Ghaemi M, Lehrke R, Rudolf J, Koulousakis A, et al. Deep brain stimulation of the subthalamic nucleus does not increase the striatal dopamine concentration in parkinsonian humans. Mov Disord. 2003;18(1):41-8.

334. Navailles S, Benazzouz A, Bioulac B, Gross C, De Deurwaerdère P, De Deurwaerdere P, et al. High-frequency stimulation of the subthalamic nucleus and L-3,4-dihydroxyphenylalanine inhibit in vivo serotonin release in the prefrontal cortex and hippocampus in a rat model of Parkinson's disease. J Neurosci. 2010;30(6):2356-64.

335. Stefurak T, Mikulis D, Mayberg H, Lang AE, Hevenor S, Pahapill P, et al. Deep brain stimulation for Parkinson's disease dissociates mood and motor circuits: A functional MRI case study. Mov Disord. 2003;18(12):1508-16.

336. Ng KL, Gibson EM, Hubbard R, Yang J, Caffo B, O'Brien RJ, et al. Fluoxetine maintains a state of heightened responsiveness to motor training early after stroke in a mouse model. Stroke. 2015;46(10):2951-60.

337. Pohodich AE, Yalamanchili H, Raman AT, Wan YW, Gundry M, Hao S, et al. Forniceal deep brain stimulation induces gene expression and splicing changes that promote neurogenesis and plasticity. Elife. 2018;7:e304301.

338. Hao S, Tang B, Wu Z, Ure K, Sun Y, Tao H, et al. Forniceal deep brain stimulation rescues hippocampal memory in Rett syndrome mice. Nature. 2015;107(15):7054-9.

339. Shirvalkar PR, Rapp PR, Shapiro ML. Bidirectional changes to hippocampal theta-gamma comodulation predict memory for recent spatial episodes. Proc Natl Acad Sci. 2010;
340. Morimoto J, Yasuhara T, Kameda M, Umakoshi M, Kin I, Kuwahara K, et al. Electrical stimulation enhances migratory ability of transplanted bone marrow stromal cells in a rodent ischemic stroke model. Cell Physiol Biochem. 2018;46(1):57-68.
341. Morshead, C, Popovic, MR, Babona-Pilipos R. Selective, directable electrotaxis of precursor cells with biphasic electrical stimulation. 2018.
342. Thrivikraman G, Boda SK, Basu B. Unraveling the mechanistic effects of electric field stimulation towards directing stem cell fate and function: A tissue engineering perspective. Biomaterials. 2018;150:60-98.
343. Perlmutter JS, Mink JW, Bastian AJ, Zackowski K, Hershey T, Miyawaki E, et al. Blood flow responses to deep brain stimulation of thalamus. Neurology. 2002;58(9):1388-94.
344. Nieoullon A, Cheramy A, Glowinski J. Release of dopamine in both caudate nuclei and both substantia nigrae in response to unilateral stimulation of cerebellar nuclei in the cat. Brain Res. 1978;148(1):143-52.
345. Nakai M, Iadecola C, Ruggiero DA, Tucker LW, Reis DJ. Electrical stimulation of cerebellar fastigial nucleus increases cerebral cortical blood flow without change in local metabolism: Evidence for an intrinsic system in brain for primary vasodilation. Brain Res. 1983;260(1):35-49.
346. Akgören N, Fabricius M, Lauritzen M. Importance of nitric oxide for local increases of blood flow in rat cerebellar cortex during electrical stimulation. Proc Natl Acad Sci U S A. 1994;91(13):5903-7.
347. Demirtas-Tatlidede A, Freitas C, Cromer JR, Safar L, Ongur D, Stone WS, et al. Safety and proof of principle study of cerebellar vermal theta burst stimulation in refractory schizophrenia. Schizophr Res. 2010;124(1-3):91-100.
348. Parker KL, Kim YC, Kelley RM, Nessler AJ, Chen K-H, Muller-Ewald VA, et al. Delta-frequency stimulation of cerebellar projections can compensate for schizophrenia-related medial frontal dysfunction. Mol Psychiatry. Nature. 2017;22(5):647-55.
349. Reis DJ, Doba N, Nathan MA. Predatory attack, grooming, and consummatory behaviors evoked by electrical stimulation of cat cerebellar nuclei. Science. 1973;182(4114):845-7.
350. Polikov VS, Tresco PA, Reichert WM. Response of brain tissue to chronically implanted neural electrodes. J Neurosci Methods. 2005;148(1):1-18.
351. Liao, E, Lin, Y, Huang, C, Tang, N, Hsieh C. Electric stimulation of ear reduces the effect of Toll-Like Receptor 4 signaling pathway on kainic acid-Induced epileptic seizures in rats. Biomed Res Int. 2018;2018: 5497256.
352. Tolias AS, Sultan F, Augath M, Oeltermann A, Tehovnik EJ, Schiller PH, et al. Mapping cortical activity elicited with electrical microstimulation using fMRI in the macaque. Neuron. 2005;48(6):901-11.
353. Herrington TM, Cheng JJ, Eskandar EN. Mechanisms of deep brain stimulation. J Neurophysiol. 2016;115(1):19-38.
354. Edamakanti CR, DO J, Didonna A, Martina M, Opal P. Mutant ataxin1 disrupts cerebellar development in spinocerebellar ataxia type 1. J Clin Invest. 2018;128:2252–65.
355. Lüscher C. Dark past of deep-brain stimulation. Nature. 2018;555:306–7.
356. Heath RG. Modulation of emotion with a brain pacemamer. Treatment for intractable psychiatric illness. J Nerv Ment Dis. 1977; 165:300-17.
357. Correa AJ, Llewellyn RC, Epps J, Jarrott D, Eiswirth C, Heath RG.Chronic cerebellar stimulation in the modulation of behavior. Acta Neurol Latinoam. 1980;26:143-53.

“Und meine Seele spannte

Weit ihre Flügel aus

Flog durch die stillen Lande

Als flöge sie nach Haus”

Mondnacht – Eichendorff

Chapter 7

General discussion

Neurons exchange signals through synapses that build up the networks, such as the cerebello-thalamic-cortical loop, in the brain. Understanding the structural and functional connectivity of synapses is one of the fundamental goals of neuroscience. So far, only few studies have addressed the basic anatomical description and systemic function of the cerebello-thalamic connection (CN-TC).

The aim of this thesis was to characterize the structural and functional properties of the CN-TC in young and adult mouse brain and to establish the cerebellar impact on the thalamus in epilepsy mouse models. In the interest of describing the detailed properties of CN-TC connection we used different tools, like optogenetics, transgenic mice and electrophysiology to unravel how the cerebellar nuclei connect to thalamic cells and what the impact is in the normal, healthy mouse brain (***Chapter 4***) and in disease (***Chapter 5***). Moreover, we wanted to investigate the building blocks studying the onset of the anatomical connection (***Chapter 2***) and recording the electrophysiological properties of cerebellar nuclei that contain the neurons which synapse in the thalamus, during various developmental stages (***Chapter 3***)**.** Moreover, we also investigated whether the Zebrin identity, and thus the location, of Purkinje cells, co-determined the firing pattern of thalamus-projecting CN neurons.

Cerebellar synaptic transfer mode

CN neurons, the output of the cerebellum, need to integrate several inputs coming from diverse sources. In the mouse brain the inhibitory input from PCs [1, 2] converges onto CN neurons with an estimated ratio of ~50 controlling the CN firing pattern most effectively in conditions of high PC synchronicity [3]. Also mossy and climbing fiber collaterals project to CN neurons. Although quantitative anatomical data is absent, these projections are thought to diverge and evoke excitatory responses that also contribute to CN action potential firing [4-6]. Tracing studies in cats showed that half of the axons originating from pontine nuclei send collateral branches terminating in the dentate nucleus [7], which indicates that 50% of mossy fibers provide excitatory inputs to CN and thus in principle compete with the inhibitory inputs from PCs (figure 1). Moreover there is a connection between the cerebellum and inferior olive as each PC receives a powerful excitatory climbing fiber input from a single inferior olive neuron.

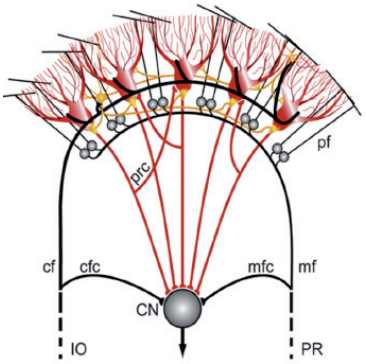

Figure 1 Scheme of connection in the cerebellum. The cerebellar cortex receives main excitatory inputs (black) from the inferior olive (IO) and pontine regions (PR) and provides via the Purkinje cell axons an inhibitory feedback (red) to the CN. Whereas the external IO and PR signals, which enter the cerebellum via the climbing fibers (cf) and the mossy fiber (mf)–parallel fiber (pf) pathway, are all excitatory, the local transmissions by the axons of the molecular layer interneurons (yellow) and recurrent collaterals (prc) of the Purkinje cells (red) are all inhibitory. mfc, Mossy fiber collaterals; cfc, climbing fiber collaterals. The local Golgi cell inhibition of granule cells (GC) is not depicted in this drawing. Adapted from Heck et al. 2013

The olivary-cortico-nuclear circuit is organized in distinct modules based on the expression of Zebrin [8]. Recent evidence indicates that PCs within the same module operate around a preferred range of intrinsically determined simple spike firing frequencies: 60 Hz for Zebrin-positive and 90 Hz for Zebrin-negative [9]. Several hypotheses have been suggested to account for the possible modes of information transfer under a regime of high inhibitory input [3, 10, 11]. One is the "synchrony coding" theory, which states that the synchronized inhibition of the PCs is phase-locking the spiking activity of the glutamatergic cells [3, 12]. On the other hand there is the "rebound spike" hypothesis, which states that the glutamatergic cells encodes the pauses of Purkinje cell activity in which hyperpolarization is released from the target cell, and this release is causing the cell to fire a burst of spikes [12, 13]. According to the "rebound spike" theory we would expect CN neurons of Zebrin-negative domain to fire less action potential as the firing frequency of PCs cells is very high and the CV is lower than in PC Zebrin-negative [9]. These firing patterns do not seem to give the opportunity to CN neurons to have a pause sufficiently long to fire a burst of spikes by activation of Ih, IT and INaP currents [12, 14, 15]. However the higher variability of the Zebrin-positive PCs' simple spike firing combined with the lower firing frequency suggests that the firing pattern is more irregular and possibly less synchronized. This could explain why we observed a lower FF in the Zebrin-positive CNs. Thus, because the

different firing pattern of Purkinje cells of different olivocerebellar modules appear to engage different CN spike activity, it seems that PCs have diverse encoding strategies dedicated for the type of behaviour they control.

It is known that CN axons are branching in diverse thalamic region, which in turn send projections to cortical areas involved in various behaviour, such as motor control, motor learning and cognitive functions (chapter 4). Of note is that it has not been proven that the nuclei receiving inhibition from Zebrin-positive or Zebrin-negative also have a preferred target in thalamus; because of the tendency of the paired-pulse depression at the CN-TC synapse upon repetitive light stimuli (chapter 4) and the fact that Zebrin-negative CN cells fire at higher frequencies than Zebrin-positive CN cells indicates that neurotransmission from Zebrin-positive CN neurons on their thalamic target neurons might be more resilient against depletion. Therefore the impact CN neurons might have on thalamic nuclei of different areas depends on their anatomical location and could even be decisive on the information transmitted to thalamocortical neurons. So it will be of interest to discern in the future, with dedicated anatomical experiments, if CN connected by PCs of different modules also project to dedicated thalamic nuclei.

Why only motor?

The cerebellar role in motor function is well recognized and recent experimental evidence, which was pioneered by Jeremy Schmahmann [16] and others, uncovered the connection between cerebellar functioning and cognitive processes, such as emotions, working memory and attention [17-19].

In general motor and cognitive functions have been viewed as independent phenomena, but they might be much more interrelated than has been previously appreciated. There is no doubt on the role of cerebellum in motor leaning [20], but in addition to that hallmark feature, several lines of evidence indicate that the mammalian cerebellum is participating in non-motor functions that are also encoded by the prefrontal cortex[21]. It has been found through neuroimaging studies that when a cognitive task increases activation in dorsolateral prefrontal cortex, it also increases activation in the contralateral cerebellum [22]. Unsurprisingly, perturbations in the correct development of the cerebellum lead also to deficits that spread to non-motor functions[23].

Lesions in adult showed a deficit in cognitive tasks [24] and children who suffered from congenital cerebellar malformations (such as Joubert syndrome) in addition to motor problems display marked cognitive defects [25, 26]. Emerging data show that neurodevelopmental disorders like autism spectrum disorders (ASD) are linked to

synaptic dysfunctional networks [27, 28]; in mutant mice that are characterized by impaired function of the postsynaptic scaffolding protein *Shank2* in cerebellar cortex social interaction deficits have been described, supporting a non-motor function of the cerebellum [29].

Perturbation during development might lead to abnormalities in the brain structure. Data gathered in mice indicate that there are critical periods in which disruption of the thalamic activity decreased the size of the correlated cortical area [30]. These findings suggest 'normal' thalamic activity is required for expansion of the cerebral cortex. In chapter 2 we investigated when the cerebello-thalamic connection is formed. Our findings suggest that there might be two different time points at which cerebellar defects could cause thalamo-cortical abnormalities, when it enters ventral thalamus (at 15.5E) and when it goes to dorsal thalamus (at 17.5). It has been shown in mice that a part of the ventral thalamus, zona incerta (ZI), when silenced, it leads to decreased synaptic activity and apical dendritic complexity of cortical neurons [31], suggesting that GABAergic projection from the ZI to cortex is essential for proper development of cortical neurons. A similar effect was shown for thalamus-barrel cortex connectivity [30], which together with the previously mentioned findings seems to indicate that it is fundamental for the normal development of thalamo-cortical networks that the neuronal activity of thalamic neurons remains undisturbed as long the axonal connections have not been completed. Cerebellar fibers are projecting both to ZI and the other nuclei of dorsal thalamus, suggesting that once these cerebellar efferents reach these target neurons they can contribute to the correct activity of thalamic and incertal neurons and thus to the proper development of their cortical targets. As shown in chapter 4, the cerebello-thalamic connection spreads to different thalamic regions affecting also areas of the cortex that are not only related to motor activity. If during invasion of the cerebellar fibers in the thalamus, the CN cells change their activity, as the correct axon growth depends on cAMP signalling and calcium influx [32], and/or target this might lead also to abnormal development of the thalamo-cortical connection also in brain areas like the prefrontal cortex increasing the chances to progress cognitive deficits.

The ventrolateral and ventromedial nuclei of the thalamus, both related to the execution and planning of motor activity, are the ones that already at E18.5 (as shown in chapter 2) receive the most of the innervation from cerebellum. However, also intralaminar nuclei receive a remarkable number of fibers in adult brain of many animal species [33-35]. So, however, we have to acknowledge that the main role of cerebellum can still be in motor function, there are evidences that the role that it plays in higher functions is of relevance.

The (strong) impact of cerebellum on thalamus

Information that has been processed by the cerebellum can end up in the thalamic complex (figure 2) and thereby reach various cerebral cortical regions. This information is spread divergently to more than one region broadening the effect that it might have on cortical activity. Taking advantage of optogenetic tools that allow us to label and activate specific cell populations in specific CNS structures [36], in chapter 4 we investigated the impact of cerebellum on thalamic nuclei related to motor function (VL and VM) and intralaminar nuclei (CL).

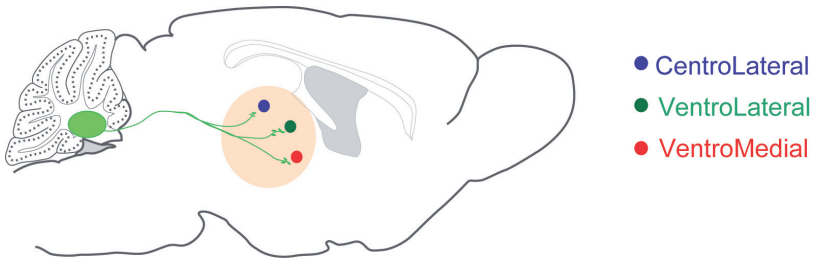

Figure 2. Schematic of cerebellar nuclei (green) innervation to dorsal thalamus (orange)

The difference in the amplitude of the evoked response suggested that the information destined for the motor thalamus (VL nucleus) needs to arrive at the target with millisecond precision and be faithfully transmitted to motor cortex. However the message passing through the intralaminar nucleus CL is smaller compared to the "main" in the motor thalamic regions, suggesting a differential impact on the cortical areas innervated by CL thalamocortical neurons. It seems plausible that the message passing through the thalamus to motor cortex could send smaller "copies " of the main message to keep higher cortical areas informed of such commands. For the cerebellar output CL seems a relevant target to get this information as for its nature, its axons diverge to many cortical areas like parietal, frontal and striatum. The connection to the striatum is also of interest, because it has been shown that cerebellar activation in mice altered the activity of striatal neurons facilitating optimal motor control [37].

This broad impact might also explain why, as seen in chapter 5, optogenetic stimulation of cerebellar terminals in thalamus could re-establish physiological thalamo-cortical network in epileptic mice. The tottering mouse phenotype is due to a mutation in the gene that encodes the Cav2.1 (P/Q-type) Ca2+ channels, which are

important for initiating synaptic transmission at most synapses formed by neurons of the mammalian central nervous system [38]. Previous studies reported that *tg* mice have impaired inhibition of thalamo-cortical cells on layer 4 pyramidal neurons [39] and impaired EPSC amplitude in VB thalamic cells upon current injection [40]. These data support the idea that both inhibitory and excitatory transmission in the thalamo-cortical networks are reduced, which could lead to pathological oscillations [41]. Thalamic cells receive, beside cortical and subcortical inputs, also inhibitory inputs from reticular nuclei. All these inputs together defines the state of the thalamic cell that upon a sudden, synchronized excitation (coming from CN) can trigger an action potential, as in the case of the potent CN-VL transmission, or a subthreshold membrane depolarization that stops oscillatory activity, as in the case of CN-VM and CN-CL transmission – both these may contribute to the eventual stop of absence seizures following single-pulse CN stimulation. Yet, since we were not able yet to investigate the impact of the tg CaV2.1 mutation, it would be of interest to dedicate a set of experiments to investigate whether CN terminals release properties, like release probability, are affected by the gene mutation and whether compensatory mechanisms, such as the upregulation of other calcium channels (N-type) [42] are at work. It is possible that although the channel composition is different, the thalamic neurons will take advantage of the summation of the input coming from synchronized cerebellar terminals to overcome the lower release probability.

To conclude, more experiments need to be performed *in vivo* to investigate in wild type animals how optogenetic stimulation of cerebellum can affect thalamic activity and behaviour. So far, the efforts in the neuroscience field [43, 44], appear too limited to make any strong statement about the different functions that the cerebellar output can have in thalamo-cortical networks. For these reasons we need to explore through behavioural tasks to test either attention, learning and memory and social behaviour, if enhancing CN output through optogentic stimulation can show significant influence on the performance. Moreover it will be worth to perturb the CN afferents during different stages in the development to investigate the impact on the cerebello-thalamo-cortical loop. In light of the cerebellar role in several neurodevelopmental disorders, it is of great interest to unravel which cerebellar and thalamic nuclei are prone to lead to specific pathological conditions and if there are sensitive time points in which restoring or helping the correct development of these fibers can prevent the onset of the disease.

References

1. Ito, M., M. Yoshida, and K. Obata, *Monosynaptic inhibition of the intracerebellar nuclei induced rom the cerebellar cortex*. Experientia, 1964. 20(10): p. 575-6.
2. Ito, M. and M. Yoshida, *The cerebellar-evoked monosynaptic inhibition of Deiters' neurones*. Experientia, 1964. 20(9): p. 515-6.
3. Person, A.L. and I.M. Raman, *Purkinje neuron synchrony elicits time-locked spiking in the cerebellar nuclei*. Nature, 2011. 481(7382): p. 502-5.
4. Wiklund, L., G. Toggenburger, and M. Cuenod, *Selective retrograde labelling of the rat olivocerebellar climbing fiber system with D-[3H]aspartate*. Neuroscience, 1984. 13(2): p. 441-68.
5. De Zeeuw, C.I., et al., *Climbing fibre collaterals contact neurons in the cerebellar nuclei that provide a GABAergic feedback to the inferior olive*. Neuroscience, 1997. 80(4): p. 981-6.
6. Najac, M. and I.M. Raman, *Synaptic excitation by climbing fibre collaterals in the cerebellar nuclei of juvenile and adult mice*. J Physiol, 2017. 595(21): p. 6703-6718.
7. Shinoda, Y., et al., *Axon collaterals of mossy fibers from the pontine nucleus in the cerebellar dentate nucleus*. J Neurophysiol, 1992. 67(3): p. 547-60.
8. Sugihara, I. and P.N. Quy, *Identification of aldolase C compartments in the mouse cerebellar cortex by olivocerebellar labeling*. J Comp Neurol, 2007. 500(6): p. 1076-92.
9. Zhou, H., et al., *Cerebellar modules operate at different frequencies*. Elife, 2014. 3: p. e02536.
10. Sudhakar, S.K., B. Torben-Nielsen, and E. De Schutter, *Cerebellar Nuclear Neurons Use Time and Rate Coding to Transmit Purkinje Neuron Pauses*. PLoS Comput Biol, 2015. 11(12): p. e1004641.
11. Uusisaari, M. and E. De Schutter, *The mysterious microcircuitry of the cerebellar nuclei*. J Physiol, 2011. 589(Pt 14): p. 3441-57.
12. Steuber, V., et al., *Determinants of synaptic integration and heterogeneity in rebound firing explored with data-driven models of deep cerebellar nucleus cells*. J Comput Neurosci, 2011. 30(3): p. 633-58.
13. Witter, L., et al., *Strength and timing of motor responses mediated by rebound firing in the cerebellar nuclei after Purkinje cell activation*. Front Neural Circuits, 2013. 7: p. 133.
14. Engbers, J.D., et al., *Signal processing by T-type calcium channel interactions in the cerebellum*. Front Cell Neurosci, 2013. 7: p. 230.
15. Tadayonnejad, R., et al., *Rebound discharge in deep cerebellar nuclear neurons in vitro*. Cerebellum, 2010. 9(3): p. 352-74.
16. Schmahmann, J.D. and J.C. Sherman, *Cerebellar cognitive affective syndrome*. Int Rev Neurobiol, 1997. 41: p. 433-40.
17. Kuper, M., et al., *Evidence for a motor and a non-motor domain in the human dentate nucleus--an fMRI study*. Neuroimage, 2011. 54(4): p. 2612-22.
18. D'Angelo, E. and S. Casali, *Seeking a unified framework for cerebellar function and dysfunction: from circuit operations to cognition*. Front Neural Circuits, 2012. 6: p. 116.
19. Koziol, L.F., et al., *Consensus paper: the cerebellum's role in movement and cognition*. Cerebellum, 2014. 13(1): p. 151-77.
20. De Zeeuw, C.I. and M.M. Ten Brinke, *Motor Learning and the Cerebellum*. Cold Spring Harb Perspect Biol, 2015. 7(9): p. a021683.
21. Diamond, A., *Close interrelation of motor development and cognitive development and of the cerebellum and prefrontal cortex*. Child Dev, 2000. 71(1): p. 44-56.

22. Raichle, M.E., et al., *Practice-related changes in human brain functional anatomy during nonmotor learning.* Cereb Cortex, 1994. 4(1): p. 8-26.
23. Limperopoulos, C., et al., *Injury to the premature cerebellum: outcome is related to remote cortical development.* Cereb Cortex, 2014. 24(3): p. 728-36.
24. Stoodley, C.J., *The cerebellum and cognition: evidence from functional imaging studies.* Cerebellum, 2012. 11(2): p. 352-65.
25. Basson, M.A. and R.J. Wingate, *Congenital hypoplasia of the cerebellum: developmental causes and behavioral consequences.* Front Neuroanat, 2013. 7: p. 29.
26. Steinlin, M., *The cerebellum in cognitive processes: supporting studies in children.* Cerebellum, 2007. 6(3): p. 237-41.
27. Peter, S., et al., *Dysfunctional cerebellar Purkinje cells contribute to autism-like behaviour in Shank2-deficient mice.* Nat Commun, 2016. 7: p. 12627.
28. Zoghbi, H.Y. and M.F. Bear, *Synaptic dysfunction in neurodevelopmental disorders associated with autism and intellectual disabilities.* Cold Spring Harb Perspect Biol, 2012. 4(3).
29. Stoodley, C.J., et al., *Altered cerebellar connectivity in autism and cerebellar-mediated rescue of autism-related behaviors in mice.* Nat Neurosci, 2017. 20(12): p. 1744-1751.
30. Moreno-Juan, V., et al., *Prenatal thalamic waves regulate cortical area size prior to sensory processing.* Nat Commun, 2017. 8: p. 14172.
31. Chen, J. and A.R. Kriegstein, *A GABAergic projection from the zona incerta to cortex promotes cortical neuron development.* Science, 2015. 350(6260): p. 554-8.
32. Averaimo, S. and X. Nicol, *Intermingled cAMP, cGMP and calcium spatiotemporal dynamics in developing neuronal circuits.* Front Cell Neurosci, 2014. 8: p. 376.
33. Teune, T.M., et al., *Topography of cerebellar nuclear projections to the brain stem in the rat.* Prog Brain Res, 2000. 124: p. 141-72.
34. Gornati, S.V., et al., *Differentiating Cerebellar Impact on Thalamic Nuclei.* Cell Rep, 2018. 23(9): p. 2690-2704.
35. Ichinohe, N., F. Mori, and K. Shoumura, *A di-synaptic projection from the lateral cerebellar nucleus to the laterodorsal part of the striatum via the central lateral nucleus of the thalamus in the rat.* Brain Res, 2000. 880(1-2): p. 191-7.
36. Deisseroth, K., *Optogenetics: 10 years of microbial opsins in neuroscience.* Nat Neurosci, 2015. 18(9): p. 1213-25.
37. Chen, C.H., et al., *Short latency cerebellar modulation of the basal ganglia.* Nat Neurosci, 2014. 17(12): p. 1767-75.
38. Catterall, W.A., et al., *Inherited neuronal ion channelopathies: new windows on complex neurological diseases.* J Neurosci, 2008. 28(46): p. 11768-77.
39. Sasaki, S., et al., *Impaired feedforward inhibition of the thalamocortical projection in epileptic Ca2+ channel mutant mice, tottering.* J Neurosci, 2006. 26(11): p. 3056-65.
40. Caddick, S.J., et al., *Excitatory but not inhibitory synaptic transmission is reduced in lethargic (Cacnb4(lh)) and tottering (Cacna1atg) mouse thalami.* J Neurophysiol, 1999. 81(5): p. 2066-74.
41. Beenhakker, M.P. and J.R. Huguenard, *Neurons that fire together also conspire together: is normal sleep circuitry hijacked to generate epilepsy?* Neuron, 2009. 62(5): p. 612-32.
42. Qian, J. and J.L. Noebels, *Presynaptic Ca(2+) influx at a mouse central synapse with Ca(2+) channel subunit mutations.* J Neurosci, 2000. 20(1): p. 163-70.

43. Popa, D., et al., *Functional role of the cerebellum in gamma-band synchronization of the sensory and motor cortices.* J Neurosci, 2013. 33(15): p. 6552-6.

44. Proville, R.D., et al., *Cerebellum involvement in cortical sensorimotor circuits for the control of voluntary movements.* Nat Neurosci, 2014. 17(9): p. 1233-9.

"Grazie a mia madre per avermi messo al mondo,

a mio padre semplice e profondo

grazie agli amici per la loro comprensione

ai giorni felici della mia generazione"

Nomadi

Appendices

Samenvatting

Summary

Curriculim Vitae

Acknowledgments

Samenvatting

Het hoofdoel van dit proefschrift was om de verbindingen tussen het cerebellum en de thalamus in het muizen te karakteriseren om zo meer antwoorden te kunnen genereren op vragen over de rol van deze verbinding in motorische en cognitieve functies, alsmede in neurologische ziekten zoals epilepsie. Om dit doel te bereiken zijn er elektrofysiologische en anatomische experimenten uitgevoerd in zowel het ontwikkelende en volwassen brein.

De resultaten in **hoofdstuk 2** geven inzicht in de vorming van de cerebello-thalamische verbinding tijdens de embryonale ontwikkeling. Het tijdspunt waarop de eerste neuronale verbindingen wordt gevormd blijkt in de laatste dagen *in utero* plaats te vinden. Deze kennis zal bijdragen aan het opbouwen van een referentiekader over hoe en vanaf welke leeftijd een cerebellaire afwijking kan leiden tot een breed pallet van neurologische aandoeningen.

De resultaten in **hoofdstuk 3** beschrijven hoe de cerebellaire kernen de door het cerebellum verwerkte informatie doorstuurt naar andere breinkernen. De Purkinje cellen zijn zowel functioneel als moleculair gecategoriseerd en in dit hoofdstuk wordt de impact van de verschillende activiteitspatronen op cerebellaire kernneuronen onderzocht.

In **hoofdstuk 4** zijn resultaten beschreven die verkregen zijn door met optogenetica selectief de axonen van cerebellaire kernneuronen te stimuleren en door middel van 'patch clamp' afleidingen de respons te meten in thalamische neuronen. Deze metingen zijn uitgevoerd in de ventrolaterale, ventromediane en centrolaterale thalamische kernen. De elektrofysiologische karakteristieken en de morfologie van deze verbindingen bleken specifiek per thalamische kern, en dus variabel. De bevindingen suggereren dat de cerebellaire verbindingen wijdverspreid en variabel effect hebben op de cerebrale schors en de daarin gecodeerde functies.

In **hoofdstuk 5** hebben we effectiviteit van de cerebellaire verbindingen naar de thalamus verder onderzocht, door de cerebellaire kernneuronen of –axonen optogenetisch te stimuleren in een muismodel voor gegeneraliseerde absence aanvallen. Deze vorm van epilepsie wordt gekenmerkt to pathologische oscillaties in de thalamo-corticale banen die gestopt kunnen worden door optogenetische stimulaties van de cerebellaire kernneuronen. In dit hoofdstuk blijkt dat stimulaties van de cerebellaire kernneuronen een variabel effect heeft op de vuurpatronen van de thalamische neuronen. Directe stimulatie van een deel van de axonen bleek minder effectief in het stoppen van absence aanvallen dan de cerebellaire kernneuronen.

Hoofdstuk 6 bevat een literatuuroverzicht van stimulatieexperimenten die als doel hadden om de rol van het cerebellum in verschillende neurologische aandoeningen te bestuderen.

Summary

The primary goal of this dissertation was to characterize the cerebello-thalamic (CN-TC) connection in mice to further elucidate questions regarding its role in motor and non-motor functions as well as in neurological disorders like epilepsy. Hereto, electrophysiological and anatomical experiments were performed in both the developing and adult mouse brain.

Chapter 2 provides insight into the formation of CN-TC connections during embryonic development and thereby reveal the time point from which the CN axons enter the thalamus and from when these axons start to form synapses. This knowledge will help to set the time point from which perturbations of the cerebellar development might lead to a dysfunctional cerebello-thalamic-cortical loop and thereby contribute to the wide range of neurological conditions reported in pediatric patients with cerebellar dysfunction.

Chapter 3 investigates the mode in which CN forward the information coming from cerebellar cortex. Previous research indicates that the peculiar organization of Purkinje cells in bands translates into differences in action potential firing patterns; we now showed that in turn CN action potential firing also adheres to the dichotomous inputs from the cerebellar cortex, which most likely also radiates to the information that is conveyed to thalamic cells.

With the use of optogenetics and whole cell patch clamp techniques in **chapter 4** we discovered the impact that the synchronization of CN terminals have on the thalamic cells positioned in different nuclei, such as the ventrolateral (VL), the ventromedial (VM) and centrolateral (CL) nucleus. As the effect was diverse in these thalamic nuclei, each of which connects to various cortical areas, we propose that cerebellar inputs can affect various cortical regions in a differential manner, and thus could affect cortical regions that encode motor behaviour different from cortical regions that contribute to cognitive functions.

This powerful connection in VL, but also the smaller amplitude responses in VM and CL raised the question how this excitatory input contributes to stop pathological thalamo-cortical oscillations during seizures. In **chapter 5** we utilized epileptic *tottering* mutant mice and optogenetics to control the action potential firing in CN neurons, or the glutamate release from their axon terminals to de-synchronize thalamic cells. We found that direct stimulation of either the CN neurons or their axons stopped absence seizures, but that CN stimulation was most effective. In **chapter 6** we discussed the role of cerebellum in epilepsy mouse models and the power of optogenetic stimulation to perturb pathological conditions and re-establish normal brain function.

Curriculum Vitae

Name: Simona Veronica Gornati
Date and place of birth: May 22, 1988 – Novara, Italy
Nationality: Italian

EDUCATION

- March 2013-September 2018: PhD candidate, Neuroscience department, Erasmus MC Rotterdam, The Netherlands
- October 2010 – December 2012 **Laurea magistrale (MSc) in Molecular Biology of Cell**, Faculty of Mathematical, Physical and Natural Sciences, University of Milan, Italy
- October 2007 - October 2010 **Laurea (BSc) in Biological Sciences,** Faculty of Mathematical, Physical and Natural Sciences, University of Milan, Italy.
- September 2002 - July 2007 **Diploma di maturità scientifica (Science Secondary School)** Liceo Scientifico Statale "Alessandro Antonelli", Novara, Italy.

RESEARCH EXPERIENCE

- March 2013-September 2018: PhD candidate, Neuroscience department, Erasmus MC Rotterdam, The Netherlands
- September 2011 –December 2012: Experimental Thesis at Department of Biomolecular Sciences and Biotechnologies, University of Milan, Italy.
- April 2010 - October 2010: Bachelor Thesis at Department of Biomolecular Sciences and Biotechnologies, University of Milan, Italy

TEACHING EXPERIENCE

- August 2015 - Neuroscience Summerschool: Patch clamp technique
- October 2015 - Master of Neuroscience: Optogenetics
- April 2014 - Medicine: Neuroanatomy

SPECIALISTIC COURSES

- January 2016: Microscopic Image Analysis- Erasmus MC, Rotterdam (Netherlands)
- October 2014: Functional Imaging and Super Resolution- Erasmus MC, Rotterdam (Netherlands)
- April 2013: Laboratory Animal Course (***Article 9***) Erasmus MC, Rotterdam (Netherlands) Principle of Laboratory animal science. Dutch legislation and ethics for the use of animal in research.

INTERNATIONAL CONFERENCES

- FENS Hertie Winter School -THALAMUS AND THALAMOCORTICAL INTERACTION, 8-15 December 2013, University Center Obergurgrl, Austria ***– selected speaker***
- 9th FENS forum of Neuroscience, July 2014, Milan, Italy- ***poster presentation***
- Gordon Research Conference -CELL CIRCUIT AND THALAMOCORTICAL INTERACTIONS- 14-19 February 2016, Ventura, CA - ***poster presentation***
- Annual Society for Neuroscience (SfN) meeting, San Diego, USA, 12-16 November 2016- ***poster presentation***

LIST OF PUBLICATIONS

Simona V. Gornati[*], Carmen B. Schäfer[*], Oscar H.J. Eelkman Rooda, Alex Nigg, Chris I. De Zeeuw and Freek E Hoebeek, Differentiating the cerebellar impact on thalamic nuclei. *Cell Reports*, in press

Oscar H.J. Eelkman Rooda, Lieke Kros, Sade J. Faneyte, Peter J. Holland, **Simona V. Gornati,** Thijs B. Houben, Huub J. Poelman, Nico A. Jansen, Else A. Tolner, Arn M.J.M. van den Maagdenberg, Chris I. De Zeeuw, and Freek E. Hoebeek, Desynchronizing epileptic thalamus activity by single pulse stimulation of cerebellar nuclei. Submitted to *Current Biology*

Daniël B. Dumas, **Simona V. Gornati**, Youri Adolfs, R. Jeroen Pasterkamp and Freek E. Hoebeek, Anatomical development of the cerebellothalamic tract in embryonic. In preparation for *Journal of Neuroscience*

Gerco Beekhof[*], **Simona V. Gornati**[*], Cathrin Canto, Avi Libster, M. Schonewille, C.I. De Zeeuw and Freek E. Hoebeek, Zebrin identity of murine cerebellar nuclei afferents corroborates neuronal firing frequency. In preparation for *Journal of Neuroscience*

Simona V. Gornati, Freek E. Hoebeek, Cerebellar stimulation: experimental and therapeutic approaches, Consensus article on Experimental Neurostimulation, submitted to *The Cerebellum*

C. Milanese, S. Gabriels, S. Cerri, **Simona V. Gornati**, I. Ulusoy, F. Blandini, F.E. Hoebeek, D. di Monte, P.G. Mastroberardino, Transferrin Receptor 2 as a target to halt nigral neurons iron overload in Parkinson's disease. In preparation for *Cell Death and Disease*

Acknowledgments

"Ingratitude is the daughter of pride"

Finally, this journey has come to an end. Many times I was about to crash, to quit, to cry..and oh boy, how much I cried... But what doesn't kill you, makes you stronger. And for sure now I am a different person than the one who entered the EMC five years ago. I would be very much unfair and proud if I wouldn't recognize that all the effort, blood, sweat and tears were shared and even sometimes carried by you guys.

Since 15th of March 2013 (happy b.day) you have always been there, Freek. To you goes my gratitude, my affection, and my esteem. I know I can be very impatience, chaotic and stubborn, but you always put the patience, the discipline and the compassion that helped me to realize that no matter how hard, how bad, how difficult, it can be done. You were (and still are) a guidance and a source of help. Niet mepien and roll up your sleeves, we are RRRRRotterdamers, proud to be.

Chris, thank you very much for your support and suggestions. Thank you for giving me the freedom and for teaching me to dare.

Thank you to all the members of my lab, and the technicians that have been the real "target" of my insanity. Oscar, thank you for always been a calm and solid companion during all the challenges that we found on our way. Carmen, you are a brilliant scientist, thank you for sharing the work and the fun in and outside the lab. Discussing science with you opened my mind; you brought a bit of "german" method in my chaos . Thank you for the loud classical music in the morning and even lauder rock in the evening. Lieke, short but intense time together, I will always bring with me the Geordie shores memories.

A special, special thanks go to the students. Although we were supposed to teach you something, in the end, you taught me a lot.

Daniel, it was special working with you. You taught me (one of the most entropic and chaotic human) patience and precision. You brought a bit of "zen" in my life. Thank you very much.

Bas, my dear, you are a volcano of ideas, feelings and emotions. A temper like yours is hard to find, no matter how tired or busy, you were always willing to help. Don't let

people convince you that your own success is more important than helping because, as cheesy as it might sound, sharing is caring, and there is nothing better at the end of the day than knowing that you made the difference for someone. So keep on going.

Vale, needless to say, that you made my days (late-in lab-nights as well) so much fun. Beside teaching me a lot of new words (mostly..you know..words of THAT kind) you reminded me that science is passion and that you have to be damn in love (or damn crazy but, isn't it the same?) with what you are doing to carry on. Otherwise, there is no way that the work is worth the effort.

Elena, you late night patcher and daytime boxeur. You are a strong badass woman, no matter how difficult it could be, you would always stand there as passionate as you could.

Thanks a lot to all the people that passed by Sverrir, Sade, Hubb, Nico ….

Thanks a lot for the great support to all the histo-dream-team! Really girls, without you I would never have achieved this. Erika, thank you for being the mom-substitute in these years, for always keeping an eye on me, for the laughs we shared and the tears you dried.

Elize, my sweet, the number of times I entered the lab ready to crush are uncountable. Your smile and "no panic" always fixed everything, also the things that I was sure were damaged irremediably. Thank you for the EM technical support but much more for the emotional support, for the sweets and the hugs.

Mandy, thank you very much for the help and laughs and for bringing in my life a bit of organization.

Daphne, thank you very much as well for your patience and kindness. I wish you all the best!

Edwin, thank you for spending some of your time with me and qPCR (not the best match) and Geeske for teaching me how to teach.

Thank you Gerard for always asking the right questions, Dick for always answering my questions (although with a lot of jokes in between) and Tom for being the great professor you are.

My gratitude goes also to the amazing OIC group and in particular to Gert and Alex. I still remember the first time I entered your office...I brought the best image I had and..well.. soon I found out it was not that amazing...thank you for teaching me what is a good image and how to analyze it. Gert, thank you for the help with macros, it was amazing sitting next to you while you were drinking tons of hot water with a bit of tea and a lot of sugar.

Alex, really, thank you for your patience. Thank you for always being there helping, although I can be a great mess changing my mind a thousand times each hour. Thank you for being kind and for being a shoulder to cry on.

Thanks also for the help to Loes and Elise that were so patient with me.

Avi thanks for the great time together, intense but lovely. You taught me a lot. Gerco, thanks for sharing the effort, for your direct comments and funny jokes.

Thanks to Chiara and Pier, for the scientific (and not) discussions we had, for believing in me and the work together.

Work hard, play hard.

This was definitely shared with a bunch of crazy scientists that became more than just colleagues and made these years not only pain but also a lot of fun.

In order of appearance, Malik, you were the first I met during a lunch break. Although many people might say it is impossible for a French and an Italian to get along together, we prove them wrong. Thank you for the amazing wine tastings and for being my lindy-hop companion. Without you, I would never have started…

Mohamed, Mimmo, doc. You are the sweetest friend someone could wish. Thank you for all your advice and for the time we spent together. Next time we'll drink one in Italy together.

Andy, my beloved. I also remember when I met you for the first time at the borrell…it was love at first beer, and MANY others were ahead of us. SO much fun we had together, Strano, French Bulldogs, Dyonisos…when you left I felt something was missing.

Licia, piccola Sbratty, if the walls of Hemradssingel could talk some epics lines came out

when we were together. Thank you for the support inside and outside the lab, for the laughs and the sgneeks (perchè essere cretine, cretine, tutte cretine è uno state of mind, e noi siamo le regine)

Farnaz, my crazy friend. Thank you for the help in the lab and for your contagious smile. You are such a positive person and I was super lucky to have you in my life.

Michiel, thank you for sharing your energy, you are a volcano. I am sure whatever you want to be in life,you will be great. But…in case it won't work, I'll wait for you in the Italian street food cart; if you need me, call me.

Franco, movie nights had a better taste with you.

Thanks to all the BAW team, Shashini, Martijn, Marlou, Sander, the sweet Yarmo and Aaron it was a pleasure working with you.

Catarina, it was short but intense. This southern-European axes made me feel close to you since the beginning. Thank you very much for listening and advising. It was hard but with you a bit less ☺

Monica, thank you for hosting me with amazing dinners, for always being friendly, your kindness and smile helped me a lot during the ups and downs of a (Italian) Ph.D. Somehow you made me feel at home. ;) E comunque, lunga vita a Vinicio.

Vincenzo, thank you for your "5 minuti di eleganza", for scientific and political discussions, you also made me feel home.

Thank you to all the colleagues that in a way or another made my time in the dept nicer: Cindy, Gustavo, Jochen, Annette, Ilja, Mana, Brian, Rossella, Lorenzo, Maria, Bastiaan, Leonoor, Francesca and Anna.

Thanks also to my sweet Italian gang Monica, Manu e Ila who shared with me joyful moments (la pizzaaaaa) a lot of laughs and a lot of tenderness. Ciao bellezze!

To the alpha-male of the "famigghia", Ale, thank you for hosting amazing evenings, dinners, for the laughs and the love.

Thank you to people that believed in me and most important to people that didn't.

Because there is nothing sweeter than prove you wrong.

Friends are the family we choose for ourselves

Saša, bro', you have been more than just a colleague. We grew up together, we faced problems together. You made me laugh a lot during the patching sessions and you helped me a lot with technical issues. You thought me "think in solutions Simo, not in obstacles" and I will always treasure it and our friendship.

Sylvie, Ma Chérie, I cannot imagine how my life would have been without you. You helped me so much in so many situations that I might need a whole chapter to list them all. A good summary is that I am extremely thankful for having you in my life and I am so happy that Olaf&Olof brought you at mine that night.

Both of you thank you for sharing the burden of standing next to me, I know I can be pretty "intense".

Thanks to my paranymph-from-distance, Negah. Although you are not here I can feel your presence, the same precious presence that helped me to go through these years. We started together and when you left it was horrible. You were my anchor, my singer-companion, my knowledgeable colleague, my sweet friend. If I made it through the super hard first year it was mostly because of you. Thank you a lot.

Chiara, tesoro, thank you for being a safe haven during the many crises I encountered during these years. The 7th floor became my refuge because you were there with your support. Thank you for the good time at yours, for all the good advice. You were (and are) a strong reference and without you, my life would have been way more miserable.

To my alter-ego Ale. Faraway so close. Although the distance I feel what you feel. It was a gift meeting you. Thank you for cheering me up, for the evenings at Labru, for the chats and fun.

Prof Ilir, thank you for feeding me (I am sure it costs a lot), for the bbq and good time together.

Thanks to my personal Spanish teacher Ivan. Gracias por toda la ayuda en estos años. I hope to see you soon in Italy.

Thanks to all the #hotpeople with #hotplans for being a lovely group of friends always ready to cheer me up in the moment of sadness. Bart, Kees and Ben, thanks a lot.

A very special thank goes to Tommi and Costi that were flatmates and soon turned into family.

Tommi, you were my father-figure during these years. Thank you for the help, for the support and for building with us the place that I learned to call home.

Costi, together since April 2013. I also wondered how life there would have been without you. I can't really answer. There was the rain, there was the laminaat, le beghe, the market, the tears and laughs. I cannot imagine going through all of these without you. There was a house to build and two girls that turned into women, together.

Life and all that it brings would be meaningless
without the best thing about it: friends.

Therefore I want to thank my friends-from-home that although far, have always been a warm hug where to go.

First of all my gratitude goes to Caro and Fede, we are not sisters by blood but sisters by heart. Life brought us far from each other but when we are together is like nothing changed. Thank you for the support, for listening and basically for being my other 2/3 of brain and heart. A special thanks go also to Francesco who was fundamental in the creation of the "quarta Maria": Zoe.

Thanks to my favorite scientist and beloved friend Claudia. You were there since the beginning ("posso sedermi qui?"). The distance never made me feel less close to you. From the cytology exam to the corrections of the doctoral thesis you have been there. And needless to say that without you I would not have made it. Our past together is epic but the best is yet to come.

Monia, thanks a lot for the infinite patience, the kindness and the support you gave me. We are friends for years and I am very happy to have you in my life. I am sure I was a pain for the covers designs but you were there. Thanks a lot.

Thanks to all my friends Matteo, Rino, Roby, Pez, Marcello, Miso, Gian, Bigno, Chiara, Dilo, Luca, Bicio, Ricky, Pol and Enci for the fun we had together.

Thanks a lot also to my "old" lab. 6B people, thanks a lot for your help. Thanks to Michele, without you I would never have replied to the email.

Thanks to Stefania, for your guidance and friendship, to Marina and Nicoletta for being always present and to Erika, MartaP, MartaG and Davide.

"Un albero senza radici è solo un pezzo di legno"

Matteo, thank you. You see all my light and you love my dark. I can find sometimes hard to express what I have in my mind but with you, I don't need to. You know it. Thank you for standing by my side, hold my hand and keep on walking.

Thanks to my family, their support, understanding and their unconditional love means a lot to me.

Grazie ai miei adorati nonni, ai miei zii e cugini. Siamo una famiglia piccola ma molto chiassosa, che a tutti i ritrovi, che sia Natale o Pasqua, riempie sempre il mio cuore. Siamo cresciuti insieme e io non potevo sperare di meglio. Grazie per avermi dato le ali per volare e la radici per tornare.

Most of all I want to thank my mother and father. Patty, thank you for teaching my kindness, to ask "how can I help you" and tell "thank you". Uzzo, thank you for giving me a strong back, able to bear the weight of work. I can only imagine how hard is to see your kid leaving home, the country, to follow her path. This thesis is not my achievement, it is our success.

E ve lo dico anche in italiano, mamma, papà, più di tutto devo ringraziare voi due. Patty, grazie per avermi insegnato la gentilezza e a chiedere "come posso aiutarti" e dire "grazie". Uzzo, grazie per avermi dato una schiena forte capace di sopportare il peso del lavoro. Posso solo immaginare quanto sia stato difficile vedere la vostra bambina lasciare casa e il paese per seguire la sua strada. Questa tesi non è il mio traguardo ma il NOSTRO successo.

Dunque io ringrazio tutti quanti
Specie la mia mamma che mi ha fatto cosi' funky